THE JOURNAL
OF
CHEMICAL PHYSICS

VOLUME 8 OCTOBER, 1940 NUMBER 10

The Infra-Red Absorption of Phenol and Its Halogen Derivatives in the Region of the Second Overtone of the OH Absorption*

OLIVER R. WULF AND ERNEST J. JONES
Bureau of Plant Industry, U. S. Department of Agriculture, Washington, D. C.

(Received May 19, 1940)

Orthohalogen and symmetrically trihalogen substituted phenols in the region of the second overtone of the OH absorption show behavior that is similar to that in the region of the first overtone but with increased displacement of the component absorptions. Subsidiary peaks are observed in the region of the second overtone and appear to stand in ordered relation to the principal peaks. In the present work the ortho- and symmetrically trichloro-, bromo-, and iodophenols as well as pentachlorophenol and phenol itself have been studied in carbon tetrachloride solution. The tendency of phenol to associate in a series of polymers has been studied by means of the phenol absorption. Relative to phenol the association of the above-mentioned substituted phenols is small.

ONE of the features of the infra-red spectra of complex organic molecules that seems to hold promise of aiding in the application of such spectra to a study of molecular structure is the influence of one group on the characteristic absorption of another group within the same molecule when the former group is near or adjacent to the latter. Perhaps the simplest illustration of this is contained in the ortho substituted phenols. A considerable number of these have been investigated in earlier work from this laboratory in the region 6500–7500 cm^{-1}, the region of the first overtone of the absorption characteristic of the OH group.[1] In general very close correspondence has been found between the actual character of the spectra and that to be expected on the basis of Pauling's theory[2] of such spectra. In the present work a study has been made of the absorption of *o*-chloro-, *o*-bromo-, and *o*-iodophenol in the region of the second overtone of OH, together with the absorption of the respective symmetrically trihalogen substituted phenols and the monohalogen benzenes, and also that of pentachlorophenol and phenol itself. The results permit a further test of Pauling's theory and afford additional data pertinent to the question of the shape of the absorption peaks.[3]

EXPERIMENTAL

The procedure was similar to that in past work from this laboratory. The substances were studied in dilute CCl_4 solution, and intensities were measured quantitatively. Owing to the weakness of the absorption in the second overtone, much higher concentrations were required than those used in the study of the first overtone. The absorption cells were of 30 cm length and the concentrations usually employed lay in the range 0.05–0.5 molal. At these concentrations phenol shows association,[4] and measurements were made at a number of concentrations in order to estimate the true molal absorption of monomeric

* Material presented at the Baltimore meeting of the American Chemical Society, April, 1939.

[1] Wulf, Liddel, and Hendricks, J. Am. Chem. Soc. **58**, 2287 (1936); Wulf and Liddel, *ibid.* **57**, 1464 (1935).

[2] Pauling, J. Am. Chem. Soc. **58**, 94 (1936); *The Nature of the Chemical Bond* (Cornell University Press, Ithaca, 1939).

[3] Wulf and Deming, J. Chem. Phys. **6**, 702 (1938).

[4] Fox and Martin, Proc. Roy. Soc. **162**, 419 (1937).

phenol, as should be obtained if the absorption were studied at higher dilutions. Cells longer than could be accommodated in the present arrangement of the apparatus would be required to make satisfactory measurements at such dilutions. The results for the halogen substituted phenols both for the mono-ortho substituted and for the symmetrically trisubstituted compounds indicated that the degree of association for these in the above-mentioned range of concentrations was very much less than for phenol, and indeed that, within the accuracy of measurement, measurable association could not be said to be present. Each of these compounds was measured at at least two concentrations, such as 0.2 and 0.4 molal, and an average of the values obtained for the apparent molal absorption coefficient was taken as representing the molal value. Because of the relatively low solubility of 2,4,6-triiodophenol, adequate concentrations were not obtainable and the intensity measurements for it are therefore not as satisfactory as for the other compounds.

These measurements, as those earlier published from this laboratory, have been made on the large glass spectrograph which records photographically the light trace of the galvanometer deflections against wave-length. In Fig. 1, an illustration is given of a record of phenol (concentration roughly 0.2 *M*).

In the course of the present work we have recalibrated the spectrograph, in order to extend to higher frequencies the earlier calibrations and to improve wherever possible the positional (frequency) measurements under the present instrumental conditions. This calibration was done entirely against mercury lines, using the values of Volk,[5] and in the higher frequency portion, also the values of Murakawa[6] and of Suga,[7] in terms of ν_{vacuum}. On the principal plates comprising the calibration, the mercury spectrum was superimposed on that of the regular tungsten lamp source, this giving the mercury spectrum under actual recording conditions and giving on all these plates the atmospheric water vapor absorption (7200–7500 cm^{-1}) which contains the reference point used for setting all actual absorption plates for measurement. In the region of the first overtone this calibration differs slightly from that earlier used, and in the sense that positions on the plate lie at higher frequencies by about 10 cm^{-1}, an amount lying within the overlap of the given limits of error. This does not of course affect materially the relative values. Working with the slit width, speed of plate motion, breadth of trace, etc. used in the present work, all of which affect somewhat the final attainable resolution and accuracy, we believe that the frequency values given in this paper should not be in error by more than ± 5 cm^{-1}. The accuracy of the value given for the position of an absorption maximum depends also of course on how well defined the particular maximum actually is, i.e., on its strength, shape, and freedom from overlapping absorption.

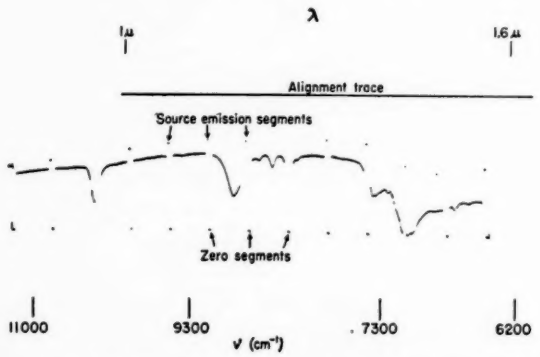

FIG. 1. An experimental record. Zero and source segments are obtained by the operation of a timing device working in five-minute cycles. The alignment trace, produced as a result of the plate moving past a fixed spot of light, allows a test to be made on each plate of the perpendicularity of the galvanometer swing and plate travel.

In the case of each substance measured, effort was made to obtain the substance in adequate purity. The attempt was made throughout not only to work with as pure materials as practicable but to utilize the several fractions of a purification to ascertain if any disturbing impurity were discernible in the absorption records, since this should have varied between the fractions.

RESULTS

The three ortho substituted phenols show, as is illustrated in Fig. 2 and as they did in the first overtone, absorptions both in the position of the normal phenol absorption (in this region *ca.* 10,320 cm^{-1}) and in a position displaced from this to lower frequencies by an amount increasing in the order *o*-chloro-, *o*-bromo-, and *o*-iodophenol.[1] These absorption peaks will be referred to, following Pauling[2] and as was done in the work in the first overtone region, as absorptions due, respectively, to a *trans*- and to a *cis*-form of these molecules. Certain complexities less evident in the first overtone region, are present in the second overtone region and require consideration before this nomenclature is satisfactory. Thus in *o*-bromophenol the absorption in the vicinity of the normal phenolic OH gives evidence of being composed of two peaks: one at about 10,300 cm^{-1}, rather closely in the position of the normal OH absorption, the other about 75 cm^{-1} to lower frequencies. Since this latter peak appears in 2,4,6-tribromophenol, while the peak at 10,300 cm^{-1} does not, it seems reasonable to conclude that the peak at 10,225 cm^{-1} is not concerned in what we may term the

[5] Volk, Dissertation, Tübingen, 1914, as given by Kayser and Konen, *Handbuch der Spectroscopie*, Vol. 7 (Hirzel, Leipzig, 1934), and by Murakawa (see reference 6).

[6] Murakawa, Proc. Physico-Math. Soc. Japan (3), **17**, 14 (1935).

[7] Suga, Sci. Papers Inst. Phys. Chem. Research No. 741, **34**, 32 (1937).

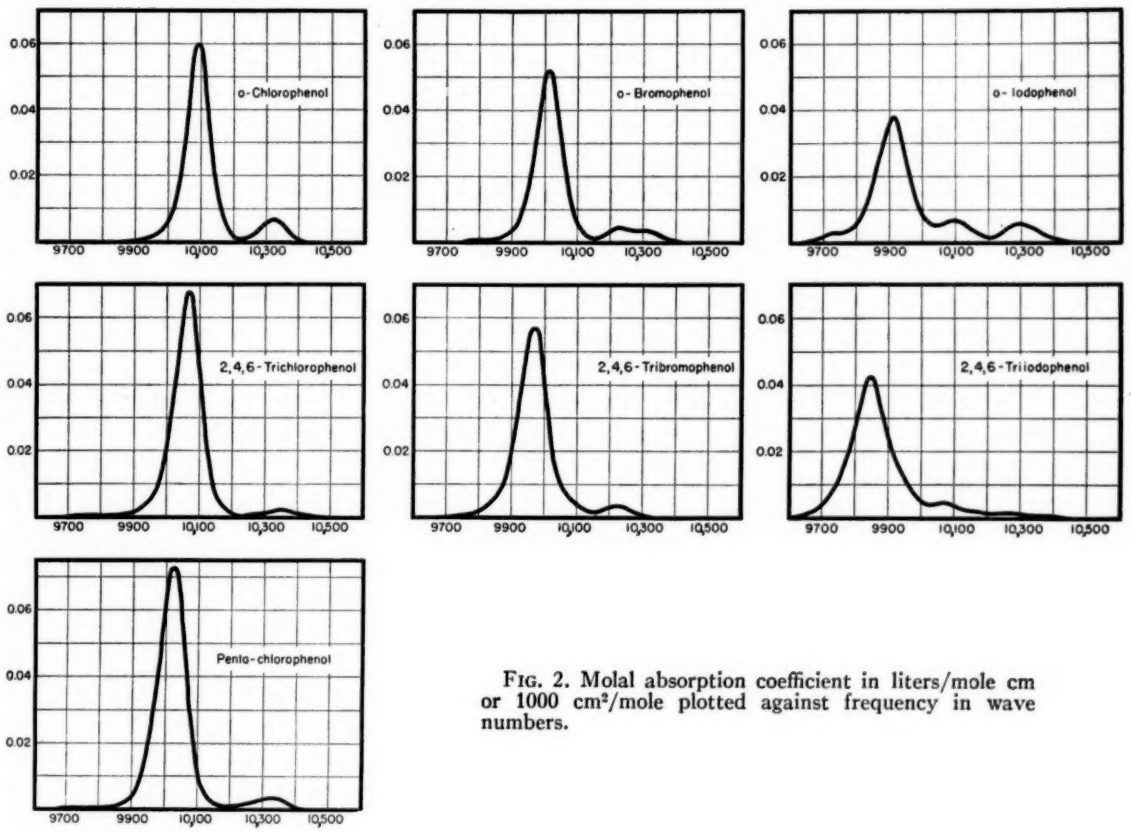

FIG. 2. Molal absorption coefficient in liters/mole cm or 1000 cm²/mole plotted against frequency in wave numbers.

trans-absorption of orthobromophenol. That this peak is, nevertheless, associated with the presence of OH in the molecule seems certain, since it does not appear in bromobenzene. The origin of this absorption will be discussed in the following paper. In reference 1 mention was made of further weak peaks in the vicinity of the *o*-chlorophenol absorption. In the second overtone region such weak peaks are clearly in evidence. Furthermore, just to low frequencies of the main (*cis*) peaks in this region there occurs very weak absorption which can in one or two cases be seen in Fig. 2. It is present in all these substances as is shown in the following paper where its origin is also discussed.

In *o*-iodophenol there appears at about 10,100 cm^{-1} a peak lying between what may be called the normal *cis*- and *trans*-peaks. This peak appears also in 2,4,6-triiodophenol, in which the orthoform (and hence the *trans*-peak) is absent. It thus seems reasonable to conclude that it is not a part of the *trans*-absorption. That it is associated with the presence of the OH group seems again to be true here, since it does not appear in iodobenzene.

This phenomenon brings rather sharply to attention the circumstance that such small absorption peaks may at times be symmetrically located under either the normal *cis*- or normal *trans*-peak of ortho substituted phenols in this region, and may thus cause the relative intensities of the two peaks to appear to be different from what they really are by themselves. This seems to be the case in this region for *o*-chlorophenol. In 2,4,6-trichlorophenol a small peak similar to the small peaks in the tribromo- and triiodo compounds occurs, and in this compound is located approximately at the position of the *trans*-peak of orthochlorophenol. Thus the intensity of this *trans*-peak presumably appears somewhat greater in the absorption as measured than that actually due to the *trans*-form of the molecule alone. And while the intensity of such a subsidiary peak may be somewhat different

in an orthohalogen substituted phenol than in the respective 2,4,6-trihalogen compound (compare the two bromophenols, Fig. 2 in which the peak is of approximately the same intensity), in estimating the relative intensities of the pure *cis*- and *trans*-peaks it seems evidently advisable to deduct from the intensity in the *trans*-peak region the intensity due to the subsidiary peak as measured in the respective trihalogen compound, assuming that this is about the same in the two compounds. Where comparison can be made there is evidence that this assumption is justified and the application of this correction undoubtedly leads to a better value for the area of the *trans*-peak than would be obtained if this correction were not applied at all. The possibility certainly exists that such weak peaks also underlie the *cis*-peak, but, as will appear later, this is much less probable. Moreover, in this case, failure to take such a weak peak into account would lead to a smaller error in the important ratio of *cis* to *trans*, since in all cases the intensity of the *cis*-peaks is much larger (of the order of tenfold) than that of the *trans*-peak.

The areas under the absorption coefficient curves for all seven substances do not vary greatly, the value being 7–8 liters/sq. cm mole. This is about one-twentieth the corresponding areas in the first overtone. Furthermore, the ratio of *trans*-peak area to *cis*-peak area is of the order of 1 : 10, as was observed also in the first overtone region. Assuming the absorption coefficients of the *cis*- and *trans*-forms to be the same, this ratio is indicative of the relative number of molecules in the two forms.[2] However, the circumstance of a subsidiary peak underlying a *trans*-peak, pointed out above and evident from the figure, makes the exact determination of the *trans*-: *cis*-area ratio difficult. This ratio taken from Fig. 2 without the deduction of the subsidiary peak ratio, for example in *o*-chlorophenol, would be misleading and the accurate determination of the area of the weak subsidiary peak is not possible from the present results. No attempt will be made, therefore, to determine this ratio for the three substances individually. It may be noted, however, that with the deduction of the subsidiary peak area from the *trans*-peak of *o*-chlorophenol, this latter probably remains somewhat greater than the true *trans*-peak area of *o*-bromophenol. The curves for the two iodophenols indicate a second subsidiary peak underlying the *trans*-peak of the ortho compound. This is confirmed in the work of the following paper. The large experimental error in the determination of the area of this small subsidiary peak leaves it entirely possible that the area of the *trans*-peak of *o*-iodophenol is less than that of *o*-bromophenol and by an amount such that the *trans*-: *cis*-area ratios decrease in the order *o*-chloro-, *o*-bromo-, and *o*-iodophenol, as would at first thought be expected from the increasing displacements of the three *cis*-peaks from the normal *trans*-position. This point, mentioned in reference 1 where an anomaly appeared to exist, is discussed in more detail in the following paper. In order that comparison may be made between the present results and those in the first overtone region,[1] the total areas under the seven curves of Fig. 2 are given in Table I.

TABLE I.

Substance	Second Overtone Molal absorption area	First Overtone (liter/cm² mole)
o-chlorophenol	6.6	135
o-bromophenol	6.4	125
o-iodophenol	6.7	125
Trichlorophenol	7.6	150
Tribromophenol	7.2	125
Triiodophenol	7.1	120
Pentachlorophenol	8.6	

After account is taken, where necessary, of the positions of these subsidiary peaks, the positions of the *trans*-peaks for these three molecules are roughly the same as that of the absorption of phenol itself. Actually they appear to decrease slightly in frequency in the order *o*-chloro-, *o*-bromo-, and *o*-iodophenol. The three *cis*-peaks lie progressively to lower frequencies, at approximately 10,099 cm^{-1}, 10,018 cm^{-1}, and 9917 cm^{-1}, respectively. These displacements relative to the normal *trans*-position are in the order of the respective polarizabilities of the halogen atoms.[1] Their values are all greater than the corresponding displacements in the first overtone. In Fig. 3 the positions of the several peaks for the six compounds just mentioned as well as for phenol and pentachlorophenol are represented diagrammatically. The removal of the final two hydrogens in 2,4,6-trichlorophenol has

in pentachlorophenol left the minor subsidiary peak at about the same position, close to the normal phenol position. The principal or *cis*-peak relative to that in 2,4,6-trichlorophenol is noticeably displaced to lower wave numbers as was the peak for this latter substance, relative to the *cis*-peak of orthochlorophenol.

The increase in displacement of the *cis*-peak relative to the *trans* in passing from the first to the second overtone is, of course, to be expected, since the two peaks represent two different absorptions possessing distinct frequencies in the fundamental also. Fox and Martin,[4] for example, have given the positions in the fundamental of the two peaks in *o*-phenyl-phenol. The separation of the two peaks increases, of course, with the number of the overtone. Because of the anharmonic character of the oscillations the overtones are in each case displaced somewhat toward lower frequencies from the exact multiple values of the two fundamental oscillations. Anharmonicities for the OH vibration in such spectra as these have been calculated by Fox and Martin[4] and by Mizushima, Uehara and Morino.[8]

The present data afford the opportunity to calculate several other values of the anharmonicity for the OH absorption. We question, however, the importance of making further estimates of this property of the OH group so long as there is, as seems to be the case, an appreciable uncertainty in the measured positions of the peaks. This uncertainty arises apparently from two quite different sources. First, there is the experimental uncertainty, as is indicated by the variance in the results. Thus, while our value for the second overtone of the OH absorption of phenol is in agreement with the value given by Mizushima, Uehara, and Morino, the values for *o*-bromophenol differ considerably. Their value for the *trans*-peak lies about 10 cm^{-1} above ours, while their value for the *cis*-peak lies somewhat more than this amount below our value. Second, there is the real physical and unknown uncertainty when the possibility exists that the maximum of absorption being measured is a composite of two (or even more) absorptions having, in general, different positions and intensities. Thus in *o*-iodophenol the absorption in the region of the first overtone *trans*-peak[1] lies at lower frequencies than would normally be expected for the position of the *trans*-peak, and it has an area, relative to that of the *cis*-peak, considerably larger than would be expected. The former circumstance, when this position is used with that in the second overtone region, leads to an unreasonable value for the anharmonicity, while the latter circumstance leads to a rather improbable situation discussed in reference 1. Both of these abnormalities are apparent only, and are caused by a subsidiary peak that is merged with the *trans*-peak in the first overtone region as is shown in the following article. To summarize, the position of the maximum of such a broad absorption peak is, to begin with, none too well defined a thing, and the possibility that the peak being measured is actually a composite of two or more peaks makes very difficult the determination of the true position of the particular peak that is of interest. Suffice it to say that the anharmonicities calculated from the present data, with the above-mentioned exception, are all about the same as the values found by the above-mentioned investigators, namely 80–95 cm^{-1}. In phenol it seems to be roughly 85 cm^{-1}. We wish to point out that this is about the same as the anharmonicity of the free OH molecule which is 82.6 cm^{-1}, its fundamental vibration frequency being 3735 cm^{-1}.[9] The frequency of infinitesimal vibration for the OH group from the above-mentioned calculations is roughly 3750–3800 cm^{-1}. For phenol this is about 3780 cm^{-1}.

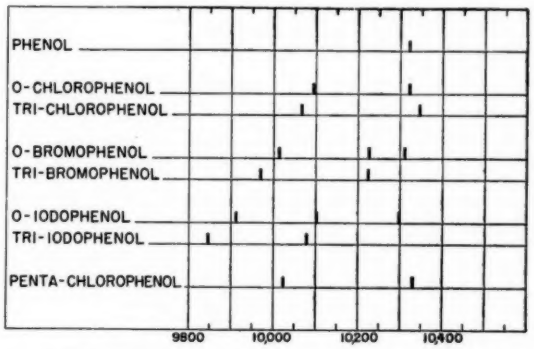

FIG. 3. Diagrammatic representation of the positions of the absorption shown in Fig. 2.

[8] The positions of the second and third overtone absorptions for phenol, *o*-chloro- and *o*-bromophenol have been measured by Mizushima, Uehara, and Morino, Bull. Chem. Soc. Japan **12**, 132 (1937).

[9] See, for example, Sponer, *Molekülspektren* (Springer, Berlin, 1935), Vol. 1.

The breadths of the peaks in the second overtone show a definite increase over those of the corresponding peaks in the first overtone. This phenomenon has been pointed out and discussed somewhat in an earlier paper[3] in connection with measurements of the fundamental and first overtone of phenol, the former measurements being those of Fox and Martin.[4] The increase in breadth in this case was closely twofold in passing from the fundamental to the first overtone. The breadths of the *cis*-peaks in the second overtone of the ortho substituted halogen phenols stand in the approximate relation of 3 to 2 with the corresponding peaks in the first overtone. The half-value widths of the *trans*-peaks are more difficult to obtain with satisfactory accuracy from measurements made at the concentrations used in the present work because of the weakness of these peaks. However, in the present work phenol has also been measured. The half-value width of its peak proves to be approximately 75 cm^{-1} while that for the fundamental and first overtone are about 25 cm^{-1} and 50 cm^{-1}, respectively.[3] It is probable therefore that the *trans*-peaks of the ortho substituted compounds show the same behavior. This increase of breadth with increase in the number of the overtone is important for the theoretical understanding of the cause of the breadth of these absorption peaks. It indicates that the curves represent the absorption of a group of oscillators differing somewhat in frequency, and distributed practically symmetrically about a most frequently occurring form, each individual oscillator in the distribution behaving independently, producing its own fundamental and overtones, and leading thus to a breadth of the absorption peak which is proportional to the number of the overtone.

The Association of Phenol[10]

The experimental results for the absorption of phenol showed, as was to be expected from much chemical evidence as well as from earlier spectroscopic work,[4] that at concentrations of several tenths molal such as employed here, appreciable association was occurring. Quantitative measurements such as the present ones can lead to a rough value for the degree of association, on the assumption that we have a measurable absorption which is really due to the monomer and which in itself obeys Beer's law. The circumstance that the degree of association cannot be measured very accurately arises from the fact that two unknowns are involved in the problem, the degree of association, of course, and also the true molal absorption of the monomer whose concentration we wish to determine by these absorption measurements. Given either one of these, a rather good value for the other could be determined, but with both unknown, as in the present problem, values for these two unknown quantities varying considerably may be chosen which at the same time represent fairly closely the experimental observations.

There seems to be no reason to doubt that the absorption due to the monomer will follow Beer's law closely. It is, however, more difficult to be sure that there exists measurable absorption which is due to the monomer alone. It is evident from the work of others as well as from the present work that not all the absorption in this region is due to the monomer. Absorption due to associated molecules is evident just to lower frequencies of the principal OH peak. If in the association of two phenol molecules the absorption of only one of the OH groups were altered in position, then the other would absorb in the same positions as the OH of the unassociated molecules. Under such conditions the principal peak, which at low concentrations is due evidently to the monomeric form, would at higher concentrations be due partially as well to the associated form. If, however, both OH bonds are affected in the process of association the principal peak might be due entirely to monomer absorption. This has been discussed in some detail by Fox and Martin.[4] We agree with the point of view that the results suggest that the interaction between two molecules in association affects both OH bonds. We shall assume in presenting our results that the absorption in the principal peak may be taken as a measure of the concentration of monomer present.

It has been found possible to represent a

[10] After the completion of this work the authors' attention was called to the work of Kempter and Mecke, Naturwiss. **27**, 583 (1939) in which the association of phenol has been measured over a wide range of concentrations in a manner similar to that described here.

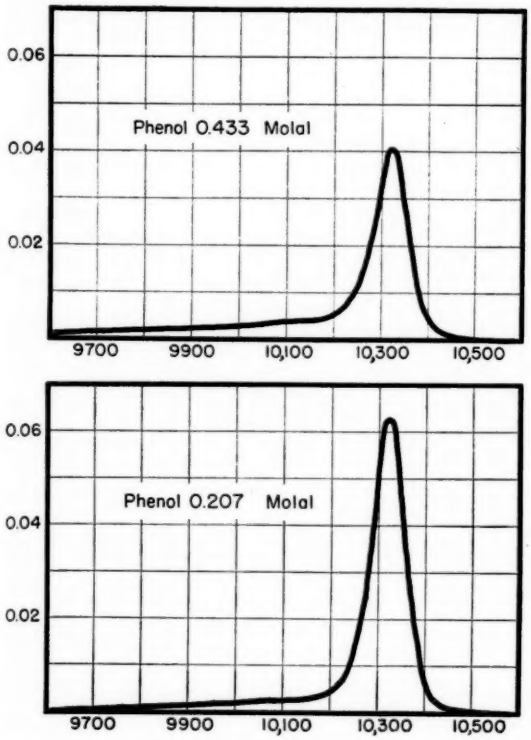

FIG. 4. Apparent molal absorption of phenol at two concentrations.

number of complex infra-red absorption curves[11] as a summation of component absorptions on the assumption that the absorptions from such molecules in solution in the infra-red are compositions of a number of symmetrical peaks. In the present instance the phenol absorption in the second overtone was decomposed into two parts by completing the peak at 10,300 cm^{-1} symmetrically with the high frequency side, obtaining thus two portions, the one taken to be the monomeric absorption at 10,300 cm^{-1} and the other, the residual absorption due to the higher polymers. Figure 4 shows the apparent molal absorption of phenol at a concentration of approximately 0.2 and 0.4 molal. It is of some interest that the shape of the absorption in the second overtone is noticeably different from that found by Fox and Martin[4] and others in the fundamental in the same range of concentration.

Using the area of the principal peak as proportional to the concentration of the monomer, it was apparent after measurements at a few concentrations that, as found also by Fox and Martin,[4] the association was not to be explained by the formation of a single polymer such as a dimer. This is to be expected from the studies which have been made on the association of phenols and other molecules in various solvents—a field which has been discussed in a comprehensive way by Lassettre.[12] In such association the apparent molecular weight of the solute often increases almost linearly with concentration. Lassettre showed that a linear increase could be accounted for by a unique set of equilibrium constants and gave an expression for the concentration in formula weights as a series in powers of the concentration of the monomer, the coefficients of the terms of the series involving the equilibrium constants of the different polymerization reactions. The equilibrium constant for any particular order of polymer was expressed in terms of the polymer number and a constant characteristic of the particular type of polymerization. Our results can be well represented by such an expression, which has the form

$$C=\sum_{l=1}^{l=\infty} lu^{l}K_{l}, \qquad (1)$$

where $K_l=(\alpha l)^{l-1}/l$, α being the equilibrium constant of the formation of the polymer $l=2$ from the monomer, that is, of dimerization, and the summation being taken over l, the polymer number. K_l is the equilibrium constant for the reaction representing the formation of the lth polymer from the monomer, u is the concentration of the monomer, and C is the total concentration of the solute expressed in formula weights. In principle the polymer number l takes on the integral numbers unity to indefinitely large numbers.

The area under the principal peak at any one total concentration is equal to the concentration of the monomer at this concentration multiplied by the true monomeric molal absorption coefficient, which is the value of the area of this peak to which extrapolation to infinite dilution leads. The concentrations of the monomer and of the

[11] Fox and Martin, Proc. Roy. Soc. **162**, 419 (1937); *ibid.* **167**, 257 (1938); J. Chem. Soc., 318 (1939); Rose, J. Research Nat. Bur. Stand. **20**, 129 (1938); Wulf and Deming, reference 3.

[12] Lassettre, Chem. Rev. **20**, 259 (1937); J. Am. Chem. Soc. **59**, 1383 (1937).

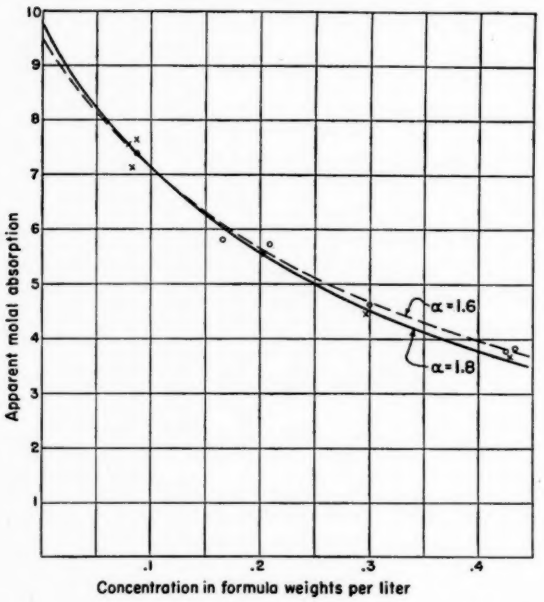

FIG. 5. Variation of the association of phenol with concentration.

various polymers are, of course, functions of the characteristic constant of the polymerization, and thus the absorption data are actually used to determine the two quantities at the same time; namely, the molal absorption coefficient of the monomer and the constant characterizing the equilibrium between the polymers of different order.

Two sets of measurements were made, one in winter and one in summer, in a room whose temperature was fairly constant; the winter range being 24–25.5°C, the summer range being 25.5–27°C. The cell was not thermostated, since the original intention of the work was not to measure the association of phenol. The calculation of the constant characteristic of the equilibrium and the true molal absorption coefficient was carried out by trial. The results of these calculations are represented in Fig. 5. $\alpha=1.8$ seems to represent best the series of measurements made in the winter while $\alpha=1.6$ favors those measurements made in the summer which is in accord with the slightly higher temperature of these readings. The winter and summer measurements are indicated on the figure by crosses and circles, respectively.

The true molal absorption area of the monomer for these two sets was 9.75 and 9.47, respectively. This quantity probably does not vary appreciably with temperature, and a mean value of 9.6 liters/mole cm² or 9.6×10^3 cm²/mole cm probably represents a fairly good value for the molal absorption area of monomeric phenol in the second overtone.

The authors gratefully acknowledge the assistance given them by Lola S. Deming in the numerical calculations.

SUMMARY

Quantitative measurements of the absorption in the region of the second overtone of the OH group have been made on the ortho and the symmetrically trisubstituted chloro-, bromo-, and iodophenols as well as on pentachlorophenol and phenol itself. In the concentration range employed of the compounds measured only phenol showed association large enough to be definitely established. The ortho substituted phenols show in the second overtone, as was found in the first, a small absorption peak in the normal phenol position and a larger peak displaced to lower frequencies, in accord with Pauling's theory of the absorption of these compounds. Subsidiary peaks are observed and are more in evidence in this region than they were in the region of the first overtone. It is pointed out that an important source of error may arise in determining the positions and intensities of small peaks such as the *trans*-peaks of these substances, when such subsidiary peaks overlap or underlie the peak being measured. Such effects actually occur in the spectra of the substances here studied. The displacements of the *cis*-peaks are in the order of the polarizability of the halogen atoms, and in amount are closely those to be expected as second overtones from those measured in the region of the first overtone. The breadths of these second overtone peaks stand about in the ratio of 3 : 2 to those of the corresponding first overtone peaks and, in the case of phenol for which there is data, in the ratio 3 : 1 to that of the fundamental. This offers further substantiation for the point of view that the breadth of the peak arises from a distribution in frequency of the absorbing oscillators around a mean or most probable frequency. The association of phenol in carbon tetrachloride at room temperature has been calculated by measuring quantitatively the absorption of the monomer. The data indicate that phenol in carbon tetrachloride associates in a series of higher order polymers, and yield values for the molal absorption coefficient of monomeric phenol and for the constant which characterizes the equilibrium between the polymers of different orders.

Combination Frequencies Associated with the First and Second Overtone and Fundamental OH Absorption in Phenol and Its Halogen Derivatives

OLIVER R. WULF, ERNEST J. JONES, AND LOLA S. DEMING
Bureau of Plant Industry, United States Department of Agriculture, Washington, D. C.

(Received May 19, 1940)

Absorption maxima occurring in the near infra-red spectra of phenol and seven of its halogen derivatives have been measured and interpreted as combination frequencies in which the valence vibration of the OH group combines with frequencies of the body of the molecule. Certain of these absorptions underlie some of the *trans*-peaks of the orthohalogen phenols causing such a *trans*-peak to appear of larger area than that due to the *trans*-peak alone. A group of the combination frequencies which lie in the range 1000–1600 cm^{-1} above the first overtone OH absorption have been observed as a group of an order of magnitude weaker intensity in the frequency range twice the values above the first overtone OH and also above the fundamental OH absorption, apparently involving two units of vibration in the combining frequencies. A close correspondence is found between the frequencies involved in these combination tones and the frequencies which have been observed in some of these compounds in the deep infra-red and in Raman spectra.

INTRODUCTION

THE second overtone absorption of the OH group in phenol and certain of its halogen derivatives, lying in the region of 10,000 cm^{-1} shows similar behavior[1] to the first overtone absorption[2] in the region of 7000 cm^{-1}. While the absorption of phenol in this region in dilute carbon tetrachloride solution consists of a single symmetrical peak, the orthohalogen substituted phenols show two peaks, a small one at approximately the same frequency as the phenol peak and a large one displaced to lower frequencies, this displacement increasing in the order chlorine, bromine, and iodine. The 2, 4, 6-trisubstituted derivatives show a single peak in each case, the position of which is approximately that of the major peak of the respective ortho derivative, although in all three cases slightly displaced to lower frequencies. Pentachlorophenol similarly shows a single peak at approximately the position of the major peak of the respective ortho derivative just as did the symmetrically trisubstituted derivative, and again with a small displacement which is slightly greater than that for the latter compound.

In addition to this principal pattern of the second overtone absorption, subsidiary peaks occur in this region comparable in intensity to the minor or *trans*-peaks of the ortho derivatives. In reference 2 mention was made of the occurrence in the vicinity of the first overtone of further weak absorption in several if not all of the compounds studied and, in particular, of two weaker peaks in *o*-chlorophenol in addition to the *cis*- and *trans*-peaks. At the concentrations used in the second overtone work, subsidiary peaks just to higher frequencies of the first overtone show clearly. As pointed out in reference 2, atmospheric water vapor absorption renders observation difficult in this region. However, such subsidiary peaks similar in character to those in the second overtone region and weak compared with the main peak, are present in the first overtone region for all the halogen derivatives.

These peaks both in the first and second overtone regions appear to be only a part of a considerable number of peaks arising through the combining of the OH valence vibration with other frequencies in the molecule. They seem to be independent of the ortho effect, occurring not only in the ortho compounds but in phenol, in the trisubstituted derivatives, and in pentachlorophenol, where the absorption characterizing the ortho effect is absent. Their intensities are an order of magnitude less than those of the principal valence vibrations on which they depend. In the ortho derivatives this is the *cis*-peak in each case, as will be seen later in this paper. It may be that a similar set of absorptions (combination frequencies) exists for the respective *trans*-peaks but they have not as yet been

[1] This journal (preceding article).
[2] (a) Wulf, Liddel, and Hendricks, J. Am. Chem. Soc. **58**, 2287 (1936); (b) Wulf and Liddel, *ibid.* **57**, 1464 (1935).

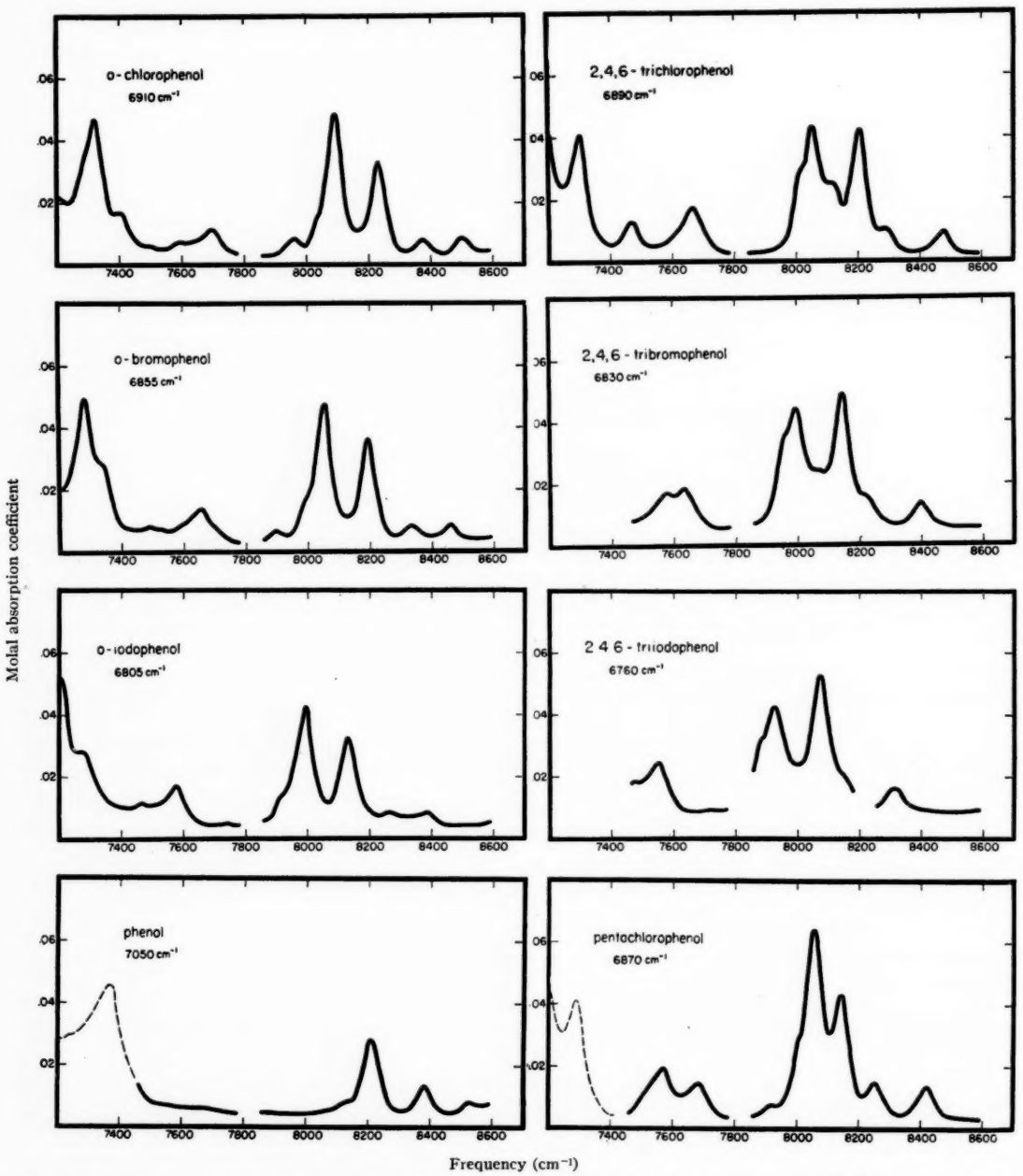

FIG. 1. Principal combination frequencies lying above the position of the first overtone OH absorption. The frequency value below the name of each substance is the position of the first overtone peak. In the ortho compounds it is the position of the *cis*-peak.

found in this work. They would be of the order of tenfold weaker again than the first set, if the intensities of these two sets were proportional to those of the two principal peaks upon which they depend, these being in the ratio of 0.1 or smaller. In addition to the above-mentioned, certain further absorptions, of an order of magnitude again weaker, have been observed, depending upon the first and second overtones and fundamental valence absorption, respectively.

Such combination frequencies offer a means of observing a considerable number of the low

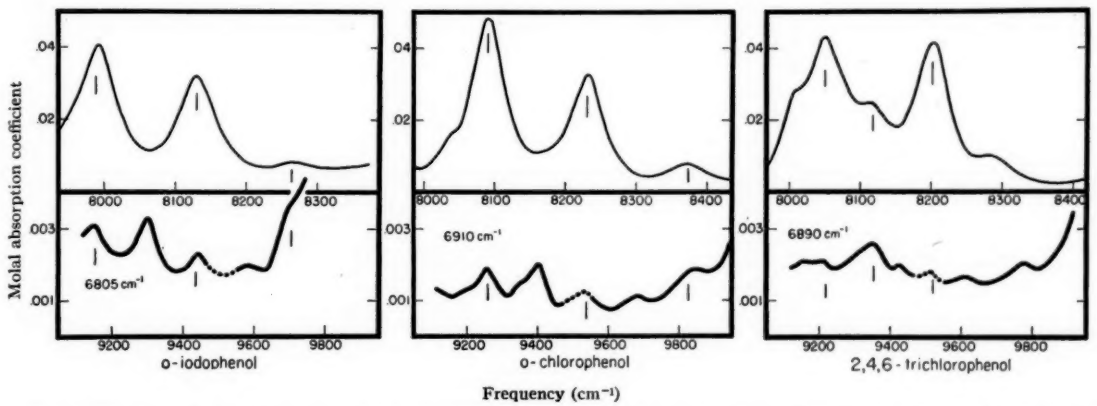

FIG. 2. Weak combination frequencies in the 9500 cm^{-1} region, with those of the 8200 cm^{-1} region of Fig. 1 placed above. The latter are on a twofold greater scale of abscissae than the former, and are so placed as to show the similarity in the relative positions of the peaks marked on the figure by short vertical lines. The frequency values at the left in the lower portions of the figure are the positions of the first overtone peak.

frequencies of a molecule in a convenient region of the infra-red, even accessible, as in the present case, with glass optics.[3] Since their intensities depend upon the character of the intramolecular forces and upon the geometry of the molecule, their interpretation should contribute considerably to the complete description of the absorbing molecule. It proves also to be the case that the existence of these absorptions explains some anomalies which had existed in the relative intensities of certain peaks in the orthohalogenated phenols.

EXPERIMENTAL

The plates, from which the data given below were obtained, were chosen from the plates taken in the work on the second overtone absorption described in the preceding article except for pentachlorophenol in the 6000 cm^{-1} region and the material lying at frequencies higher than 10,600 cm^{-1}. The several peaks representing the combination frequencies to be discussed in the present paper are in many instances relatively weak on these plates, in some instances very weak, still higher concentrations being required if accurate measurements of the intensities of these peaks were desired. The plates, however, afforded the opportunity to make a survey of the combination frequencies.

RESULTS

The combination frequencies in the region above the first overtone for the eight compounds measured are shown in Figs. 1 and 2. These are curves of the molal absorption coefficient, as used in past work from this laboratory. In each case the accompanying carbon tetrachloride (pure solvent) plate served as a blank. However, no correction has been made for turbidity in the solution plate, as has been done in past work and as was done in reference 1. This means that the absolute values of the absorption coefficients are in all cases somewhat high, by an amount which varies from case to case.[4] This same applies to the results in the 9500 cm^{-1} region shown in the lower portion of Fig. 2, where, because of the high concentration of the solutions used in the plates from which these results were read, the effect of turbidity is magnified. The material shown in the upper portion of Fig. 3 in the region above 10,400 cm^{-1} and the pentachlorophenol results in the 6000 cm^{-1} region shown in the lower portions of Fig. 4 rest on an indirectly determined reference line. The absorption coefficients are correspondingly less accurate.

The heavy black line used in the curves represents the measurements made on plates

[3] Rumpf and Mecke, Zeits. f. physik. Chemie **B44**, 299 (1939). This article came to the authors' attention when this manuscript was nearly completed.

[4] The absorption coefficient curve for phenol, while similar in form to the others, shows considerably weaker absorption. This is undoubtedly due to the association known to be present at these concentrations. However, this means that some of the observed absorption may be due to the polymers. In view of this, absorption coefficients based on the concentration of the monomer, which is known approximately from the work in reference 1, cannot be fairly given. The character of the curve suggests, however, that at least the main part of the detail shown is due to the unassociated phenol molecule.

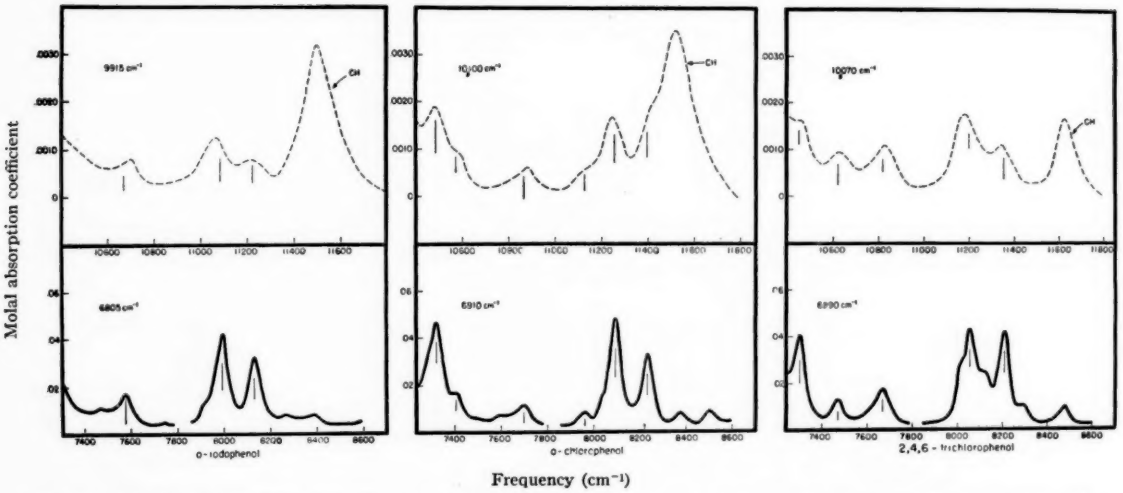

FIG. 3. Principal combination frequencies lying above the position of the second overtone OH absorption, with the corresponding first overtone frequencies of Fig. 1 shown below. The frequency value in the left-hand portion of each curve is, in the upper three curves, the position of the second overtone peak, while in the lower three curves it is the position of the first overtone peak. The comparison indicates that the same frequencies are involved in these combination tones as in those above the first overtone. The peak designated by CH in each of the three upper portions of the figure is principally, but in general not entirely, the third overtone CH valence absorption.

for which there were corresponding pure solvent plates. The long-dash line represents measurements which are based on indirectly determined reference lines, and hence are correspondingly less accurate than the other measurements. The portions of the heavy-line curves shown in heavy dots, represent sections missing from the principal plates which were filled in from other plates. These similarly are less accurate than the heavy curves. The thin full lines of Figs. 2 and 4 are used to represent curves of Fig. 1, simply redrawn on a scale of abscissae twofold greater than that of Fig. 1.

DISCUSSION OF RESULTS

The prominent combination frequencies, as shown in the figures, lie principally in the region up to 1600 cm^{-1} greater than the valence absorption upon which they depend, and were most readily observed in the present work in the region to higher frequencies of the first overtone. They are characterized by a particularly strong group of five or six frequencies in the region 1000–1600 cm^{-1} greater than the first overtone absorption. This will be called the 1200 cm^{-1} group hereafter. In the region 2000–3000 cm^{-1} above the first overtone, very weak absorption is perceptible in the present plates, similar though not identical to the pattern of the strong 1200 cm^{-1} group. It will be spoken of below as the 2400 cm^{-1} group. In the upper portions of Fig. 2 the 1200 cm^{-1} group is plotted on a twofold greater scale of abscissae and oriented so as to show the resemblance of the patterns to be discussed further below. In the region to higher frequencies of the second overtone, i.e., 10,400–11,800 cm^{-1}, certain of these combination frequencies can be seen to be present up to and including the strong 1200 cm^{-1} group (Fig. 3). Their positions with respect to the second overtone agree well with the positions of the corresponding frequencies above the first overtone. The weak group at about 2400 cm^{-1} above the first overtone, little more than visible at the concentrations employed in the present work, is too weak to be seen above the second overtone.

However, if this 2400 cm^{-1} combination absorption also occurs with the fundamental valence vibration, as would be expected after the close correspondence of the stronger combination frequencies following the first and second overtones, this group should appear in the 6000 cm^{-1} region with an intensity easily observable. This is the region of strong first overtone CH absorption, and absorption in this region in

phenol and its derivatives as well as all CH-containing compounds has long been known. It lies within the range of the glass spectrograph used in the present work.

The study of pentachlorophenol from 5400 cm^{-1} to higher frequencies afforded an opportunity of observing all absorption due to OH, free of CH absorption. In the region of 6000 cm^{-1} there appears a series of relatively strong peaks whose intensity is of the same order as that of the 1200 cm^{-1} group above the first overtone, showing that in the range 5600–6200 cm^{-1} important OH absorption occurs, and that the absorption in this region of the CH first overtone is, in phenol and its derivatives, in part due to OH. Because of the relatively low solubility of pentachlorophenol and the resulting low concentration at which it was studied, the absorption for it in the 9500 cm^{-1} region was very weak. Nevertheless, five members of this weak group as they appear about 2400 cm^{-1} above the first overtone can be seen sufficiently clearly that their pattern can be checked with that in the 6000 cm^{-1} region. Within experimental error the pattern of these peaks is the same, as is clear in Fig. 4, and furthermore the group lies above the estimated position of the fundamental by a frequency difference which is the same as that above the first overtone, leaving little doubt that the same group of frequencies is concerned in the combination frequencies observed in the 6000 cm^{-1} and 9500 cm^{-1} regions. So far as the authors are aware the position of the fundamental OH absorption of pentachlorophenol in carbon tetrachloride solution has not been reported. The position estimated from the first and second overtone absorptions assuming linear anharmonicity is 3530 cm^{-1}. In the upper portion of Fig. 4, as in Fig. 2, the 1200 cm^{-1} group of pentachlorophenol is shown on a twofold greater scale of abscissae, and so oriented as to show the resemblance of the patterns.

Several further combination frequencies (Fig. 1) occur in these compounds, representing combinations of the OH valence vibration with frequencies in the molecule lower than 1000 cm^{-1}. Some of these vary considerably in frequency and intensity from compound to compound and in phenol several of them are either of very low intensity or are absent. Most of these peaks can be seen in the figures; the others are the "subsidiary peaks" (peaks in the vicinity of the valence vibration itself) dealt with in the preceding article. These latter prove to be of considerable importance in interpreting the intensities of the principal absorptions of the ortho substituted phenols in the first and second overtone regions as will be described further on.

The pattern of the 1200 cm^{-1} group is nearly the same in the three ortho compounds, indi-

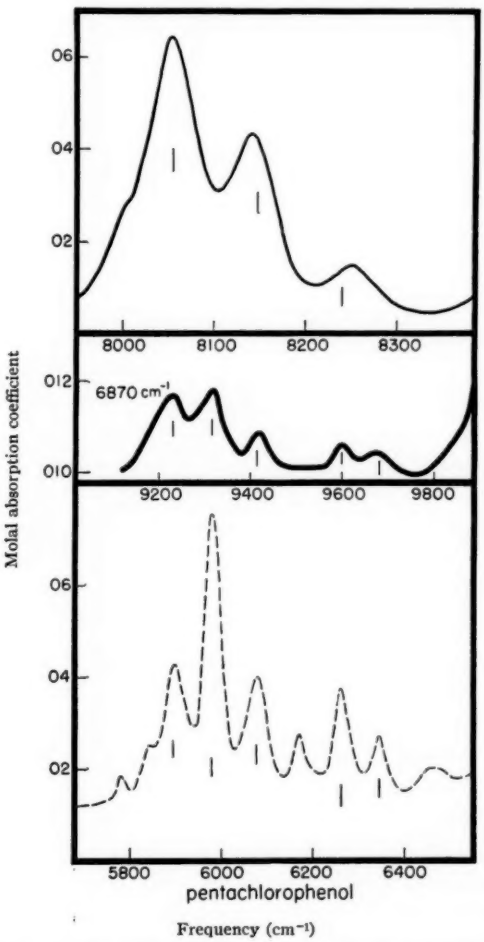

FIG. 4. The combination frequencies in pentachlorophenol in the region 6000 cm^{-1} compared with those lying in the 9500 cm^{-1} region. As in Fig. 2, comparison is also made with the principal combination frequencies in the 8200 cm^{-1} region. The 6000 cm^{-1} group lies above the fundamental OH absorption by apparently the same interval as does the 9500 cm^{-1} group above the first overtone absorption. The number in the upper left corner of the middle portion of the figure is the position of the first overtone absorption. Concerning the lower portion of the figure, the position of the fundamental calculated from the positions of the first and second overtones is approximately 3530 cm^{-1}.

cating that these frequencies depend but little on the particular halogen. A tendency for these peaks to broaden in passing from *o*-chloro and *o*-bromo to *o*-iodo is reminiscent of the behavior of the first and second overtone valence OH absorptions upon which these depend.

The actual positions of the members of this group of frequencies shift for the various compounds in accordance with the shift of the principal (*cis*) first overtone peak, as is to be expected if the former are combination frequencies that involve the latter. In *o*-bromophenol, for example, this pattern is displaced to lower frequencies, relative to that in *o*-chlorophenol, by the same amount as the first overtone *cis*-peak of the *o*-bromophenol is shifted to lower frequencies relative to that of *o*-chlorophenol. The same applies to *o*-iodophenol. The pattern in phenol, while somewhat different, clearly tends to obey the same relation and for two of the peaks the agreement is very close. The pattern changes a little in passing to the symmetrically trisubstituted compounds, but again within this latter group it is nearly constant. The second overtone CH absorption on the other hand remains at about the same position in these compounds with the following values for the frequency of its apparent maximum in cm^{-1}: phenol, 8795; *o*-iodophenol, 8810; *o*-bromophenol, 8825; *o*-chlorophenol, 8825; tri-iodophenol, 8840; tribromophenol, 8880; trichlorophenol, 8895. It is due to this circumstance that the shift of the 1200 cm^{-1} group in passing from phenol to *o*-chlorophenol has apparently resulted in the removing of the highest frequency peak of the OH pattern of the former out from under the second overtone CH absorption. In phenol its presence seems indicated as an asymmetry under the low frequency side of the CH absorption.

The *Cis-Trans* Absorptions of the Orthohalogenated Phenols

In the interpretation of the spectra of the orthohalogen phenols[5] considerable importance attaches to the question as to whether the absorption coefficients in the valence absorption of the *cis*- and *trans*-forms in any one ortho substituted phenol are essentially equal or whether they differ considerably. It seems probable for the following reason that they are approximately the same.[6] In the symmetrically trisubstituted compounds, if the concept of *cis*- and *trans*-forms of the ortho compounds be generally right, all the molecules are necessarily in one form, namely the *cis*-form. Yet the area of the absorption peak is roughly the same as for phenol. This seems to be a fair test, for the *cis*-form of the trisubstituted compound (in this case the only form present) should, if it differs at all, differ somewhat more from phenol than the *cis*-form of the ortho substituted compound, because the molecule itself differs more, being more extensively substituted.

The possibility of important differences in the relative absorption coefficients of the *cis*- and *trans*-forms arose in earlier work[2a] when it became clear that the displacement of a *cis*-peak by an ortho group did not appear to go hand in hand with the difference in free energy between the *cis*- and *trans*-forms as determined from the ratio of the areas of the *cis*- and *trans*-peaks. This lack of correspondence between the magnitude of the displacement of the *cis*-frequency and the free energy difference between the two forms seemed, while physically not impossible, nevertheless somewhat surprising. In using the ratio of the two absorption areas as a measure of the free energy difference (i.e., of the constant of the equilibrium between the two forms), it had, however, been assumed that the absorption coefficients of the two forms were the same, for otherwise this ratio would not be a measure of the ratio of the concentrations of the two forms. This assumption, which, if invalid, might permit a reconciliation of the observations with the expectation that the displacement of the *cis*-peak should go hand in hand with the free energy difference between the two forms, appears from the above for all practical purposes to be valid.

Against this point of view it might be pointed out that a relatively small difference in the absorption coefficients for the *trans*- and *cis*-

[5] Pauling, J. Am. Chem. Soc. **58**, 94 (1936); *The Nature of the Chemical Bond* (Cornell University Press, Ithaca, 1939).

[6] See, however, Kozima and Mizushima, Sci. Papers Phys. Chem. Inst. Tokyo **30–31**, 296 (1936–37).

forms would avoid the apparent discrepancy, as can be seen by comparing the results for *o*-bromo and *o*-iodophenol.[2a] From the respective absorption areas one would estimate about the same ratio for the number of trans to the number of *cis*-molecules, or even a somewhat greater ratio for the iodo derivative, in spite of the fact that the displacement of the *cis*-peak in the latter is considerably greater than that for the bromo derivative. However, the difference in the molal absorption of the two *trans*-forms, or even also of the *cis*-forms necessary to make the estimated ratio somewhat smaller in the iodo derivative than in the bromo derivative, would evidently not have to be very large.

This unsatisfactory state of affairs has, however, been removed by the study of those members of the combination frequencies lying close to the principal first and second overtone absorptions and called, in this work, the subsidiary peaks. These, varying from compound to compound as explained above, take up positions which in some cases underlie the *trans*-peaks and lead in this way to mistaken estimations of both the intensities and the positions of the *trans*-peaks.

The possibility of recognizing this situation lay in the measurements of the combination frequencies observable in both the first and second overtone regions. For, since these combination tones are built on the *cis*-peaks, and since the *cis-trans* displacement is different in the first and second overtone, if a subsidiary peak underlies the trans peak in the region of one of the overtones it will not in general do so in the other, since it remains separated from the *cis*-peak by the same amount in each case, while the displacement of the *cis*-peak from the *trans*-peak changes considerably. Thus in *o*-bromophenol the displacement of the *cis*-peak from the *trans* in the first overtone is about 195 cm^{-1}, while in the second overtone region a subsidiary peak shows at about 215 cm^{-1} greater than the *cis*-peak. It seems clear from this that what appears to be the *trans*-peak in the first overtone of *o*-bromophenol is really the superposition of two peaks, the actual *trans*-peak and a subsidiary peak. The area of the actual *trans*-peak is certainly smaller than the total apparent area and it will be noticed that its position, judging from the position of the subsidiary peak, lies to slightly lower wave numbers than the maximum of the composite peak.

In *o*-iodophenol a rather surprising state of affairs had appeared to exist. The apparent *trans*-peak, besides being large in area, lay quite a little below the normal phenol position; among other things this gave an anharmonicity that, when used in conjunction with second overtone measurement, deviated widely from the other values. Here again, however, these difficulties arise from an underlying subsidiary peak. The displacement of the *cis*-peak in the first overtone is about 215 cm^{-1}, while in the second overtone a subsidiary peak is found lying about 190 cm^{-1} above the *cis*-peak. Thus a subsidiary peak not only underlies the first overtone *trans*-peak but, judging from the position of the actual maximum, appears to be the larger part of the absorption in this position, and accounts at the same time for the large apparent displacement of this *trans*-peak, some 30 wave numbers to lower frequencies from the normal phenol position. It seems probable, therefore, that the three ortho-halogen derivatives show *trans*-peaks all of which lie at approximately the normal phenol position and whose areas decrease in the order *o*-chloro, *o*-bromo, and *o*-iodophenol. Thus it appears probable that these compounds do behave as would be expected, not alone with regard to the displacement of the *cis*-peak, but also with regard to the ratio of the numbers of molecules in the *trans*- and *cis*-forms. It would seem that this must be regarded as further strong support for Pauling's theory of these spectra.

In the case of *o*-chlorophenol a subsidiary peak is indicated in the second overtone region at about 250 cm^{-1} above the *cis*-peak. There should thus be a subsidiary peak at about 7150 cm^{-1} in the first overtone region of *o*-chlorophenol. It has already been pointed out[1] that such a peak was mentioned[2a] and it appears clearly on the plates of the present work. From the measurements in the second overtone region it seems probable that no strong subsidiary peak underlies the *trans*-peak of this substance in the first overtone, and that its apparent area approximates the true area of the *trans*-peak.

Interpretation of the Combination Frequencies

The relations existing in the above figures seem to leave little doubt that the numerous absorption maxima shown therein arise from frequencies which represent the combination of the OH valence vibration with other frequencies of the molecule. Such combination frequencies are possible because of the anharmonic character of the motions, and in molecules such as these, symmetry considerations limit but little the number of allowed combinations. A tangible connection between the OH valence vibration and the rest of the molecule may perhaps be visualized by recalling that, in speaking of the OH valence vibration itself, a mode of vibration of the entire molecule is meant, the amplitude of the motion being predominately in the OH group. However, in this motion other portions of the molecule move with very small amplitude, as for example, the carbon atom to which the OH group is attached. This atom is, of course, an intimate part of the main portion of the molecule and in particular of the six-carbon ring constituting the benzene nucleus. This six-carbon ring possesses modes of vibration, certain of which are characteristic of many of the derivatives of benzene and in the field of Raman spectra are sometimes called constant lines, since these frequencies do not change greatly throughout such compounds.

From the close similarity of the results for pentachlorophenol with those of the other compounds it seems clear that none of the important combination tones involves the CH groups, either in a valence (which frequency is much too high anyhow) or bending sense. This leaves the benzene nucleus with its heavy substituents and the OH group itself (bending motion) as the source of the frequencies with which the OH valence vibration may combine to give the combination frequencies. Even in phenol itself the possible vibrations of the molecule other than OH vibrations must evidently be looked upon as those of a substituted benzene, since the molecule is a benzene ring with a heavy substituent upon it, namely the OH group. It would not be surprising if motion in the C−O group, which is the link connecting the OH group to the rest of the molecule, were to play a part in the combination tones.

The figures indicate about a dozen frequencies with which the OH valence vibration is combining to give absorption maxima of appreciable intensity. They range from very low frequencies such as 200 cm^{-1} to as high as 1600 cm^{-1}, the highest involved in the 1200 cm^{-1} group. It will be noted that the intensities of the low frequency combinations and of the stronger members of the 1200 cm^{-1} group are comparable.

The lowest frequency in benzene is 405 cm^{-1} and the existence in the present compounds of frequencies as low as two hundred wave numbers is undoubtedly due to the circumstance that the OH vibration is combining here with frequencies involving the heavy substituent and in a bending motion. Phenol itself and, for example, monochlorobenzene show in their Raman spectra[7] frequencies as low as 200 cm^{-1}.

The 1200 cm^{-1} group, comprising five or six frequencies over the range 1000–1600 cm^{-1}, is a particularly characteristic feature of these compounds. As a contributor to this group one might look to the OH bending frequency whose value lies in this region. There seems, however, to be some evidence that this does not take part in these combinations with appreciable intensity. This frequency would probably maintain its identity fairly well, as does the OH valence frequency, and if present should be identifiable with one of the peaks. Now while the pattern of the group changes somewhat in passing from the ortho substituted compounds to the trisubstituted compounds, *within each of these two sets* of compounds the pattern is remarkably constant in spite of the change of halogen. Through these same two sets the OH valence vibration shows pronounced change in its position with change of halogen.[1,2] While it is not, apparently, a necessary conclusion that the OH bending frequency should also show such a change, it seems not unreasonable to expect that it would, and hence to accept the apparent absence of such an effect in the 1200 cm^{-1} group as some evidence that the OH bending motion is not contributing appreciably to the pattern of this group. In any case, since the

[7] Hibben, *The Raman Effect and Its Chemical Applications* (Reinhold, New York, 1939).

group is composed of five or six frequencies, the principal portion of it at least must be explained in terms of other frequencies of the molecule.

To explain the 1200 cm^{-1} group it is natural to look to frequencies of the benzene nucleus, and first, since there is reason for believing that the OH group of phenol is constrained to lie in the plane of the benzene ring,[5] to frequencies involving motion in the plane of the ring. In benzene there are several carbon vibrations of the order of 1200 cm^{-1}, namely, 993, 1010, 1485, and 1595 cm^{-1}, which are the frequencies $A_{1g}{}^{(C)}$, $B_{1u}{}^{(C)}$, $E_u{}^{-(C)}$, and $E_g{}^{+(C)}{}_2$, respectively,[8] the last two of which are degenerate. Each of these two last would presumably appear in the present compounds as two frequencies. In total these would represent six possible frequencies. Moreover, these are all motions in the plane of the ring. It seems probable that combination of the OH valence vibration with such ring frequencies gives rise to the 1200 cm^{-1} group and its characteristic pattern in these eight phenols.

At the same time, it would be reasonable to look for a correspondence between deep infra-red and Raman observations on the one hand and the present combination frequencies on the other. The infra-red measurements of Williams, Hofstadter, and Herman[9] on phenol vapor show that such correspondence does exist. There is a close resemblance between the frequencies observed by them up to 1590 cm^{-1} and the combination frequencies observed in the present work. (These authors have also suggested the identification of certain of the frequencies observed by them in the region 1000–1500 cm^{-1}, in terms of the frequencies of benzene.) It is true that in the present work comparison cannot as satisfactorily be made with phenol itself because, at the concentrations employed, phenol is considerably associated. This will lead to some distortion or broadening of the spectrum, as is illustrated by the absorption due to higher polymers just to lower frequencies of the valence absorption of the monomer.[1] The 1200 cm^{-1} group, however, seems characteristic of all of these compounds. The resemblance between the results of Williams, Hofstadter, and Herman and the present work is clear from Table I. The present absorption maxima, observed in solution, would of course be expected to be broader than those observed in the vapor phase.

Similarly the Raman data show a correspondence with the frequencies observed in the present work involved in combination frequencies. So far as the authors are aware, there are Raman data only for *o*-chlorophenol, *o*-bromophenol, and phenol itself, of the compounds studied in the present work. But there is an additional compound for which the Raman data are of interest here, and this is *o*-fluorochlorobenzene. The OH group is both halogen-like and of nearly the same mass as the fluorine atom, and since we are interested in all the frequencies of *o*-chlorophenol exclusive of those within the OH group, *o*-fluorochlorobenzene should be of much help. Actually there is very marked similarity in the Raman data for these compounds,[10] and up to 1600 cm^{-1}, the Raman lines for *o*-fluorochlorobenzene are nearly the same as those for *o*-chloro- and *o*-bromophenol. As is clear from the table, essentially all the frequencies observed in the combination frequencies in the present work are found in the Raman lines of

TABLE I.

Raman			Infra-Red	Combination Frequencies							
o-Fluorochloro benzene	*o*-Chlorophenol	*o*-Bromophenol	Phenol vapor	Phenol	*o*-Chlorophenol	*o*-Bromophenol	*o*-Iodophenol	Trichlorophenol	Tribromophenol	Tri-iodophenol	Pentachlorophenol
375	378	296		325	410	425	400	410			420
498	498	474			490	485	475	575			695
530	539										
552	561	550									
680	678	650			685	630	660		740	715	
748	750	743	800		785	800	770	775	805	790	810
824	833	825	876								
	1000	933									
1026	1030	1023	1010								
1069		1065	1057		1050	1045					1050
1125	1124	1114		1075	1125	1120	1110	1125	1130	1125	1135
1150	1154	1153	1177	1160	1180	1200	1190	1160	1165	1165	1185
1234	1246	1247	1250					1225	1240		
1264	1290	1289									
	1337	1328	1329	1330	1320	1335	1325	1315	1315	1310	1270
1485	1456		1487	1475	1465	1480	1460	1395	1385	1390	1380
1589	1588	1584	1590		1590	1605	1580	1580	1565	1550	1550

[8] See for example, Wilson, Phys. Rev. **45**, 706 (1934); Ingold *et al.*, J. Chem. Soc. (London), 976 (1936); and Langseth and Lord, Kgl. Danske Vidsk. Selsk. math.-fys. Medd. **16**, No. 6 (1938).

[9] Williams, Hofstadter and Herman, J. Chem. Phys. **7**, 802 (1939).

[10] Kohlrausch and Pongratz, Sitzber. Akad. Wiss. Wien, Abt. IIb, **143**, 551 (1935); Kohlrausch and Ypsilanti, *ibid.* **144**, 417 (1935).

these substances. The low frequencies involved in the combination tones lying just above the first and second overtone absorption and comprising what has been called in this and the preceding article "subsidiary peaks," probably arise from carbon-halogen bending motions.

The absorption in the 9500 cm^{-1} region, shown for four of the present compounds in Figs. 2 and 4, undoubtedly represents the combination of the OH valence vibration with two units of vibrational energy in the same frequencies of the body of the molecule which led to the 1200 cm^{-1} group. Though measured less accurately because of their weakness, several of the peaks in the 9500 cm^{-1} region have positions which indicate the same pattern as that in the 1200 cm^{-1} group. This is shown in Figs. 2 and 4, in which the upper portions are simply the corresponding 1200 cm^{-1} groups redrawn on a twofold greater abscissa scale. Furthermore the mean intensity of the 2400 cm^{-1} group is an order of magnitude less than that of the 1200 cm^{-1}, a circumstance to be expected if the present interpretation is correct. The relative intensities among the several peaks are not, however, the same in the two groups, which again might reasonably be expected on this interpretation. Evidence has been presented in Fig. 4 that the absorption in pentachlorophenol in the 6000 cm^{-1} region involves the same frequencies with the fundamental OH absorption as does the weak group in the 9500 cm^{-1} region in combination with the first overtone OH absorption. This identification of the pentachlorophenol absorption in the 6000 cm^{-1} region is, of course, no further evidence for the interpretation proposed here of the 2400 cm^{-1} group, except in that the pattern of the group again resembles closely that of the 1200 cm^{-1} group, as shown in the upper portion of the figure.

Concerning motion in the C−O group, the frequency of the valence vibration of this linkage is generally taken from Raman work[7] to be about 1030 cm^{-1}. That this should be involved in such combination frequencies seems probable since it is the link coupling the OH group with the body of the molecule, vibrations of which appear in the combination tones. It may be, however, that, in the present compounds, the amplitude of motion in the C−O group is considerable in two or three different characteristic vibrations of the body of the molecule and that the C−O vibration is distributed among these two or three modes of motion. It would, however, contribute one more frequency to the total number of frequencies in this range characteristic of the heavy atoms in the phenols. In addition to the six mentioned above as derivable from the benzene nucleus and lying in the range 1000–1600 cm^{-1}, this would add a seventh frequency in this region that might appear in the combination tones. From Table I it seems that seven frequencies may characterize the combination tones in this group somewhat better than do six.

Since in all but one of the compounds studied in the present work the molecule contained CH as well as OH, it would be natural to inquire to what extent combination tones built upon the CH valence vibration were also playing a part in the present spectra. The CH valence vibrations show clearly, of course, in their respective positions in these compounds. The results for pentachlorophenol indicated not only that the combination frequencies built upon the OH valence vibration did not involve the CH groups, but also that none of the prominent combination frequencies shown in the figures was built upon the CH valence vibration. This does not mean, however, that combination frequencies built upon the CH vibration do not exist in the other seven compounds, which contain CH, in other portions of the spectrum, or even, if they are weak, in the same portions of the spectrum as covered by the present figures.

The spectra of hydrocarbons, and in particular benzene, show absorption[11] in the region 6800–7400 cm^{-1}. It seems probable that this represents combination frequencies involving characteristic vibrations of the six-carbon ring similar to those observed in the phenols in the present work. Rumpf and Mecke[3] have recently found such combination frequencies in aromatic CH-containing compounds above the overtones of CH absorption in the photographic infra-red. Identification of such combination frequencies built upon the CH vibration is somewhat more difficult than those of the OH vibration because

[11] Liddel and Kasper, Bur. Stand. J. Research **11**, 599 (1933).

(as pointed out by Rumpf and Mecke) the CH valence absorption of benzene and its derivatives is not single,[12] while in the OH absorption of phenol and its derivatives it is. This would presumably lead to complexity in the pattern of the combination tones, and this seems indeed to characterize the above-mentioned absorption of benzene in the 6800–7400 cm^{-1} region. However, the first overtone CH absorptions show one peak stronger than the others which, in carbon tetrachloride solution, lies at about 5970 cm^{-1}. The above-mentioned group of frequencies in benzene, nearly two orders of magnitude weaker in the 6800–7400 cm^{-1} region, show two prominent peaks which lie to higher frequencies of the valence absorption by about 1010 cm^{-1} and 1190 cm^{-1}, respectively. These may be two of the frequencies characteristic of the carbon ring, as those in the 1200 cm^{-1} group of the present compounds. The rather complicated pattern of the benzene absorption in the 6800–7200 cm^{-1} region is probably explainable as due to approximately the same six frequencies of the body of the molecule as are represented in the 1200 cm^{-1} group in the present compounds, built upon the two- or three-peaked first overtone CH absorption. Absorption similar to that in the 7000 cm^{-1} region in benzene can be seen also on the plates of the monohalogen benzenes mentioned in the preceding article.

It is clear that weak absorption in the vicinity of the first overtone of the OH group measured at concentrations where the OH combination frequencies are strong (and where the valence absorption is complete at its center), may involve CH absorption;[2a] namely, the CH combination frequencies just discussed. It is with reserve, therefore, that we wish to suggest an interpretation of a weaker peak that appears in at least the three trisubstituted compounds of the present work, which lies closer to the first overtone than does the "first subsidiary peak" of the preceding article. In tri-iodophenol this peak is so close in, that it appears as a wing on the high frequency side of the main first overtone peak, the displacement from the center of the main peak being about 80 cm^{-1}. In this instance a similar wing is visible at a corresponding position on the low frequency side of the main peak, it being of somewhat lower intensity than the high frequency wing. This evidently suggests that the two wings may represent sum and difference tones.

In tribromophenol the separation of this weaker peak from the main first overtone peak is greater, and it can be seen distinct from the latter. The separation is roughly 120 cm^{-1}. In trichlorophenol this separation is considerably greater still, being roughly 210 cm^{-1}. The values obtained suffice for the present purposes in that they show that this frequency in the three compounds is very low, and that it is strongly halogen dependent, provided, of course, that the identification of these three peaks as correponding peaks is correct.

The separation of this peak in these three compounds from the main first overtone peak is surprisingly small, especially in the tri-iodophenol, even for a bending frequency involving atoms such as these. Such absorption would answer the description of that to be expected from the librational motion of the OH group about the C–O bond perpendicular to the plane of the molecule, which was discussed in an earlier paper[13] in connection with the theory of the shape and breadth of single absorption peaks such as those of the present work. It seems possible that this absorption, observed in the first overtone of the three trihalogen compounds, may arise from such librational motion. It would, however, be difficult to distinguish it in the present results from any other low frequency vibration, except insofar as the particularly low absolute value of the frequency argues for it. The displacement with change of halogen is probably significant, for not only is it even greater fractionally than the change in the ortho (*cis-trans*) effect itself, but it is in the reverse sense, being greatest for the chloro and least for the iodo compound. Interpreted in terms of the librational motion, this would indicate weakening of the restoring force involved in the motion perpendicular to the plane of the molecule with increasing attractive force between the hydrogen of the OH group and the halogen atom, and with the accompanying increase of the O–H distance.

[12] Fox and Martin, Proc. Roy. Soc. London **A167**, 257 (1938).

[13] Wulf and Deming, J. Chem. Phys. **6**, 702 (1938).

The positions of this peak explain a circumstance noted throughout the first and second overtone measurements of these compounds, that the first and second overtone peaks are considerably broader in the iodophenols than in the bromo and chloro compounds. In the former the position of this peak is so close to the main first and second overtone peak that it underlies it, leading, in conjunction with the difference tone, to a peak considerably broader than the principal central member alone. In the bromo and chloro compounds the position of this weak peak is sufficiently distant from the principal peak that it does not underlie it and hence the latter is observable alone.

The greater breadth manifested by the iodo peak in the first and second overtone also seems to be present in the combination tones, as may be seen by reference to Fig. 1. If this arises from the same cause, this is evidence in support of the suggestion that these particular peaks lying close in to the main peak of the first and second overtone absorption are, indeed, the librational motion of the OH group, since they represent frequencies superimposed on the OH absorption no matter where it appears, that is to say, not only in the pure valence absorptions, but also when these appear in combination with another frequency such as a member of the group of ring frequencies discussed above. This, of course, is what would be expected of such librational motion, since it is a characteristic of the vibrational motion of the OH group, whether it appears alone or in combination with other frequencies.

Concerning the general subject of combination tones involving very low frequencies and observed in solution, mention should be made of the possibility that such low frequencies may arise from an interaction of solute and solvent molecules.[14] In the present instance a compound molecule might be thought of wherein a phenol molecule and a CCl_4 molecule were weakly bound, for example, electrostatically through the action of the electric moment in the OH group. In such a case combination frequencies involving the OH vibration and a low frequency of the solvent environment might result. Evidence that the very low frequency peak, discussed above in terms of the out-of-the-plane motion of the OH group, does not arise from a frequency of such a loosely bound solute-solvent complex, lies in the marked halogen dependence which this peak exhibits. This change with change of halogen substituent is reasonable if the low frequency is in the phenol molecule adjacent to the halogen substituent (a condition which would be met by the out-of-the-plane motion of the OH group), but it would be less expected if the low frequency were in the solvent environment.

The authors wish to make grateful acknowledgment to Urner Liddel, Sterling B. Hendricks, and G. E. Hilbert, who through their participation in earlier infra-red work in this laboratory have contributed much to the present results. The authors also wish to thank Professor E. Teller for very helpful discussion.

[14] See for example the work of West and Edwards, J. Phys. Chem. **5**, 14 (1937) on the absorption of HCl in CCl_4 solution.

Summary

Absorption maxima occurring in the near infra-red spectra of a number of the halogen derivatives of phenol have been measured and interpreted as combination frequencies in which the valence vibration of the OH group combines with frequencies of the body of the molecule. These have been observed principally in the region above the first overtone OH valence absorption, but combination tones involving some of the same frequencies have also been observed above the second overtone and above the fundamental OH absorption. The existence of these combination frequencies makes it possible to observe a number of the low frequency vibrations of such molecules in a relatively accessible region of the infra-red.

The positions of certain of these combination frequencies are such that they underlie some of the *trans*-peaks of the orthohalogen phenols in the first and second overtone regions. The apparent areas of these *trans*-peaks have until now appeared to be somewhat anomalous. When proper allowance for the areas of these combination frequency peaks is made in estimating the areas of the *trans*-peaks, it appears that the ratio of the *trans*-area to *cis*-area throughout these compounds decreases with increasing displacement of the *cis*-peak, both in the first and second overtone region, in accord with the simplest expectation from the theory of the origin of the *cis*- and *trans*-peaks.

A pronounced group of five or six frequencies, in the region 1000–1600 cm^{-1} above the first overtone OH absorption, occurs weakly again at higher frequencies in the form of a combination of the first overtone OH absorption with two units of vibrational energy in the frequencies of the body of the molecule which are involved in this group. In the spectral region of 6000 cm^{-1}, which is the corresponding region above the position of the fundamental OH absorption, there is strong CH absorption (valence

first overtone) in compounds containing the CH group. But in pentachlorophenol, which is free of CH absorption, the same combining frequencies were observed in this region of the spectrum, indicating that the absorption in the region of the first overtone of CH in phenol and its halogen derivatives is in part also OH absorption.

The frequency differences between the observed combination frequencies and the OH valence absorption upon which they depend, that is, the frequencies characteristic of the body of the molecule, have been compared with existing deep infra-red and Raman results. A close correspondence exists between these. The higher members of these frequencies that enter into the combinations appear to be principally vibrations of the six-carbon ring in which the motion lies in the plane of the ring. The very low frequencies entering into the combinations are probably carbon-halogen bending vibrations.

A discussion is included of combination frequencies built upon the CH valence vibration. In the halogen-substituted phenols these are weak compared to those built on the OH valence vibration in the region studied. A weak peak lying very close to the first overtone OH absorption in trichloro, tribromo, and triodophenols is interpreted as due to out-of-the-plane motion of the OH group about the C—O bond, and some experimental evidence is adduced in support of this interpretation.

OCTOBER, 1940 JOURNAL OF CHEMICAL PHYSICS VOLUME 8

The Ultraviolet Absorption of NO_2*

LOUIS HARRIS, G. W. KING, W. S. BENEDICT† AND R. W. B. PEARSE‡
Massachusetts Institute of Technology, Cambridge, Massachusetts

(Received July 5, 1940)

A system of eight discrete and several diffuse bands in the ultraviolet absorption spectrum of NO_2 has been analyzed. From the positions of the bands and their temperature coefficient of absorption the upper state intervals have been determined as 523 and 714 cm^{-1}, those of the lower state as 749 and 1319 cm^{-1}. The latter are not the same as the fundamentals deduced from infra-red data. Different possibilities of reconciling these intervals are discussed.

THE nitrogen dioxide molecule, NO_2, is of great importance in the quantum theory of molecular structure, being unique among the stable triatomic molecules in having an odd electron. Quantitative information about molecular orbitals would be considerably increased by determination of the structure and energy levels of NO_2 from its spectrum. However, probably because of the odd electron that supplies the interest, the spectrum is exceedingly complicated.

In the ultraviolet, however, there are bands with relatively simple structure, which, incidentally, represent one of the few band systems of an asymmetric rotator with apparent regularities. The gross structure has been identified as a Q branch but the detailed structure has not yet been properly analyzed.

EXPERIMENTAL PROCEDURE

To further the investigation of the vibrational and rotational analysis, we have obtained spectra under a variety of conditions of temperature and pressure of NO_2. Spectra were taken with Hilger E315 and E1 prism instruments, the M.I.T. 21-foot (first- and second-order) and 35-foot gratings. The quartz absorption tubes varied in length from 2 mm to $2\frac{1}{2}$ meters. The $2\frac{1}{2}$-meter quartz tube was 7 cm diameter at one end and 3 cm at the other end. This conical structure provided the tube with an aperture equal to that of the 21-foot grating. By suitable mirrors light was passed twice through this tube giving an effective absorption path of 5 meters.

This long path was primarily designed for investigations in the photographic infra-red (which results will be presented at another time) but also in the study of the ultraviolet region, to permit the use of very low pressures in the hope of sharpening the rotational structure. Although these very low pressure spectra were only ob-

* Contribution No. 455 from the Research Laboratory of Physical Chemistry, Massachusetts Institute of Technology.

† Present address: General Chemical Company, Long Island City, Long Island.
‡ Present address: Astrophysics Department, Imperial College of Science and Technology, London.

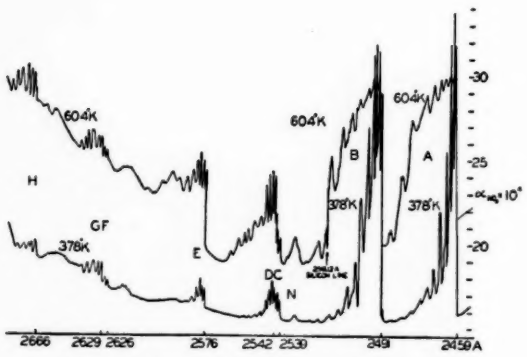

FIG. I-1. Absorption coefficient of NO_2 in the ultraviolet (E1). Ordinates are $\alpha_{NO_2} \times 10^4$.

tained on the prism spectrograph, the rotational lines remained less sharp than the atomic spectra photographed simultaneously. We concluded that the natural width of the lines limits the resolution of the rotational structure of the ultraviolet system.

LOADING OF APPARATUS WITH NO_2

In all experiments the NO_2 used was prepared and purified very carefully. NO_2 was generated by heating $Pb(NO_3)_2$ or by desiccation of fuming HNO_3 with concentrated phosphoric acid. Oxygen was then bubbled through the liquid $NO_2-N_2O_4$, dried with P_2O_5. The nitrogen dioxide was then frozen with liquid air and pumped; allowed to warm to $-78°C$ when it was pumped again. The resulting NO_2, free of O_2, N_2, and NO was sublimed into the side arm of the absorption cells. This procedure produced a clear white solid on freezing to liquid-air temperatures and permitted rapid movement of NO_2 from side arm to cell and vice versa. After the gas was kept at high temperatures for several hours it was found necessary to allow the tube to cool before freezing out the NO_2; otherwise the decomposition product NO formed a blue solid (N_2O_3), and the permanent gas produced, O_2, prevented rapid condensation in the side arm. A technique which avoided contact of NO_2 with grease, mercury, or other substances known to react with NO_2, was used throughout.

CONDITIONS OF EXPERIMENTS

The tubes were surrounded by well lagged furnaces permitting temperature regulation to within 5°C through the length of the quartz tube.

The total pressure in the absorption cells was controlled by the vapor pressure of $NO_2-N_2O_4$ condensed as solid or liquid in a side arm, whose temperature was kept constant to 0.1°C by various eutectic mixtures. The absolute values of the vapor pressures were determined separately in this laboratory and agree in general with those of Giauque and Kemp.[1]

Quantitative intensity measurements were made with the prism spectrograph (E1) using

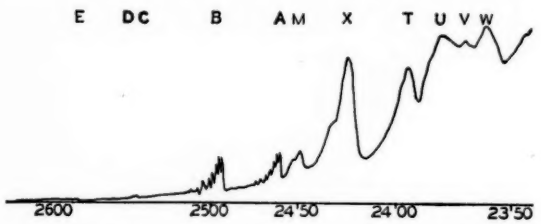

FIG. I-2. Microphotometer trace of NO_2. Absorption between 2300A and 2600A (E2).

calibrated screens. Long exposures were necessary to bring out the weak bands (at wavelengths greater than 2580A) at high temperatures due to the strong background absorption from 2400 to 2800A. The blackening of the photographic plate was corrected for deviation from the reciprocity law.

TREATMENT OF DATA

The resulting light transmissions are related to the absorption coefficients by the use of Beer's law,

$$\text{Log } I/I_0 = -\Sigma\beta_i(\lambda)x_i p_0 l = -\alpha p_0 l = -\alpha p l \frac{273.1}{T},$$

where l is the path length, p is the total pressure, p_0 this pressure reduced to 273.1°C and x_i are the mole fractions of the various components which have specific absorption coefficients β_i.

In the experiments with a one-meter tube the partial pressures of NO_2 were determined from the total pressures by the use of Bodenstein's equilibrium data.[2] The $2\frac{1}{2}$- and 5-meter path lengths permitted pressures low enough for the absorption due to N_2O_4 to be negligible.

[1] W. F. Giauque and J. D. Kemp, J. Chem. Phys. **6**, 40 (1938).
[2] M. Bodenstein, Zeits. f. physik. Chemie **100**, 68 (1922).

The results from many spectrograms are summarized in Fig. 1 in which α is plotted against wave-lengths. It is seen that there is a background absorption throughout the ultraviolet with a considerable temperature coefficient. The discrete absorption stands out above the background absorption. We found it quite easy to separate the discrete from the continuous absorption. The former, attributed to single NO_2 molecules is defined as β, the absorption above the background. It is this quantity, β, which is used in the analysis of the vibrational and rotational structure.

A microphotometer trace of the absorption between 2350A and 2600A as obtained with a Hilger E2 spectrograph is shown in Fig. 2. Tracings of the 2491A band have been published by Henri.[3] (E1).

The most characteristic feature of this band system is the comparative wide spacing of "lines" in each "sharp" band. Under higher resolution these lines turn out to be heads of what we shall henceforth call subbands. (Even a medium-sized Hilger instrument is adequate to give partial resolution of the subbands.)

Our photographs have extended this band system to include several new bands having the same rotational structure as the others, as well as many new diffuse bands. In addition, the band at 2540A has been found to consist of two bands

[3] V. Henri, *The Structure of Molecules* (Ed. P. Debye, 1932), p. 132.

TABLE I. *Ultraviolet bands of* NO_2.

Band designation	Wave-length	Origin	Intensity	$\beta_{MAX}\times10^4$	Appearance of Band
(10 bands)	(2,050 to 2,353A)		*s*		diffuse and broad*
W	2,353 A	42,490 cm^{-1}	*sss*		diffuse; sharp head, band degraded to red
V	2,364	(42,280)	*m*		diffuse; band head not well defined
U	2,373	(42,120)	*m*		diffuse; broad
T	2,392	41,790	*s*		diffuse; sharp head, band degraded to red
X	2,421	41,285	*ss*		diffuse; sharp head, band degraded to red
Y	2,430	(41,136)	*w*		diffuse; sharp head, band degraded to red
M	2,447	40,844	*w*		diffuse; sharp head, band degraded to red
A	2,459	40,658	*m*	18.2	slightly diffuse
B	2,491	40,130.0	*m*	16.5	sharp
N	2,529	39,524	*w*		diffuse; sharp head, band degraded to red
C	2,539	39,381	*w*	1.7	sharp
D	2,542	(39,335)	*w*	2.3	slightly diffuse
E	2,576	38,811	*w*	1.7	sharp
F	2,626	38,070	*ww*	.9	sharp
G	2,629	(38,032)	*ww*	.7	slightly diffuse
H	2,666	37,504	*ww*	.9	sharp

* The positions of these bands have been given by Lambrey, Ann. d. Physik 14, 95 (1930).

TABLE II. *Wave numbers of subband heads.*

Band	*A* 2459A		*B* 2491A		*C* 2539A		*D* 2542A		*E* 2576A		*F* 2626A		*G* 2629A		*H* 2666A	
Sub-band	cm^{-1}	Δ cm^{-1}	cm^{-1}	Δ cm^{-1}	cm^{-1}	Δ cm^{-1}	cm^{-1}	Δ cm^{-1}	cm^{-1}	Δ cm^{-1}	cm^{-1}	Δ cm^{-1}	cm^{-1}	Δ cm^{-1}	cm^{-1}	Δ cm^{-1}
$K=0$	40,653		40,130.0		39,381		(39,335)		38,811		38,070		38,032		(37,504)	
		3		4.0		4		(12)		4		4		16		(4)
1	40,650		40,126.0		39,377				38,807		38,066				37,500	
		13		11.6		13				12		13				11
2	40,637		40,114.4		39,364		39,323		38,795		38,053		38,016		37,489	
		18		18.7		20		22		18						19
3	40,619		40,095.7		39,344		39,301		38,777						37,470	
		27		26.7				25		28						25
4	40,592		40,069.0				39,276		38,749						37,445	
		35		34.1				37		35						39
5	40,557		40,034.9				39,239		38,714						37,406	
		41		40.2				40		44						
6	40,516		39,994.7				39,199		38,670							
		48		49.3						54						
7	40,468		39,945.4						38,616							
		54		54.5												
8	40,414		39,890.9													

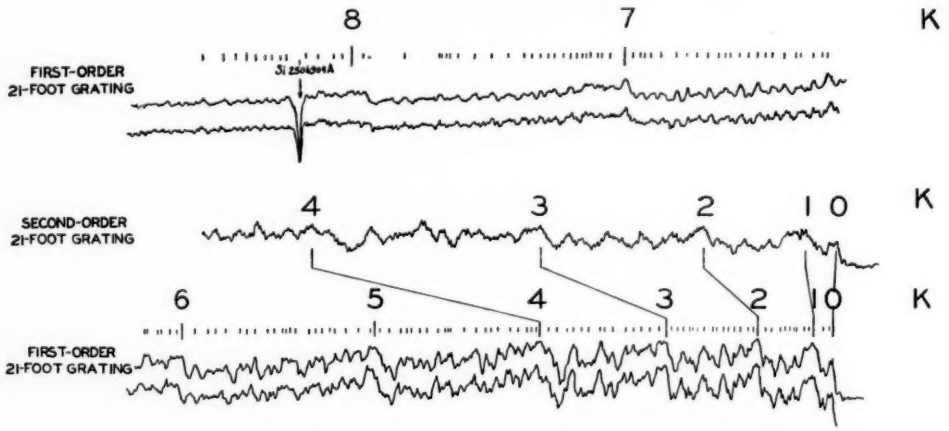

FIG. I-3. Microphotometer traces of NO_2. Absorption near 2500A (band *B*) (Grating). The subbands are indicated by values of *K*. The distances of the absorption peaks shown from the band origin are given in Table III. The two first-order curves are from entirely different plates.

each with rotational structure similar to the structure of the bands at 2459, 2491, and 2576A. The band origins and other pertinent data are presented in Tables I and II. All the bands listed above 2350A have sharp heads near the position of maximum absorption and are degraded to the red, except the diffuse bands of medium or weak intensity which do not have sharp heads (but are not symmetrical).

Microphotometer tracings of the grating spectrograms for the 2491A band are shown in Fig. 3. Although the grating spectrograms show sharp lines in the subbands the microphotometer tracings reveal a very complex and erratic structure to these lines. The tracings obtained from different plates show identical contours showing that the complex structure is real and not due to plate grain.

Wave numbers corresponding to the peaks are given in Table III. The wave numbers reported are smoothed values obtained from several first- and one second-order plate.

Although more lines are reported than previously for the same spectral region, we are of the opinion that the lines are not completely resolved and that the natural line width precludes the resolution.

In the succeeding paper we describe how, on account of the regular spacing of the subbands, even this unresolved structure can be made to yield approximate values of the spectroscopic constants of NO_2, and, equally important, the positions of the origins of these bands. The origins are essentially at the head of the first subband. This permits us to enter into a vibrational analysis with some definite wave number intervals.

VIBRATIONAL ANALYSIS

The rotational analysis has determined the origins of the discrete bands of this system (to about 2 cm^{-1}) and indicates to 20 cm^{-1}, the origins of the diffuse bands. Thus intervals can be determined with the corresponding certainty. All the discrete bands have essentially the same rotational constants, indicating they belong to the same system.

The absorption coefficients of the bands of this system were determined with tolerable accuracy and were of value in the analysis inasmuch as several pairs of bands had exactly the same coefficients. The temperature variation of the absorption of these bands determined approximately the initial or lower energy levels.

This system is composed of sharp, slightly diffuse and very diffuse bands presumably due to predissociation. This phenomenon was very useful in locating the relative positions of the upper state levels.

Finally, considerable assistance was afforded by the selection rule for an electronic dipole transition; namely, that the initial and final states must have the same symmetry. The possible symmetry classes for nonlinear triatomic

molecules have been given by Mulliken,[4] *viz.*, A_1, A_2, B_1, B_2, the first being the totally symmetric representation. The rotational structure in all the bands of the same symmetry will be the same and determined by the direction of the electric moment produced by the displacement of electrons, relative to the principal axes of the molecule as a rotator.

It is possible to have transitions between two electronic states as a result of quadripole and not dipole radiation, e.g., $A_1 \rightleftarrows A_2$. For such transitions (which will be weaker than the dipole transitions) the rotational structure of the bands is determined by the motion of the nuclei in the initial and final states, i.e., by the infra-red selection rules. This may account for the comparative low intensity of absorption of this system but it does not solve other difficulties encountered below.

(a) Discrete bands

The strongest of the discrete and semidiscrete bands, B and A, have almost exactly the same absorption coefficient, temperature coefficient of absorption and rotational constants. Therefore, we believe that these bands have a common lower level ($A''=B''$) and that their upper levels are 523 cm^{-1} apart. This interpretation is substantiated by the relative diffuseness of A, indicating that its upper level is near predissociation.

Bands A and B have negative temperature coefficients of absorption at their heads (near the band origins) even without correcting for the background absorption. Thus the lower level of A and B is either the ground state or very close to it (see below); at any rate, it certainly is the lowest of the levels occurring in the discrete bands.

Towards the red, 1319 cm^{-1} from A and 1319 cm^{-1} from B there are two more bands D and E, likewise of the same intensity (although weaker than A and B), and each with the same temperature coefficient of absorption[5] and rotational constants. The interval $D-E$ is 524 cm^{-1}, the same as the interval $A-B$. The band E is just as sharp as band B, and E's shorter wave-length partner, D, is more diffuse than E, just as A is more diffuse than B. Thus we conclude that these two bands, D and E, have the same upper levels as A and B ($D'=A'$; $E'=B'$) and have a common lower state ($D''=E''$) which is 1319 cm^{-1} above the lower levels of A and B ($A''=B''$). The temperature coefficient of absorption for bands D and E corresponds to an excitation of about 1300 cm^{-1}.

A strong confirmation of this analysis is that still further to the red we encounter another pair of bands, G and H, with the same characteristics. The band nearer the red is very sharp, the other band slightly diffuse, but otherwise they are alike in having the same absorption coefficient (weaker than D and E), the same temperature dependence (now corresponding to an excitation of about 2600 cm^{-1}) and the same rotational constants.

The interval $G-H$ was not measured with as great an accuracy as intervals $A-B$, $D-E$, but is of nearly the same magnitude, 528 cm^{-1}. This pair, then, seems to be the result of transitions to the same upper states as $B'=E'$, sharp, and $A'=D'$, semidiffuse, from a common lower state

TABLE III. *Wave numbers of peaks on microphotometer curves of grating spectra of 2491A band.*

K	cm^{-1} from band origin	K	cm^{-1} from band origin	K	cm^{-1} from band origin	K	cm^{-1} from band origin	K	cm^{-1} from band origin	K	cm^{-1} from band origin
(0)	.0	(3)	34.71	(5)	95.53	(6)	136.23	(7)	185.15	(8)	240.03
	.72		36.12		96.50		137.19		188.11		242.41
	1.91		38.23		99.31		138.42		190.31		244.84
			39.63		101.58		140.34		190.75		247.82
(1)	3.97		41.50		103.96		141.25		192.36		250.75
	4.64		42.88		104.91		143.42		193.42		
	5.66		45.69		106.66		143.88		194.20	(Si)	252.04
	7.10		47.40		107.83		144.68		195.51		(2506.904A)
	7.84		48.30		109.30		146.86		196.34		
	8.87		50.34		112.09		149.31		197.78		254.39
	10.11		52.03		113.29		150.00		199.72		255.68
	10.79		54.04		114.35		152.43		201.05		258.23
	12.79		55.29		114.88		154.71		202.79		259.21
	13.90		57.46		116.52		156.55		204.31		261.05
			59.19		118.09		157.96		206.07		263.04
(2)	15.75				120.54		159.95		208.93		264.82
	16.45	(4)	61.00		122.41		161.55		212.60		268.09
	17.51		61.53		123.81		163.49		216.16		272.18
	19.34		62.45		126.77		164.41		219.48		
	20.00		63.69		128.71		165.77		221.77		
	21.64		65.53		130.44		167.71		222.44		
	22.70		67.20		133.28		170.28		223.37		
	24.09		69.60				172.41		223.56		
	25.04		71.17				174.64		230.61		
	26.81		72.20				177.68		237.55		
	28.08		74.50				179.80				
	29.09		76.99				181.27				
	29.73		79.48				182.34				
	31.18		80.05				183.57				
	32.69		80.85								
	33.61		82.21								
			84.65								
			86.20								
			87.78								
			88.71								
			89.97								
			92.47								
			94.64								

[4] R. S. Mulliken, Phys. Rev. **52**, 275 (1933).

[5] Overlapping of band C may confuse temperature coefficient of D.

TABLE IV. *Vibrational analysis from ultraviolet spectrum.*

Bands to level B' (sharp)

π'' / δ''	0	1	2
0	B	E	H
1	G	F	too weak

Bands to level A' (slightly predissociated)

π'' / δ''	0	1	2
0	A	D	G
1		missing ——	

2624 cm^{-1} above $B''=A''$, and 1305 cm^{-1} above $D''=E''$.

The system, A, B, D, E, G, H, forms a self-consistent scheme of energy levels as shown in Table IV. The origin of the system seems to be at 40,130.0 cm^{-1} but later discussion casts some doubt upon this. The intervals between the vibrational levels in the lower electronic state are 1319 cm^{-1} and 2624 cm^{-1}, and one interval between vibrational levels in the upper electronic state is 523 cm^{-1}, which is in the neighborhood of the predissociation region.

The interval 1319 cm^{-1} occurs again between the completely diffuse bands M and N. The band M does not have a positive temperature coefficient and N behaves like D and E, i.e., as if it corresponded to an excitation of about 1300 cm^{-1} above the ground state. The bands M and N therefore verify 1319 cm^{-1} as an interval in the lower electronic state and determine a new upper level: $M'=N'$, 714 cm^{-1} above B'.

It is easy to prove the frequency 1319 cm^{-1} is a symmetrical frequency A_1, because we have several pairs of bands with a common upper level and lower levels differing by 1319 cm^{-1}. Alternate bands would be missing if the 1319 cm^{-1} frequency were of a σ type vibration, according to the electronic-transition selection rule.

There remain two other discrete sharp bands, C and F, whose connection with the above set is not easy to make. Before discussing them we shall first investigate the completely diffuse bands toward shorter wave-lengths.

(b) Diffuse bands

Bands M and N lead us toward the further ultraviolet where there are more diffuse bands, stronger than the discrete bands, and of which some have sharp heads and are degraded to the red, properties characteristic of the discrete bands. If M and N belong to the same system they should be due to transitions to higher levels in the upper electronic state, and so one would expect to find a recurrence of the 523 cm^{-1} and 714 cm^{-1} frequencies as harmonics if they are fundamentals, or of combinations of these numbers if they are merely differences.[6]

The strongest of the diffuse bands are X and W, 1192 and 2397 (=1192+1205) cm^{-1}, respectively, from B. All the bands (out to 44,000 cm^{-1} where the character of the band structure changes, indicating the appearance of another system) can be accounted for with 710 and 523 cm^{-1} as upper state fundamentals, the strongest progression being B, X, W at intervals of $1200=710+523$ cm^{-1} (see Table V).

No values for the intervals of the lower state are obtained from the analysis of the diffuse bands (other than $M-N$), nor is there any indication whether B is the (000) level or a slightly excited level.

(c) Bands *C* and *F*

The absorption in the neighborhood of D is different in appearance from that at A, B, E, H. This we interpret as due to overlapping by another band C, for the following reasons:

(1) The spacings of the first three peaks (of the band which we call C) are practically the same as the first three peaks of A, B, E, H.

TABLE V. *Vibrational analysis of diffuse bands.*

710 / 523	0	1	2	3
0	B	M		
1	A	X	U	
2	Y	T	W	
3	—	V		
4	—			

(2) The subband heads of C are much sharper than those in the part we call D, and the subbands of D are more confused than those of A, B, E, and H, due to the supposed tail of C.

[6] Symmetry laws tell us that only vibrational levels of the type A_1 can occur in transitions from the ground state; i.e., the π and δ fundamentals and all their overtones, and even overtones of σ. The latter, however, according to the Herzberg-Teller rule will be relatively weak. Thus we must try to account for all the strong bands with but two fundamental frequencies in the upper state.

(3) C has a distinctly smaller temperature coefficient of absorption than have the peaks of D. In A, B, E, H the temperature coefficient varies smoothly throughout the band.

(4) We cannot account for the appearance of a *single band* of the appearance of $C-D$ on the basis of our rotational analysis.

Similarly, the absorption at G is more complicated than at A, B, E, H. The structure at G, which resembles that at D, is due to the overlapping of another band F. This conclusion is arrived at on the basis of the same observations as noted for the band C. In addition, if it is assumed that F, G and C, D are single bands with a rotational structure different from other bands, and that their intervals from H and E, respectively, are the same as the interval $B-A$, one would then have to explain why A has the simpler structure. Moreover, the interval between $F-C$ is 1311 cm^{-1}, not 1319 cm^{-1} nor 1305 cm^{-1}, intervals found between $B-E$, $A-D$ and $E-H$ and $D-G$, respectively.[7]

The fact that this interval is different from the other two intervals shows that the lower level of C is not the same as $A''=B''$ (the lowest level). Therefore we expect C to start from another elevated state and F to start from that level combined with the 1319 cm^{-1}.

This affords another proof that 1319 cm^{-1} is of symmetry type A_1 for whatever the symmetry of C'', $C'=F'$ have the same symmetry, and therefore F'' has the same. Thus the symmetry is not changed in passing from C'' to F'' which differ by the frequency $\sim$1319 cm^{-1}.

The temperature coefficient of absorption of band C corresponds to that of a band arising from a level about 700 cm^{-1} above the ground level, and certainly less than 1319 cm^{-1} above the ground level. The temperature coefficient of F, being about the same as G, indicates also that $C''<1319$ cm^{-1} above $A''=B''$. The sharpness of both C and F indicates that their common upper state is below A'. Taken together, these facts require that the lower level of C is $0<C''<1319$ cm^{-1}. Since C is 749 cm^{-1} from B (which, having a negative temperature coefficient, may be the origin) we should naturally ascribe it to a transition from a fundamental of frequency 749 cm^{-1}, and F from the combination 749+1319 cm^{-1} of the lower electronic state. If this be the case, it is easy to show that the 749 cm^{-1} fundamental is of symmetry A_1.

Some considerations, however, make one uneasy about this conclusion. A remarkable feature of this band system is the identical intensity in the pairs $A-B$, $D-E$, and $G-H$ showing that the Franck-Condon transition probabilities to the two upper levels A' and B' (523 cm^{-1} apart) are practically the same, at least for the three A_1 levels discovered, $A''=B''$, $D''=E''$, and $G''=H''$. Now, if C'' is also of symmetry A_1, and more especially as 749 cm^{-1} and 523 cm^{-1} are probably the δ'' and δ' vibrations, one would expect also a transition from C'' to A' giving rise to a band 523 cm^{-1} toward shorter wave-lengths from C of comparable intensity. There is no trace of a band at the calculated position.

The negative temperature coefficient of A and B indicates their lower level is the ground state, and the above discussion shows the upper level of B is the lowest, and only sharp level of the upper state. Hence we would say B corresponds to the origin of the system and 1319 and 749 cm^{-1} are the two symmetrical fundamentals, π and δ, of the lower electronic state as summarized in Table IV. By the Herzberg-Teller rule, we not only expect to find these symmetrical vibrations, but also, finding one we expect to find the other, and do not expect to find the third, σ type vibration (which infra-red data, *vide infra*, indicates as 1615 cm^{-1}). However, neither 1319 cm^{-1} nor 749 cm^{-1} are found in the infra-red spectrum of NO_2.

Comparison with the Infra-Red Spectrum

The infra-red spectrum

If NO_2 is a wide-angle molecule, the σ vibration band should be of the parallel type, and the π and δ vibration bands should be of the perpendicular type. That is, two of the fundamental bands should have the same contours ($\perp$), and one should have a different contour ($\parallel$). Two of

[7] Qualitatively, this slight difference is real; the spectrograms show clearly that the extent of overlapping of F and G is greater than that of C and D, three peaks of C preceding the short wave-length edge of D while only two precede the short wave-length edge of G. In order to bring the intervals $F-C$ to the same value as the interval $E-H$ or $D-G$ an error of 5 cm^{-1} would have to exist in the measurement of the head of G, which is unlikely.

the observed[8] intense bands are reported to be "doublets" (641 and 1615 cm^{-1}), and one reported as having a single maximum (1373 cm^{-1}). The latter, however, is somewhat confused by the 1274-cm^{-1} band of N_2O_4.

It has been suggested,[9] therefore, that the 1373-cm^{-1} band corresponds to the σ vibration. However, this interpretation does not fit the rest of the spectrum. In the infra-red all odd combinations of the σ vibration (i.e., those involving one B_2 level) should have the same rotational structure, all other bands between A_1 levels having a different rotational structure. The band at 2910 cm^{-1} (1615+1373 cm^{-1}) is undoubtedly a doublet with exactly the same envelope as the band at 2226 cm^{-1} (presumably 1615+641 cm^{-1}) which, according to the above interpretation should have the other type of rotational structure. Further, if the 1373-cm^{-1} infra-red band is due to the same fundamental as our ultraviolet 1319-cm^{-1} frequency, it cannot be the σ vibration because the ultraviolet frequency has been shown to be of the symmetrical A_1 type.

We shall attempt to show that the σ vibration should be ascribed to the 1615-cm^{-1} band and the π and δ vibrations to the 1373-cm^{-1} and 641-cm^{-1} bands by showing that bands involving B_2 levels are doublets. Bands between A_1 levels will give another type but as none of these have been observed under the grating, agreement and discrepancies cannot be taken seriously until they have been examined with a grating.

Rotational structure of the infra-red bands

Our analysis of the rotational structure of the ultraviolet system, giving the constants of the ground electronic state of NO_2, enables us to predict the rotational structure of the infra-red. The occurrence of a small moment of inertia (the molecule being "nearly linear") enables us to sort out the rotational structure into branches of widely separated subbands (each subband containing P, Q, and R branches of closely spaced lines); for parallel bands there is a Q branch of subbands; for perpendicular bands, P and R branches.[10] Band envelopes obtained by allowing the ΔB_σ (B_σ determines the separation of the widely spaced rotational levels) to tend to zero in the formulae[11] given for the parallel bands show that the subbands crowd on top of one another. Presumably the fine structure constant ΔB_J also tends to zero, whereby the subbands become symmetrical with P and R branches on each side of the subband origins. When the lines are drawn with the correct weight and exponential factors, as in the following paper, the interval from the origin to the region of maximum intensity in the P and R branches turns out to be 20 cm^{-1}. The result is the usual type of parallel band with a strong central peak of Q branches. However, as was described by Eyster[10] for the hydrazoic acid bands, the small moment of inertia (which determines the subband separations) will have a strong dependence upon the vibrational state so that we expect the subbands to shift somewhat, masking the Q branches. The parallel B_2 type of band will, then, have a doublet envelope with peaks 40 cm^{-1} apart, and origin in the middle.

When the envelopes of the 2226-cm^{-1} and 2910-cm^{-1} bands are plotted on the same wave number scale, they are almost identical and the separation of the doublet about as predicted for the B_2 type bands. The band at 1615 cm^{-1} (not examined as carefully as the 2226- and 2910-cm^{-1} bands) is also a doublet. Thus, we believe that these three bands are of the σ, B_2 type, and that the 1615 cm^{-1} is the σ vibration.

A further proof, irrespective of the actual shape of the band contours, is as follows. A simple arithmetical analysis shows that both the 2910- and 2226-cm^{-1} doublets must contain the fundamental 1615 cm^{-1}, for combinations avoiding 1615 are less likely on account of intensity or anharmonicity considerations. It thus appears that 2910 and 2226 cm^{-1} between them must contain all three fundamentals. With the aid of the selection rule we can then prove: (1) They cannot be both perpendicular bands because one of them

[8] A. B. D. Cassie and R. L. Bailey, Nature **131**, 239 (1933); R. Schaffert, J. Chem. Phys. **1**, 507 (1933). The bands of the infra-red have been examined only with prism spectrometers, excepting three, at 1615, 2226 and 2910 cm^{-1}, which were examined with a grating by Sutherland, Proc. Roy. Soc., **A145**, 278 (1934). The band at 1615 cm^{-1}, however, was not separated from the water vapor absorption in this region.

[9] See G. B. B. M. Sutherland and W. G. Penney, Nature **136**, 146 (1935). These authors, however, believe instead that the data warrants the assignment of 1373 to the π vibration.

[10] This approach has been used by E. Eyster, J. Chem. Phys. **8**, 135 (1940).

[11] Following paper, Eqs. (6), (7), (8).

must contain the σ vibration. (2) If 2226 cm^{-1} were parallel and 2910 cm^{-1} perpendicular, the 641 cm^{-1} is the σ vibration, an unlikely assignment. (3) It is impossible to have the assignment 2226 cm^{-1} perpendicular and 2910 cm^{-1} parallel, if, as the ultraviolet indicates, 1319 cm^{-1} is the symmetrical vibration. Therefore we believe both are parallel bands and 1615 cm^{-1} is the σ vibration. Further, these combination bands are the only strong ones, in agreement with this assignment.

The frequencies of the other two fundamentals obtained by subtracting 1615 cm^{-1} from 2910 and 2226 cm^{-1} are 1295 cm^{-1}+anharmonicity, and 611 cm^{-1}+anharmonicity. The latter may be identified with the band reported at 641 cm^{-1}; the 1295 cm^{-1}, with Schaffert's[8] 1373 cm^{-1}, if one can accept such a large anharmonicity, or with our 1319 cm^{-1}.

The two symmetrical fundamentals will probably have no characteristic feature under the resolution of prism instruments. Cassie and Bailey[8] reported a doublet structure for 641 cm^{-1} whereas Schaffert[8] found only a single peak for the 1373 cm^{-1} band. This difference may not be real, for in a similar case the sharp single peak of the 2910 cm^{-1} band under resolution turned out to be a doublet when examined with a grating.[12, 8]

Correlation with the ultraviolet

The difficulty is, however, to identify the 1373 cm^{-1} of the infra-red with the 1319 cm^{-1} of the ultraviolet. The 1319 cm^{-1} frequency lies well outside Schaffert's curve. The discrepancy may be due in part to the fact that the origin of a perpendicular band is at $\nu_{vib}+B_K''$, B_K'' being a rotational constant of the lower electronic state. In the case of NO_2, the magnitude of B_K is about 20 cm^{-1}.

Another difficulty is that, although the selection rules permit the appearance of the other symmetric frequency (beside the 1319 cm^{-1}) in an electronic transition, and the Franck-Condon principle leads one to expect to find it with detectable intensity, we do not find a progression of 641 cm^{-1} in the ultraviolet. Indeed, the only frequency from the ground electronic state, other than those of the 1319 cm^{-1} progression is indicated by band C, which is 749 cm^{-1} from B'', the lowest level of the 1319–523 scheme. Since 749 cm^{-1} is not found in the infra-red but rather 641 cm^{-1}, we must account for this extra band C (and also F) by the other symmetrical frequency, 641 cm^{-1}. The most reasonable explanation is that A'', B'' is not the lowest vibrational level of the lower electronic state but rather the 641 cm^{-1} level. Then C'' could be 1373 cm^{-1} above (000), leaving $C''-B''=1373-641=732$ cm^{-1} and accounting for D, 1319 cm^{-1} from B, as originating from the level 641+1373 cm^{-1}, less anharmonicity. All such assignments give bands in conformity with the selection rules cited.

The negative temperature coefficient is not proof that A and B arise from the ground state, for reference to Eq. (16) of the following paper shows that if the partitition function changes more rapidly with temperature than the factor $\exp(E^0-E)/kT$ for an excited level, a band from this level can also have a negative temperature coefficient. A numerical estimate shows, however, that this is impossible for the 641 cm^{-1} level unless there are unknown low-lying levels, which is not likely in view of Giauque and Kemp's thermodynamic investigations.[2, 13]

The main objection to this assignment, summarized in Table VI, is that transitions from the ground state seem to be absent. We do not expect the Franck-Condon principle to be so effective in such a short interval as 641 cm^{-1}.

Another difficulty is that the interval between the fundamental C'' and its first harmonic F'' is measured as 1311 cm^{-1}, which, since the infra-red

TABLE VI. *Vibrational analysis based on ultraviolet and infra-red data.*

	Bands to B'				Bands to A'			
δ'' \ π''	0	1	2		δ'' \ π''	0	1	2
0	missing	C	F		0	missing		
1	B	E	H		1	A	D	G

[12] L. Harris and G. W. King, J. Chem. Phys. **2**, 51 (1934)

[13] The continuous background may be an integral part of the absorption transitions, in which case the lower levels are above the ground state. The energy of the lower continuum levels, obtained from the temperature coefficient of the continuous absorption presented in Fig. 1 varies from 2400 cm^{-1} at 2600A, to 1600 cm^{-1} at 2520A, rising again to 2000 cm^{-1} at 2460A. The continuum may then correspond to transitions from excited levels of the ground state to configurations on the potential bowl of the upper state lying above the dissociation lip, proceeding simultaneously with the discrete transitions.

gives the fundamental at 1373 cm^{-1} indicates an unusually large anharmonicity factor.

Other explanations of the band C are:

(1) The band C is due to a transition from 641 cm^{-1} above the lowest vibrational state to a level 100 cm^{-1} below B'. This introduces a new vibrational frequency in the upper electronic state which it is impossible to fit into any reasonable scheme.

(2) The band C may be from the lowest vibrational state to an upper level, 749 cm^{-1} below B'. The objections to this are: (a) the temperature coefficient of absorption is not zero, and (b) there do not appear to be other transitions to this new upper state level, although its symmetry is the same as all the others.

(3) A third possibility is that C'' might be at 2×641 cm^{-1} above B'' and go to A' which would account for a somewhat smaller temperature coefficient of C than D. However, C is not diffuse like A, and all other levels ending at A' are diffuse.

Further possibilities explaining C and also 1319 cm^{-1} as contrasted with 1373 cm^{-1} of the infra-red are:

There may be two different low electronic states lying close together, one being identified with the ground state of the molecule (and manifesting itself in the infra-red data), the other being the lower electronic state of the ultraviolet band system. The negative temperature coefficients of the bands A and B indicate that the new low-lying electronic state would have to be <1000 cm^{-1} from the real ground state. However, the agreement between equilibrium data and spectroscopic calculations is the strongest evidence against such a postulate.

In a nearly linear molecule such as NO_2 seems to be, there may be considerable interaction of the π and δ frequencies, which are A_1 levels, with rotation about the σ axis, giving levels belonging to representations of the group of the symmetric rotator. Since the selection rule for an electronic transition requires transition from a state of one representation to another of the same representation, whereas the infra-red permits other transitions, different rotation vibration levels will combine in the electronic than in the infra-red bands. This may result in essentially a splitting of the π and δ vibrations into two levels, 1373 and 1319, and 749 and 641 cm^{-1}, respectively.

Summary

From measurement of intervals, intensity of absorption and consideration of predissociation of the band system at 2500A we find: (1) Upper electronic state energy levels of 714 and 523 cm^{-1} presumably the π and δ frequencies, with the strongest progression $n(\pi+\delta)$. (2) Lower electronic state energy level intervals of 1319, 2624 (1319+1305), 749 and 2060 (749+1311) cm^{-1}.

Temperature coefficients, in particular the negative temperature coefficient of the heads of the 2459 and 2491A bands lead us to suppose (a) the origin of this system is at 2491A, 40,130 cm^{-1}, and (b) that the above intervals in the lower electronic state, 1319 and 2624 cm^{-1} are the fundamental and first harmonic of a symmetrical frequency, the interval 749 cm^{-1} being the other fundamental, and 2060 cm^{-1} the combination level.

In order to make the vibrational frequencies of the lower electronic state of the ultraviolet system compatible with the accepted vibrational frequencies of NO_2 derived from infra-red data, we are forced to assume that 2459 and 2491A bands come from a level 641 cm^{-1} above the vibrationless state in spite of the negative temperature coefficient of the heads. This assumption leads to the following assignment of intervals for the lower (ground) state as derived from the ultraviolet bands:

$$\begin{aligned} \pi \text{ to } 2\pi &= 1311 \text{ cm}^{-1}, \\ \pi+\delta \text{ to } 2\pi+\delta &= 1319 \text{ cm}^{-1}, \\ 2\pi+\delta \text{ to } 3\pi+\delta &= 1305 \text{ cm}^{-1}, \\ \pi-\delta &= 749 \text{ cm}^{-1}. \end{aligned}$$

Difficulties of this scheme are mentioned and alternative explanations discussed, but a clarification of the situation awaits a grating analysis of the infra-red bands at 1373 cm^{-1} or the analysis of other electronic transitions in the visible or near infra-red absorption spectrum of NO_2.

The Rotational Structure of the Ultraviolet Bands of NO_2 *

LOUIS HARRIS AND G. W. KING
Massachusetts Institute of Technology, Cambridge, Massachusetts

(Received July 5, 1940)

The rotational structure of the 2491A band in the ultraviolet absorption spectrum of NO_2 is not completely resolved, but the spectroscopic constants have been determined from the spacing of the subbands (groups of transitions with the same K), their intensity, the temperature coefficients of absorption and finally from the comparison of synthetic spectra constructed from arbitrary constants with the observed spectra. The O−N−O angle in the lower state is 154° and the N−O distance is 1.28A. For the excited state the angle remains essentially the same, the internuclear distance increasing to 1.41A.

§1. INTRODUCTION

OF all the bands in the absorption spectrum of NO_2 in the visible and ultraviolet regions of the spectrum those near 2500A have the most clearly defined structure. The outstanding feature of eight of these bands is a regularly spaced Q branch of subbands with sharp heads. In the band at 2491A fairly well-developed parabolae are partly resolved in each of the subbands.[1] Thus two rotational quantum numbers are required to represent the spectrum. Therefore, at least one state is nonlinear, and since transitions between a linear and a nonlinear molecule cannot occur for nonzero values of two rotational quantum numbers, both states involved in this ultraviolet system are nonlinear. In this paper we determine the moments of inertia of the NO_2 molecule in the upper and lower states of this ultraviolet system from the rotational structure, in particular from that of the 2491A band which is the best resolved.

The spacing of subbands shows that the formulae to be used for all the line positions and their intensities are the equations of nearly symmetrical rotors (in each state) with intensities given by selection rules for the induced moment parallel to the axis of (approximate) rotational symmetry. Our grating spectrograms showed that the close spacing of the subband lines, in preventing their resolution, prohibits a precise analysis; nevertheless we believe that the spectrum can be satisfactorily interpreted with these formulae.

§2. ANALYSIS OF THE SPACING OF THE SUBBAND HEADS

A plot of the interval ($\Delta\nu$) between successive subband heads[2] in the 2491, 2459 and 2576A bands is shown in Fig. II-1. As the intercept of the line through the experimental points cuts the $\Delta\nu=0$ axis at some half-quantum number, presumably $-\frac{1}{2}$, the formula for the heads must be

$$\nu=\Delta B_\sigma K^2+\text{constant} \qquad (1)$$

and

$$\Delta\nu=\Delta B_\sigma(2K+1) \qquad (2)$$

and not of the form $\nu=\Delta B_\sigma J(J+1)+\text{constant}$, since the latter form requires the intercept at a whole number (-1). (ΔB_σ is the constant of

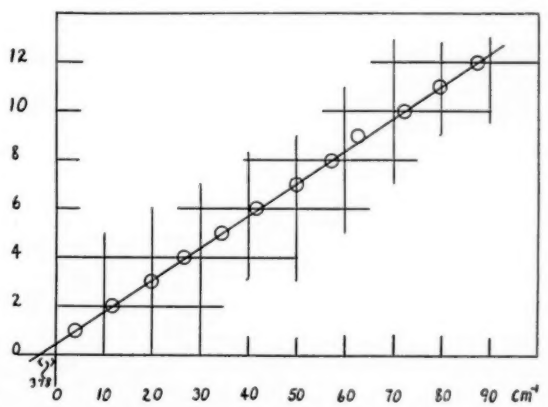

FIG. II-1. The abscissa is the interval between the $n+1$th and the nth peaks, where n is the ordinate. The intervals have a negative sign since the bands are degraded to the red.

* Contribution No. 456 from the Research Laboratory of Physical Chemistry, Massachusetts Institute of Technology.

[1] L. Harris, Proc. Nat. Acad. Sci. **14**, 690 (1928).

[2] Due to the lack of resolution of the subbands into discrete lines the exact location of the heads cannot be determined. In what follows the head is defined as the short wave-length edge of the subband as shown by the microphotometer traces of the grating spectra, Fig. I-3 of the previous paper.

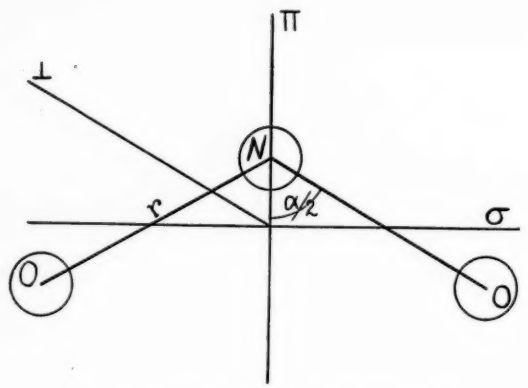

FIG. II-2. Diagram of NO_2 molecule with notation used here.

the parabola identified below.) As a result[3] the assignment of the proper K to each subband is obtained. The slope of the straight line of Fig. II-1, $2\Delta B_\sigma$, is -7.56 cm^{-1}; hence $\Delta B_\sigma = -3.78$ cm^{-1}. The intercept at $K=0$ equals ΔB_σ which from the plot is -3.8 cm^{-1}, in satisfactory agreement with the value derived from the slope.

Examination of the symmetry of the levels of a bent triatomic molecule shows that whatever the nuclear spins of the atoms there would be no missing subbands in this kind of parabola.

The parabola (1) fits the subband head positions to an accuracy of 1 cm^{-1}. This means that the K levels are not staggered more than this in either state from the simple parabolic equation of the approximately symmetrical rotor. Calculation shows that the energy levels fit the parabolic equation (1) to within 1 cm^{-1} if the angle is $>120°$.

Since $|\Delta B_\sigma|$ is comparatively large and since B_σ'' must be still larger (subbands degraded to red), the moment of inertia corresponding to B_σ'' must be very small. The only possible model satisfying this condition is a wide-angled molecule. The transitions in this band are all of the $\Delta K=0$ type, from which it follows that the dipole induced by the ultraviolet absorption must be along the σ axis (Fig. II-2), that is, parallel to the axis of symmetry of the approximate symmetric rotor, but perpendicular to the molecular axis of symmetry. It is not the precise geometrical symmetry but the symmetry of the effective rotating ellipsoid which prescribes the band structure.

[3] See also the discussion, §3.

§3. Rotational Energy Levels and Permitted Transitions

This determination of the approximate symmetry of the molecule as a rotor in the two states, and the direction of the induced dipole fixes the formulae to which the spacing of the lines of the whole spectrum (fine structure included) and their intensities should conform.

The rotational energy levels are given by

$$E_r(J,K)=B_J J(J+1)+B_K K^2+\cdots, \quad |K|\leqslant J \tag{3}$$

$$B_K=B_\sigma-\tfrac{1}{2}(B_\pi+B_\perp), \tag{4}$$

$$B_J=\tfrac{1}{2}(B_\pi+B_\perp), \tag{5}$$

where B_σ, B_π, $B_\perp$ are the spectroscopic constants which correspond to principle moments of inertia around the orthogonal axes defined[4] in Fig. II-2, with $B_\perp \cong B_\pi$ and $B_\sigma \gg B_\pi > B_\perp$. These relationships become more accurate the larger the angle.

With the dipole parallel to σ, the frequency of the lines of the branches in this band system will be represented by the following equations to an extent depending on the approximation to rotational symmetry.[5] The equations give the distance from the band origin.

$$\nu(Q^{J'\ K'}_{J''\ K''})=\Delta B_J J(J+1)+\Delta B_K K^2+\cdots, \tag{6}$$

$$\nu(P^{J'-1\ K'}_{J''\ K''})=\Delta B_J J^2-\overline{2B}_J J+\Delta B_K K^2+\cdots, \tag{7}$$

$$\nu(R^{J'\ K'}_{J''-1\ K''})=\Delta B_J J^2+\overline{2B}_J J+\Delta B_K K^2+\cdots, \tag{8}$$

$$\Delta B_J=B_J'-B_J'',$$

$$\overline{2B}_J=B_J'+B_J''.$$

When ΔB_K is much greater than $\overline{2B}_J$, the position of the lines as given by the above equations are such that those with a given value of K group themselves together forming a "subband." The subband origins are spaced according to $\Delta B_K K^2$, whereas the positions of

[4] The other configuration of a triatomic molecule as a symmetric rotor, where $B_\sigma \cong B_\pi$ would make $B_K = B_\perp - \frac{1}{2}(B_\pi+B_\sigma)$ a negative quantity, which is contrary to the observed intensity relations (see Eq. (15)).

[5] Equation (6) is not in agreement with Mecke's Eq. (4b), Eucken-Wolf, *Hand- und Jahrbuch der Chemischen Physik* (Leipzig, 1934), p. 322.

maximum intensity are given approximately by

$$\nu-\nu_{00}=(\Delta B_J+\Delta B_K)K^2=\Delta B_\sigma K^2,$$

ΔB_σ being the constant evaluated from the measurements, §2.

The equations in the case of the induced electric moment being perpendicular to the axis of the approximate symmetrical rotator are

$$\nu(Q_J^{J\ K\pm1})=\Delta B_J J(J+1)+\Delta B_K K\pm 2B_K'K+B_K', \quad (6a)$$

$$\nu(P_J^{J-1\ K\pm1})=\Delta B_J J^2-\overline{2B}_J J+\Delta B_K K^2\pm 2B_K'K+B_K', \quad (7a)$$

$$\nu(R_{J-1\ K}^{J\ K\pm1})=\Delta B_J J^2+\overline{2B}_J J+\Delta B_K K^2\pm 2B_K'K+B_K'. \quad (8a)$$

Here we have subbands identical with those of Eqs. (6), (7), (8), spaced, however, not according to $\Delta B_K K^2$ but to

$$\Delta B_K K^2\pm 2B_K'K+B_K', \quad (1a)$$

with

$$\Delta\nu=\Delta B_K(2K+1)\pm 2B_K'. \quad (2a)$$

This leads to a pair of parabolae. Although the observed spectrum does show a doubling of the subbands (see §9) the graph of the interval, Fig. II-1, gives an intercept not in agreement with (2a) unless $2B_K'$ is zero, which is impossible.

With complete resolution then, analysis from the disposition of spectral lines will give the constants B_J', B_J'' and ΔB_σ, but not B_σ'' or B_σ'. The constant B_σ'' is obtained from intensity relationships.

Substitution of reasonable values of B_J'' and B_J' in the above equations show, and the high resolution spectrograms confirm, a considerable blending and superposition so that it will be impossible to derive B_J'' and B_J' by the orthodox methods of intervals. However, values of these constants can be found by trial and error in the construction of synthetic spectra and comparison with the observed.

To make a correct comparison, and indeed to obtain a first approximation to the constants, intensities again must be taken into consideration.

§4. Intensities

The intensities of the lines comprising a band can be expressed as a product of transition probability, weight factor, an exponential function of B_J'' and B_σ'' and the rotational term of the partition function. The probabilities of transition when the induced dipole is parallel to the axis of least inertia are[6]

$$(A_{J\ K}^{J\ K})^2=\frac{K^2}{4J(J+1)}, \quad (9)$$

$$(A_J^{J-1\ K}{}_K)^2=\frac{J^2-K^2}{4J(2J-1)}, \quad (10)$$

$$(A_{J-1\ K}^{J\ K})^2=\frac{J^2-K^2}{4J(2J+1)}. \quad (11)$$

The weight factor for the $K=0$ levels is $2J+1$. For $K>0$ the weight factor is usually $2(2J+1)$, but here, it is $2J+1$, because only one of the doubly degenerate ($\pm K$) levels exists due to the zero nuclear spin of oxygen. (In the $K=0$ levels no Q, and only alternate P and R lines occur.)

The intensity factors, including transition probability and weight factors, for all the lines are, then:

$$I(Q_{J\ K}^{J\ K})=\frac{K^2(2J+1)}{4J(J+1)}, \quad (12)$$

$$I(P_J^{J-1\ K}{}_K)=\frac{(J^2-K^2)(2J+1)}{4J(2J-1)}, \quad (13)$$

$$I(R_{J-1\ K}^{J\ K})=\frac{(J^2-K^2)(2J-1)}{4J(2J+1)}. \quad (14)$$

The exponential factors in the intensity expression

$$\exp-[(B_J''J(J+1)+B_K''K^2)/kT] \quad (15)$$

are functions of the initial (lower) levels. An interpretation of intensities should therefore give an estimate of B_K'' and B_J''.

§5. Temperature Coefficient of Absorption

The states of NO_2 involved in this ultraviolet system have one set of rotational levels so widely spaced that absorption lines arising from these levels have a detectable temperature coefficient.

[6] Dennison, Rev. Mod. Phys. **3**, 280 (1931).

The measured absorption coefficient of any line is given by

$$\log_{10}\beta=\frac{-0.4343}{kT}E''(J,K)$$
$$+\log_{10}c(J,K)-\log_{10}\sigma(T)+\text{constant.} \quad (16)$$

Here, $\sigma(T)$ is the partition function, which formulates the shift of the population of the lower state with temperature; $c(J,K)$ is the combined weight factor and transition probability, E'' is the energy of the initial level equal to $E_r''(J,K)$ of Eq. (3) plus vibrational and, possibly, electronic energy, which is constant throughout the band.

The microphotometer traces of the 2491 and 2459A bands under the rather low resolution of the prism instruments show the subbands clearly separated from one another. The peak of a subband is, then, composed mostly of transitions with the same K. The absorption coefficient data obtained with the prism instruments in which the structure of the subbands are unresolved can therefore be treated quantitatively by considering the subbands as single absorption "lines," functions of K alone. This interpretation of the peaks would permit us to consider all the highly populated levels of different J, but the same K value, which on the energy level scheme occurs as a closely spaced group widely separated from the groups with quantum number $K\pm1$, as one level at $E_r''\cong B_K''K^2$.

The intensity of a subband peak is then obtained by summing (12), (13), (14) with (15).

$$I(\text{peak})=c(K)\exp -B_K''K^2/kT, \quad (17)$$

$$c(K)=K^2\Big[\sum_Q\frac{2J+1}{4J(J+1)}e^{-\Theta}$$
$$-\sum_P\frac{2J+1}{4J(J-1)}e^{-\Theta}-\sum_R\frac{2J-1}{4J(2J+1)}e^{-\Theta}\Big]$$
$$+\Big[\sum_P\frac{J^2(2J+1)}{4J(2J-1)}e^{-\Theta}+\sum_R\frac{J^2(2J+1)}{4J(2J-1)}e^{-\Theta}\Big], \quad (18)$$
$$\Theta=[(B_JJ(J+1)+B_KK^2)/kT],$$

the summation being over those J's (different for P, Q and R branches) which compose the peaks. Although the range of the summations is slightly different in successive peaks (J being always greater than K) the quantities in the square brackets vary but slowly with K.

The variation of the absorption coefficients of the unresolved subband peaks with K and T, as governed by Eq. (17) should permit a determination of B_K''. The measured absorption of subband peaks is given by a modification of (16),

$$\log_{10}\beta(\text{peak})=-0.4343/kT\,B_K''K^2$$
$$+\log_{10}c(K)-\log_{10}\sigma'(T)+\text{const.} \quad (19)$$

with $c(K)$ given by (18) and $\sigma'(T)$ equal to the sum over the $B_K''K^2$ levels.[7]

The experimental values of β(peak) for 378° and 604°K were given in Fig. I-1 of the previous paper.

The most outstanding feature of this experimental data is the actual decrease with increasing temperature of the absorption of the earlier peaks in the bands at 2491A and 2459A. This is due to the partition function in (19), i.e., to the effect of the shift of the population to levels of higher energy but greater degeneracy (in K). This observation gives support to the treatment of peaks described above.

Evaluation of B_σ''

(a) The variation of peak intensity with K serves to evalute B_K''. The fundamental intensity equation (19) shows that at constant temperature B_K'' could be determined from the slope of $\log\beta-\log\ c(K)$ plotted against ν^2; $B_K''=2.303kT\Delta B_\sigma\times$slope. At high K's where the Q branch (6) and (12) predominates $c(K)$ is approximately K^2. This value was used in drawing curves representing $\log\beta-\log c(K)$ *vs.* ν^2 slopes at high K's and derived values of B_K'' are given in Table I.

(b) The shift of maximum absorption to subbands of higher K as the temperature is increased gives an approximate value of B_K''. By equating the differential of (17) (18) to zero we obtain

$$K^2_{\max}=kT/B_K''. \quad (20)$$

The values of B_K'' obtained from an estimation of $K_{\max}$ at various temperatures are given in Table II.

(c) A more detailed treatment of the temperature variation of the absorption coefficient of

[7] Obtained by successive approximation. The sum over the J levels, and vibrational levels, is not required in the calculations of this section.

every peak leads to nearly the same value of B_K''. Reference to Eq. (19) shows that the variation of the absorption coefficient of any one subband is given by

$$\log \beta_K(T_2) - \log \beta_K(T_1) = \frac{0.4343E''}{k}\left[\frac{1}{T_1}-\frac{1}{T_2}\right]+\log\frac{\sigma'(T_1)}{\sigma'(T_2)}. \quad (21)$$

The partition coefficient can be estimated from tentative values of the vibrational and rotational levels and then the equation solved for E''. Such a treatment indicates a value of B_K'' much greater than the minimum value $|\Delta B_\sigma| = 3.78\ \text{cm}^{-1}$, namely, about $20\ \text{cm}^{-1}$.

Although none of the treatments outlined above give accurate values, the order of magnitude of $B_K'' \cong B_\sigma''$ is clearly indicated as being much greater than ΔB_σ, probably about $20\pm5\ \text{cm}^{-1}$. This value is verified by the agreement with experiment of the intensities obtained by actually constructing a spectrum from our final values of the spectroscopic constants.

§6. Analysis of Fine Structure

The reproduction of the first-order grating spectrograms (Fig. I-3) indicates a regular sequence of lines within each subband, especially for $K=4$. These lines have been fitted fairly well to parabolae by Hermann[8] and by Ionescu[9] who used prism instruments. Although all the strong lines were not accounted for, Ionescu ordered the majority of lines into P, Q, and R branches and obtained B_J'' and B_J' from his analysis. The spectroscopic constants thus derived are not consistent with the assumption of a symmetric top, nor will the constants reproduce the observed spectrum with the intensity relationships given above. When the line positions are measured more accurately, as they are from our microphotometer traces, the regularities mentioned above disappear to a large extent, showing that the "lines" (peaks in the microphotometer traces) are actually blends of numerous lines.

Table I.

	Temp. °K	Slope	B_K''
Band 2491A	378	0.008	18
	510	.006	18
	606	.004	15
Band 2459A	378	.008	18
	505	.006	18
	605	.004	15

Table II.

$T°K$	K_{max}	B_K''
373	3.5	21
504	4	22
606	4.5	21

Equations (6), (7), (8) and (12), (13), (14) show the P, Q, and R branches are repeated[10] in every subband with only slight modifications of intensity. These branches start from subband origins which are distributed according to the parabola $\Delta B_K K^2$. Even in the event of considerable blending the pattern of the subband should be repeated in the next[11] subband according to this parabolic law. It is apparent in Fig. I-3 that this is true to a certain extent, giving a value of ΔB_K, the spacing constant for the subband origins, almost the same as ΔB_σ, the spacing constant for the subband heads. We estimate $\Delta B_J = \Delta B_\sigma - \Delta B_K$ is $<0.2\ \text{cm}^{-1}$.

From the lack of complete reproduction[12] of the pattern, we conclude that there is insufficient resolution for a unique assignment of J and K values to the peaks in the fine structure of the subbands. However, the order of magnitude of the spectroscopic constants can be determined with some accuracy by finding what values of B_σ'', B_σ', B_J'', and B_J' when substituted into Eqs. (6), (7), (8), for line spacings, and Eqs. (12), (13), (14), (15) for intensities, will reproduce the general appearance of the spectrum; namely, the sharp strong heads, the diminution of intensity within a subband, and the close spacing of the lines. The labor accompanying this approach can be considerably reduced by an *a priori* knowledge of the range of the magnitude of the molecular constants.

[8] A. Hermann, Ann. d. Physik **15**, 89 (1932).
[9] A. Ionescu, J. de phys. et rad. **7**, 8, 369 (1937).

[10] Lines for which $J=K$ are missing in the $K+1$ subband.
[11] Or in the next but one if the levels are split by the asymmetry of the rotor and only alternate J levels exist.
[12] As will be seen, this is due to the fact that the peak of a blend is shifted because the intensities of the component P, Q, and R lines vary differently with K (Eqs. (12), (13), (14)).

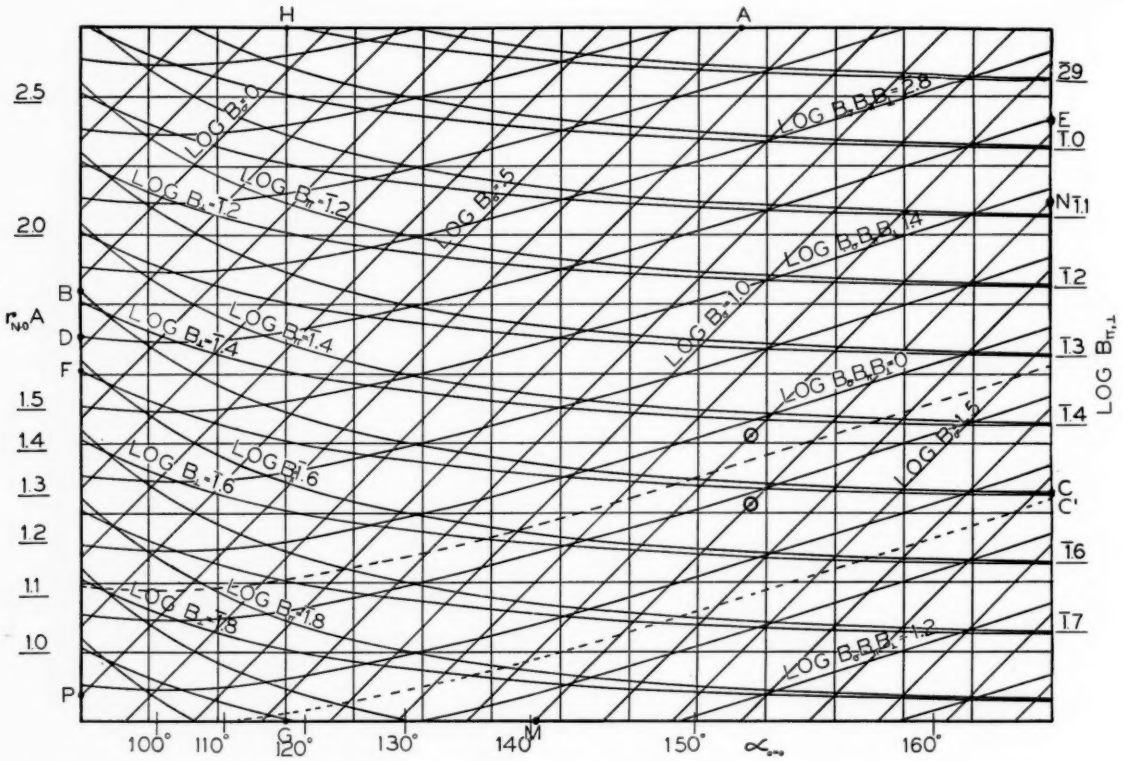

FIG. II-3. Spectroscopic constants of NO_2. Ordinates, log r; abscissae, log cos $\alpha/2$. Values of r and α are indicated. For angles greater than 160° (at the right of diagram) B_π and $B_\perp$ are practically equal and the corresponding values of log $B_{\pi,\perp}$ are given. The lower circle is the representative point for the lower electronic state, the upper circle for the upper electronic state.

§7. Magnitude of Spectroscopic Constants for NO_2

The theory of molecular structure makes it unreasonable to expect N−O distances less than 1A or greater than 2.5A or an angle α (Fig. II-2) less than 90°. Thus B_σ and B_J are limited to a definite range of values for the two electronic states involved. Figure II-3 is an outline of a chart from which the spectroscopic (molecular) constants of NO_2 can be read off for all values of r and α between the above limits. Any point on the diagram corresponds to some definite r and α (given by the ordinate and abscissa), i.e., to some definite molecular shape. Points on lines at 45° (parallel to PA) represent configurations having the same B_σ values; curves parallel to BC connect r, α values for which B_π is constant, lines parallel to FC', those values for which $B_\perp$ is constant. The appropriate values of r and α for any state is determined by the intersection of the B_σ with either B_π or $B_\perp$ lines. The constants derived from the spectrum are expected to lie somewhere on this chart.

The thermodynamic functions of the gas permit a determination of the product of the three moments of inertia (of the ground state). Curves parallel to DE in the plot connect r, α configurations which have the same $I_\sigma I_\perp I_\pi$ product. The intersection of the correct B_σ line and $B_{\pi,\perp}$ curves fixes the value of this product. Or, given the appropriate value of the product, the intersection with B_σ fixes B_π.

Vertical lines on Fig. II-3 connect models of the same degree of asymmetry. The maximum asymmetry permitted by the fit of the subband head parabola is represented by the vertical line GH. Hence the possible r, α values for both electronic states lie to the right of GH. The determination of B_σ'' as 20 cm^{-1} indicates r, α values on the line MN. Therefore, α'' is now fixed at a value greater than 140°, whereas the

minimum value limited by the fit of the subband head parabola was about 120°.

To fix r'' it is necessary to find $B_J''(\cong B_\perp'' \cong B_\pi'')$. This was accomplished by comparison of spectra drawn with various values of B_J' and B_J'' delimited to the range of Fig. II-3

§8. Construction of the Spectrum from Assumed Constants

A salient feature of the bands of this band system is the sharp and intense subband heads. The reproduction of this phenomenon, caused by the R branch heads being very close to the subband origins, is the first requirement demanded of the synthetic spectrum.

Trial spectra were constructed with the ratio $\Delta B_J/\overline{2B}_J$ varying from 0 to 1 in steps of 0.1. This ratio determines the relative positions of the branches, i.e., gives the outline of the band except for a scale factor. It was immediately evident that the ratio could not be less than 0.10, in order that the R branch should not spread too far to the shorter wave-length side of the subband heads, especially for $K=0$; nor greater than 0.3, in order to produce the sharp subband heads. Possible values of the spectroscopic constants are thus between AB and CD of Fig. II-4.

Another simplification is that if we can assume the internuclear distance is less than 2.0A and greater than 1.0A, B_J'' must lie between 0.14 and 0.55 cm^{-1}. Thus, the spectrum must correspond to constants represented by a point within the area $EFGD'$ of Fig. II-4. We have actually constructed line for line spectra corresponding to all the points marked by circles in Fig. II-4. These spectra were obtained with the use of integral ratios of $\overline{2B}_J/\Delta B_J$, which made plotting easier but gave a spectrum less rich in lines than those obtained with nonintegral values.

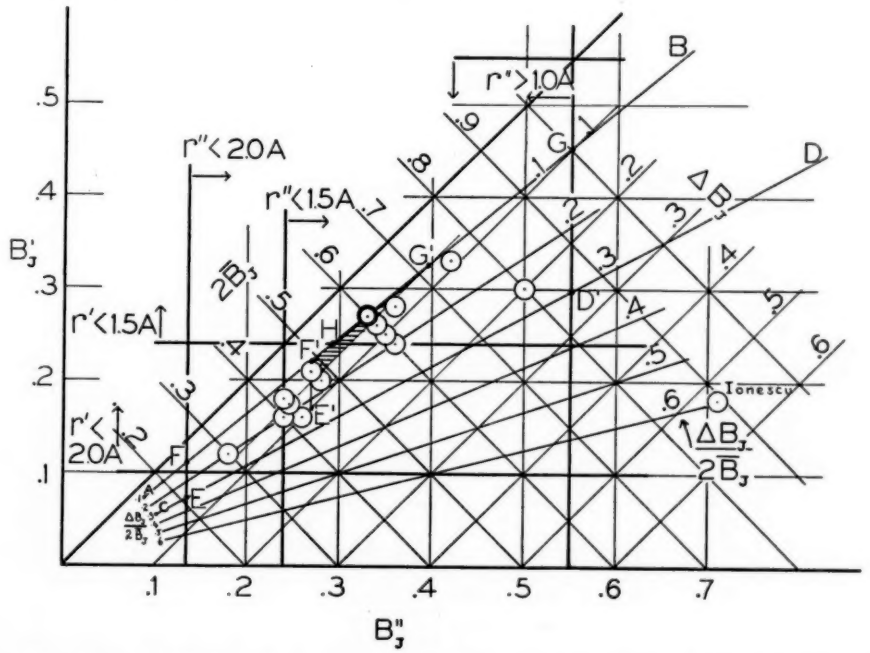

Fig. II-4. Possible combinations of B_J' and B_J'' for the ultraviolet bands. Since the subbands are degraded to the red, $B_J''>B_J'$ and the points above the 45° diagonal through the origin are not valid. The range of the B_J's for $1.0<r_{N-O}<2.0$A are indicated by heavy lines, horizontal for r', vertical for r''. The limitations apply only if the molecule is essentially a symmetrical rotor, i.e., $\alpha>120°$, and hence do not apply to Ionescu's point. The lines at ±45° are the corresponding values of ΔB_J and $\overline{2B}_J$ which enter in the formulas for the positions of the spectral lines. The construction lines fanning out from the origin of the figure are lines of constant $\Delta B_J/2B_J$. The circles indicate values of B_J', B_J'' (hence ΔB_J and $\overline{2B}_J$) for which spectra were drawn up. The point with the heavy circle corresponds to spectroscopic constants which give a synthetic spectrum most nearly like the observed spectrum. The sign of ΔB_J is omitted in the figure and in §8.

Closer estimates of the constants can now be obtained by examination of these drawings for correct reproduction of (a) the spacing of the fine structure peaks of the microphotometer traces at grating resolution, and (b) of the distribution of intensity in the envelopes of the subbands of the prism spectrograms.

For (a), in order to make the comparison with the finite resolution of the grating, each line is replaced by an exponential envelope whose half-width is known from the observed tracing of atomic Si lines. Typical hills and valleys at the correct intervals are produced only for[13] $0.05 < \Delta B_J < 0.10$. This limits the representative point to $F'E'G$ in Fig. II-4.

To reproduce the appearance of the absorption spectrum under the resolution of a prism instrument the correct procedure seems to be to consider Eqs. (6), (7), (8) and (12), (13), (14) as continuous functions of J and ν but at the same time to multiply the intensity by the density of lines.[14] In order to reproduce the sudden increase of intensity from the tail of a subband to head of the next (see Fig. I-1) the intensity factor $\exp -B_J''J(J+1)/kT$ must become effective in the tail[15] (high J's). Numerical trials show B_J'' is to be as large as possible, certainly >0.25 cm^{-1}. In addition, to minimize the overlapping of subbands which nullify this discontinuity at the heads, ΔB_J must be less than 0.07 (restricting the spread of possible values to the shaded area in Fig. II-4). At the same time, $\Delta B_J > 0.05$, otherwise, since $\Delta B_J/\overline{2B}_J \sim 0.1$, $\overline{2B}_J$ (and hence B_J'') would have to be so small that the exponential factor would be relatively inoperative.

These two tendencies, small ΔB_J and large B_J'', cannot be satisfied unless $\Delta B_J/\overline{2B}_J$ is a minimum value ($\overline{2B}_J \cong 2B_J''$ since $\Delta B_J = B_J' - B_J''$ is small). This has already been given as 0.1, so that the representative point is now forced to the line $F'G'$ in Fig. II-4, a small ΔB_J pulls the point to F', a high B_J'' to G', the two requirements fixing values close to $\Delta B_J = -0.06$ and $\overline{2B}_J = 0.6$ from which $B_J'' = 0.33$ and $B_J' = 0.27$ cm^{-1}. In addition, we might be permitted to restrict the point to this value (actually between H and G') by the reasonable guess that $r' < 1.5$A. Thus B_J'' is probably between 0.30 and 0.36, our best value being 0.33 cm^{-1}.

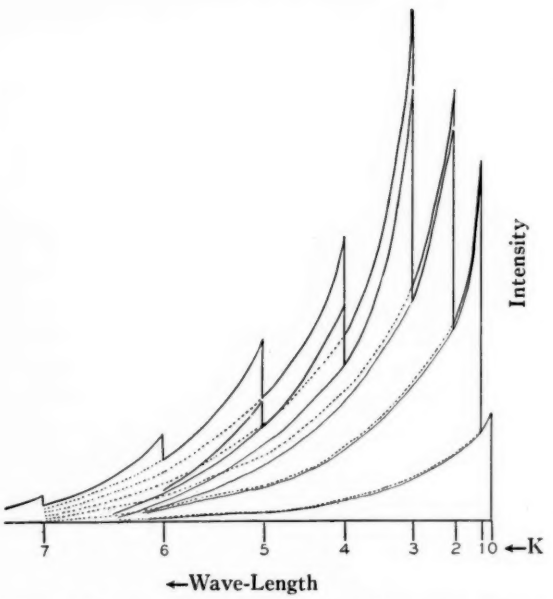

FIG. II-5. Synthetic band spectrum. Appearance of band under the relatively low resolution of a prism spectrograph. The upper curve is for $T = 400$°K, the lower for 290°K. The constants for both curves are $B_J' = 0.27$, $B_J'' = 0.33$, $B_\sigma'' = 20$ and $\Delta B_\sigma = -3.78$ cm^{-1}. The dotted curves mark the contribution of each subband in the succeeding subband for 400°K, and the thin lines for 290°K. The correction for the change in the value of the partition function has been omitted.

These values do indeed give the correct distribution in intensity when treated by the method mentioned above. The smeared-out spectra corresponding to the prism resolution are drawn for two temperatures in Fig. II-5 showing the similarity with the observed absorption. Construction of the grating line spectra with these constants gives the correct disposition of peaks and valleys, and also some details such as the strong isolated line 54.04 cm^{-1} in Table I-3.

§9. Spin-Rotation Doubling

No line of the spectrum of symmetrical rotators of this type is double from rotational degeneracy, for since oxygen has no nuclear spin, only one of the $\pm K$ levels exists. The odd electron of NO_2 however causes all states to be spin doublets.

[13] The term $\overline{2B}_J$ in Eqs. (7), (8) is of secondary importance in determining the spread of the branches.

[14] The decreased weight factor for $K = 0$ mentioned in §4 is extremely important in reducing the overlapping by the $K = 0$ subband.

[15] Reference to Eqs. (12), (13), (14) shows that the other factors in the intensity formulae increase with J.

The double series of heads mentioned by Hermann[8] and Ionescu[9] may be the splitting of lines due to spin-rotation coupling. As a molecule becomes more and more linear the rotational quantum number K becomes an electronic quantum[16] number Λ, so that in such a nearly linear molecule as NO_2 we should expect "K-type" doubling of the order of magnitude of Λ-type doubling.

In this way all the degeneracy of the lines is removed. Hence a magnetic field will not cause any rotation of the plane of polarization as it does in doublet states of diatomic molecules, explaining Hermann's[8] negative results with magnetic fields.

§10. Conclusions

The constants of the spectrum analysis are:

ΔB_σ	(from head spacing)	-3.78 ± 0.02 cm^{-1}
B_σ''	(from temperature variation of absorption coefficient)	20 ± 5 cm^{-1}
B_σ'	(from $B_\sigma''+\Delta B_\sigma$)	16 ± 5 cm^{-1}
ΔB_J	(from intensity of and spacing within subbands)	-0.06 ± 0.01 cm^{-1}
$\overline{2B}_J$	(from intensity of and spacing within subbands)	0.6 ± 0.15 cm^{-1}

$$B_J''=(\tfrac{1}{2}(\overline{2B}_J-\Delta B_J)) \quad 0.33\pm0.03 \text{ cm}^{-1},$$

$$B_J'=(\tfrac{1}{2}(\overline{2B}_J+\Delta B_J)) \quad 0.27\pm0.03 \text{ cm}^{-1}.$$

Thus, $r''=1.28\pm0.03$A, $\alpha''=154\pm4°$, and $r'=1.41\pm0.06$A, $\alpha''=154\pm6°$.

It is seen from Fig. II-3 that the angle is determined almost entirely by B_σ'' and the internuclear distance by B_J''. Several independent estimates show that B_σ'' and hence the angle, is large, and our trial spectra limit B_J'' enough to show r'' is definitely larger than the value 1.14A in NO.

The angle of the molecule does not change appreciably in the transition from the lower to the upper state, whereas the internuclear distance increases appreciably (1.28 to 1.41A). This shows that the orbital of the odd electron, which presumably is concerned in the optical absorption of NO_2, has little directional effect, but some bonding energy.

The other bands in this ultraviolet system described in the previous paper, have essentially the same rotational structure, and hence the same rotational constants as the 2491A band.

The above analysis shows then that the origins of all the bands are very close to the band heads. The accurate values for the origins thus obtained are essential for the vibrational analysis.

§11. Discussion

The large angle of 154° obtained is reasonable on theoretical grounds. The NO_2 molecule can be treated as linear CO_2 plus an odd electron. This would enter a strongly antibonding orbital[17] which is stabilized to some extent by kinking of the molecule. The molecular angle, then, can be considered as a perturbation from 180°, in contrast to that in other nonlinear triatomic molecules in which the angle is perturbed from the first order directed valence value of 90°.

The odd electron has a choice of entering orbitals which may be crudely described as p_σ and p_π. The energy separations of these states when the molecule is kinked cannot be even roughly estimated.[18] There may, therefore, be three low-lying states of approximately the same energy.

It is very important in calculating the thermodynamic functions of NO_2 from spectroscopic data to decide how many of these states are of importance in the partition function. Further, on account of the weakness of the absorption and the difficulties in the vibrational analysis of this system, it might be suggested that the lower state of this ultraviolet system may not be the ground state.

Giauque and Kemp[19] have determined $(R/2)\times\ln I_\sigma I_\pi I_\perp + R\ln p_e$ from thermodynamic data, p_e being the degeneracy of the ground state. The constancy of their value with temperature indicates there are no nearby states. Jahn and Teller[20] have shown that a nonlinear molecule cannot have orbital degeneracy, so that p_e for

[16] The rotational degree of freedom of a nonlinear molecule together with the deformation vibration form the doubly degenerate vibration of the linear molecule which has angular momentum.

[17] R. S. Mulliken, J. Chem. Phys. **3**, 720 (1935).

[18] Reference 17, p. 738.

[19] W. F. Giauque and J. D. Kemp, J. Chem. Phys. **6**, 40 (1935).

[20] H. A. Jahn and E. Teller, Proc. Roy. Soc. **A161**, 220 (1937).

NO_2 is 2 (spin degeneracy). However, if the last electron went into the p_π orbital giving a $^2\Pi$ linear state, this would split into two states, each spin doublets, neither having orbital degeneracy but requiring $p_e=4$ in the thermodynamic sum of states, as these two levels would have essentially the same energy. This value was used by Zeise.[21] Such states, however, would have an angular momentum matrix element connecting them which would be revealed by the magnetic susceptibility. The magnetic moment[22] is only $\frac{1}{2}$ (for spin), showing $p_e=2$.

Our rotational analysis in conjunction with Giauque's work confirms the value of $p_e=2$. In Fig. II-3 the lower dashed curve is log $B_\sigma B_\pi B_\perp$ derived from the thermodynamically determined value of $(R/2)$ ln $I_\sigma I_\pi I_\perp + R$ ln p_e if $p_e=4$; the upper curve is for $p_e=2$. The representative point for our best values of r and α lies closer to the $p_e=2$ curve.

[21] H. Zeise, Zeits. f. Elektrochemie **42**, 785 (1936).

[22] G. G. Havens, Phys. Rev. **41**, 337 (1932).

OCTOBER, 1940 JOURNAL OF CHEMICAL PHYSICS VOLUME 8

The Absorption Spectra of Gaseous Methylamine and Dimethylamine in the Photographic Infra-Red*

A. P. CLEAVES,† H. SPONER AND L. G. BONNER
Physics Department, Duke University, Durham, North Carolina

(Received July 23, 1940)

The absorption spectra of gaseous methylamine and dimethylamine have been measured in the region from 6000 to 12,000A using a 105-foot stainless steel absorption tube and a 3-m grating spectrograph. Absorption bands were observed at 7940, 9100, 9940, 10,070, 10,330 and 11,800A in methylamine and at 7940, 8045, 9100, 10,360, 10,625 and 11,800A in dimethylamine. The only band showing resolvable fine structure was that at 9940A in methylamine. Wherever possible the observed bands have been assigned to overtones and combinations of the fundamental N−H and C−H valence vibrations.

INTRODUCTION

PREVIOUS studies of the absorption spectra of the amines in the photographic infra-red have been confined largely to liquids and solutions. In the region from 0.8 to 1.2μ investigations of homologous series of amines in these forms by M. and R. Freymann[1] have included methylamine and dimethylamine, while P. Barchewitz[2] gives a report of a similar study for the region from 0.6 to 1.0μ. Absorption in the region of the first overtone of N−H valence frequencies has been reported by Liddel and Wulf.[3] It has seemed desirable to supplement these results by observations in gaseous amines, since measurements for the gas, where intermolecular forces do not come into play, lead to more reliable values for the molecular constants. Thompson and Skinner[4] have made this addition for methylamine vapor. In the present work, as part of a larger program, the absorption spectra of the vapors of methylamine[5] and dimethylamine have been photographed in the region from 6000–12,000A.

EXPERIMENTAL

The absorption tube used in this research was the 105-foot stainless steel pipe line recently described.[6] Pressures less than one atmosphere

* A second paper abstracted from a dissertation submitted by A. P. Cleaves to the Graduate School of Arts and Sciences of Duke University in partial fulfillment of the requirements for the degree of Doctor of Philosophy.

† Now at Langley Field, Virginia.

[1] M. Freymann, Comptes rendus **202**, 1674 (1936); **203**, 721 (1936); M. and R. Freymann, J. de phys. et rad. **7**, 476 (1936).

[2] P. Barchewitz, Comptes rendus **204**, 246 (1937); Ann. de physique **11**, 261 (1939).

[3] U. Liddel and O. R. Wulf, J. Am. Chem. Soc. **55**, 3574 (1933).

[4] H. W. Thompson and H. A. Skinner, J. Chem. Phys. **6**, 775 (1938); H. W. Thompson, J. Chem. Phys. **7**, 448 (1939). The first of these papers appeared when this research was already in progress.

[5] A preliminary report was given at the meeting of the Am. Phys. Soc., April, 1939.

[6] H. Sponer and L. G. Bonner, J. Chem. Phys. **8**, 33 (1940).

were used. The light source consisted of the two filaments of a Mazda prefocused headlight bulb connected in series and operated at 14 volts. A concave spherical mirror was placed behind the source to improve the intensity of the light. As spectrograph a 3-m grating with 14,438 lines per inch was used in an Eagle mounting. Most measurements were made in the first order. Slit width was usually 0.06 mm and the dispersion was 5.3A/mm. Eastman spectroscopic plates of types III-N, 144-P, 144-Q and I-Z were used. Exposure times ranged from a few minutes to fifty hours. Standards of wave-length were secured from higher orders of the spectrum of a Pfund iron arc.

The amines used were anhydrous Kahlbaum products triply distilled in vacuum. The near infra-red spectrum of the methylamine and boiling point determinations of a sample of the dimethylamine** demonstrated the absence of the most probable impurities such as water, ammonia and alcohol.

Results

Methylamine

Strong bands of absorption by methylamine vapor have been found in the photographic infra-red at 10,330, 9940 and 7940A at pressures of 5 cm, 20 cm and 60 cm, respectively. There is also evidence at the highest pressure mentioned, of weak absorption at 9100, 10,070 and at about 11,800A. Microphotometer traces of the bands at 10,330 and 7940A revealed no fine structure while the microphotometer trace of the band at 9940A showed a number of separate Q branches definitely resolved on either side of an intensity minimum. Figure 1 shows a microphotometer

TABLE I. *Infra-red bands of methylamine.*

Authors A	Authors cm^{-1}	Thompson and Skinner, Thompson A	M. & R. Freymann (liquid) A	Liddel and Wulf (solution in CCl_4) A	Assignment	Anharmonicity cm^{-1}
7,940	12,590	7,940			$4\nu NH_{\parallel}$	70
9,100	11,000				$4\nu CH_{\perp}$	73
9,940	10,055	9,950	10,064		$3\nu NH_{\perp}$	60
10,070	9,930		10,168		$2\nu NH_{\perp}$	
					$+\nu NH_{\parallel}$	
10,330	9,680	10,310	10,450		$3\nu NH_{\parallel}$	67
11,800	8,470	11,730			$3\nu CH_{\perp}$	70
				15,200	$2\nu NH_{\parallel}$	70

** The boiling point determination was very kindly made by Professor L. A. Bigelow of the Chemistry Department.

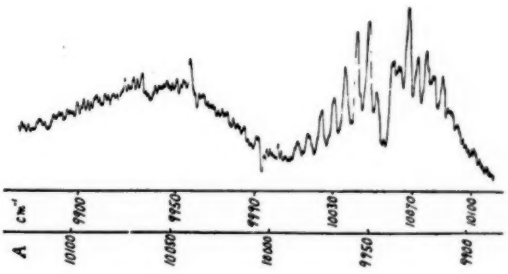

FIG. 1. Microphotometer tracing showing the absorption bands at 9940 and 10,070A in methylamine.

record of the band and also shows the weak band at 10,070A in which there is no definite indication of resolved fine structure. Table I gives our measurements together with those of previous authors for comparison.

Dimethylamine

The more prominent bands of absorption by gaseous dimethylamine have been located at 7940, 8045, 10,360 and 10,625A at a pressure of 25 cm. The microphotometer trace of the first two together with a comparison trace from an exposure through the empty tube is reproduced in Fig. 2. These bands are evidently unresolved, but not of equal intensity, and the same is true of the other two. The difference in intensity is greater, however, in the case of the pair of longer wavelength bands, the band at 10,360A being the most intense in the spectrum. Careful investigation with pressures up to 45 cm did not reveal absorption in the 10,000A region for dimethylamine. At the highest pressure mentioned, however, there was evidence of weak absorption at 9100A and also near the limit of the sensitivity range of the type Z plates, as was the case for methylamine mentioned above. The results together with other authors' measurements are exhibited in Table II.

Discussion of Results

Methylamine

Of the three strong bands at 10,330, 9940 and 7940A the second, reproduced in Fig. 1, shows fine structure. The band is of the perpendicular type, and has clearly resolved P and R branches with a minimum between them. It has been discussed in detail by Thompson and Skinner and by Thompson[4] and molecular structural con-

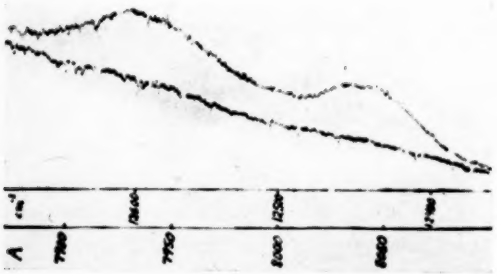

FIG. 2. Microphotometer tracing showing the pair of bands at 7940 and 8045A in dimethylamine, together with a trace from an exposure through the empty tube.

stants have been derived by these authors. We assign the band to $3\nu_{NH}\perp$, i.e., to the threefold excitation of the unsymmetrical amino valence vibration. This is in agreement with Thompson's second paper. With the fundamental value of 3470 known from the Raman effect[7] this gives an anharmonicity $\omega_0 x_0$ of 60 cm^{-1}.

The other two strong bands at 10,330 and 7940A are continuous, and this suggests immediately that they be interpreted as parallel bands whose fine structure, depending on the two largest moments of inertia, could not be resolved with the 3-m grating spectrograph. Even with a 6-m grating instrument Thompson[4] was not able to detect any structure. We associate the bands with the parallel N−H valence vibration, interpreting the band at 10,330A as the second overtone and the band at 7940A as the third overtone of $\nu_{NH}||$. Thompson and Skinner and Thompson[4] took the same interpretation as one possibility of two, the other one being for instance for the 10,330 band $\nu_{NH}\perp+2\nu_{NH}||$. Independent calculations for both bands, using 3360 cm^{-1} as fundamental,[8] lead to anharmonicities of 70 cm^{-1} and 67 cm^{-1}, respectively, which is a good agreement considering the difficulty of locating the centers of the bands correctly. Liddel and Wulf[3] have observed an intense band for a solution of methylamine in carbon tetrachloride at 6580 cm^{-1}. Taking this as the first harmonic in our series we calculate an anharmonicity of 70 cm^{-1} which fits well with the other values. Between the 9940A discrete band and the strong continuous band at 10,330A there appears a much weaker band at 10,070A. It is shown in Fig. 1 on the left side of the 9940 band. From its appearance we conclude that the band is not resolved. We interpret it as $2\nu_{NH}\perp+\nu_{NH}||$. This assignment can be simply checked by calculating whether this band lies one-third from $3\nu_{NH}\perp$ between $3\nu_{NH}\perp$ and $3\nu_{NH}||$ which is exactly the case. That the other combination of $\nu_{NH}\perp+2\nu_{NH}||$ could not be found is perhaps related to the weakness of the fundamental $\nu_{NH}\perp$ in the infra-red. The suggested explanation involves a strong interaction between the two valence N−H vibrations.

Noticeable absorption has been observed also in the region of 11,800A. Its center can be estimated only roughly on account of the decreasing sensitivity of the plate in that region. We believe that this absorption is associated with the C−H valence vibrations, more specifically, we interpret it as the second overtone of $\nu_{CH}\perp$, that is as $3\nu_{CH}\perp$. Locating its center at 8470 cm^{-1} this assignment, together with the value of 2968 cm^{-1} of the fundamental,[8] would result in an anharmonicity of 70 cm^{-1}. Calculation of the third overtone using this anharmonicity leads to a value of 11,030 cm^{-1}. Now a weak band has been found at about 9100A or 11,000 cm^{-1} which we would like to interpret as $4\nu_{CH}\perp$.

TABLE II. *Infra-red bands of dimethylamine.*

Authors A	Authors cm^{-1}	Barchewitz (liquid) A	M. & R. Freymann (liquid) A	Liddel and Wulf (solution in CCl_4) A	Assignment
7,940	12,590	8,010			$4\nu_{NH}$?
8,045	12,430	8,109			
		8,316			
~9,100	11,000	9,100			$4\nu_{CH}\perp$
		9,300			
10,360	9,650		10,452		$3\nu_{NH}$?
10,625	9,410		10,723		
~11,800	8,470				$3\nu_{CH}\perp$
				15,280	$2\nu_{NH}$

Thompson and Skinner have concluded that there can be no free rotation in the methylamine molecule. We agree with their conclusion. Recently the potential barrier has been calculated for the hindered rotation in methyl alcohol[9] to be about 1345 cal./mole. We would expect a slightly higher value for methylamine.

[7] J. S. Kirby-Smith and L. G. Bonner, J. Chem. Phys. **7**, 880 (1939).

[8] A. P. Cleaves and E. K. Plyler, J. Chem. Phys. **7**, 563 (1939); C. R. Bailey, S. C. Carson and E. F. Daly, Proc. Roy. Soc. London **A173**, 339 (1939); R. G. Owens and E. F. Barker, J. Chem. Phys. **8**, 229 (1940).

[9] J. S. Koehler and D. M. Dennison, Phys. Rev. **57**, 1006 (1940).

Dimethylamine

Examination of the observed bands indicates that it is not possible at present to give a unique interpretation. In agreement with Barchewitz we associate the pairs of bands at 8000 and at 10,500A with the N−H valence vibration. Since, however, the fundamental[10] and the first overtone[3] are single it seems difficult to relate more than one band of each pair to this vibration. Barchewitz[2] takes the band at 8109 in the liquid as $4\nu_{NH}$ and another observed by him at 6714A as $5\nu_{NH}$. Taking the fundamental as 3343 cm^{-1} from Raman measurements in the liquid[11] and the band observed by M. and R. Freymann at 10,452A as $3\nu_{NH}$ one obtains values of $\omega_0 x_0$ of 78, 87 and 91 cm^{-1}, respectively for the series. This steady increase in the value of the constant is not surprising in view of the high degree of anharmonicity to be expected in the liquid.

In the gas, however, the situation is much more complex. If we take the fundamental in the gas[10] as 3384 cm^{-1} we obtain from Liddel and Wulf's value an anharmonicity of 111 cm^{-1}. If we now continue the series with the band 9410 cm^{-1} as $3\nu_{NH}$ and 12,430 cm^{-1} as $4\nu_{NH}$ we obtain $\omega_0 x_0$ values of 107 and 92 cm^{-1}.

There seems, however, one objection to this series. Instead of the band at 10,625A it seems more logical to take the stronger band at 10,360A as $3\nu_{NH}$ in analogy to the corresponding band in methylamine. If we do that and also take the stronger band at 7940 of the next pair as $4\nu_{NH}$, this leads to anharmonicities of 84 and 78 cm^{-1}, respectively. This leaves Liddel and Wulf's value completely outside the series. We feel that at present no preference can be given to either interpretation and we have no interpretation to offer for the two bands not taken as NH overtones.

The situation is more favorable for the CH vibrations. Bands have been observed at about the same positions as for methylamine; also the fundamental of the unsymmetrical CH valence vibration is much the same so that the interpretation of these bands as second and third harmonics of this vibration seems safe.

It may be of interest to note that a calculation of the C−H bond energy from the CH series leads to a value of 95 kcal. while values of 93 and 99.5 have been reported from thermochemical calculations.[12]

In conclusion we wish to express our indebtedness to the Penrose Fund of the American Philosophical Society, the National Research Council and Duke University Research Fund for grants-in-aid which made this research possible.

[10] J. S. Kirby-Smith and L. G. Bonner, Phys. Rev. **55**, 1113A (1939).
[11] K. W. F. Kohlrausch, Monatsh. f. Chemie **68**, 349 (1936).
[12] Taken from H. A. Stuart, *Molekülstruktur* (1934), p. 349.

OCTOBER, 1940 JOURNAL OF CHEMICAL PHYSICS VOLUME 8

Note on the Zeeman Effect of Chrome Alum

J. H. VAN VLECK
Harvard University, Cambridge, Massachusetts

(Received July 2, 1940)

It is shown that the Zeeman patterns observed by Spedding and Nutting are comprehensible if and only if the lines in question are intersystem combinations.

SPEDDING and Nutting[1] have studied the Zeeman effect of lines of chrome alum in the vicinity of 15,000 cm^{-1}. They find that the Zeeman pattern consists of unshifted lines, and of lines displaced by twice the normal Lorentz separation i.e. by $\pm 2\beta H$, where $\beta = he/4\pi mc$. It is our purpose to examine what information concerning the energy levels can be derived from this fact. The spectroscopic behavior of the chromic ion is, of course, entirely different in the solid state from in the free gaseous condition, for enormous crystalline fields are present in the

[1] F. H. Spedding and G. C. Nutting, J. Chem. Phys. **3**, 369 (1935).

former. The alums are cubic crystals, but x-ray data[2] show that the fields acting on the paramagnetic ion are not quite cubic, and instead have only trigonal symmetry. Full cubic symmetry, however, is achieved macroscopically, as the unit cell contains four different Cr^{+++} ions whose trigonal axes are related as are the four body-diagonals of a cube. It is known from susceptibility data that the energy levels of the ground state are

$$W_0 \pm \beta H, \quad W_0 \pm 3\beta H, \tag{1}$$

corresponding to the spin-only value of the magnetic moment yielded by $S=\frac{3}{2}$. The upper levels must consequently have Zeeman energies $\pm\beta H$ and/or $\pm 3\beta H$ for otherwise the Zeeman energy cannot change by $0, \pm 2\beta H$. The outer components $\pm 3\beta H$ are of course present only if the state is a quartet. The upper as well as lower levels undoubtedly come from the configuration d^3. The latter yields, besides numerous doublets, the following quartet states in a trigonal, but almost cubic field:

$$^4F\Gamma_2A,\ ^4F\Gamma_4E,\ ^4F\Gamma_4A,\ ^4F\Gamma_5A,\ ^4F\Gamma_5E,\ ^4P\Gamma_4A,\ ^4P\Gamma_4E. \tag{2}$$

Because the crystalline Stark effect decomposes the energy levels, more letters are required to specify a stationary state than for a free ion. The first letter is associated in the usual way with the azimuthal quantum number, the second is the cubic representation in Bethe's notation,[3] and the third is the trigonal representation in Mulliken's terminology,[4] wherein A and E denote singly and doubly degenerate orbital states in a trigonal field. The ground level is $^4F\Gamma_2A$.

We will now show that the upper state cannot be any of the ^4A states. The four spin components of a ^4A level will coincide only if the field is cubic, as can be shown from group theory. Since, actually, the field has only trigonal symmetry, the quartet will be decomposed by spin-orbit interaction into two twofold levels even without an applied magnetic field. This decomposition is very weak as long as the ^4A level is derived from a nondegenerate cubic level, such as Γ_2, but is much larger if the ^4A is associated with a degenerate cubic representation such as Γ_4 or Γ_5, for the quenching of orbital angular momentum is very much less complete in the latter, being due solely to the noncubic portion of the crystalline field, or possibly the Jahn-Teller effect. Consequently in the case of the ground term $^4F\Gamma_2A$, the spin-orbit decomposition of the quartet is of no consequence. It is, in fact, known from data on adiabatic demagnetization and paramagnetic relaxation[5] to be only 0.17 cm^{-1}, and can be disregarded in comparison with Spedding's Zeeman shifts, which are over 2 cm^{-1}. Thus here $\pm\beta H$ and $\pm 3\beta H$ belong effectively to the same state, except for the Zeeman displacements themselves. On the other hand, in the case of the $^4\Gamma_4A$ and $^4\Gamma_5A$ terms, which by (2) are the only possible ^4A levels available for the upper states of Spedding and Nutting's measurements, the quartet will be resolved into two twofold levels whose separation $h\Delta\nu$ is of the same order 5 cm^{-1} as that calculated by Siegert[6] for the ground state of vanadium, which is analogous in that it is derived from a degenerate cubic representation. This separation is large compared with the Zeeman displacement, and so we must regard the displacements $\pm 3\beta H$ as relating to a different origin, or field-free level, than those of type $\pm\beta H$. Furthermore, the Zeeman patterns will have the simple structure $\pm\beta H$ or $\pm 3\beta H$ only as long as the magnetic field is applied parallel to the trigonal axis. Actually there are four different trigonal axes, corresponding to four sub-groups of Cr ions, and so the field must be oblique to some of these axes. The result will be a vastly more complicated Zeeman pattern than for the ground state, where the spin was bound only to the negligible extent 0.17 cm^{-1} and so behaved practically isotopically. If we neglect $H\beta$ in comparison with the spin-orbit splitting $h\Delta\nu$ of the quartet into two pairs, then the explicit formulas for the Zeeman levels associated with $^4\Gamma_5A$ or $^4\Gamma_4A$ are easily seen[7] to be

$$\begin{aligned} W &= W_0 + h\Delta\nu \pm 3\beta H\cos\theta, \\ W &= W_0 \pm \beta H(1+3\sin^2\theta)^{\frac{1}{2}}, \end{aligned} \tag{3}$$

[2] H. Lipson and C. A. Beevers, Proc. Roy. Soc. **148**, 664 (1935); H. Lipson, *ibid.* **151**, 347 (1935).

[3] For explanation of the cubic Stark effect, and underlying group theory, see H. A. Bethe, Ann. d. Physik **3**, 133 (1929).

[4] R. S. Mulliken, Phys. Rev. **43**, 279 (1933).

[5] Data in course of publication independently by Bleaney, by Casimir and du Pré, and by Gorter and Teunissen all give roughly the same separation; also see F. K. du Pré, Physica **7**, 79 (1940).

[6] A. Siegert, Physica **4**, 138 (1937); van den Handel and Siegert, *ibid.* **5**, 871 (1938).

[7] The result (3) can, for instance, be obtained by solving the secular problem connected with the Hamiltonian function $\frac{1}{2}h\Delta\nu S_z^2 + H\beta(S_z\cos\theta + S_x\sin\theta)$.

and thus depend markedly on the angle θ between the magnetic field and the trigonal axis, making the total pattern very involved and of a quite different type from that observed by Spedding and Nutting.

Anisotropic and complicated Zeeman patterns are also to be expected for ^4E states. The quantitative formulas, however, will presumably be somewhat different from (3), since the orbital degeneracy is lifted only in virtue of the Jahn-Teller effect, and there probably is resonance through two or more equivalent configurations.

The assumption of a quartet upper state, either of the A or E type, thus will not work. It may be objected that our argument is based entirely on the not completely certain, though highly probable, assumption that $h\Delta\nu > H\beta$. However, the selection principles rule out quartet upper states in the other case $h\Delta\nu < H\beta$. Then the upper Zeeman pattern, to be sure, has the isotropic structure (1) instead of (3), but the most intense lines would be those without any Zeeman shifts, contrary to experiments. This is true, since the crystalline field decouples the spin from the orbit, so that there is no inducement for the spin to alter its orientation when the orbital quantum numbers change, and we thus have the unacceptable selection rule $\Delta M_s = 0$. Hence the upper state cannot be a quartet in any case.

On the other hand, if the upper state is a doublet $S = \frac{1}{2}$, so that the lines are intersystem combinations, the Zeeman behavior is accounted for nicely. The orbital moment is quenched either in virtue of the natural trigonal field or the Jahn-Teller effect. The spin is effectively free, inasmuch as by Kramers' theorem on double degeneracy, both orientations must have the same energy except for the applied magnetic field. The energy levels become $W_0 \pm \beta H$, and we have Spedding and Nutting's pattern if we have the selection rule that the quantum numbers M_s cannot change by more than one unit.

Precisely this selection rule is indeed yielded by theory for intersystem combinations, since the effect of the spin-orbit interaction is to allow states to combine which differ by up to one unit in M_s. This is because the matrix elements of $A\mathbf{L}\cdot\mathbf{S}$ are of the form $\Delta M_s = 0, 1$ (also $\Delta L = 0, \pm 1$; $\Delta S = 0, \pm 1$) and in the first approximation of perturbation theory, only those states will be blended which can be connected by matrix elements of $A\mathbf{L}\cdot\mathbf{S}$. In other words, the wave function which would be pure quartet without spin-orbit perturbations is "contaminated" with a trace of doublet function which can differ by one unit in M_s, and it is only because of this contamination that intersystem combinations are possible. The transition $\Delta M_s = 0$ is no longer unduly favored as in the case of lines which are not intersystem combinations. Since the lines are now visible only in virtue of the spin-orbit distortion, the $\Delta M_s = 0, \pm 1$ of the blending effect now modulates the possible changes in M_s, so that M_s need no longer be invariant. The transitions $\Delta M_s = \pm 1$ should thus be about as intense as those in which M_s is unaltered. This is what is observed experimentally. The theory does not seem sufficiently refined as yet to account for the polarization rules, or why the relative intensities of the Zeeman components vary as they do when the orientation of the magnetic field relative to the crystallographic axes is changed. Some variation with orientation is not unreasonable, but a detailed quantitative explanation would involve knowledge of just how the orbital selection principles, especially the Laporte rule, are broken down by the crystalline field. As the lines are intersystem combinations, as well as contrary to the Laporte rule, they are highly forbidden by the ordinary selection rules, but this need not cause concern, in view of the enormous concentration of atoms in the solid state. They may be due to dipole transitions caused by coupling with crystal vibrations, to magnetic dipole radiation, or to quadrupole radiation.[8] Which of these is the true cause is as yet unknown.

It is interesting to examine the atomic spectral terms which can give rise to the upper levels observed by Spedding and Nutting. This problem is considered in the following paper, where it is shown that there are doublets which fall in approximately the correct position when allowance is made for the breakdown of Russell-Saunders coupling by the crystalline field.

[8] Cf., for instance, J. H. Van Vleck, J. Phys. Chem. **41**, 67 (1937).

On the Energy Levels of Chrome Alum

R. FINKELSTEIN AND J. H. VAN VLECK
Harvard University, Cambridge, Massachusetts

(Received July 2, 1940)

The energy levels for the configuration d^3 of the chrome ion in chrome alum are calculated by starting with the empirical spectroscopic data on the free Cr^{+++} ion, and then making the assumption that the interatomic forces in the solid state can be represented by a crystalline potential of cubic symmetry, whose magnitude is taken from Schlapp and Penney's theory of the magnetic susceptibility. The particular point to be tested is whether in the solid there is a doublet level only 15,000 cm^{-1} above the basic quartet state, as predicted in the preceding paper from the study of Spedding and Nutting's data on the Zeeman effect. The computed deepest doublet is about 18,200 cm^{-1} higher than the ground level, but the discrepancy is not excessive in view of uncertainties in the parameters of the crystalline field and the fact that any "one-atom" model is only an approximation in the solid state. As already suggested by Spedding and Nutting, it is very essential in computing the positions of *excited* levels, to include elements of the crystalline potential which are nondiagonal in the quantum number L, for without them the lowest doublet is much too high, *viz.* 30,000 cm^{-1} above the ground term. On the other hand, the effect of these nondiagonal members is shown to be unimportant for the *ground* level of greatest multiplicity, not merely for Cr^{+++} but also for other salts of the iron group, so that previous calculations by various writers on magnetic susceptibilities are not appreciably impaired by their assumption of Russell-Saunders coupling.

INTRODUCTION

USUALLY the spectra of solids are characterized by continuous bands rather than discrete lines. Sharp lines, however, are sometimes observed in salts of the iron or rare earth groups, associated with transitions of electrons in incomplete inner shells. Comparatively little has been done in studying these lines theoretically, although the problem is obviously much simpler than that of the energy bands associated with conduction electrons. The comparative simplicity arises from the fact that the electrons may, at least approximately, be regarded as remaining on the same atom, and the interatomic forces may be represented by a crystalline potential. We thus have a one-atom problem, rather than a dynamical system involving infinitely many atoms.

It is the purpose of the present paper to consider the case of potassium chrome alum ($KCr(SO_4)_2 \cdot 12H_2O$). Most of the energy levels belonging to the configuration $3d^3$ of the free Cr^{+++} ion are known from ordinary spectroscopic measurements, and we shall endeavor to estimate the corresponding positions of the levels in solid chrome alum. In the latter, the ion is subject to a field of dominantly cubic character, whose potential may, without loss of generality,[1] be taken to be

$$V=\sum_i V_i \quad \text{with} \quad V_i=D[x_i^4+y_i^4+z_i^4-\tfrac{3}{5}r_i^4]+f(r_i). \tag{1}$$

The sum in (1) is over the three $3d$ electrons. The additive term $f(r_i)$ will vanish if the potential satisfies Laplace's equation, as we shall henceforth assume. Very likely it does not do so, but the resulting correction is merely an additive constant common to all levels of the configurations $3d^3$ and so is of no importance for us.

It will be necessary to calculate only the energy levels belonging to the configuration $3d^3$, for orbits associated with other configurations are not sufficiently sequestered in the interior of the atom to give rise to sharp lines, and also usually involve too high an energy to be involved in absorption lines in the optical region. The observed lines are thus internal to the configuration $3d^3$, and so violate the Laporte rule, as discussed in the preceding paper.

[1] The generality results because higher harmonics than those of the fourth degree in development of the crystalline potential make no contribution for d electrons. See, for instance footnote 4 of J. H. Van Vleck, J. Chem. Phys. **7**, 61 (1939).

It is not necessary for us to include the modifications of the energy levels resulting from spin-orbit coupling, or from the fact that, strictly speaking, the crystalline potential has trigonal rather than perfectly cubic symmetry, for we only endeavor to locate the energy levels to within an error of the order 10^3 cm^{-1}. This is sufficient accuracy to answer the question as to whether it is reasonable that there be doublet levels 15,000 cm^{-1} above the ground level state, as predicted in the previous paper from the study of the Zeeman measurements of Spedding and Nutting. To essay higher accuracy would be presumptuous in view of the qualitative and provisional nature of existing models of forces in solid salts.

In the ordinary Penney-Schlapp theory[2] of magnetic ions in the solid state, elements of the crystalline potential which are nondiagonal in the quantum number L are neglected. This approximation is equivalent to assuming that L is a good quantum number. This supposition is not warranted in the case of the doublet states of chrome alum, although we shall later see (cf. end of article) that it is reasonably adequate for the quartets, and in particular the ground state $d^3\,{}^4F\Gamma_2$ involved in determinations of the magnetic susceptibility. Spectroscopic measurements, however, can involve excited doublet states, and so we must allow for the breakdown of L coupling, and so consider matrix elements nondiagonal in L. We shall, however, neglect elements of the crystalline potential nondiagonal in the principal quantum number n. Such elements express the fact that this potential blends $3d^3$ with other configurations, but fortunately the latter involve such high energies that the resulting modifications are probably not important.

The LS System of Representation

One way of finding the necessary matrix elements would doubtless be to use Kramers'[3] symbolic $\xi\eta$ method, closely related to group theory. For our purpose, however, it is simpler and more straightforward to utilize explicit wave functions. Some of the wave functions appropriate to Russell-Saunders coupling for the configurations d^3 have been given by Condon and Shortley,[4] and the rest can be obtained by a procedure fully described by them.

These characteristic functions, of $\mathfrak{L}^2$, $\mathfrak{S}^2$, $\mathfrak{L}_z$ and $\mathfrak{S}_z$, are as follows, omitting the quartet states and those doublet states given by Condon and Shortley:

$$
\begin{aligned}
({}^2H\,1) &= [8\beta+6\theta+4P-3V-R+3X-2Z-\zeta]/(210)^{\frac{1}{2}},\\
({}^2H\,0) &= [\lambda+\gamma+4Y-2\alpha-2\eta-W+2Q-S]/(42)^{\frac{1}{2}},\\
({}^2G\,1) &= [12\beta-6\theta+6P+6R-12V-3X+7Z-4\zeta]/(840)^{\frac{1}{2}},\\
({}^2G\,0) &= [\lambda-\gamma+2\alpha-2\eta-2W+2S]/(28)^{\frac{1}{2}},\\
({}^2F\,1) &= [4\beta+6\theta-6P+2R+4V-X+Z]/(120)^{\frac{1}{2}},\\
({}^2F\,0) &= [-\lambda-\gamma+4Y-2\alpha-2\eta+2W-4Q+2S]/(60)^{\frac{1}{2}},\\
(a\,{}^2D\,1) &= [\beta-\theta+V-R]/2, \quad (a\,{}^2D\,0) = [\alpha-\eta+W-S]/2,\\
(b\,{}^2D\,1) &= [-\beta-3\theta-4P+V+3R+2X-2\zeta]/(84)^{\frac{1}{2}},\\
(b\,{}^2D\,0) &= [-2\lambda+2\gamma+3\alpha-3\eta-3W+3S]/(84)^{\frac{1}{2}},\\
({}^2P\,1) &= [-9\beta+9\theta+6P+6V-12R+X+4Z-5\zeta]/(630)^{\frac{1}{2}},\\
({}^2P\,0) &= [-3\lambda-3\gamma+2Y-\alpha-\eta-4W+8Q-4S]/(210)^{\frac{1}{2}}.
\end{aligned}
$$

The value of M_L is indicated by the last index on the left side (0 or 1) and we have supposed in each

[2] W. G. Penney and R. Schlapp, Phys. Rev. **41**, 194 (1932); Schlapp and Penney, *ibid.* **42**, 666 (1932).
[3] H. A. Kramers, Proc. Amst. Acad. **33**, 953 (1930); **34**, 965 (1931).
[4] E. U. Condon and G. Shortley, *The Theory of Atomic Spectra* (Cambridge University Press, 1935), p. 226.

instance that $M_S=+\frac{1}{2}$. We have used the abbreviations:

$$P=(2^+1^--2^+),\quad Q=(2^+0^--2^+),\quad R=(2^+1^+-2^-),\quad S=(2^+0^+-2^-),\quad V=(2^-1^+-2^+),$$

$$W=(2^-0^+-2^+),\quad X=(2^+0^--1^+)\sqrt{6},\quad Y=(1^+0^--1^+),\quad Z=(2^+0^+-1^-)\sqrt{6},\quad \alpha=(1^+0^+-1^-),$$

$$\beta=(1^+1^--1^+),\quad \gamma=(2^+-1^--1^+)\sqrt{6},\quad \zeta=(2^-0^+-1^+)\sqrt{6},\quad \eta=(1^-0^+-1^+),\quad \theta=(1^+0^-0^+),$$

$$\lambda=(1^+1^--2^+)\sqrt{6},$$

where a notation such as $(0^+-2^-2^+)$ means an antisymmetrical wave function in which one electron has $m_l=0$, another has $m_l=-2$, and, the third has $m_l=+2$. The superscripts refer to the two spin possibilities $M_S=\pm\frac{1}{2}$. The electrons of course all have $l=2$, since the configuration is d^3. To get $\psi(-M_L)$, we reverse the sign of all the m_l, and multiply by $(-1)^{M_L}$, and to obtain states for $M_S=-\frac{1}{2}$ we reverse the sign of all the superscripts.

Since the potential is of the form ΣV_i, its matrix components are simply expressible in terms of those of a single electron. The diagonal elements are

$$(a_1\cdots a_n|\,V\,|a_1\cdots a_n)=\textstyle\sum_{i=1,\cdots N}(a_i|\,V_i\,|a_i).$$

The only other nonvanishing elements are of the form

$$(a_1\cdots a_k\cdots a_n|\,V\,|a_1'\cdots a_l'\cdots a_n')=\epsilon(a_k|\,V\,|a_l')$$

with $a_1'\cdots a'_{l-1}\,a'_{l+1}\cdots a_N$ restricted to be merely a permutation of $a_1\cdots a_{k-1}a_{k+1}\cdots a_n$. The factor ϵ is $+1$ or -1 according as this permutation is even or odd. Since we are dealing with a three-electron system, the value of N is 3.

For the matrix $(m_l|\,V_i\,|m_l')$ we have[2]

$$(m_l|\,V\,|m_l')=\tfrac{1}{2}\{\tfrac{1}{6}(35m_l^4-155m_l^2+72)\delta_{m_l,m_l'}+10\delta_{m_l,m_l'+4}+10\delta_{m_l,m_l'-4}\}Dq, \tag{2}$$

where m_l, $m_l'=-2,-1\cdots+2$, and where Dq is the constant of Penney and Schlapp,[2] *viz.*

$$2(m_l|r^4|m_l)/105.$$

The $L\Gamma$ System of Representation

Our functions represent eigenstates of $\mathfrak{L}$ and $\mathfrak{S}$, but it is not necessary to diagonalize $\mathfrak{J}$, as we are neglecting spin-orbit coupling, which is subordinate in the solid state. On the other hand, it is advisable to use as basis functions those which diagonalize the potential (1) apart from elements non-diagonal in L. Such functions must be classified according to their cubic representation[5] Γ rather than according to M_L. In other words, they diagonalize $\mathfrak{L}^2$ but not $\mathfrak{L}_z$. The secular equations associated with the passage from the M_L to the Γ systems of representation have been given by Penney and Schlapp up to $L=4$ and the case $L=5$ can be treated by similar methods. (In their first paper they considered $J=4$ rather than $L=4$, but the mathematical structure is similar.)

The transformation matrix $(L\Gamma|\,LM_L)$ can thus be calculated, and is shown in Table I.

The representations Γ_4 and Γ_5 are triply degenerate, and in each case two of their wave functions are obtained by using the two sign possibilities in the left side of Table I, while the third is found either in the central or in the right portion. Each doubly degenerate state Γ_3 has one wave function in the central part and one on the right. There are two threefold states of the form ${}^2H\Gamma_4$, and they are distinguished by the indices α and β.

---

[5] For explanation of the different cubic representations, see H. A. Bethe, Ann. d. Physik **3**, 133 (1929).

TABLE I.*

$M_L=$	∓ 5	∓ 1	± 3
$^2H\Gamma_5$	$\frac{1}{5}(30)^{\frac{1}{2}}$	$-\frac{1}{4}\sqrt{7}$	$-\frac{1}{8}\sqrt{6}$
$^2H\Gamma_4\alpha$	$-\frac{1}{5}d^{\frac{1}{2}}$	$\frac{1}{3}ad^{\frac{1}{2}}/(10)^{\frac{1}{2}}$	$-\frac{1}{6}ed^{\frac{1}{2}}/\sqrt{5}$
$^2H\Gamma_4\beta$	$\frac{1}{5}c^{\frac{1}{2}}$	$\frac{1}{3}bc^{\frac{1}{2}}/(10)^{\frac{1}{2}}$	$\frac{1}{6}fc^{\frac{1}{2}}/\sqrt{5}$
$^2G\Gamma_5$	0	$\frac{1}{4}\sqrt{2}$	$-\frac{1}{4}(14)^{\frac{1}{2}}$
$^2G\Gamma_4$	0	$\frac{1}{4}(14)^{\frac{1}{2}}$	$\frac{1}{4}\sqrt{2}$
$^2F\Gamma_5$	0	$-\frac{1}{4}(10)^{\frac{1}{2}}$	$\frac{1}{4}\sqrt{6}$
$^2F\Gamma_4$	0	$\frac{1}{4}\sqrt{6}$	$\frac{1}{4}(10)^{\frac{1}{2}}$
$^2D\Gamma_5$	0	1	0
$^2P\Gamma_4$	0	1	0

	$+2$	-2
$^2H\Gamma_5$	$\frac{1}{2}\sqrt{2}$	$\frac{1}{2}\sqrt{2}$
$^2H\Gamma_3$	$\frac{1}{2}\sqrt{2}$	$-\frac{1}{2}\sqrt{2}$
$^2G\Gamma_5$	$\frac{1}{2}\sqrt{2}$	$-\frac{1}{2}\sqrt{2}$
$^2G\Gamma_3$	$\frac{1}{2}\sqrt{2}$	$\frac{1}{2}\sqrt{2}$
$^2D\Gamma_5$	$\frac{1}{2}\sqrt{2}$	$-\frac{1}{2}\sqrt{2}$
$^2D\Gamma_3$	$\frac{1}{2}\sqrt{2}$	$\frac{1}{2}\sqrt{2}$
$^2F\Gamma_5$	$\frac{1}{2}\sqrt{2}$	$\frac{1}{2}\sqrt{2}$
$^2F\Gamma_2$	$\frac{1}{2}\sqrt{2}$	$-\frac{1}{2}\sqrt{2}$

	$+4$	-4	0
$^2H\Gamma_4\alpha$	$\frac{1}{2}a^{\frac{1}{2}}/\sqrt{6}$	$\frac{1}{2}a^{\frac{1}{2}}/\sqrt{6}$	$-\frac{1}{6}ba^{\frac{1}{2}}/\sqrt{5}$
$^2H\Gamma_4\beta$	$\frac{1}{2}b^{\frac{1}{2}}/\sqrt{6}$	$\frac{1}{2}b^{\frac{1}{2}}/\sqrt{6}$	$\frac{1}{6}ab^{\frac{1}{2}}/\sqrt{5}$
$^2H\Gamma_3$	$\frac{1}{2}\sqrt{2}$	$-\frac{1}{2}\sqrt{2}$	0
$^2G\Gamma_4$	$\frac{1}{2}\sqrt{2}$	$-\frac{1}{2}\sqrt{2}$	0
$^2G\Gamma_3$	$(7/24)^{\frac{1}{2}}$	$(7/24)^{\frac{1}{2}}$	$-(5/12)^{\frac{1}{2}}$
$^2G\Gamma_1$	$(5/24)^{\frac{1}{2}}$	$(5/24)^{\frac{1}{2}}$	$(7/12)^{\frac{1}{2}}$
$^2F\Gamma_4$	0	0	1
$^2D\Gamma_3$	0	0	1
$^2P\Gamma_4$	0	0	1

* Here $a=6+(21)^{\frac{1}{2}}$, $b=6-(21)^{\frac{1}{2}}$, $c=\frac{1}{14}[153+33(21)^{\frac{1}{2}}]$, $d=\frac{1}{14}[153-33(21)^{\frac{1}{2}}]$, $e=19+4(21)^{\frac{1}{2}}$, $f=19-4(21)^{\frac{1}{2}}$.

The elements of V in the $L\Gamma$ representation, measured in multiples of Dq, are now found to be

^2H	^2G	^2F	^2D_a	^2D_b
-1.335	-1.605	-1.055	7.30	-1.595
	1.86	2.535	-2.935	3.84
		-0.335	5.775	2.525
	$(^2\Gamma_5)$		-2	2.18
				1.81

^2H	^2H	^2G	^2F	^2P
2.61	0	6.17	1.73	0.588
	-2.61	4.45	-0.635	4.98
		-1	-1.73	-2.78
	$(^2\Gamma_4)$		1	-5.88
				0

	^2H	^2G	^2D_a	^2D_b
	2	9.64	5.48	-1.195
		-0.285	5.86	-7.66
	$(^2\Gamma_3)$		3	-3.27
				-2.715

^4F	^4P
6	4
$(^4\Gamma_4)$	0

$(^2F\,\Gamma_2|\,V|\,^2F\,\Gamma_2)=-2$

$(^2G\,\Gamma_1|\,V|\,_2G\,\Gamma_1)=-2$

$(^4F\,\Gamma_5|\,V|\,^4F\,\Gamma_5)=-2$

$(^4F\,\Gamma_2|\,V|\,^4F\,\Gamma_2)=-12$

These of course include elements nondiagonal in L as well as those elements which blend together the two D states. Only states corresponding to the same cubic representation and same multiplicity combine. Since the determinants are symmetrical, we omit writing the elements below the diagonal. The Dirac notation has been used for the representations occurring only once, whose elements are, of course, entirely diagonal.

To the matrix of the crystalline potential it is now necessary to add the matrix of the Russell-Saunders energy E of the free ion. The matrix elements for the states occurring once are all diagonal in the $L\Gamma$ system of representation and are as follows expressed in wave number units measured upward from the ground state[6]

$$^4F=0,\quad ^4P=14{,}200,\quad ^2G=15{,}200,\quad ^2P=19{,}400,\quad ^2H=21{,}200,\quad ^2F=(33{,}700)\ \text{cm}^{-1}. \tag{3}$$

The elements corresponding to the two D states are

$$(^2D_a|\,E\,|^2D_a)=27{,}500,\quad (^2D_a|\,E\,|^2D_b)=12{,}700,\quad (^2D_b|\,E\,|\,D_b)=46{,}600\ \text{cm}^{-1} \tag{4}$$

with characteristic values

$$^2D=20{,}600,\qquad ^2D'=(53{,}500)\ \text{cm}^{-1}. \tag{5}$$

[6] For spectroscopic data on the free Cr IV ion, see I. S. Bowen, Phys. Rev. **52**, 1153, (1937). The writers are much indebted to Professor Bowen for communicating to them his determinations of the positions of the ^2P and low ^2D terms, which he has not published, but which we have incorporated in (3) and (5).

Entries in parenthesis mean that a direct spectroscopic determination is not available, and that the levels have been located approximately by extrapolation from isoelectronic configurations or by means of the "*FG*" relations of Slater-Condon-Shortley.

There are two useful checks which we have used against numerical errors in writing down the various preceding matrices. In the first place, the elements of the crystalline potential down the principal diagonal correspond to the conventional Penney-Schlapp theory,[2] and can be obtained, as they show, in a purely algebraic fashion independent of wave functions, by using essentially the methods of group theory. The latter does not determine a proportionality constant, but this can be obtained by using the Goudsmit[7] method of diagonal sums.[6] (The two ^2D states cannot, however, be resolved by this method.) In the second place, when all the Russell-Saunders energies are arbitrarily taken equal, i.e., (3) and (4) omitted, the L quantization becomes extraneous, and the electrons are individually quantized in the cubic field. Under these circumstances, the energy of an individual electron is $-4Dq$ or $6Dq$, since solution of the characteristic value problem connected with (2) yields roots $-4Dq$ and $6Dq$, occurring three and two times, respectively. Hence the roots of the related secular equation must in this other limiting case be of the form $n\cdot(-4Dq)+(3-n)\cdot 6Dq$ $(n=1,2,3)$. An interesting but somewhat involved argument based on group theory and explained below in fine print, shows that the correlation of the different roots with the various secular equations is as follows for the doublet levels, in multiples of Dq:

$$\Gamma_1\colon -2;\quad \Gamma_2\colon -2;\quad \Gamma_3\colon -12,-2,-2,+18;\quad \Gamma_4\colon -12,-2,-2,8,8;\quad \Gamma_5\colon -12,-2,-2,8,8. \tag{6}$$

If we regard the diagonal elements of the determinants as known, from the conventional Penney-Schlapp theory or otherwise, then when the secular determinants are quadratics, the off-diagonal elements can be determined without the use of explicit wave functions by the Goudsmit inspection method,[7] i.e., simply by the requirement that the roots reduce properly to (6) in the corresponding limit. In particular, the formulas for the quartets can be obtained entirely by this inspection method, and we have consequently not bothered to write out the wave functions for them.

Proof of (6). When the Russell-Saunders energies are all taken equal, the electrons can be separately quantized in the crystalline field, and the wave functions considered to be simple products,[8] rather than sums of products of the individual functions as previously. The individual factors are characteristic functions of the "one-electron" secular problem connected with (2), and correspond to Γ_3 or Γ_5 of the cubic group, for these are the cubic resolution of the representation $l=2$ of the rotation group. To apportion roots to the secular equations associated with the three-electron problem, we must evaluate the irreducible representations contained in the triple direct product. The theory of characters shows that

$$\begin{gathered}\Gamma_3\times\Gamma_3\times\Gamma_3=[\Gamma_1+\Gamma_2+\Gamma_3]+2\Gamma_3,\quad \Gamma_5\times\Gamma_5\times\Gamma_5=[\Gamma_1+\Gamma_4+2\Gamma_5]+(\Gamma_2)+2\Gamma_3+2\Gamma_4+2\Gamma_5,\\ \Gamma_3\times\Gamma_3\times\Gamma_5+\Gamma_3\times\Gamma_5\times\Gamma_3+\Gamma_5\times\Gamma_3\times\Gamma_3=[\Gamma_4+2\Gamma_5]+(\Gamma_4)+4\Gamma_4+4\Gamma_5,\\ \Gamma_3\times\Gamma_5\times\Gamma_5+\Gamma_5\times\Gamma_3\times\Gamma_5+\Gamma_5\times\Gamma_5\times\Gamma_3=[\Gamma_1+\Gamma_2+2\Gamma_3+\Gamma_4+\Gamma_5]+(\Gamma_4+\Gamma_5)+2\Gamma_1+2\Gamma_2+4\Gamma_3+4\Gamma_4+4\Gamma_5.\end{gathered} \tag{7}$$

Here we have included in square and round parentheses the parts of the total direct product which are absorbed by the symmetrical and antisymmetrical direct products, respectively. The symmetrical product corresponds to an orbital wave function symmetrical in three electrons, and so is not allowed by the exclusion principle, while the antisymmetrical product obviously embodies the quartet states. The portion not enclosed in either type of parenthesis represents an intermediate type of symmetry appropriate to doublet states. The occurrence of these states is just half as great as that indicated by (7), because two states of this intermediate orbital symmetry are required in order to construct one totally antisymmetric wave function when the spin is included.[9]

The result (6) then follows from (7) on noting that a factor Γ_5 or Γ_3 on the left side of (7) corresponds, respectively, to an energy $-4Dq$ and $6Dq$ for a single electron. (We must correlate $-4Dq$, $6Dq$ with Γ_5, Γ_3 rather than vice versa, because triple and double roots of the secular problem connected with (2) must correspond to three- and twofold representations, respectively.)

The derivation of (7) itself requires some discussion, which we now give. The reduction of the total direct product is obtained by standard methods of group theory. The symmetrical direct product of the form $a\times a\times a$ can be reduced by

[7] S. Goudsmit, Phys. Rev. **31**, 946 (1928); **35**, 1325 (1930).

[8] The wave function is, of course, expressible as a simple product only before "antisymmetrization" with respect to spin and orbit combined. Our classification of symmetry types in the section in fine print relates to purely orbital permutation, and of course only an antisymmetrical representation is allowed when spin is included.

[9] Cf. E. Wigner, Zeits. f. Physik **40**, 492 (1927); *Gruppentheorie*, Chap. XXII.

rules given by Tisza.[10] There is no antisymmetrical portion involved in $\Gamma_3\times\Gamma_3\times\Gamma_3$, since an antisymmetric triple product cannot be constructed when only two functions are available, as is the case for a doubly degenerate representation like Γ_3. With Γ_5 there are three functions available, so that one antisymmetrical product can be built. This must correspond to a onefold representation. Hence Γ_2 represents the antisymmetrical part of $\Gamma_5\times\Gamma_5\times\Gamma_5$, inasmuch as Γ_1, the only other onefold representation contained in the total direct product, has already been absorbed by the symmetrical portion. To find the symmetrical and antisymmetrical parts of $[a\times a]\times b$ we use the following rule: If a given representation occurs n times in $[a\times a]\times b$, it is contained n times in the symmetrical or antisymmetrical parts of $[a\times a]\times b+[a\times b\times a]+[b\times a\times a]$ according as it arises from $[a\times a]_{\text{sym}}\times b$ or $[a\times a]_{\text{anti}}\times b$. This statement follows from the fact that one symmetrical or antisymmetrical wave function can be built from a triple product if two factors are already symmetrized or antisymmetrized, and the third is unlike the other two.

Results

To evaluate the roots of our secular determinants numerically, we take the constant Dq equal to 1500 cm^{-1}, as this is the round value indicated by susceptibility data.[11,12] The levels in solid chrome alum then prove to be

$^2\Gamma_5$ 76,500 cm^{-1}	$^2\Gamma_4$ 47,500 cm^{-1}	$^2\Gamma_5$ 25,900 cm^{-1}
$^2\Gamma_3$ 75,600	$^2\Gamma_4$ 40,500	$^4\Gamma_4$ 23,100
$^2\Gamma_4$ 59,000	$^2\Gamma_3$ 36,400	$^2\Gamma_4$ 19,300
$^2\Gamma_3$ 55,900	$^4\Gamma_4$ 36,100	$^2\Gamma_3$ 18,200
$^2\Gamma_5$ 48,700	$^2\Gamma_5$ 34,600	$^4F\Gamma_5$ 15,000
$^2\Gamma_5$ 48,700[12]	$^2\Gamma_4$ 34,400	$^4F\Gamma_2$ 0.
$^2\Gamma_2$ 48,600	$^2G\Gamma_1$ 30,200	

Here the origin is taken at the ground state in the solid state, which is depressed $12Dq=18{,}000$ cm^{-1} as compared with the ground state of the free ion. The corresponding levels for the free Cr^{+++} ion, which are basic to the calculation, are given in (3) and (5).

According to (8) the lowest doublet level is 18,200 cm^{-1} above the ground state. Our interpretation[13] of Spedding and Nutting's measurements[14] on the Zeeman effect requires that there be doublet levels only 14,900 cm^{-1} above the basic term. The discrepancy of about 3000 cm^{-1} probably seems rather large to atomic spectroscopists accustomed to specifying an energy level to within less than a wave number. However, the agreement seems adequate when it is remembered that calculations on the solid state are necessarily more or less qualitative and lack the precision of the refined theory of the spectra of free atoms. It is to be emphasized that we are making a somewhat different application than usual of the theory of the crystalline potential, as we are using the latter to locate the position of excited levels rather than merely to determine the magnetic susceptibility of the ground state. The rough accord achieved with experiment by our calculations can be regarded both as a confirmation of our interpretation of Spedding and Nutting's data, and of the real physical significance of the constant Dq of the Penney-Schlapp cubic crystalline potential. The discrepancy may be due to the fact that our assumed value 1500 cm^{-1} of Dq, although correct as regards rough order of magnitude, may be a little low. There are no adequate determinations of Dq available for chrome alum, and it is necessary for us to base our estimates on salts not merely of different chemical composition, but also of different valence.[15] The best measurements of Dq are furnished by susceptibility data on Tutton or other closely related salts of nickel. The doublets are brought to within the proper distance 14,900 cm^{-1} of the basic quartet if we take Dq about 1820 cm^{-1}, and such a change

[10] L. Tisza, Zeits. f. Physik **82**, 48 (1933).

[11] Cf. reference 2 and J. H. Van Vleck, J. Chem. Phys. **7**, 81 (1939).

[12] The entry 48,700 appears twice because there is approximately a double root of the $^2\Gamma_5$ secular equation at this position.

[13] J. H. Van Vleck, J. Chem. Phys. **8**, 790 (1940).

[14] F. H. Spedding and G. C. Nutting, J. Chem. Phys. **3**, 369 (1935).

[15] It is hard to tell whether Dq should increase or decrease in going from nickel to chromium, as the trivalent rather than divalent behavior tends to diminish the mean value of $x^4+y^4+z^4$, whereas the lesser nuclear charge acts in the opposite direction. Furthermore, changes in $x^4+y^4+z^4$ may be more than compensated by corresponding alterations in the distance R to the nearest water molecules, since increasing valence diminishes R, and since Dq is proportional to R^{-5} or R^{-6} according as the molecules act as point charges or as dipoles. The observations of Dq directly for chromium salts by Janes and others are not made on alums, and are not reliable, since determinations of Dq in chromium from susceptibility measurements are inordinately difficult because they require the precise determination of a very small deviation of the susceptibility from the "spin only" value. Cf. reference 11.

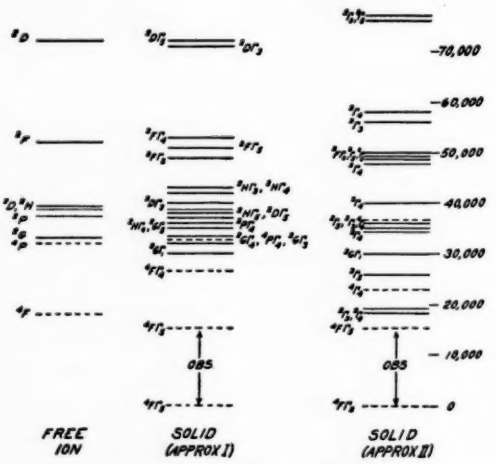

FIG. 1. The left side of the figure gives the empirical energy levels for the free ion, while approximations I and II show the corresponding positions in the solid alum, and are, respectively, exclusive and inclusive of matrix elements nondiagonal in the quantum number L. Doublet states are indicated by solid lines, and quartets by dashed. The preceding paper shows that the "observed" discrete absorption represents intersystem combination. Hence to obtain agreement with experiment, a solid line should coincide with the upper end of the arrow.

in the value of Dq does not seem excessive in view of the elements of uncertainty just mentioned. Quite irrespective of the question of the size of Dq, there are other errors latent in the calculations which are sufficient to explain the discrepancy. The field is, in the first place, not accurately cubic, and furthermore the "one-atom" method envisaged by the use of a crystalline potential is itself only an approximation.[16] Actually in the solid state one has all the intricacies of the "many-atom" problem, in particular the complications due to the Jahn-Teller effect, as previously discussed by one of the authors,[16] and also possible overflowing of the electrons onto adjacent atoms,—an effect recognized in the method of molecular orbitals but not in that of crystalline potentials.

One thing stands out clearly from the calculations, and that is that in the case of the doublet states it is very essential to include the effect of the matrix elements nondiagonal in L. In fact, without them, the deepest doublet level would be a $^2G\Gamma_1$ term 30,200 cm^{-1} above the ground state, far too high. It was our perplexity at this disagreement that led us to undertake the detailed calculations of the present paper inclusive of nondiagonal elements in L. The blending of various doublet states caused by the nondiagonal elements in L is so complete that the quantum number L usually loses all meaning, and it is impossible to classify the levels as ^2G, ^2H, etc. (except for the representations Γ_1, Γ_2 involving only one value of L). Spedding and Nutting[14] have already suggested that the calculation would probably yield this result. For the quartets, however, the error involved in dropping nondiagonal terms in L is not serious. Without the diagonal terms, the $^4F\Gamma_4$ and $^4P\Gamma_4$ states would fall at 27,000 and 32,200 cm^{-1} instead of 23,100 and 36,100 cm^{-1}, respectively.

The results of our calculations are shown graphically in Fig. 1, where approximations I and II are, respectively, exclusive and inclusive of the nondiagonal elements in L. The bottom level in approximation I is considerably deeper than that for the free ion because the ground state $^4F\Gamma_2$ is depressed $12Dq=18{,}000$ cm^{-1} by the crystalline potential. There is no commensurate depression of the doublet states unless we include nondiagonal elements in L, and it is for this reason that with Russell-Saunders coupling the doublet-quartet interval turns out to be 30,200 cm^{-1} even though the line $^4F-{}^2G$ falls at 15,200 cm^{-1} in the free ion. It will be noted that there is little correspondence between the energy levels of the solid and gas, and theories[17] of the solid state based on the assumption that the displacement between the solid and gaseous state amounts to only a few hundred cm^{-1} are obviously spurious.

It will be noted that according to our computations the $^4F\Gamma_5$ state is not far removed from the upper states studied by Spedding and Nutting. The Zeeman pattern resulting from the transition $^4F\Gamma_2-{}^4F\Gamma_5$ would be quite different from that of the observed lines, as stressed in the preceding paper.[13] One wonders why the line $^4F\Gamma_2-{}^4F\Gamma_5$ has escaped observation. The answer is, no doubt, that all the excited levels are somewhat lower than shown in the figure, since otherwise the $^2\Gamma_3$ state does not fall at the right position and that consequently the quartet is displaced down to a region where it is masked

[16] For further discussion see, for instance, J. H. Van Vleck, J. Chem. Phys. **7**, 61 (1939).

[17] E.g. O. Deutschbein, Zeits. f. Physik **77**, 489 (1932); D. M. Bose and S. Datta, Zeits. f. Physik **80**, 376 (1933).

by the continuum associated with transitions of exterior ($4s$, $4p$, etc.) rather than d^3 electrons. This continuum has a rift merely between about 14,000 and 16,000 cm^{-1}.[18] The narrowness of this gap makes it impossible to try to observe most of the levels shown in Fig. 1. Spedding and Nutting have observed several levels in the narrow region accessible to observation, but it would be futile to try to identify them with the individual roots of our secular determinant. In the first place, degenerate cubic states will be split by the noncubic portions of the crystalline field, and besides this, some of the states may be repeated at intervals of the order 10 to 10^2 cm^{-1} due to vibrational structure. Hence the various levels found experimentally are not necessarily to be identified with different electronic states.

States of Highest Multiplicity in Vanadium, Cobalt, and Nickel

Because of the reciprocal character of the configurations d^3 and d^7 our calculations also apply to Co^{++}, with merely a change in sign of the constant Dq. It can be shown [19] that the determinants for the quartets also apply to the corresponding triplets in $V^{+++}(d^2)$ and $Ni^{++}(d^8)$ with a sign change in Dq for V^{+++}, but not for Ni^{++}, as in the latter there are two compensating sign changes. These observations enable one to study how far the susceptibility calculations for vanadium and cobalt are modified by the partial loss of significance of the quantum number L as suggested by Spedding. In the case of chromium, this question does not enter, as the ground state is the only one belonging to the representation $^3\Gamma_2$. In vanadium the interval $^3F-{}^3P$ for the free ion is 13,000 cm^{-1}, and we find on solving our secular equation for $^3\Gamma_4$ states, that the basic state $^3F\Gamma_4$ is of the form

$$\psi = (0.94)^{\frac{1}{2}}(^3F) - (0.06)^{\frac{1}{2}}(^3P). \qquad (8)$$

This result was quoted in a previous paper by one of the writers and shows that in Siegert's calculations, the assumption of Russell-Saunders coupling is much closer to the truth than that of complete breakdown.[20] In the case of Co^{++} the interval $^3F-{}^3P$ is somewhat wider than in V^{+++}, and the coefficients are about $(0.95)^{\frac{1}{2}}-(0.05)^{\frac{1}{2}}$. The "contamination" by ^4P is too small to alter materially[21] Schlapp and Penney's calculation of the susceptibility of cobaltous compounds made on the assumption that the basic state is pure ^4F.

[18] There is also a rift in the vicinity of 22,000 cm^{-1}, and sharp lines are also observed in this vicinity (cf. F. H. Spedding and G. C. Nutting, J. Chem. Phys. **2**, 421, 1934). Reference to our table of calculated levels for the solid shows that these lines probably arise from $^2\Gamma_5$ or $^4\Gamma_4$ upper states, when allowance is made for the fact that our computed positions of excited levels are probably 3000 cm^{-1} or so too high. It would be interesting if Zeeman observations were available on these lines, for the preceding paper (reference 13) shows that the behavior of the Zeeman patterns would be quite different according as the lines are doublets or quartets.

[19] There is a reciprocal relation between the behavior of the triplet states of d^3 (or d^7) and the quartet levels of d^4 (or d^6), for the filled states in the latter can be correlated with "holes" in the Stark pattern of the former inasmuch as a d level has five spatial substates. There is, however, a sign reversal in Dq when one goes from one case to the other. See J. H. Van Vleck, Phys. Rev. **41**, 208 (1932).

[20] The results mentioned in fine print on p. 69 of a previous paper, reference 1, follow from the fact that the departures from Russell-Saunders coupling reduce the orbital moment of the $^3F\Gamma_4$ state by a factor $a^2-\frac{2}{3}b^2$ as compared with ideal R-S coupling, where a and b are, respectively, the first and second coefficients in (8). The values of a^2 and b^2 corresponding to complete breakdown of this coupling (i.e., individual quantization) would be $\frac{4}{5}$, $\frac{1}{5}$.

[21] The incipient breakdown of the Russell-Saunders coupling lowers the orbital moment matrix for the $^4F\Gamma_4$ state of cobalt by about 8 percent, and so perhaps reduces by about 16 percent the deviations of the calculated susceptibility of cobalt from the spin only value, since the susceptibility involves the magneton number quadratically. (Exact, reliable figures cannot, however, be given without long calculations, which do not seem worth while.) This change is in the right direction, but not large enough.

Fine Structure of the 3.35μ Band of Ethylene

LINCOLN G. SMITH
Palmer Physical Laboratory, Princeton, New Jersey
(Received July 27, 1940)

The fine structure of the parallel-type band due to the C−H stretching vibration of ethylene has been obtained with a 7500-line grating. From the measured wave numbers of the lines of this band the mean of the two large moments of inertia of C_2H_4 has been determined as 30.08×10^{-40} g cm². This value combined with the value $C=5.70\times10^{-40}$ g cm² for the small moment gives for the large moments of inertia $A=33.20\times10^{-40}$ g cm² and $B=27.50\times10^{-40}$ g cm². These values are in good agreement with those previously reported.

PREVIOUS studies under high resolution of the near infra-red bands of ethylene[1] have not revealed the rotational structure of any of the parallel-type bands. This structure has been obtained with a new prism-grating instrument for the parallel band at 3.35μ corresponding to the C−H stretching vibration. It is the purpose of this paper to present the results of measurements on this band and to compare them with results obtained from Raman and photographic infra-red data.

EXPERIMENTAL

The spectrograph, equipped with a rocksalt foreprism giving ample dispersion at 3μ, has given excellent results with some of the new replica echelette gratings made by Professor R. W. Wood of The Johns Hopkins University. The grating used in the present work has a surface $6\frac{3}{4}$ in.×4 in. ruled with 7500 lines to the inch. The detecting device is a compensated vacuum thermocouple constructed by Professor C. Hawley Cartwright of the Massachusetts Institute of Technology. This is connected to a double galvanometer amplifying system which differs from the usual type in the inclusion of a pair of photoelectric cells and an FP-54 amplifier in place of a thermorelay or photronic cell. The over-all stability of the system is excellent, the sensitivity being limited chiefly by the Brownian motion of the first galvanometer (connected to the thermocouple). Thorough shielding of the entire spectrograph, especially of the detecting and amplifying systems, and thermostatic control of the room temperature have made difficulties due to drift for the most part inappreciable. Results are obtained by recording on photographic paper 30 in.×20 in. the deflections of the second galvanometer. This paper is wrapped on a drum connected through a chain of gears to the grating circle, both of which are driven by a small motor. Calibration lines across the picture are put on with a light mounted beside the second galvanometer which is flashed manually at regular angular intervals.

The ethylene used in the present experiment was obtained from the sample used by Delfosse and Hipple[2] to check previous mass-spectrograph

TABLE I.

J''	$\tilde{\nu}_R$(cm⁻¹)	$\tilde{\nu}_P$(cm⁻¹)	δ''	δ'
1		2985.29		
2	2992.71	83.16		(0.955)
3	94.44	81.43	(0.931)	(0.929)
4	96.06	79.62	(0.918)	(0.910)
5	98.03	77.91	0.921	(0.915)
6	99.91	75.80	0.935	0.927
7	3001.53	73.73	0.935	0.927
8	03.30	71.86	0.929	0.925
9	05.11	69.93	0.929	0.926
10	07.09	68.00	0.928	0.931
11	08.91	66.15	0.930	0.930
12	10.64	64.29	0.931	0.927
13	12.53	62.37	0.928	0.929
14	14.04	60.53	0.931	0.923
15	15.89	58.56	0.920	0.925
16	17.42	56.97	0.927	0.916
17	19.71	54.73	0.922	0.928
18	21.34	52.90	0.932	0.925
19	23.32	50.77	0.928	0.930
20	24.87	48.99	0.929	0.925
21	26.49	47.11	0.925	0.923
22	28.27	45.29	0.924	0.922
23		43.37	0.923	
24		41.53		
25		39.91		
26		37.93		

[1] A. Levin and C. F. Meyer, J. Opt. Soc. Am. **16**, 137 (1928).

[2] J. Delfosse and J. A. Hipple, Jr., Phys. Rev. **54**, 1060 (1938).

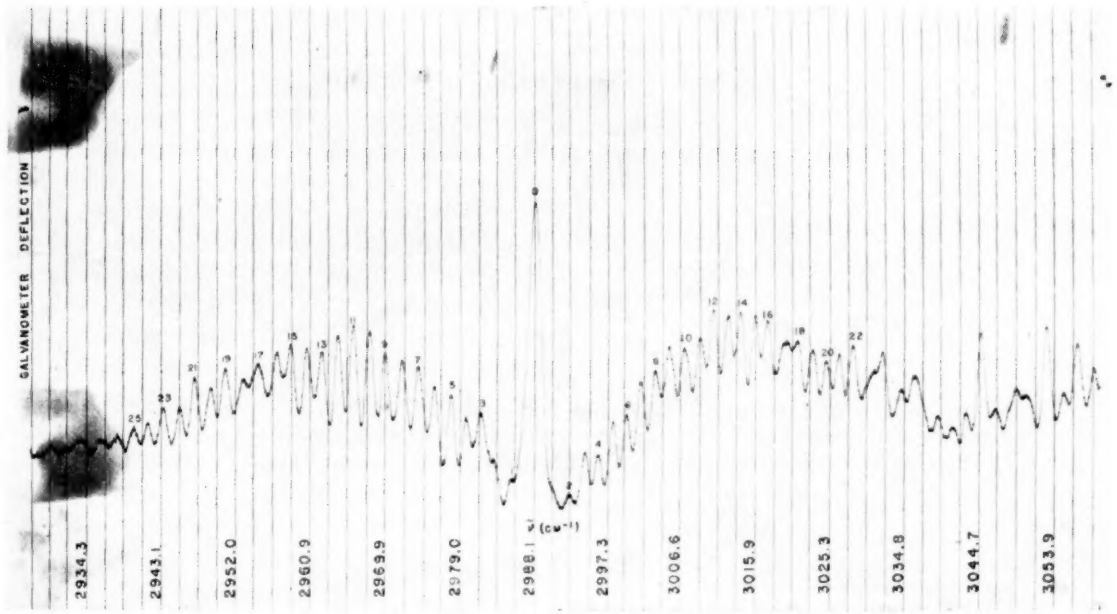

FIG. 1. Automatic record of the 3.35μ band of C_2H_4. The lines are labeled with the J values of the lower state. (At the right appear several lines of the perpendicular C−H band whose center is at 3107.4 cm^{-1}.)

results on C_2H_4. Its purity is further assured by the absence of any detectable absorption in the 3.3μ region due to other hydrocarbon molecules. The gas was contained in an 8-cm cell provided with rocksalt windows. The pressure in the cell was 95 mm of Hg.

RESULTS AND DISCUSSION

A reproduction of the experimental results appears in Fig. 1. The zero energy readings taken at either end of the picture show that very little drift occurred during the recording time (35 minutes). The spectral slit width was 0.55 cm^{-1}. The wave numbers of the lines of the band are shown in Table I. For calibration of the grating the wave number for the Q branch of the band was taken as 2988.20 cm^{-1} from the results of Levin and Meyer.[1]

It is well known that C_2H_4 may be treated to a fairly good approximation as a symmetric top molecule. For determining the mean of the two large moments of inertia (D) we may therefore use the combination relationships:

$$\delta''=\frac{h}{8\pi^2cD''}=\frac{R(J-1)-P(J+1)}{2(2J+1)}$$

(for the ground state),

$$\delta'=\frac{h}{8\pi^2cD'}=\frac{R(J)-P(J)}{2(2J+1)}\quad\text{(for the upper state).}$$

Values of δ'' and δ' for various J values are listed in columns 4 and 5 of Table I. From the averages of these values 0.9274 cm^{-1} and 0.9241 cm^{-1}, respectively, we obtain for the ground state $D''=30.08\times10^{-40}$ g cm^2 and for the first excited state of the vibration in question $D'=30.17\times10^{-40}$ g cm^2. The first value is in good agreement with the value $D''=30.0\times10^{-40}$ g cm^2 obtained by Lewis and Houston[3] from Raman studies of C_2H_4. With the value $C=5.70\times10^{-40}$ g cm^2 for the small moment of inertia given by Badger[4] this value gives for the two large moments of inertia: $A=33.20\times10^{-40}$ g cm^2, and $B=27.50\times10^{-40}$ g cm^2. The values agree well with those given by Badger.[4]

[3] C. M. Lewis and W. V. Houston, Phys. Rev. **44**, 903 (1933).
[4] R. M. Badger, Phys. Rev. **45**, 648 (1934).

The Mercury Photosensitized Decomposition of Ethane

IV. The Reaction at High Temperatures

E. W. R. STEACIE* AND R. L. CUNNINGHAM†
Physical Chemistry Laboratory, McGill University, Montreal, Canada

(Received June 21, 1940)

The mercury photosensitized decomposition of ethane has been investigated at temperatures up to 475°C. It is found that the products of the reaction are very similar to those at low temperatures. It is concluded that the primary step is a C−H bond split, and that the most important secondary reactions are

$$H+C_2H_6\rightarrow C_2H_5+H_2$$
$$H+C_2H_5\rightarrow 2CH_3.$$

The quantum yield approximately doubles on going from 100° to 475°C. No evidence of chain characteristics is found up to 475°C, and it is concluded that the mechanism of the reaction at high temperatures does not differ essentially from that at low temperatures.

INTRODUCTION

A NUMBER of previous investigations of the mercury photosensitized decomposition of ethane have been made, the first being that of Taylor and Hill.[1] Early work served to establish the fact that ethane was attacked by excited mercury atoms yielding a variety of saturated hydrocarbons, and indicated that free radicals were undoubtedly involved in the process.[2,3] A more complete investigation of the reaction was made by Steacie and Phillips.[4–6] They used both a circulating[5] and a continuous flow system.[6]

In the circulatory system it was found by improved trapping methods that it was possible to remove butane from the system as fast as it was formed, and thus the occurrence of secondary reactions was largely prevented. Under these circumstances the products of the reaction consisted of methane, propane and butane. Using the continuous flow method considerable hydrogen production was found, and it was concluded that the primary step was a C−H split. Steacie and Phillips suggested the following mechanism

$$C_2H_6+Hg(^3P_1)\rightarrow C_2H_5+H+Hg(^1S_0), \quad (1)$$
$$H_2+Hg(^3P_1)\rightarrow 2H+Hg(^1S_0), \quad (2)$$
$$H+C_2H_6\rightarrow CH_4+CH_3, \quad (3)$$
$$H+C_2H_6\rightarrow C_2H_5+H_2, \quad (4)$$
$$2CH_3\rightarrow C_2H_6, \quad (5)$$
$$CH_3+C_2H_5\rightarrow C_3H_8, \quad (6)$$
$$2C_2H_5\rightarrow C_4H_{10}, \quad (7)$$
$$2H\rightarrow H_2. \quad (8)$$

Work on the cadmium photosensitized reaction[7] indicates a very similar mechanism.

It was suggested by Taylor[8] that the production of methane in this and other reactions could be better accounted for by dropping reaction (3) in the above scheme and substituting the reaction

$$H+C_2H_5\rightarrow 2CH_3. \quad (9)$$

This modification of the mechanism has received theoretical support from papers by Rice and Teller[9] and Gorin, Kauzmann, Walter and Eyring.[10] The investigation of the reaction of

* Present address: National Research Laboratories, Ottawa, Canada.

† Holder of a Studentship from the National Research Council of Canada.

[1] H. S. Taylor and D. G. Hill, Zeits. f. physik. Chemie **B2**, 449 (1929); J. Am. Chem. Soc. **51**, 2922 (1929).

[2] W. Kemula, Rocz. Chem. **10**, 273 (1930).

[3] W. Kemula, S. Mrazek and S. Tolloczko, Coll. Czech. Chem. Comm. **5**, 263 (1933).

[4] E. W. R. Steacie and N. W. F. Phillips, J. Chem. Phys. **6**, 179 (1938).

[5] E. W. R. Steacie and N. W. F. Phillips, Can. J. Research **B16**, 303 (1938).

[6] E. W. R. Steacie, W. A. Alexander and N. W. F. Phillips, Can. J. Research **B16**, 314 (1938).

[7] E. W. R. Steacie and R. Potvin, J. Chem. Phys. **7**, 782 (1939).

[8] H. S. Taylor, J. Phys. Chem. **42**, 763 (1938).

[9] F. O. Rice and E. Teller, J. Chem. Phys. **6**, 489 (1938).

[10] E. Gorin, W. Kauzmann, J. Walter and H. Eyring, J. Chem. Phys. **7**, 633 (1939).

hydrogen atoms with propane[11] and butane[12] also furnishes strong experimental support for the occurrence of reaction (9).

The above work has been of considerable interest in connection with the question of the applicability of the Rice-Herzfeld free radical mechanism to the thermal decomposition of ethane.[13] Much work has been done which has a bearing on the subject.[14] In general it may be said that the evidence points to the untenability of free radical mechanisms in the case of the ethane decomposition. However, in view of the importance of the evidence from experiments on the mercury photosensitized decomposition of ethane, it seemed desirable to extend the results to high temperatures near the range at which the thermal decomposition of ethane became appreciable.

Experimental

Reaction system

The experiments were made in a continuous "single-pass" flow system. This type of apparatus suffers from certain manipulative disadvantages, but it allows the maximum possible elimination of secondary reactions. This is very important in the present case. Hydrogen quenches λ2537 about 60 times more strongly than does ethane. As a result, if hydrogen is allowed to build up in the products, the reaction soon ceases to be the mercury photosensitized decomposition of ethane, and becomes the reaction of atomic hydrogen with ethane.

The main features of the apparatus are shown in Fig. 1. The gas at constant pressure enters the system through a calibrated capillary *C*, made from a piece of thermometer tubing. A ballast bulb *V* of 500 cc capacity is used to smooth out pressure fluctuations. The entering ethane then passes over the hot mercury surface of the saturator *S* which is maintained electrically at

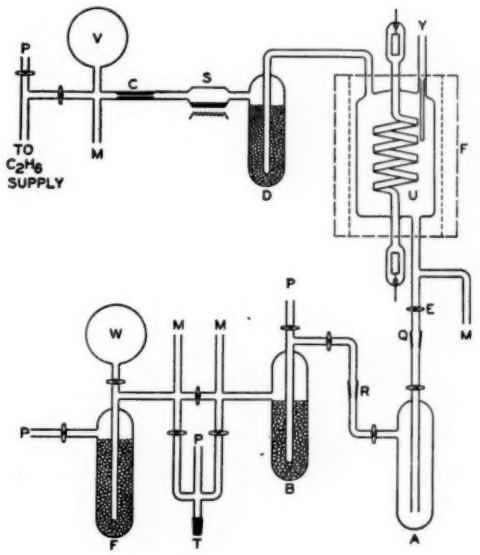

FIG. 1. Apparatus.

about 70°C by a heating coil. The gas then passes through a desaturating trap *D*, filled with iron pellets and maintained at 25°C, where excess mercury vapor is removed.

The gas and mercury vapor then pass into the reaction vessel *U*, the pressure in which can be regulated by controlling the outflow of the gases by using a file-scratched stopcock, *E*, as an adjustable leak. After irradiation the gas flows through this stopcock into a series of three traps, cooled with liquid air, *A*, *B*, and *F*. The first of these, *A*, is initially empty and serves to collect all the ethane and any higher products that may be formed. The second, *B*, is packed with silica gel and adsorbs nearly all the methane and some hydrogen. Trap *F* contains activated charcoal and adsorbs the remaining hydrogen and a trace of methane. A 500-cc expansion bulb *W* was connected to the carbon trap and was used when large amounts of hydrogen were being collected. The different parts of the system could be separately evacuated through all connections marked *P* in Fig. 1. The pumping system consisted of the usual Hyvac, mercury diffusion pump, liquid-air trap, McLeod gauge, etc. Manometers were connected to all points marked *M* in the figure.

By means of a ground joint *T* gas could be pumped with a Toepler pump into a portable mercury gas-holder, and transferred to the

[11] E. W. R. Steacie and N. A. D. Parlee, Trans. Faraday Soc. **35**, 854 (1939); Can. J. Research **B17**, 371 (1939).
[12] E. W. R. Steacie and E. A. Brown, J. Chem. Phys. **8**, 734 (1940).
[13] F. O. Rice and K. F. Herzfeld, J. Am. Chem. Soc. **56**, 284 (1934).
[14] See E. W. R. Steacie, Chem. Rev. **22**, 311 (1938) for a review of the literature, and later papers by L. Küchler and H. Theile, Zeits. f. physik. Chemie **B42**, 359 (1939); F. O. Rice and K. F. Herzfeld, J. Chem. Phys. **7**, 679 (1939); E. W. R. Steacie and G. Shane, Can. J. Research, **B18**, 203 (1940).

analytical apparatus. Trap *A* was removable, so that the liquid products of the reaction could be conveniently handled.

Light source

The source of λ2537 was a high voltage, low pressure mercury discharge lamp very similar to that described by Steacie and Phillips.[15] The lamp-reaction vessel system was enclosed in an electric furnace, with the electrodes projecting from the furnace. The furnace was thermostatically controlled to ±1°C. Temperatures were measured by means of a Chromel-Alumel thermocouple.

As with other lamps of this type the output was very reproducible at a given temperature. The absolute output was determined by measuring the rate of hydrolysis of 0.5*N* monochloracetic acid in the reaction vessel at 60°C. (This temperature was necessary to obtain proper operation of the lamp.) According to Rudberg[16] the quantum yield of the hydrolysis is approximately unity. Recent work by Leighton, Smith, and Leighton,[17] however, indicates values considerably lower than this. There are, however, certain indications from work done in this laboratory that the quantum yield may be higher at the very high light intensities used here. Pending a re-examination of the question, and for the sake of comparison with our earlier work, we have used Rudberg's values. In any case, the main interest attaches to the products of the reaction, and to the effect of temperature on the quantum yield rather than to its absolute value.

On the above basis the mean of a number of concordant observations gave for the total intensity of λ2537 entering the reaction vessel at 60°C a value of 1.15×10^{-5} Einstein per second. As the measurements of Steacie and Phillips showed, there is virtually complete absorption of this radiation in the reaction vessel with the mercury vapor concentration and ethane pressures used in this work, except at the lower pressures. At these pressures the data of Steacie and Phillips were used to calculate the amount of radiation absorbed.

The variation with temperature of the output of lamps of this type is comparatively small. It is, however, appreciable. To determine it, a hole was ground in the outer Pyrex jacket of the reaction vessel, and spectrophotometric determinations of the relative intensity of λ2537 were made over the temperature range employed. It was found that the output of λ2537 increased approximately linearly with temperature, and was about 50 percent greater at 400°C than at 100°C.

Materials

Ethane was obtained in cylinders from the Ohio Chemical and Manufacturing Company. It was stated to be 97 percent pure. As in the flow system used the ratio of products to unreacted ethane is small, it was necessary to purify the ethane very thoroughly. To accomplish this the cylinder gas was passed through a 60-cm tube at 300°C containing copper oxide to remove hydrogen. It was then bubbled through bromine water and into a two-liter vessel illuminated with a Point-o-lite lamp to bring about bromination of unsaturates, then through a 40 percent solution of potassium hydroxide, and finally through a trap at −80°C. The gas was then fractionated, the end fractions being discarded. The purified gas was condensed into steel cylinders by means of liquid air, and stored under pressure. Samples of the purified gas showed no detectable impurities with the analytical methods used.

Analysis

The products of the reaction were analyzed by means of a low temperature distillation apparatus of the Podbielniak type. Since a very large amount of unreacted ethane was present in comparison with the amount of products, it was necessary to carry out the distillation extremely slowly, some ten or fifteen hours being required. In view of the tedious nature of the operation, the control of the still was made automatic.

In the analysis hydrogen and methane were taken off together, and this fraction was analyzed by combustion.

Some liquid products were also found. Vapor pressure measurements, as well as carbon-hydrogen balances indicated that the liquid products were predominantly hexanes, and they have therefore been reported as C_6H_{14}.

[15] E. W. R. Steacie and N. W. F. Phillips, Can. J. Research **B16**, 219 (1938).
[16] E. Rudberg, Zeits. f. Physik **24**, 247 (1924).
[17] W. G. Leighton, R. N. Smith and P. A. Leighton, J. Am. Chem. Soc. **60**, 2566 (1938); **61**, 2299 (1939).

TABLE I. *Preliminary runs at various pressures. Volume of system, 1300 cc; mercury vapor pressure, 1.3×10^{-3} mm; resonance radiation (at 60°C), 1.15×10^{-5} Einstein per sec.; ethane flow, 2.41 cc per sec. at NTP.*

Temperature °C	Pressure cm	Quantum Yield	Products, mole percent					Ratio $\frac{H_2}{CH_4}$
			H_2	CH_4	C_3H_8	C_4H_{10}	"C_6H_{14}"	
88	5	0.28	45.6	15.4	10.7	8.6	19.7	2.9
100	2	0.28	40.8	19.2	12.1	11.7	16.2	2.1
100	5	0.31	42.8	18.7	10.3	9.7	18.7	2.2
100	7	0.37	—	—	—	—	—	4.3
165	18	0.53	—	—	—	—	—	14

Results

Table I gives the results of runs made at high flow rates at various pressures. In Table II results are given for runs at slower flow rates and 5 cm pressure, and in Table III at 10 cm pressure The data in Table I were obtained in preliminary runs and are not as reliable as the later data, since the analytical methods were not as satisfactory.

Discussion

A comparison of the results in Tables I and II shows that there is no appreciable change in the reaction with change in flow-rate. It may therefore be concluded that secondary reactions have been reduced to a minimum.

The results show a comparatively small change in quantum yield with increasing temperature, the yield being slightly less than doubled on going from 100° to 475°C.

On the whole the products change relatively little with change in temperature, although the results show that the H_2/CH_4 ratio decreases considerably with increasing temperature. An increase in ethane pressure increases the ratio somewhat. Runs were not made over a wide pressure range, because at lower pressures the absorption of λ2537 is incomplete, while at higher pressures a layer of polymer deposited on the walls of the lamp and strongly decreased the transmission.

The results are entirely compatible with the mechanism previously proposed[5] as modified by Taylor,[8] *viz.*:

$$C_2H_6+Hg(^3P_1)\rightarrow C_2H_5+H+Hg(^1S_0), \quad (1)$$

$$H_2+Hg(^3P_1)\rightarrow 2H+Hg(^1S_0), \quad (2)$$

$$H+C_2H_6\rightarrow C_2H_5+H_2, \quad (4)$$

$$H+C_2H_5\rightarrow 2CH_3, \quad (9)$$

$$2CH_3\rightarrow C_2H_6, \quad (5)$$

$$CH_3+C_2H_5\rightarrow C_3H_8, \quad (6)$$

$$2C_2H_5\rightarrow C_4H_{10}, \quad (7)$$

$$2H\rightarrow H_2, \quad (8)$$

$$CH_3+H\rightarrow CH_4. \quad (10)$$

At higher temperatures we must also consider the reactions

$$C_2H_5+H_2\rightarrow C_2H_6+H, \quad (11)$$

$$CH_3+H_2\rightarrow CH_4+H, \quad (12)$$

$$CH_3+C_2H_6\rightarrow CH_4+C_2H_5. \quad (13)$$

Reaction (11), however, will have little real effect, since it is merely the reverse of (4). Reaction (12) is undoubtedly responsible at least in part for the decrease in the H_2/CH_4 ratio at higher temperatures. The indications in the past were that reaction (13) had a relatively high activation energy.[8,10] Recent work of Smith and Taylor[18] indicates a value of the activation energy of *ca.* 8 kcal. In any case reaction (13) will be of importance in the production of methane at higher temperatures.

The increase in quantum yield at higher temperatures is undoubtedly due to the increasing occurrence of (4), which has an activation energy

TABLE II. *Experiments at 5 cm pressure. Ethane flow, 0.37 cc per sec. at NTP. Other conditions as in Table I.*

Temperature °C	Products, mole percent					Quantum Yield	Ratio $\frac{H_2}{CH_4}$
	H_2	CH_4	C_3H_8	C_4H_{10}	"C_6H_{14}"		
100	47.1	14.4	9.1	9.1	20.3	0.29	3.30
100	46.4	13.6	10.4	9.5	19.1	0.27	3.41
170	46.5	14.8	9.3	9.6	19.8	0.44	3.16
250	46.1	15.1	9.6	9.3	19.9	0.55	3.07
325	41.4	16.3	14.5	13.3	14.5	0.58	2.53
325	41.9	15.3	14.1	14.5	14.2	0.57	2.71
400	40.6	18.1	15.3	13.5	12.5	0.55	2.24
400	41.6	15.7	14.5	14.1	14.1	0.55	2.65
475	41.3	21.1	9.9	9.4	18.3	0.51	1.97

[18] J. O. Smith and H. S. Taylor, J. Chem. Phys. **7**, 390 (1939).

of about 8 kcal., as compared with the recombination reaction (8). The effect of increased pressure will be to increase (1), as compared with (2). Less of the hydrogen formed in the reaction will therefore be destroyed by (2), and the amount of hydrogen in the products rises. Furthermore, at higher ethane pressures (4) will be favored as compared with (9).

The results show that there is little change in the products of the reaction, or in the quantum yield on going from room temperature to 475°C. The mechanism at high temperatures is therefore in the main the same as that at low temperatures. Since the quantum yield is still less than unity at 475°C, it is evident that no chain processes are coming into play.

This raises the question whether the equilibrium in the reaction

$$C_2H_6 \rightleftarrows C_2H_4+H_2 \qquad (14)$$

is such as to permit the detection of appreciable amounts of ethylene at 475°C under our experimental conditions. Pease and Byers[19] have recently discussed this equilibrium in detail. Their results indicate that at the pressures used in this investigation the equilibrium dissociation of ethane should be in the neighborhood of 10 percent at 475°C. With the "single-pass" flow system used in our work, the amount of decomposition of ethane varied from 3 to 20 percent, being of the order of 12 to 15 percent in most experiments. It follows, therefore, that if the products of the reaction had been ethylene and hydrogen only, and equilibrium had been reached, the amount of reaction would have been about the same as that observed. In other words the position of equilibrium in the reaction

$$C_2H_6 \rightleftarrows C_2H_4+H_2 \qquad (14)$$

does not in any way prevent the formation and detection of ethylene under our experimental conditions.

[19] R. N. Pease and A. M. Byers, J. Am. Chem. Soc. 60, 2489 (1938).

TABLE III. *Experiments at 10 cm pressure. Ethane flow—0.37 cc per sec. at NTP. Other conditions as in Table I.*

Temperature °C	Products, mole percent					Quantum Yield	Ratio $\frac{H_2}{CH_4}$
	H_2	CH_4	C_3H_8	C_4H_{10}	"C_6H_{14}"		
115	52.2	9.7	7.8	7.2	23.1	0.39	5.41
170	49.4	9.9	7.1	6.2	27.4	0.58	4.94
250	52.9	10.4	7.2	7.0	22.5	0.68	5.10
250	52.1	10.5	7.5	6.6	23.3	0.66	5.00
325	39.5	17.6	(17.5)	11.1	14.3	0.73	2.24
400	37.7	20.5	14.2	14.1	13.5	0.72	1.86
400	36.2	19.9	16.3	17.0	10.6	0.73	1.84
475	40.0	20.1	12.3	11.2	16.4	0.72	2.00
475	41.6	21.5	8.1	8.7	20.1	0.72	1.90

However, the equilibrium in the reaction

$$C_2H_4+H \rightleftarrows C_2H_5 \qquad (15)$$

must also be considered. It is well known that reaction (15) proceeds rapidly from left to right at low temperatures and fairly high hydrogen atom concentrations, and the Rice-Herzfeld mechanism for the thermal decomposition of ethane depends on it going from right to left at higher temperatures. In the present case, however, the stationary concentration of atomic hydrogen produced by reactions (1) and (2) is presumably much higher than that which would exist in the thermal decomposition if the Rice-Herzfeld mechanism held. This forces reaction (15) over to the right, and prevents the formation of appreciable amounts of ethylene in the products.

It may therefore be concluded that the present results cannot decide the question of the tenability of the Rice-Herzfeld mechanism. The results do show that the mechanism of the mercury photosensitized reaction at high temperatures is not greatly different from that at low temperatures. The difficulties which have been previously encountered in applying the Rice-Herzfeld mechanism to the thermal decomposition of ethane[14] still exist, therefore, and it may be concluded that no satisfactory modification of this mechanism has yet been devised.

Lifetime of Fluorescence in Diacetyl and Acetone

G. M. Almy and Scott Anderson
Department of Physics, University of Illinois, Urbana, Illinois

(Received July 3, 1940)

The mean lifetime of the fluorescence of diacetyl vapor has been determined by direct measurement with a phosphoroscope to be 1.65×10^{-3} sec. Quantitative measurement of the diffusion of the excited molecules from a beam of exciting illumination, at different pressures, has also been made and the results are compatible with this lifetime. Integration of the absorption coefficient over the band associated with the fluorescence leads, on the other hand, to a lifetime of the excited state of 10^{-5} sec. To explain this discrepancy and other facts known about the fluorescence various mechanisms are considered, of which the most satisfactory seems to be this: Following light absorption, $X\rightarrow A$, the diacetyl molecule goes without radiation into a long-lived state M, lying near A. Fluorescence occurs only upon return to A. M may correspond to a tautomeric rearrangement of the molecule. Acetone, radiated with λ3130, shows fluorescence identical with that of diacetyl radiated with λ4358, but the fluorescence grows with time. It can be produced immediately with high intensity by adding diacetyl. The growth curve has been determined and is of form, $I_t=I_0\ (1-e^{-kt})$. Diffusion experiments show the lifetime of the fluorescence in acetone to be equal to that in diacetyl and that the lifetime, or rate of decay, is independent of exciting intensity. The conclusion is that the same molecule, presumably diacetyl, is responsible for the fluorescence in both cases. Possible mechanisms for the excitation of diacetyl in acetone are discussed.

THE study of the fluorescence of polyatomic molecules may lead to information about their behavior after absorption of light which is of fundamental importance in understanding photochemical processes. The fluorescence of the diacetyl molecule offers such an opportunity for several reasons. First, the fluorescence of diacetyl occurs in water solution as well as in the vapor.[1] Second, similar fluorescence occurs in several compounds containing the $O=C-C=O$ group, e.g., benzil in solution,[2] indicating that properties of diacetyl obtained from a study of the fluorescence may be to some extent common to a large class of molecules. The same fluorescence is found to occur in the vapor of other compounds containing acetyl radicals (CH_3CO), e.g., acetone, when they are radiated with light which will decompose the molecules.[1,3] Third, the fluorescence is strongly quenched by oxygen,[1] the oxygen being consumed. Thus a process of photo-oxidation can be studied by means of the fluorescence. Fourth, there is the practical reason that the green diacetyl fluorescence is especially easy to study. It is excited intensely by the Hg arc groups of strong lines near λλ3650, 4047, 4358 and it can readily be observed by visual, photographic or photoelectric methods.

In a previous study[1] several properties of the fluorescence were observed and could be accounted for by the assumption of a simple fluorescence process. Rough estimates of the lifetime of the excited molecule were compatible with this model. Further experiments, which are the subject of the first part of this paper, have led to more accurate determinations of the lifetime of the fluorescence, which proves to be much longer than the rough estimate, and also much longer than one would estimate from the probability of the transition between the states involved in the absorption leading to the fluorescence. Various possible implications of these facts have been considered and the most satisfactory interpretation is the introduction of a long-lived state, with approximately the same energy as the state reached on absorption, into which the excited molecule can go for a time, before returning to the original excited state to emit the fluorescence.

In the second part of the paper some experiments are described which have to do with the fluorescence of acetone and acetone-diacetyl mixtures. They establish further the identity of the emitting molecule, very probably diacetyl, in the fluorescence of diacetyl and acetone vapors. They throw some light on the question of the process of excitation in acetone.

[1] Almy, Fuller and Kinzer, J. Chem. Phys. **8**, 37 (1940).
[2] P. R. Gillette, Master's Thesis, University of Illinois, 1939.
[3] Matheson and Noyes, J. Am. Chem. Soc. **60**, 1857 (1938).

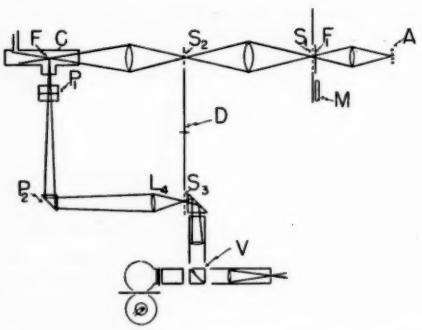

FIG. 1. Phosphoroscope arrangement to measure the lifetime of the fluorescence. A, high pressure water-cooled mercury arc. S_2 and S_3, radial slots in the disk D. C, fluorescence chamber, P_1, reversing prism. V, visual photometer.

DIRECT MEASUREMENT OF LIFETIME WITH PHOSPHOROSCOPE

To obtain a direct measurement of the mean lifetime of the fluorescence we employed the phosphoroscope shown in Fig. 1. It consisted of a disk D, 30 cm in diameter, with radial slots 1 mm wide spaced every 4° around the circumference, rotated by a direct-current motor whose speed was varied by a resistance in the primary. The speed of the disk was measured with a tachometer. The arc at A was a General Electric high pressure water-cooled arc with a quartz envelope. This was focused through a filter onto the slit S_1 which had its image focused upon a slit in the disk. An image of the latter was formed in the Pyrex chamber C into which the vapor was introduced. The fluorescence occurring at F was focused on a slit S_3 opposite S_2 by means of the prisms P_1 (for reversing the image), P_2, and the lens L_4. This lens was provided with a calibrated screw adjustment. The point of focus could be arranged so that when the disk was turning at a constant velocity, one could view the fluorescence through S_3 a measurable time after the exciting light was cut off at S_2. Thus by measuring the intensity of the fluorescence coming through S_3 with the visual photometer V, the intensity of the fluorescence still left at measured times after excitation could be determined. The photronic cell at M enabled us to check the variation in the intensity of the exciting arc, which proved to be negligible. The voltage on the bulb in the visual photometer was kept constant.

Employing this phosphoroscope we measured the decay of the fluorescence in diacetyl at room temperature (26°C). It was found that the decay was exponential in time; when $\log I_t/I_0$ was plotted against delay time a straight line was obtained, of which the negative reciprocal of the slope is the mean lifetime (τ). The data for six runs gave a mean lifetime for the fluorescence of $1.65\pm0.2\times10^{-3}$ sec. at 26° C. There was no perceptible variation with pressure.

To study the variation of the lifetime with the wave-length of the exciting light we inserted filters at F_1. For light of the longer wave-lengths we employed a Corning Noviol glass which transmits about 5 percent of 3800A increasing to 70 percent at 4400A. The Corning 986 glass was inserted to transmit wave-lengths less than about 4000A. There was no appreciable difference in the two lifetimes measured and they were each in agreement with the measurement previously made with the full arc. It should be noted here that in both of these cases the intensity of the incident light was much less than when employing the full arc as in all the previous measurements. This indicates that the lifetime is independent of intensity; a point which is verified in experiments on diffusion of the fluorescence to be described later.

The lifetime for the fluorescence of diacetyl in an aqueous solution was also determined. The results of one attempt, with a concentration of 1 part in 50, revealed a much shorter lifetime, of the order of 6×10^{-5} sec.

DIFFUSION OF FLUORESCENCE

An altogether different means of gaining information concerning the lifetime of fluorescing molecules is a quantitative study of the diffusion of excited molecules before fluorescing. Heil[4] and Almy, Fuller and Kinzer[1] performed such an experiment to secure qualitative values of the lifetime for fluorescence of NO_2 and diacetyl, respectively. We have refined this experiment by making a quantitative measurement of the fluorescence intensity and hence of the distribution of the excited particles since the intensity is proportional to concentration of the excited particles. From an analysis of the diffusion

[4] Heil, Zeits. f. Physik **77**, 563 (1932).

pattern, the product of the diffusion coefficient (D) and the lifetime (τ) is obtained. Thus, assuming a reasonable value of D, we can calculate τ or, conversely, using the value of τ measured directly with the phosphoroscope, D and thus the collision cross section of excited against unexcited particles, is determined. These measurements were carried out on diacetyl.

The experimental arrangement is shown in Fig. 2. The high pressure mercury arc was placed at A. A uniformly illuminated slit at S was focused in the center of the Pyrex chamber C. The beam of light in the chamber as seen by the camera had the dimensions shown in the inset at (A). At low pressures of diacetyl the excited molecules diffused out into the shadow before fluorescing. The resulting fluorescence pattern was photographed. The distribution of intensity in the diffusion pattern was obtained by photographic photometry.

The interpretation of these diffusion patterns is as follows. Consider a beam of excited molecules initially between the infinite planes $x=0$ and $x=-b$. The rate at which the concentration will vary in space if these molecules are permitted to diffuse out of the beam is given by the usual diffusion equation

$$-\partial C/\partial t = D\partial^2 C/\partial x^2 \qquad (1)$$

subject to the boundary conditions that at $t=0$

$$C=\begin{cases} a \text{ for } -b<x<0 \\ 0 \text{ for } x>0 \text{ and } x<-b, \end{cases}$$

where C is the concentration of excited molecules. These boundary conditions correspond physically to the situation in the chamber about 10^{-2} sec. after illumination begins, i.e., the concentration of excited particles in the beam has come to equilibrium but no diffusion has occurred. A solution of this equation under these conditions is seen to be

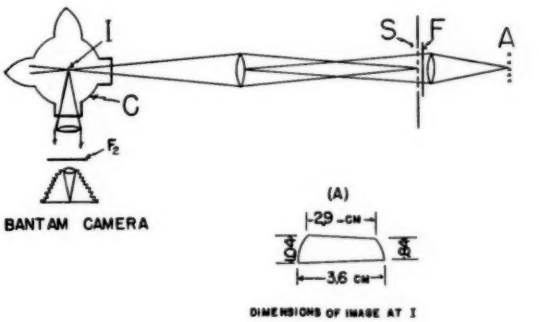

FIG. 2. Apparatus for studying the diffusion of the fluorescence. A, high pressure arc. C, Pyrex chamber. F_2, Wratten 12 filter. The inset (A) gives the actual dimensions of the image at I with high diacetyl pressure in the tube.

$$C=\frac{a}{\sqrt{\pi}}\int_0^{(x+b)/2(Dt)^{\frac{1}{2}}} e^{-\beta^2}d\beta - \frac{a}{\sqrt{\pi}}\int_0^{x/2(Dt)^{\frac{1}{2}}} e^{-\beta^2}d\beta. \qquad (2)$$

Therefore, if t represents the elapsed time since the molecules were excited and q represents the number per cc that are excited per second in the beam, then under equilibrium conditions the contribution (dC) to the concentration at x from molecules having been generated in the previous interval of time between $-t$ and $-t+dt$ is given by the expression (2) if a is set equal to qdt. If the excitation of the molecules takes place only when they are in the beam, the fraction that will still be excited at time t is $e^{-t/\tau}$, where τ is the mean lifetime of the excited molecules. Now in the steady state the molecules at x may have received their excitation at all previous times between 0 and ∞. Therefore the concentration of excited molecules (C^*) at x after the equilibrium is attained is given by the equation

$$C^*=\frac{q}{\sqrt{\pi}}\int_0^\infty e^{-t/\tau}\left\{\int_0^{(x+b)/2(Dt)^{\frac{1}{2}}} e^{-\beta^2}d\beta - \int_0^{x/2(Dt)^{\frac{1}{2}}} e^{-\beta^2}d\beta\right\}dt. \qquad (3)$$

Performing the integration with respect to β by parts, we have

$$C^*=\frac{q\tau}{\sqrt{\pi}}x\int_0^\infty \frac{e^{-x^2/4Dt-t/\tau}}{4\sqrt{Dt^3}}dt - \frac{q\tau(x+b)}{\sqrt{\pi}}\int_0^\infty \frac{e^{-(x+b)^2/4Dt-t/\tau}}{4\sqrt{Dt^3}}dt. \qquad (4)$$

If in the first integral we let $t/\tau=A^2w^{-2}$, where $A^2=x^2/4Dt$ and in the second let $t/\tau=B^2w^{-2}$,

where $B^2=(x+b)^2/4D\tau$ we get

$$C^*=\frac{q\tau}{\sqrt{\pi}}\int_0^\infty e^{-w^2-A^2w^{-2}}dw - \frac{q}{\sqrt{\pi}}\int_0^\infty e^{-w^2-B^2w^{-2}}dw. \quad (5)$$

Therefore

$$C^*=\frac{q\tau}{2}e^{-x/(D\tau)^{\frac{1}{2}}}(1-e^{-b/(D\tau)^{\frac{1}{2}}}). \quad (6)$$

Since the intensity of the fluorescence at any point is proportional to the concentration of excited particles at that point, we can write

$$\log C^*/C_0^*=\log I/I_0=-x/(D\tau)^{\frac{1}{2}}, \quad (7)$$

where C_0^* is the concentration at the edge of the beam, I_0 the intensity of fluorescence there, and I the intensity of the fluorescence at any point x. If we reduce this to atmospheric pressure we have

$$\log I/I_0=-x(p/760D_0\tau)^{\frac{1}{2}}, \quad (8)$$

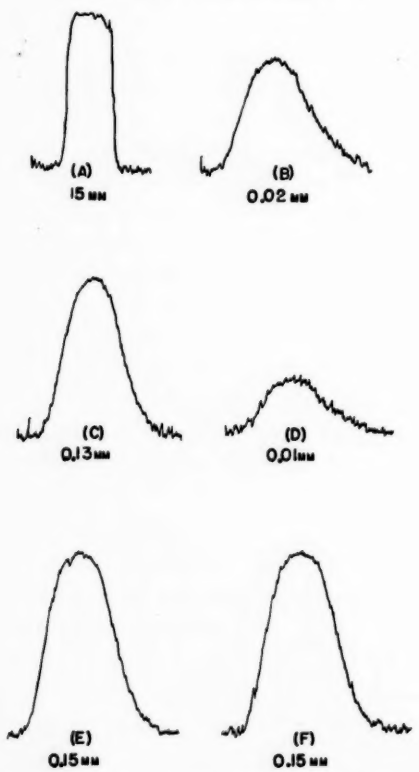

FIG. 3. Microphotometer traces of diffusion pattern of fluorescence in diacetyl at the pressures indicated. *A*, pattern at high pressure; *B*, *C*, *D*, used to determine $D_0\tau$ in Fig. 4. *E* and *F* used to show τ independent of exciting intensity. *F* (15-second exposure) obtained with nine times intensity used in *E* (3-minute exposure).

where p is the pressure of the vapor, and D_0 is the diffusion coefficient at atmospheric pressure at the temperature of the experiment (26°C). Thus, plotting $(760/p)^{\frac{1}{2}}\log I/I_0$ against x, we should get a straight line, the negative reciprocal of whose slope should equal $(D_0\tau)^{\frac{1}{2}}$. If by an independent measurement one or the other of these two quantities is known, the other is determined.

Microphotometer traces of the diffusion patterns for four diacetyl pressures are shown in Fig. 3. In Fig. 4, $(760/p)^{\frac{1}{2}}\log I/I_0$ is plotted against x, the distance from the edge of the illuminated beam, which is sharply defined at high pressures. The data at three pressures are used and all fit reasonably well on the same straight line, as predicted. The slope of the line is $1/(D_0\tau)^{\frac{1}{2}}$, according to Eq. (8). From the estimated slope one finds $D_0\tau=5.34\times10^{-5}$ cm². No value of D_0 for diacetyl is available, for the diffusion of either excited or unexcited molecules. Neither has the coefficient of viscosity been measured from which D, equal to η/ρ could be estimated. For several somewhat similar molecules η is about 10^{-4} c.g.s. units; for acetone it is 0.95×10^{-4}. Assuming $\eta=10^{-4}$, D_0 is 2.7×10^{-2} and $\tau=2.0\times10^{-3}$ sec., in good agreement with the lifetime measured with the phosphoroscope.[5]

Conversely, assuming $\tau=1.65\times10^{-3}$ sec., the value found by the phosphoroscope method, we calculate the value for D_0 to be 3.2×10^{-2} cm²/sec. as the diffusion coefficient of excited diacetyl molecules among unexcited ones. Using the kinetic theory relation between the diffusion coefficient and collision cross section (S),[6] we calculate a value of $S=11.2\times10^{-15}$ cm² which for spherical molecules is equivalent to a collision diameter of 5.9A. This is roughly what one would expect for unexcited molecules of this mass and structure.

This apparatus was well suited for detecting any change in lifetime for fluorescence under different intensities of excitation. Since the diffusion pattern is determined by the product $D_0\tau$, any change in τ would be reflected in the

[5] From visual observation of the fluorescence pattern (reference 1) the lifetime had been estimated to be 10^{-5} sec., or longer. The quantitative measurements show the visual method to be unreliable.

[6] See, for example, Kennard, *Kinetic Theory of Gases* (McGraw-Hill, 1938), p. 194.

diffusion pattern. With a given pressure of diacetyl in the chamber we took pictures of the fluorescence with different intensities of the exciting light. Since the intensity was lowered by the interposition of screens at F_1, the time of exposure of the films was increased by such an amount that the maximum blackening was the same on all plates. Fig. 3 shows the microphotometer traces of two such plates for which the intensity of the exciting radiation differed by ninefold. It is obvious that the two traces are almost identical, showing that the lifetime does not depend upon the intensity of the exciting light.

Lifetime Estimated from Integrated Absorption Coefficient

To shed more light on the processes associated with the fluorescence of diacetyl, the lifetime of the state reached on absorption was determined from the absorption coefficient integrated over the band which is connected with the fluorescence. In a molecule the complete band system arising from a single electronic transition corresponds to a single line in an atomic spectrum. If the spectrum is continuous or consists of lines so close together as to overlap throughout the absorption band, the integrated absorption coefficient, $\int k_\nu d\nu$, can be obtained by measuring k_ν at various wave-lengths, plotting it as a function of wave number, and integrating graphically over the band. The lifetime is calculated from the relation[7]

$$\tau=\frac{n}{8\pi c\nu^2}g'/g''\frac{1}{\int k_\nu d_\nu}, \qquad (9)$$

where $n=2.7\times10^{19}$ molecules per cc; k_ν=absorption coefficient, defined by $I_\nu=I_\nu{}^0e^{-k_\nu l}$, l being the path in cm of gas at 0°C and one atmosphere pressure; ν=wave number, cm^{-1}; g', g''=statistical weights of upper and lower states.

To obtain the absorption spectrum of diacetyl vapor we employed the same high pressure mercury arc used in the other experiments. The various regions of the spectrum were selected by the use of a quartz monochromator whose exit slit was focused through a Pyrex cell containing the vapor onto a potassium hydride photo-cell. Each setting of the monochromator admitted a spectral range of approximately 100A.

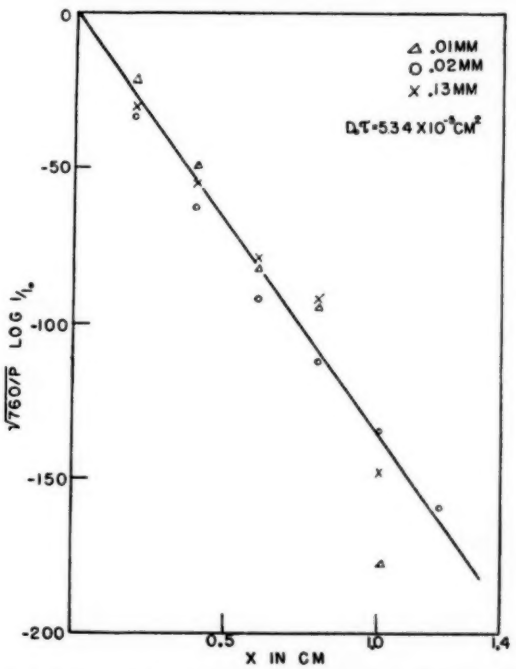

FIG. 4. Plot of data from the diffusion of the fluorescence. Data taken with three pressures of diacetyl, 0.01 mm, 0.02 mm, and 0.13 mm, all at temperature of 26°C. Slope of straight line equals $-1/(D_0\tau)^{\frac{1}{2}}$.

The plot of k_ν against ν is given in Fig. 5. The area under the curve is 7340 cm^{-2}. The assumption was made that the spectrum could be treated as continuous. This assumption was tested (1) by showing that Beer's law holds over a pressure range of 43 mm to 0.01 mm and (2) by comparing the integrated absorption coefficient with that obtained from data taken by Lardy[8] for diacetyl in hexane solution, in which case the lines of the band system should be considerably broadened. The area under the curve from Lardy's data is 7265 cm^{-2}. This is subject to an increase of about twenty percent on account of a correction factor $(n_0{}^2+2)^2/9n_0$, where n_0=the index of refraction of the solvent, which must be applied in the case of absorption spectra of solutions.[9] The agreement is certainly close enough to justify the use of $\int k_\nu d\nu$ of the vapor in calculating the order of magnitude of τ.

[7] See Mulliken, J. Chem. Phys. 7, 14 (1939) for a summary of intensity relations.

[8] Lardy, Dissertation, Zurich (1924).

[9] Chako, J. Chem. Phys. 2, 644 (1934).

Substituting our value of $\int k_\nu d\nu$ in Eq. (9), τ comes out to be 8.5×10^{-6} second, if we assume $g'/g''=1$. There may be a large error in this last assumption but in any event the order of magnitude of the lifetime of the upper state of the absorption transition required by the integrated absorption coefficient is 10^{-5} sec. This is a hundred times smaller than the directly measured mean life of the fluorescence.

Discussion of Diacetyl Fluorescence

The most important facts concerning the fluorescence of diacetyl vapor from the present and previous work can be summarized as follows.

The fluorescence is produced by absorption within the band extending from λ3500 to λ4650. The fluorescence consists mainly of three bands, with fine structure, with maxima at λλ5120, 5610, 6135. There is a gap between fluorescence and absorption in which both are very weak, if present at all.

The spectrum of the fluorescence of diacetyl vapor is independent of pressure (0.1 mm to 60 mm), temperature (10° to 100°C), exciting wave-length (λ3650−λ4358) and the pressure of added gases.

The quantum yield of the fluorescence is about 0.035 at λ4358, 0.03 at λ3650. The yield at λ4358 is independent of the exciting intensity and pressure. Henriques and Noyes[10] find that at λ3650 the yield is enhanced by increasing the pressure.

The mean lifetime of the fluorescence in the vapor is 1.65×10^{-3} sec. On the other hand, the lifetime corresponding to the integrated absorption coefficient over the band associated with the fluorescence is about 10^{-5} sec. The lifetime of the fluorescence is independent of pressure and exciting intensity as shown by both phosphoroscope and diffusion experiments.

The lifetime and the quantum yield both decrease as the temperature is increased, but with different temperature coefficients.

The radiation which excites the fluorescence (at least up to λ4358) is also capable of decomposing the molecule, eventually into CO and hydrocarbons.

[10] Henriques and Noyes, J. Am. Chem. Soc. **62**, 1038 (1940).

In view of the available experimental facts, what is the most likely mechanism of the fluorescence emission? Three sorts of process have been considered. (1) Simple fluorescence, that is to say, absorption, followed by vibrational redistribution and then, reemission. (2) Delayed fluorescence, in which absorption (call it $X\rightarrow A$) is followed by transition into a long-lived state (M) lying near state A. Fluorescence occurs only when the molecule is returned by collisions to a state, presumably A, which can combine with the ground state. The long-lived state might be a tautomeric form of the diacetyl molecule. (3) Processes involving the recombination or reaction, of radicals, or radicals and molecules.

Of these three types of mechanism, (1) and (3) can be shown to be very improbable. Simple fluorescence, while adequate to account for many of the observed facts,[1] will not admit the results of measurements of lifetime. The mean life of the fluorescence is 1.65×10^{-3} sec.; the quantum yield is only 0.035 which means, on this mechanism, that while the molecule is in the excited state a competing process is

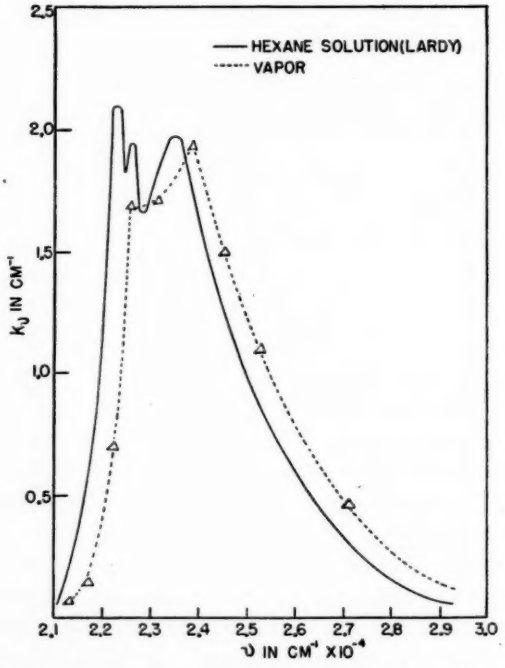

FIG. 5. Absorption spectrum of diacetyl. Solid line plotted from data taken by Lardy on diacetyl in a hexane solution. Broken line determined for diacetyl vapor. k_ν, absorption per cm path at atmospheric pressure.

about 30 times as probable as the fluorescence. It is, therefore, the competing process which is mainly responsible for the observed rate of decay; the lifetime against fluorescence must be 30 times that observed, or about 0.05 sec. On the other hand, the lifetime against the same transition, estimated from the absorption coefficient, is 10^{-5} sec. This large discrepancy rules out this simple process.

The third type of mechanism involving the recombination of radicals or the attack of molecules by radicals might conceivably occur in many different ways. Of these, emission accompanying a recombination of radicals is excluded by the following arguments:

(1) It has been shown[1] that the density of radicals under the conditions used cannot be great enough to account for the observed rate of decay.

(2) In such a bimolecular process, the rate of decay of the fluorescence should be smaller the lower the initial concentration of radicals, that is to say, the lower the exciting intensity. It was observed, however, especially in the diffusion experiment, that the rate of decay was independent of intensity. A ninefold change in intensity caused no change in the form of the diffusion pattern, hence no change in the rate of decay. In such a process, moreover, the decay curve should not be exponential, as observed.

(3) Dilute aqueous solution (e.g. 1 : 200) of diacetyl fluoresces strongly. Under these conditions the recombination of radicals (except of those just separated) should be greatly hindered.

(4) The slow growth of the identical fluorescence in acetone (described below), as contrasted with its immediate appearance in diacetyl is difficult to understand if the emission is a recombination spectrum. It should not require minutes or hours in one case, about 10^{-3} sec. in the other, to establish equilibrium between production and recombination of the same radicals.

The first three of these arguments apply also against a process of chemiluminescence, in which the energy released in a bimolecular reaction between radicals excites a third molecule. Argument three (occurrence of fluorescence in dilute aqueous solution) also applies against chemiluminescence caused by the energy released in a radical-diacetyl reaction going to excite another diacetyl molecule. This argument is against any process which involves the diffusion of radicals before reaction.

Still another possibility of this type is the formation of an excited molecule by a sticking collision of a radical and a diacetyl molecule, which compound molecule later emits the fluorescence. If the slow rate of decay measures the rate at which effective collisions of this type occur the rate should depend upon the pressure of diacetyl; no variation of lifetime with pressure is observed (Fig. 4). If, on the other hand, the effective collision requires only a short time, say 10^{-7} sec. at 1 mm pressure, the problem of accounting for the long observed lifetime has merely been transferred to another molecule.

The second mechanism suggested, delayed fluorescence, is capable of accounting for all of the observations. In this process diacetyl absorption ($X \rightarrow A$) is followed by a transition without radiation into a long-lived state M, which may be a tautomeric form of the molecule, separated by a potential barrier from state A. The chemical reactions which have been observed, decomposition and photo-oxidation if oxygen is present, may occur while the molecule is in either state A or M. Fluorescence occurs when the molecule returns to a state, presumably A, which can combine with the ground state X. The state A reached on absorption is the one described by McMurry and Mulliken[11] as forbidden by electronic selection rules to combine with the ground state. The lifetime of 10^{-5} sec. against this transition, which we compute from the absorption coefficient, is compatible with this assignment.

This mechanism is similar to the one proposed by Henriques and Noyes.[10] They introduce three excited states: B^0, corresponding to state A here, the state reached on absorption; B^1, analogous to our metastable state M; and B^2 from which fluorescence occurs and which in our model is a low vibrational level of electronic state A. At $\lambda 3650$ they find the fluorescence intensity increases with increasing pressure. This may be due primarily to the rapid removal of vibrational energy by collisions, reducing the

[11] McMurry and Mulliken, Proc. Nat. Acad. Sci. **26**, 312 (1940).

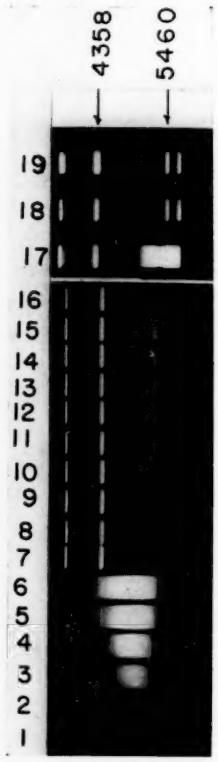

FIG. 6. Plate showing growth of green fluorescence in acetone under λ3130 radiation. Spectra 1–6, density marks. Spectra 7–15, consecutive one-minute exposures during first nine minutes of excitation of static acetone. Spectrum 16, taken during 10th minute of radiation with glass plate transmitting only $\lambda > 3400$A before arc. Spectra 1–16 on Eastman 40 plate. Spectrum 17, mixture of 14 mm diacetyl and 99 mm of acetone, five-minute exposure with λ3130 excitation. Spectrum 18, same as in 17 with glass plate as in 16. Spectrum 19, flowing acetone with mean pressure of 108 mm, five-minute exposure with λ3130 excitation. Spectra 17, 18, and 19 all on Eastman 50 plate.

probability of chemical processes, such as decomposition, and thereby enhancing the chance of fluorescence. When the molecule is excited with λ4358 the initial vibrational energy is much less and the effect of pressure in shifting the relative probabilities of chemical processes and fluorescence may be negligible.

The simplest adequate form of our proposed mechanism is one in which it is assumed that the processes competing with the fluorescence for the excitation energy all occur in state A, rather than M. In this case the fluorescence quantum yield is given by $I_f/I_A = k_v/(k_v+k_c)$ where k_v is the probability of fluorescence and k_c is the probability of the occurrence of a competing process. The lifetime is then determined primarily by K_{MA}, the rate of return from M to A. This mechanism allows the introduction of two activation energies: E_c in k_c and E_{MA} in k_{MA}, which control the temperature dependence of the competing chemical process and lifetime, respectively. From the roughly measured dependence of yield[12] and lifetime $(1/k_{MA})$ on temperature, from the observed quantum yield[13] (0.035) and k_v (10^5 sec.$^{-1}$), one can calculate, $E_c = 2100$ cal. per mole, $E_{MA} = 3900$ cal. per mole, $k_c = 28 \times 10^5$ sec.$^{-1}$.

One can easily write down the kinetic equations for the case in which chemical changes occur in both states A and M, with rates depending on temperature. No simple interpretation, as in the above case, can be inferred from the more complicated expressions for yield and rate of decay.

EXPERIMENTS WITH ACETONE

It has recently become clear that the green fluorescence observed when acetone is radiated with λ3130 is identical with the fluorescence of diacetyl when radiated with λ4358. Not only do the same three broad bands appear in the spectrum in both cases, but the finer superimposed structure is identical.[1] Matheson and Zabor[14] have also shown that several compounds containing the radical CH_3CO, e.g., acetaldehyde and methyl ethyl ketone, have a similar fluorescence spectrum. In addition there is chemical evidence that diacetyl is present in acetone after radiation with λ3130.[15,16]

If the fluorescence in acetone is due to the accumulation of diacetyl under the action of light the fluorescence should grow from zero intensity with continued radiation. To determine the course of growth of the fluorescence,

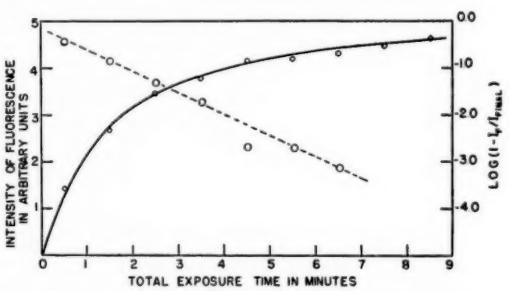

FIG. 7. Typical growth curve of green fluorescence in acetone radiated with λ3130. Points determined from Fig. 6 by taking the integrated intensity of each successive interval as the intensity for the midpoint of that interval. Full curve: intensity of fluorescence, I_f. Dotted curve: log $(1-I_f/I_0)$, I_0 = final intensity.

[12] Unpublished measurements of Almy and Gillette. Also measured by Henriques and Noyes (reference 10) who found a somewhat more rapid change with temperature.

[13] Fuller, Phillips and Almy, J. Chem. Phys. **7**, 973 (1939).

[14] Matheson and Zabor, J. Chem. Phys. **7**, 536 (1939).

[15] Spence and Wild, J. Chem. Soc. 352 (1937).

[16] Barak and Style, Nature **135**, 307 (1935).

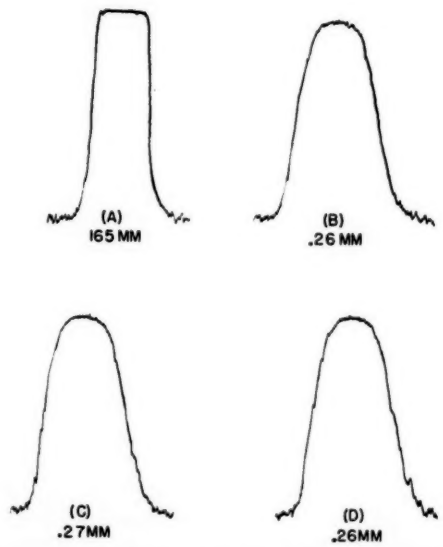

FIG. 8. Microphotometer traces of diacetyl, and diacetyl-acetone mixtures. (A) 150 mm of acetone plus 15 mm of diacetyl, one-second exposure; (B) 0.26 mm pressure (1 part diacetyl, 10 parts acetone), ten-minute exposure; (C) 0.27 mm of diacetyl, fifteen-second exposure; (D) same vapor as in (B) with exciting intensity reduced to $\frac{1}{3}$, thirty-minute exposure. *A*, *B* and *D*, λ3130 radiation; *C*, λ4358 radiation.

thoroughly outgassed acetone was flowed through a Corex fluorescence chamber where it was radiated with light from a quartz mercury arc, filtered by an aqueous solution of the iron-free sulphates of nickel and cobalt which transmitted principally the λ3130 line. The fluorescence spectrum was photographed with a Steinheil spectrograph equipped with one glass prism and an f: 3.5 camera. After getting a spectrogram of the fluorescence of the flowing acetone, the flow was arrested and a series of consecutive exposures was taken of the fluorescence of the static acetone. A series of such exposures is shown in Fig. 6.

From a study of a number of such plates the following facts appear:

(1) With rapidly flowing acetone radiated principally with λ3130, a negligible amount of green fluorescence is produced. Practically all the fluorescence is in the blue beginning at about 4700A and extending toward the ultraviolet.

(2) When the flow of acetone is stopped the intensity of the green fluorescence grows from a very low value towards a maximum as is shown by the successive exposures. With the aid of the density marks the intensity of the fluorescence in the successive exposures in Fig. 6 was determined and plotted against time in Fig. 7. The justification for plotting the curve through the origin is obtained from a comparison of exposures 7 and 19. The former is an exposure taken during the first minute of radiation of static acetone; the latter is an exposure of five minutes with flowing acetone at a pressure about $\frac{2}{3}$ of the first and on a plate much faster in the green. This comparison shows that the average intensity of the green fluorescence in the first minute of radiation of stationary acetone is ten to one hundred times stronger than in a flowing system and that, therefore, one is justified in plotting a point of sensibly zero intensity at zero time in Fig. 7. In the same figure the straight line shows that the fluorescence grows according to the relation $I_f = I_0(1 - e^{-kt})$ where I_0 is the final intensity, approached asymptotically.

(3) When a little diacetyl is added to the acetone the green fluorescence appears immediately with full intensity upon radiation with λ3130 (exposure 17). Furthermore, this fluorescence is not due to the direct excitation of diacetyl by a small amount of blue light which might pass the filter. This is demonstrated by the disappearance of the fluorescence when a glass plate transmitting only light of wave-lengths longer than 3400A is interposed.

(4) The blue fluorescence present in a system of flowing acetone grows weaker on continued radiation of the static vapor (exposures 1–9).

We attempted in a second experiment to detect the formation of diacetyl in acetone radiated by λ3130 by measuring the absorption of light of wave-length 4358A which is absorbed by diacetyl but not by acetone. The few rough trials gave positive evidence of absorption at λ4358 suggesting that a small amount of diacetyl was formed, but at most no more than a partial pressure of a few tenths of a mm. Furthermore, apparently an equilibrium between its creation and decomposition was soon established for one could get as much absorption of λ4358 after fifteen minutes of radiation as after several hours.

In addition to these experiments, we measured the lifetime for the fluorescence in acetone by the method of the diffusion of the fluorescence.

This we did by comparing the diffusion patterns of an acetone-diacetyl mixture radiated with λ3130 and diacetyl radiated with λ4358 at equal pressures. As seen from Fig. 8 the microphotometer traces of the photographs are identical. This shows that the lifetime in the two cases is nearly the same since their diffusion coefficients surely are not greatly different. We also decreased the intensity of the exciting light by a factor of three and compensated by increasing the exposure time by three and found that the diffusion pattern is unaltered, indicating (1) that the lifetime in the case of acetone, as in diacetyl, is unaltered by the variations in the intensity of the exciting light and (2) that, assuming photographic reciprocity, the intensity of the green fluorescence in the acetone-diacetyl mixture is proportional to the intensity of the exciting light. In this experiment there was present much more diacetyl than occurred in radiated acetone, even on long radiation.

In conclusion, what can be said about the origin of the green fluorescence in acetone? What is the molecule which emits it and by what process is it excited? The fluorescence spectrum is identical in acetone excited by λ3130 and diacetyl excited by λλ3650, 4047, 4358. It does not appear in pure acetone flowing rapidly. It appears when diacetyl is added or when, on continued radiation, diacetyl has accumulated in the tube. The presence of diacetyl appears to be necessary for the production of the fluorescence and the simplest assumption is that the diacetyl molecule is the emitter.

Further relations between acetone and diacetyl fluorescence are seen in the diffusion experiments. At the same total pressures the diffusion patterns of pure diacetyl and acetone plus a small amount of diacetyl are identical. This means that, assuming the same diffusion coefficients, the lifetimes are identical; a ten-percent difference could easily be detected. This constitutes a further check on the identity of the emitter or emitting process in the two cases. Recombination or chemiluminescence processes are ruled out by arguments given in the discussion of diacetyl fluorescence. The fluorescence must be due to a long-lived molecule, presumably diacetyl, excited while in the illuminated region.

The process by which the diacetyl molecule is excited must involve a reaction between an excited molecule and diacetyl. Diacetyl does not fluoresce with appreciable intensity when radiated with λ3130 unless acetone is present. Hence, the simplest picture of the excitation of diacetyl is a collision of the second kind between excited acetone and diacetyl. It cannot be that a diacetyl-producing reaction between excited acetone and another molecule or radical leaves the diacetyl produced in a condition to emit the fluorescence, for in that case the fluorescence in pure acetone should be present almost immediately with full intensity.

The simple nature of the growth curve of the fluorescence should shed some light on the processes of production, excitation, and disappearance of the diacetyl. However, just because several steps are involved between absorption by acetone and the appearance of the fluorescence, there is no series of processes which will uniquely account for the growth.

Quenching Efficiency of Oxygen

The fluorescence of diacetyl is apparently strongly quenched by oxygen,[1] but recovers in time, indicating that the oxygen is consumed. It was shown that an oxygen pressure of 0.013 mm brought the fluorescence to one-half intensity. Assuming a collision diameter of 3×10^{-8} cm, a lifetime of the excited molecule of 10^{-5} sec. was required to make fluorescence and quenching collisions equally probable. We now find, however, that the molecule actually remains in an excited state 10^{-3} sec. Therefore, about 100 collisions (to within 3×10^{-8} cm) between excited diacetyl and oxygen occur, on the average, before a quenching collision takes place. The quenching process thus owes its apparent high efficiency to the long lifetime of the excited molecule.

The Rate of Solution of Metals in Acids as a Function of Overvoltage*

I. The Diffusion Potential

GEORGE E. KIMBALL AND ALVIN GLASSNER
Department of Chemistry, Columbia University, New York, New York

(Received July 2, 1940)

The problem of simultaneous conduction and diffusion through a constrained diffusion layer is discussed. An exact solution is obtained for the case of an ideal dilute solution containing only two ionic species. The special case of divalent ions diffusing into a uni-divalent electrolyte is also solved by numerical methods. It is shown that for diffusion layers of thicknesses of the order of 50μ the potential drop across the layer for currents of the order of magnitude of 100 milliamperes per sq. cm is less than one millivolt. It is therefore legitimate to neglect the diffusion potential in comparison with the double layer potential at an electrode surface.

IN discussions of the theory of electrode reactions it is assumed that the potential difference across the diffusion layer surrounding an electrode is negligible in comparison with that across the electrical double layer.[1] The relationship between potential and current in a region where both ionic conduction and diffusion are taking place must be known before this assumption can be justified. This paper is therefore devoted to a discussion of this relationship.

Consider a portion of an electrolyte solution bounded by two parallel planes separated by a distance δ and of unit cross section. Let the coordinate x be in a direction perpendicular to these planes, such that $x=x_1$ at the left-hand boundary, $x=x_2$ at the right-hand boundary, and $x_2-x_1=\delta$. Physically, we shall require that $x=x_1$ correspond to the interface between the diffusion and electrical double layers, that $x=x_2$ correspond to the interface between diffusion layer and solution.

Within this layer there exist ions of several types, each variety being denoted by a subscript i. The average velocity of the ith ion, v_i, will be given by[2]

$$v_i=-U_i[N_0\partial\mu_i/\partial x+z_i\mathfrak{F}\partial V/\partial x], \qquad (1)$$

where U_i is the mobility of the ith ion (i.e., the velocity produced by a force of one dyne acting on a mole of ions), μ_i is the chemical potential *per ion*, z_i the valence. V is the potential at any point x of the diffusion layer; $\mathfrak{F}$ is the Faraday constant, and N_0 the Avogadro number. If we assume an ideal solution we may write

$$\mu_i=\mu_i^0+kT\ln C_i, \qquad (2)$$

where C_i denotes the concentration of the ith variety of ion at the point x in moles per cc. Then

$$v_i=-U_i\left[\frac{RT}{C_i}\frac{\partial C_i}{\partial x}+z_i\mathfrak{F}\frac{\partial V}{\partial x}\right]. \qquad (3)$$

The number of moles of ions of the ith type crossing a unit surface in one second at the point x is given by

$$M_i=C_iv_i. \qquad (4)$$

Accordingly the current in the diffusion layer due to the ith ion is

$$\begin{aligned} I_i&=z_i\mathfrak{F}M_i \\ &=-z_i\mathfrak{F}U_i[RT\partial C_i/\partial x+z_i\mathfrak{F}C_i\partial V/\partial x]. \end{aligned} \qquad (5)$$

There will be one such equation for each of the ion varieties. These, together with the Poisson equation,

$$\frac{\partial^2V}{\partial x^2}=-\frac{4\pi}{K}\sum_i z_i\mathfrak{F}C_i, \qquad (6)$$

where K is the dielectric constant, constitute a system of differential equations the solution of which gives a complete picture of the diffusion layer.

If we substitute numerical constants into Eq.

* Publication assisted by the Ernest Kempton Adams Fund for Physical Research of Columbia University.

[1] E.g., Kimball, J. Chem. Phys. **8**, 199 (1940).

[2] MacInnes, *Principles of Electrochemistry* (Reinhold, 1939), p. 461.

(6), using the value $K=80$, there is obtained

$$\sum_i z_i C_i = -0.7\times 10^{-16}\,\partial^2 V/\partial x^2. \tag{7}$$

It follows that ordinary values of $\partial^2 V/\partial x^2$ lead to values of $\sum z_i C_i$ which are below the limits of experimental accuracy. Hence it is legitimate to assume

$$\sum z_i C_i = 0, \tag{8}$$

that is, electrical neutrality of the solution, without simultaneously assuming that $\partial^2 V/\partial x^2 = 0$ and thus $\partial V/\partial x = \text{constant}$.[3] With the aid of Eq. (8) we may further simplify Eq. (5).

First, however, we may put (5) into a more convenient form by substituting the equivalent conductance of an ion, λ_i, for the mobilities in accordance with the equation

$$\lambda_i = n_i U_i \mathfrak{F}^2, \quad n_i = |z_i|. \tag{9}$$

In this way we obtain from (5)

$$I_i = -\lambda_i\left[\frac{z_i RT}{n_i \mathfrak{F}}\frac{\partial C_i}{\partial x} + n_i C_i \frac{\partial V}{\partial x}\right]. \tag{10}$$

If we define a quantity J_i by means of the equation

$$J_i \equiv n_i I_i/\lambda_i, \tag{11}$$

we obtain from (10)

$$J_i = -\left[z_i \frac{RT}{\mathfrak{F}}\frac{\partial C_i}{\partial x} + n_i^2 C_i \frac{\partial V}{\partial x}\right] \tag{12}$$

and

$$J \equiv \sum J_i = -\left[\frac{RT}{\mathfrak{F}}\sum z_i \frac{\partial C_i}{\partial x} + \frac{\partial V}{\partial x}\sum n_i^2 C_i\right]. \tag{13}$$

By means of (8) we see that

$$\sum_i z_i\, \partial C_i/\partial x = 0. \tag{14}$$

If we also let

$$S = 2\mu = \sum n_i^2 C_i, \tag{15}$$

where μ is the ionic strength, Eq. (13) becomes

$$\partial V/\partial x = -J/S. \tag{16}$$

[3] Hermans, Rec. des trav. chim. **56**, 635 (1937).

Substitution of (16) into (12) leads to

$$J_i = -\left[z_i \frac{RT}{\mathfrak{F}}\frac{\partial C_i}{\partial x} - \frac{n_i^2 C_i}{S} J\right]. \tag{17}$$

These equations can be solved exactly in the particular case of a solution of a simple salt, such that the system contains but two varieties of ions. In this case

$$J_1 = -\frac{RT}{\mathfrak{F}} z_1 \frac{\partial C_1}{\partial x} + \frac{z_1^2 C_1}{S} J, \qquad J_2 = -\frac{RT}{\mathfrak{F}} z_2 \frac{\partial C_2}{\partial x} + \frac{z_2^2 C_2}{S} J, \tag{18a}$$

$$\partial V/\partial x = -J/S \tag{18b}$$

with the supplementary relations

$$J = J_1 + J_2, \quad S = z_1^2 C_1 + z_2^2 C_2, \quad z_1 C_1 + z_2 C_2 = 0. \tag{19}$$

By algebraic manipulations Eqs. (18a) may be transformed to

$$\frac{\partial C_1}{\partial x} = -\frac{\mathfrak{F}}{RT}\frac{z_2}{z_2 - z_1}\left(\frac{J_1}{z_1} + \frac{J_2}{z_2}\right), \qquad \frac{\partial C_2}{\partial x} = +\frac{\mathfrak{F}}{RT}\frac{z_1}{z_2 - z_1}\left(\frac{J_1}{z_1} + \frac{J_2}{z_2}\right). \tag{20}$$

Thus both C_1 and C_2 vary linearly with x. Hence S too is a linear function of x, and we may write

$$S = Ax + B. \tag{21}$$

Combining this with (18b) we find

$$\partial V/\partial x = -J/(Ax+B), \tag{22}$$

which, upon integration between the limits x_1 and x_2, yields

$$V_2 - V_1 = -\frac{J}{A}\ln\frac{Ax_2+B}{Ax_1+B} = -\frac{J}{A}\ln\frac{S_2}{S_1}. \tag{23}$$

To determine A we have from (19) and (21)

$$A = \partial S/\partial x = z_1^2 \partial C_1/\partial x + z_2^2 \partial C_2/\partial x. \tag{24}$$

With the use of Eqs. (20) this reduces to

$$A=\frac{\mathfrak{F}}{RT}(z_2J_1+z_1J_2)$$
$$=\frac{\mathfrak{F}}{RT}\left(\frac{n_1z_2I_1}{\lambda_1}+\frac{n_2z_1I_2}{\lambda_2}\right). \tag{25}$$

B is the value of S at the point $S=0$.

If $S_1=S_2$, so that no diffusion takes place, then $A=0$, and

$$J=-B\partial V/\partial x=-S\partial V/\partial x. \tag{26}$$

Since J and S are constant, this shows that $\partial V/\partial x$ is constant. Substituting for J and S,

$$\frac{n_1I_1}{\lambda_1}+\frac{n_2I_2}{\lambda_2}=-(n_1^2C_1+n_2^2C_2)\frac{\partial V}{\partial x}. \tag{27}$$

Equation (27) is obviously equivalent to the ordinary conduction equations:

$$I_1=-n_1\lambda_1C_1\partial V/\partial x,$$
$$I_2=-n_2\lambda_2C_2\partial V/\partial x. \tag{28}$$

In the case of simple diffusion without conduction

$$I=I_1+I_2=0 \tag{29}$$

and therefore

$$J=(n_1/\lambda_1-n_2/\lambda_2)I_1,$$
$$A=\frac{\mathfrak{F}}{RT}\left(\frac{n_1z_2}{\lambda_1}-\frac{n_2z_1}{\lambda_2}\right)I_1. \tag{30}$$

Substitutions of Eqs. (30) into (23) yields

$$V_2-V_1=\frac{n_1\lambda_2-n_2\lambda_1}{n_1\lambda_2z_2-n_2\lambda_1z_1}\frac{RT}{\mathfrak{F}}\ln\frac{S_2}{S_1}, \tag{31}$$

which in the case of a uñi-univalent electrolyte correctly reduces to

$$V_2-V_1=\frac{\lambda_2-\lambda_1}{\lambda_2+\lambda_1}\frac{RT}{\mathfrak{F}}\ln\frac{C_2}{C_1}$$
$$=(t_2-t_1)\frac{RT}{\mathfrak{F}}\ln\frac{C_2}{C_1}, \tag{32}$$

where t_1 and t_2 are the transference numbers of the ions.

In the experimental work reported in the following paper of this series it was necessary to consider a diffusion layer containing (1) cadmium ions, (2) hydrogen ions, and (3) sulfate ions. It was further assumed that the sulfate ions took no part in carrying the current. In this case the differential equations to be satisfied are

$$J_1=-\frac{2RT}{\mathfrak{F}}\frac{\partial C_1}{\partial x}+\frac{4C_1}{S}J,$$
$$J_2=-\frac{RT}{\mathfrak{F}}\frac{\partial C_2}{\partial x}+\frac{C_2}{S}J,$$
$$0=+\frac{2RT}{\mathfrak{F}}\frac{\partial C_3}{\partial x}+\frac{4C_3}{S}J, \tag{33}$$
$$\partial V/\partial x=-J/S.$$

Let

$$J_2=-\gamma J_1, \tag{34}$$

γ being some numerical parameter. Then

$$J=(1-\gamma)J_1 \tag{35}$$

and the differential equations become

$$\frac{\partial C_1}{\partial x}=\frac{\mathfrak{F}}{2RT}\left[\frac{4C_1}{S}(1-\gamma)J_1-J_1\right],$$
$$\frac{\partial C_2}{\partial x}=\frac{\mathfrak{F}}{RT}\left[\frac{C_2}{S}(1-\gamma)J_1+\gamma J_1\right],$$
$$\frac{\partial C_3}{\partial x}=\frac{\mathfrak{F}}{2RT}\left[-\frac{4C_3}{S}(1-\gamma)J_1\right], \tag{36}$$
$$\frac{\partial V}{\partial x}=-(1-\gamma)\frac{J_1}{S}.$$

We now define three new variables:

$$y=-\frac{J_1\mathfrak{F}}{RT}\frac{x}{C_3^{(0)}},$$
$$C_i'=C_i/C_3^{(0)}, \tag{37}$$
$$V'=\mathfrak{F}V/RT,$$

where $C_3^{(0)}$ is a parameter enabling us to define concentrations in whatever units we please. Thus Eqs. (36) become

$$\partial C_1'/\partial y=(-2(1-\gamma)C_1'+\tfrac{1}{2}S')/S',$$
$$\partial C_2'/\partial y=(-(1-\gamma)C_2'-\gamma S')/S',$$
$$\partial C_3'/\partial y=2(1-\gamma)C_3'/S', \tag{38}$$
$$\partial V/\partial y=(1-\gamma)/S'.$$

TABLE I. *Numerical integration of Eqs. (38) for $\gamma=0.025$.*

y	$C'_{SO_4^{--}}$	C'_{H^+}	$C'_{Cd^{++}}$	S'	$\frac{\partial C'_{SO_4^{--}}}{\partial y}$	$\frac{\partial C'_{H^+}}{\partial y}$	V'
0	1.000	2.000	0.000	6.000	0.325	−0.350	0.000
1	1.307	1.723	0.446	8.734	0.292	−0.217	0.134
2	1.591	1.537	0.822	11.191	0.277	−0.159	0.231
3	1.761	1.373	1.074	12.715	0.270	−0.130	0.283
4	2.028	1.255	1.400	14.969	0.264	−0.107	0.355
5	2.290	1.157	1.711	17.163	0.260	−0.0907	0.414
6	2.549	1.072	1.963	19.320	0.257	−0.0791	0.468
7	2.805	0.997	2.306	21.443	0.255	−0.0703	0.516
8	3.059	0.930	2.594	23.542	0.253	−0.0635	0.560
9	3.311	0.870	2.876	25.618	0.252	−0.0581	0.599
10	3.563	0.814	3.156	27.690	0.251	−0.0536	0.636
11	3.813	0.762	3.432	29.742	0.250	−0.0500	0.669
12	4.063	0.713	3.706	31.791	0.249	−0.0469	0.701
13	4.312	0.668	3.978	33.828	0.249	−0.0443	0.731
14	4.561	0.625	4.248	35.863	0.248	−0.0420	0.759
15	4.809	0.584	4.517	37.888	0.248	−0.0400	0.785
16	5.057	0.545	4.784	39.911	0.247	−0.0383	0.811
17	5.304	0.508	5.050	41.924	0.247	−0.0368	0.834

TABLE II. *Numerical integration of Eqs. (38) for $\gamma=0.05$.*

y	$C'_{SO_4^{--}}$	C'_{H^+}	$C'_{Cd^{++}}$	S'	$\frac{\partial C'_{SO_4^{--}}}{\partial y}$	$\frac{\partial C'_{H^+}}{\partial y}$	V'
0	1.000	2.000	0.000	6.000	0.317	−0.367	0.000
1	1.299	1.705	0.446	8.687	0.284	−0.236	0.131
2	1.576	1.500	0.826	11.108	0.270	−0.178	0.228
3	1.841	1.320	1.181	13.408	0.261	−0.144	0.305
4	2.099	1.188	1.505	15.604	0.256	−0.122	0.371
5	2.353	1.074	1.816	17.750	0.252	−0.107	0.428
6	2.604	0.973	2.117	19.859	0.249	−0.0965	0.479
7	2.852	0.881	2.412	21.936	0.247	−0.0881	0.524
8	3.098	0.796	2.700	23.988	0.245	−0.0815	0.565
10	3.585	0.644	3.263	28.036	0.243	−0.0718	0.639
12	4.069	0.508	3.815	32.044	0.241	−0.0651	0.702
14	4.550	0.383	4.358	36.017	0.240	−0.0601	0.758
16	5.029	0.267	4.896	39.965	0.239	−0.0563	0.808
18	5.506	0.158	5.427	43.890	0.238	−0.0534	0.853
20	5.982	0.054	5.955	47.802	0.238	−0.0511	0.895
22	6.459	−0.047	6.482	51.719	0.237	−0.0491	0.933

TABLE III. *Numerical integration of Eqs. (38) for $\gamma=0.075$.*

y	$C'_{SO_4^{--}}$	C'_{H^+}	$C'_{Cd^{++}}$	S'	$\frac{\partial C'_{SO_4^{--}}}{\partial y}$	$\frac{\partial C'_{H^+}}{\partial y}$	V'
0	1.000	2.000	0.000	6.000	0.308	−0.383	0.000
1	1.291	1.686	0.448	8.642	0.276	−0.255	0.128
2	1.559	1.461	0.828	11.011	0.262	−0.198	0.222
3	1.818	1.278	1.179	13.266	0.254	−0.164	0.299
4	2.068	1.126	1.556	15.426	0.248	−0.142	0.364
5	2.320	0.992	1.824	17.568	0.244	−0.127	0.421
6	2.563	0.871	2.128	19.633	0.241	−0.116	0.471
7	2.805	0.760	2.425	21.680	0.239	−0.107	0.516
8	3.044	0.656	2.716	23.696	0.238	−0.101	0.557
9	3.281	0.558	3.002	25.690	0.236	−0.0950	0.594
10	3.517	0.465	3.284	27.671	0.235	−0.0906	0.629
11	3.752	0.376	3.564	29.640	0.234	−0.0867	0.661
12	3.986	0.291	3.840	31.597	0.233	−0.0835	0.691
13	4.219	0.209	4.114	33.543	0.233	−0.0808	0.720
14	4.453	0.129	4.388	35.495	0.232	−0.0784	0.747
15	4.684	0.0516	4.659	37.420	0.232	−0.0763	0.773
16	4.917	−0.0232	4.929	39.359			0.796

This set of equations, involving the parameter γ, cannot be solved exactly except in the particular cases $\gamma=0$ and $\gamma=1$. In the latter case we immediately obtain

$$\begin{aligned} C_1' &= \tfrac{1}{2}y + \text{constant}, \\ C_2' &= -y + \text{constant}, \\ C_3' &= \text{constant}, \\ V' &= \text{constant}. \end{aligned} \tag{39}$$

The case $\gamma=0$ corresponds to the physical situation in which the current is being carried by cadmium ions alone, that is, cadmium ions diffusing through a sulfuric acid solution. The solution then obtained is

$$\begin{aligned} C_1' &= C_3' - 1/(C_3')^{\frac{1}{2}}, \\ C_2' &= 2/(C_3')^{\frac{1}{2}}, \\ V' &= \tfrac{1}{2}\ln C_3', \\ y &= 4C_3' + \frac{2}{(C_3')^{\frac{1}{2}}} - 6. \end{aligned} \tag{40}$$

TABLE IV. *Numerical integration of Eqs. (38) for $\gamma=0.15$.*

y	$C'_{SO_4^{--}}$	C'_{H^+}	$C'_{Cd^{++}}$	S'	$\frac{\partial C'_{SO_4^{--}}}{\partial y}$	$\frac{\partial C'_{H^+}}{\partial y}$	V'
0	1.000	2.000	0.000	6.000	0.283	−0.433	0.000
1	1.267	1.632	0.451	8.504	0.253	−0.313	0.119
2	1.502	1.389	0.807	10.627	0.240	−0.261	0.204
3	1.737	1.147	1.163	12.749	0.232	−0.227	0.276
4	1.966	0.933	1.499	14.795	0.226	−0.204	0.338
5	2.190	0.738	1.821	16.782	0.222	−0.187	0.392
6	2.411	0.557	2.132	18.231	0.219	−0.175	0.440
7	2.629	0.387	2.435	20.643	0.216	−0.166	0.484
8	2.844	0.225	2.731	22.527	0.215	−0.158	0.523
9	3.058	0.070	3.023	24.394	0.213	−0.152	0.558
10	3.270	−0.080	3.350	26.240			0.592

TABLE V. *Numerical integration of Eqs. (38) for $\gamma=0.30$.*

y	$C'_{SO_4^{--}}$	C'_{H^+}	$C'_{Cd^{++}}$	S'	$\frac{\partial C'_{SO_4^{--}}}{\partial y}$	$\frac{\partial C'_{H^+}}{\partial y}$	V'
0	1.000	2.000	0.000	6.000	0.233	−0.533	0.000
1	1.220	1.522	0.459	8.238	0.207	−0.429	0.099
2	1.420	1.120	0.860	10.240	0.194	−0.377	0.175
3	1.610	0.761	1.229	12.119	0.186	−0.344	0.238
4	1.793	0.429	1.580	13.931	0.180	−0.321	0.292
5	1.971	0.116	1.913	15.652	0.176	−0.305	0.339
6	2.146	−0.096	2.194	17.264			0.382

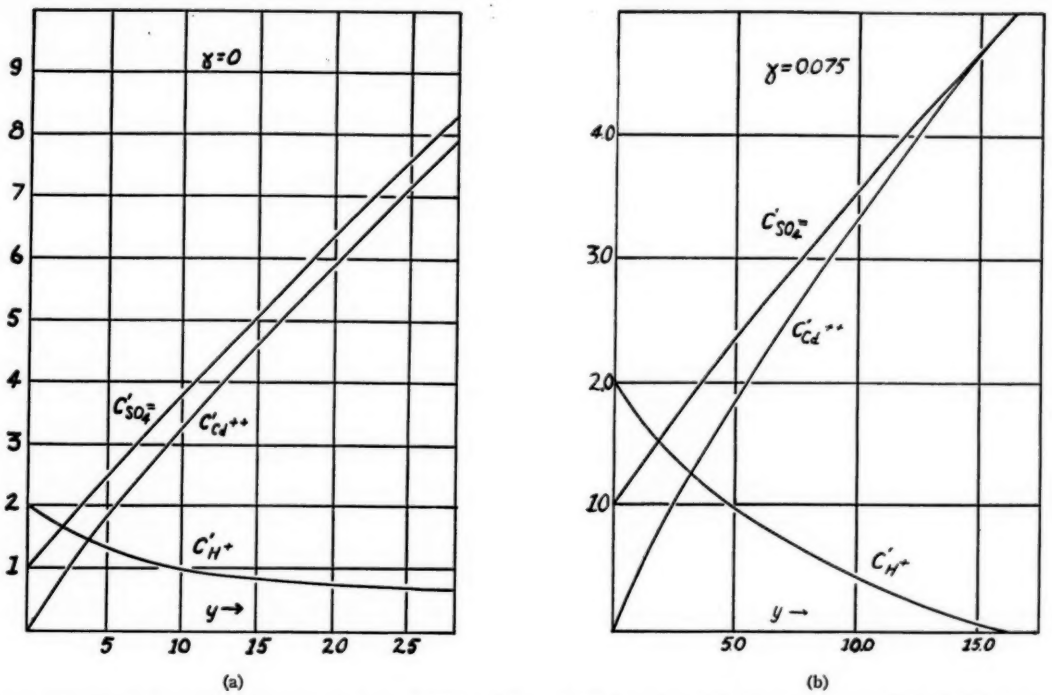

FIG. 1. The variation of the concentrations of Cd^{++}, H^+, and $SO_4^=$ in the diffusion layer on a $Cd-H_2SO_4$ electrode. The unit of concentration is the concentration of $SO_4^=$ in the main body of the solution. The coordinate y measures the distance inward from the interface between the solution and the diffusion layer, in units defined in the text. In Fig. 1(a), $\gamma=0$, i.e., the entire current is carried by the Cd^{++}. In Fig. 1(b), a fraction of the current is carried by H^+, as shown by the value of γ.

For other values of γ resort must be had to numerical integration. In Tables I–V the required data for the integrations are presented. In Fig. 1 graphs are given of the concentration *versus* y; in Fig. 2, graphs of V' *versus* y are given for various values of γ. The values at $y=0$ denote the values at the solution-diffusion layer interface.

In order to convert the primed quantities into quantities having the customary dimensions we must make use of Eqs. (37). For a $1N$ sulfuric acid solution at 25°C

$$\begin{aligned} 6.40\times10^{-6}\frac{\lambda_{Cd}}{I_{Cd}}y&=x \text{ cm},\\ \tfrac{1}{2}C_i'&=C_i \text{ mole/liter},\\ 0.0256V'&=V \text{ volt}, \end{aligned} \tag{41}$$

where I_{Cd} is given in amperes.

Values of the thickness of the diffusion layer as they appear in the literature[4] vary between

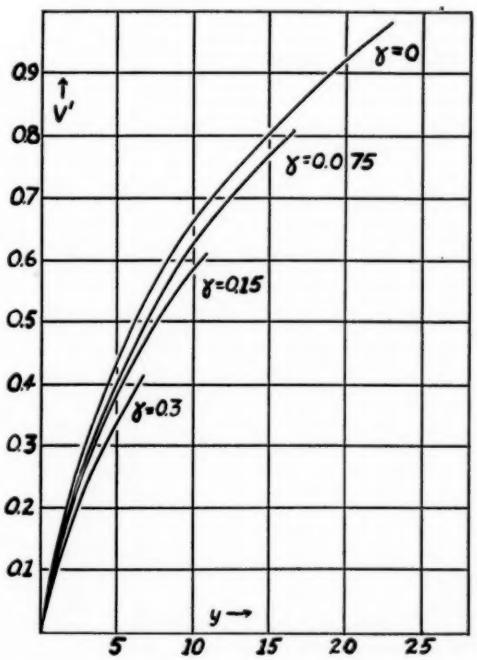

FIG. 2. The variation of electrostatic potential in the diffusion layer on a $Cd-H_2SO_4$ electrode.

[4] Roller, J. Phys. Chem. **39**, 221 (1935).

20–50μ, as obtained from kinetic measurements interpreted in accordance with the Nernst theory, to 0.0025μ, as obtained by ultramicroscopic examination of water flowing slowly in pipes. If we assume the width of the diffusion layer to be 50μ, $\lambda_{Cd}=50$, and $I_{Cd}=0.1$ ampere per sq. cm, it is found that the potential drop across the diffusion layer amounts to less than a millivolt. This value is negligible in comparison with the voltage necessary to produce the current mentioned. Thus the assumption that the diffusion potential at an electrode is negligible in comparison with the double layer potential receives some theoretical justification.

OCTOBER, 1940 JOURNAL OF CHEMICAL PHYSICS VOLUME 8

The Rate of Solution of Metals in Acids as a Function of Overvoltage*

II. The Solution of Cadmium in Sulfuric Acid

GEORGE E. KIMBALL AND ALVIN GLASSNER
Department of Chemistry, Columbia University, New York, New York

(Received July 2, 1940)

The rate of solution of cadmium in sulfuric acid has been measured as a function of the hydrogen overvoltage at the electrode surface. The rate was found to be constant at a given potential, independent of the concentration of sulfuric acid used. The rate increases with the electrode potential in accordance with the theory of Kimball. From the dependence of the rate on the speed of stirring, and also from the behavior on varying the potential, it is concluded that the solution process is diffusion controlled. The effect of surface inhomogeneities was too great to permit an evaluation of the absolute rate.

1. INTRODUCTION

WHEN a metal atom or ion leaves the surface of an electrode, it must traverse three regions before it arrives in the main body of the solution. Likewise, before an ion from the solution can be discharged, it must traverse the same three regions in reverse order. The first step in the solution of a metal is the transfer of an ion from the electrode surface through the layer of adsorbed atoms to the layer of adsorbed ions, which, together with its electrical image in the electrode, constitutes the electrical double layer surrounding the electrode surface. The ion must then be transported through the diffusion layer which surrounds the layer of adsorbed ions.

The rate at which these processes take place has been discussed by numerous authors.[1] The object of the present paper is to attempt to confirm experimentally the theory which has been developed by Eyring, Glasstone, and Laidler and by Kimball. According to this theory, the rate of the first step is determined by the rate at which the ions cross a potential energy barrier lying somewhere between the electrode surface and the adsorbed ion layer.

It has been shown theoretically[2] that the current I_a carried by the ionic species A from an electrode surface should be given by an equation of the form

$$I_a=\epsilon_a\lambda\{e^{\epsilon_a(V-V_a)/kT}[A]-[A^+]\}, \qquad (1)$$

where ϵ_a is the charge on the ion A^+, $[A]$ is the activity of the discharged form, and $[A^+]$ is the activity of the ion A^+ in the body of the solution. V is the potential difference across the electrical double layer surrounding the electrode surface, and V_a is the potential difference when the

* Publication assisted by the Ernest Kempton Adams Fund for Physical Research of Columbia University.

[1] Nernst and Brunner, Zeits. f. physik. Chemie **47**, 52, 56 (1904); Tafel, *ibid.* **50**, 641 (1905); Centnerszwer, *ibid.* **A141**, 297 (1929); Erdey-Grúz and Volmer, *ibid.* **A150**, 203 (1930); Gurney, Proc. Roy. Soc. (London) **A134**, 137 (1931–2); Frumkin, Zeits. f. physik. Chemie **A164**, 121 (1933); Hammett, Trans. Faraday Soc. **29**, 770 (1933); Butler, Proc. Roy. Soc. (London) **A157**, 423 (1936); Bowden and Agar, Ann. Reports Chem. Soc. **35**, 90 (1938); Horiuti and Okamoto, Bull. Chem. Soc. Japan **13**, 216 (1938); Eyring, Glasstone and Laidler, J. Chem. Phys. **7**, 1053 (1939); Kimball, *ibid.* **8**, 199 (1940).

[2] Kimball, reference 1.

electrode is at equilibrium with both A and A^+ at unit activity, i.e., the standard electrode potential. Both V and V_a are to be reckoned positive when the electrode is at a higher potential than the solution.

The factor λ in Eq. (1) is given by

$$\frac{1}{\lambda}=\frac{1}{P}e^{\epsilon_a\alpha(V-V_a)/kT}+\frac{1}{Q} \tag{2}$$

in which Q is the rate of diffusion through the diffusion layer when the difference in activity of the ion A^+ on the two sides of the diffusion layer is unity. P is the rate of formation, or discharge, of A^+ across the electrical double layer when $V=V_a$ and $[A]=1$. The factor α denotes that fraction of the double layer potential operating between the adsorbed ion layer and the potential energy barrier which must be surmounted by an ion in order to cross from the adsorbed ion layer to the electrode surface.

There are two special cases of Eq. (2) which are of importance. If $P \ll Q$, the reaction is diffusion controlled, and Eq. (2) reduces to

$$\lambda=Q. \tag{3}$$

In this case Eq. (1) takes the form

$$I_a=\epsilon_a Q\{e^{\epsilon_a(V-V_a)/kT}[A]-[A^+]\}. \tag{4}$$

It should be noticed that Eq. (4) is independent of the quantity α.

In the other special case $P \ll Q$. Then

$$\lambda=Pe^{-\epsilon_a\alpha(V-V_a)/kT} \tag{5}$$

and Eq. (1) takes the form

$$I_a=\epsilon_a P\{e^{(1-\alpha)\epsilon_a(V-V_a)/kT}[A]-e^{-\epsilon_a\alpha(V-V_a)/kT}[A^+]\}. \tag{6}$$

The remainder of this paper will describe an experimental check on the validity of Eq. (1) for the solution of a typical metal, cadmium, in sulfuric acid.

2. Experimental Procedure

The reaction between cadmium and sulfuric acid is a typical irreversible electrode reaction. At the interface two distinct processes take place: the solution of cadmium as cadmium ions, Cd^{++}, and the liberation of hydrogen from the acid. If a piece of cadmium is simply dipped into sulfuric acid, both reactions take place in such a way that the current I_{Cd} carried from the cadmium by the cadmium ions is equal to the current I_H carried to the cadmium by the hydrogen ions. (It is assumed throughout this work that no current is carried in any other way, e.g., by sulfate ions.)

The theory predicts that these two electrode reactions proceed independently of each other, except insofar as they are both governed by the potential drop at the electrode surface. For a given potential drop, therefore, the rate of solution of cadmium should be independent of the actual rate at which hydrogen is evolved, and hence independent of the solution in which the cadmium is dissolving.

In order to verify this conclusion, the experiments were carried out in such a way that the ratio of the hydrogen current to the cadmium current could be varied. This was accomplished by using a second electrode as a polarizing electrode. If a large current is passed from the cadmium to the polarizing electrode, the reaction at the cadmium surface becomes simply

$$Cd \rightarrow Cd^{++}+2\epsilon$$

and the hydrogen current disappears. If the current is reversed the cadmium solution stops, and the current is entirely carried by the reaction

$$2H^+ + 2\epsilon \rightarrow H_2.$$

For intermediate currents, any ratio of I_{Cd} to I_H can be obtained.

In order to measure the potential drop at the cadmium surface a saturated calomel electrode was used as a reference electrode. The potential difference, E, between this electrode and the cadmium is actually the sum of three separate potential differences, namely: (i) the potential drop V across the double layer at the cadmium-solution interface; (ii) the potential drop across the diffusion layer (concentration polarization); and (iii) the ohmic drop due to the resistance of the leads and that portion of the solution between the cadmium and the reference electrodes. We have shown in the previous paper that the second of these is negligible. The third, however, is far from being negligible, and allow-

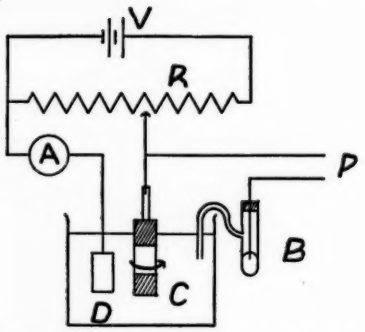

FIG. 1. Schematic diagram of electrical apparatus.

ance must be made for it. If R is the effective resistance of the solution and leads, the ohmic drop is IR, where I is the total current. Hence we may set

$$E=V+IR. \tag{7}$$

In terms of the measured quantities I_{Cd}, I, and E, Eq. (1) becomes

$$I_{Cd}=2\epsilon\lambda\{e^{2\epsilon(E-IR-V_{Cd})/kT}[Cd]-[Cd^{++}]\}. \tag{8}$$

We may put $[Cd]=1$, and since the concentration of cadmium ions in solution was always kept very low, we may also put $[Cd^{++}]=0$. Then Eq. (8) simply reduces to

$$I_{Cd}=2\epsilon\lambda e^{2\epsilon(E-IR-V_{Cd})/kT}. \tag{9}$$

If the solution is diffusion controlled this becomes

$$\begin{aligned} I_{Cd}&=2\epsilon Q_{Cd}e^{2\epsilon(E-IR-V_{Cd})/kT} \\ &=I_0{}^q e^{2\epsilon(E-IR)/kT}, \end{aligned} \tag{10}$$

where

$$I_0{}^q=2\epsilon Q_{Cd}e^{-2\epsilon V_{Cd}/kT}. \tag{11}$$

If, on the other hand, the reaction is activation controlled.

$$\begin{aligned} I_{Cd}&=2\epsilon P_{Cd}e^{2\epsilon(1-\alpha)(E-IR-V_{Cd})/kT} \\ &=I_0{}^p e^{2\epsilon(1-\alpha)(E-IR)/kT} \end{aligned} \tag{12}$$

where

$$I_0{}^p=2\epsilon P_{Cd}e^{-2\epsilon(1-\alpha)V_{Cd}/kT}. \tag{13}$$

Whether the reaction be activation or diffusion controlled, the cadmium current should follow an equation of the form

$$I_{Cd}=I_0e^{\beta(E-IR)}, \tag{14}$$

where $\beta=2\epsilon/kT$ if the reaction is diffusion controlled, or $\beta=2\epsilon(1-\alpha)/kT$ if the reaction is activation controlled. Taking logarithms

$$\log I_{Cd}=\log I_0+BE-BIR, \tag{15}$$

where $B=\beta/2.303$. If we let $E=E_0+\Delta E$, where E_0 is any convenient potential (usually chosen as the potential of the floating electrode),

$$\log I_{Cd}=\log I_0+BE_0+B\Delta E-BIR \tag{16}$$

or

$$\log I_{Cd}-B\Delta E=\log I_0+BE_0-BIR. \tag{17}$$

Hence if the theory is correct, a plot of $\log I_{Cd}-B\Delta E$ against I should give a straight line, whose intercept for $I=0$ is $\log I_0+BE_0$ and whose slope is $-BR$.

A schematic diagram of the electrical apparatus used is presented in Fig. 1. Two 2-volt storage batteries (V) were used as a source of potential. In order to maintain constant potential of the cadmium electrode throughout a run, manual operation of the rheostat (R) and potentiometer system was necessary. The potentiometer (P) used was a Leeds and Northrup student potentiometer 7658C. The ammeter (A) used was a Weston d.c. milliammeter graduated in units of 5 milliamperes. The electrodes were immersed in 2.5 liters of sulfuric acid solution contained in a 3-liter beaker placed in a thermostat. The cadmium electrode (C) was made to rotate by means of an electrically driven motor, the variation in speed of rotation during a run being less than 1 percent. The polarizing electrode consisted of a rectangle of smooth platinum (D) attached to a cylindrical iron support, contact being made by means of mercury. All potentials were measured with the aid of a saturated calomel electrode (B). Throughout all experiments, nitrogen was bubbled through the solution.

The sulfuric acid used in the experiments was obtained by dilution of the commercial 18M product. The concentration was determined by titration with standard sodium hydroxide. Since the presence of oxygen has an adverse effect on the measurement of the potential of the cadmium electrode and since its presence interferes in the analytical determination of cadmium by the polarograph method, the sulfuric acid solution was boiled and allowed to cool in an atmosphere of nitrogen.[3] After cooling, the sulfuric acid was

[3] The loss in volume of solution during this process varied between 20–30 cc and was replaced by an equivalent

placed in a 2.5-liter bottle, air swept out by nitrogen, and placed in the thermostat over night.

The cadmium used was obtained in the form of cylindrical rods of *ca.* 0.8 cm diameter from the Mallinckrodt Company. A qualitative analysis by means of the polarograph did not show the presence of metallic impurities. The surface was cleaned and polished with rough and then fine emery paper. Petroleum ether was used to remove any grease. Each of the cadmium rods was attached to either a brass or an iron rod with a mercury cup at one end so that satisfactory contact could be made. A satisfactory coating for unexposed portions of the surface was obtained by using a Bakelite lacquer BL-3128.[4]

When not in use, all cadmium rods were kept in 1*N* sulfuric acid. All cadmium surfaces used in the experiments were thus acid etched. The surface was inclined to develop small pits,

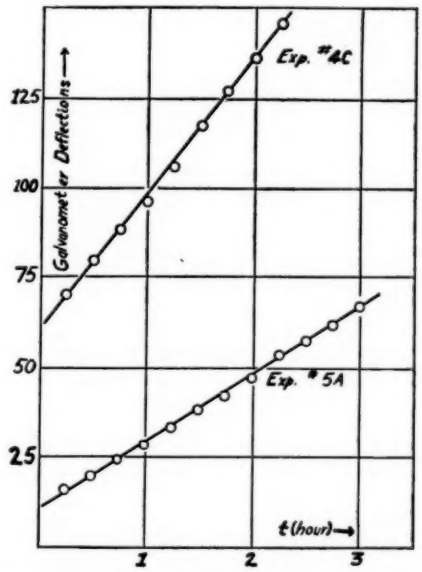

FIG. 2. Typical experimental rate curves. The ordinate is Cd^{++} concentration; the abscissa, time in hours. Electrode potential and stirring rate held constant.

TABLE I.

Exp.	S	I_{Cd}	$\frac{I_{Cd}}{S}$	ΔE	I	$\frac{I}{S}$	$\frac{I}{I_{Cd}}$
12*A*	5.71	7.56	1.34	0.01	4.5	0.79	0.60
8*A*	6.32	5.63	0.821		2.6	0.41	0.46
11*A*	6.32	6.29	0.995		4.0	0.63	0.64
7*A*	11.4	10.5	0.921		7.9	0.69	0.75
7*C*	11.4	10.2	0.895		8.6	0.75	0.84
6*A*	11.9	10.7	0.899		8.2	0.69	0.77
4*B*	13.8	10.4	0.754		5.2	0.38	0.50
5*A*	17.4	9.97	0.573		7.6	0.44	0.76
5*C*	17.4	10.1	0.580		6.6	0.37	0.65
10*A*	17.4	12.2	0.701		7.8	0.45	0.64
12*B*	5.71	18.1	3.17	0.02	16.5	2.9	0.91
8*B*	6.32	9.34	1.48		7.1	1.1	0.76
11*B*	6.32	13.7	2.17		12.3	1.9	0.90
7*B*	11.4	20.8	1.82		20.1	1.8	0.97
7*D*	11.4	20.8	1.82				
6*B*	11.9	17.0	1.43		15.9	1.3	0.94
4*C*	13.8	20.3	1.47		12.8	0.93	0.63
5*B*	17.4	19.9	1.14		20.0	1.1	1.01
5*D*	17.4	19.5	1.12		18.0	1.0	0.92
10*B*	17.4	25.5	1.47		21.7	1.2	0.85
12*C*	5.71	28.2	4.94	0.03	28.0	4.9	0.99
11*C*	6.32	24.3	3.84		26.0	4.1	1.07
7*E*	11.4	31.8	2.79		30.2	2.6	0.95
7*G*	11.4	32.0	2.81		30.2	2.6	0.94
10*C*	17.4	34.9	2.01		35.3	2.0	1.01
11*D*	6.32	30.9	4.89	0.04	43.0	6.8	1.39
7*F*	11.4	41.7	3.66		42.4	3.7	1.02
7*H*	11.4	41.7	3.66		42.4	3.7	1.02
10*D*	17.4	47.5	2.73		52.0	3.0	1.09

probably due to the presence of minute bubbles of alien gas absorbed in the process of manufacture.

All reactions took place in a thermostat maintained at a temperature of 25.00±0.01°C.

All analyses for cadmium were made by the polarographic method[5] with the aid of the "Electropode."[6] The instrument was calibrated for solutions ranging in strength from 1–30 mg Cd^{++} per liter in both 1*N* and 0.4*N* sulfuric acid solutions. A linear relation was found between galvanometer deflections and cadmium concentration in the region between 5–30 mg. This linearity persisted to concentrations up to at least 500 mg per liter with an error less than 1 percent. Below a concentration of 5 mg per liter, the error was much greater and the linearity no longer present. Samples to be analyzed were swept free of oxygen by means of nitrogen, and during the analysis itself nitrogen was allowed to flow over the surface of the solution. In analyzing samples the increment method[7] was used.

Samples of the solution (about 10 cc) were withdrawn from the reaction vessel and the concentration of cadmium determined. It was found that the concentration increased linearly with time (see Fig. 2) in accordance with the

amount of sulfuric acid of the proper strength. In view of the independence of the rate of solution of cadmium from the concentration of acid no significant error is to be expected.

[4] Supplied by Bakelite Corporation, Bound Brook, N. J.

[5] Kolthoff and Lingane, Chem. Rev. **24**, 1 (1939).

[6] Designed by the Fisher Scientific Co., Pittsburgh, Pa.

[7] Müller and Petras, J. Am. Chem. Soc. **60**, 2990 (1938).

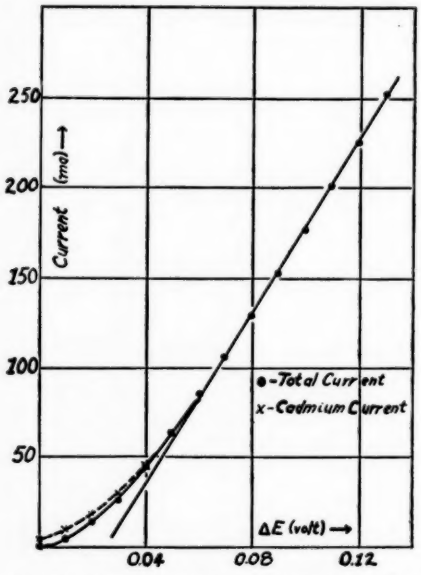

FIG. 3. Variation of rate of solution of cadmium with potential. Solid line—total current from electrode. Broken line—cadmium current.

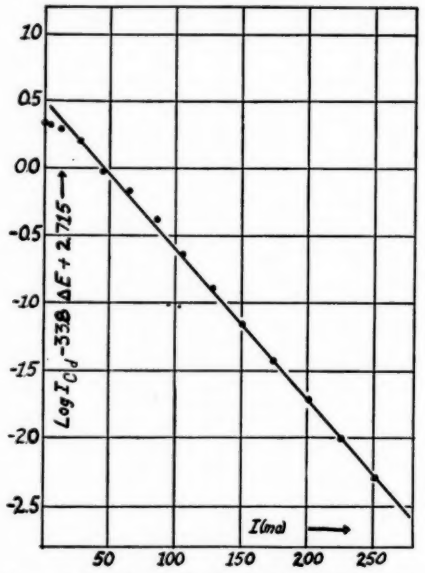

FIG. 4. Experimental verification of Eq. (17), on assumption $B=33.81$ (doubly charged cadmium ions).

zero-order rate equation

$$dC/dt=k/v, \tag{18}$$

v being the volume of solution. All rate constants were calculated by a least-square evaluation. Knowing the volume of the solution, the current of cadmium from the electrode is easily computed from the rate constant.

Experiments were first conducted with cadmium rods whose apparent surface areas were measured. The results obtained are reproduced in Table I. The second column gives the measured surface in sq. cm, the third the cadmium current in milliamperes, the sixth the total current in the same units. In the fifth column is given the difference in volts between the potential used for the experiment and the equilibrium potential of the cadmium rod obtained for $I=0$.

It will be noted that in the last column the values of the ratio I/I_{Cd} are fairly constant at constant potential difference. This ratio increases with increasing potential difference until it reaches a value unity, indicating that at this point the entire current is carried by cadmium ions. Assuming that the ratio of the equivalent conductances of the ions is independent of the potential, it is possible to obtain from the last column of Table I the value of γ defined in Eq. (34) of the previous paper. For

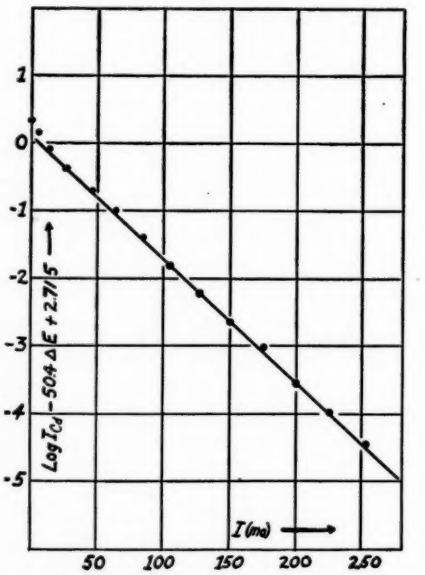

FIG. 5. Experimental verification of Eq. (17), on assumption $B=50.73$ (triply charged cadmium ions).

$$\gamma=-\frac{1}{2}\frac{I_H}{I_{Cd}}\frac{\lambda_{Cd}}{\lambda_H}$$
$$=-\frac{1}{2}\frac{\lambda_{Cd}}{\lambda_H}\left(\frac{I-I_{Cd}}{I_{Cd}}\right) \tag{19}$$
$$=\frac{1}{2}\frac{\lambda_{Cd}}{\lambda_H}\left(1-\frac{I}{I_{Cd}}\right).$$

When $I=I_{Cd}$ it is seen that $\gamma=0$. When $I=0$, then $\gamma\leqq 0.075$. Thus the values of γ pertinent to these experiments lie between these extremes.

It will further be noted that at constant potential the ratios I_{Cd}/S are not constant, but apparently decrease with increase of surface area. This has all the appearances of an edge effect, possibly due to unequal distribution of surface inhomogeneities, such as the small pits. This effect is more predominant for smaller areas than for larger ones, thus accounting, at least qualitatively, for the apparently greater rate of solution of the smaller surfaces. For this reason it was decided that in future experiments a complete determination of the rate constants at the various potentials for a given surface would be completed in one day.

In Fig. 3 we give plots of both the cadmium and total currents *versus* the potential ΔE. E_0 is taken to be the potential of the floating electrode ($I=0$). It will be noticed that for large values of the total current and potential, the relationship between these quantities is linear:

$$I=C+D\Delta E. \tag{20}$$

Experimentally it was found that increase of ΔE above 0.04 v caused a deposition of cadmium on the platinum electrode. Thus cadmium currents calculated by analysis in this region of potential would yield low results. However, in view of the fact that in the neighborhood of $\Delta E=0.04$ v it was found that $I=I_{Cd}$, it seems a fair assumption that this relationship persists to higher potentials.

TABLE II. *Values of* $\Delta \log I_{Cd}/\Delta(\Delta E)$ *1N* H_2SO_4*; 600 r.p.m.*

$\Delta E_2-\Delta E_1$	0.01 −0.00	0.02 −0.01	0.03 −0.02	0.04 −0.03
	31.8	29.0	14.9	12.7
	36.0	31.0	25.6	12.7
	36.9	30.5	20.4	14.6
	33.5	21.8	20.1	24.4
	38.9	31.2	25.3	14.3
	27.9	32.6	19.0	18.5
	31.2	23.8	21.5	17.6
		33.0	25.5	27.2
		35.2	13.0	
		39.1	20.7	
		40.1		
		32.8		
		31.2		
		29.7		
		24.8		
		31.6		
Average	33.7	31.1	20.6	17.7
a.d.	±1.1	±0.9	±1.0	±1.5

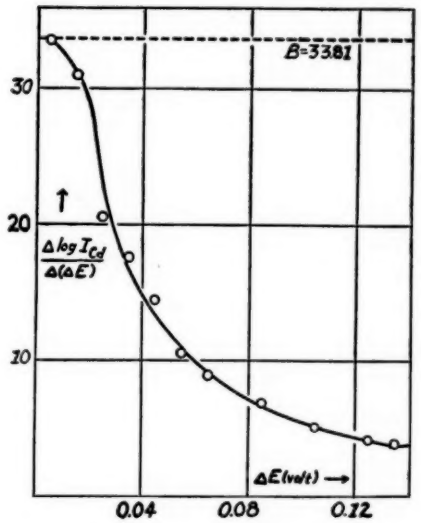

FIG. 6. Experimental determination of B.

3. RESULTS AND DISCUSSION

The theoretical value of B for cadmium in Eq. (17) is 33.81 if diffusion controlled, or 33.81 $(1-\alpha)$ if activation controlled. In Fig. 4 we have plotted for a typical run the experimentally determined values of $\log I_{Cd}-B\Delta E$ *versus* I using the value $B=33.81$. In Fig. 5 the same points are plotted using the value $B=50.43$, corresponding to a triple positive charge on the cadmium ion. Both values of B seem to fit the data equally well, the first few points lying on opposite sides of the straight line. Values of B were determined by the least-square method such that all points would lie on the best straight line. In all cases the calculated value of B corresponded to a charge on the cadmium ion varying between 2 and 3, the average lying very close to 2.5. It is believed that this resulted from the greater experimental inaccuracy in the determination of cadmium currents at the smaller potentials rather than from the existence of any triply charged cadmium ions. None such are known to exist in solution. Thus a value of $B=33.81$ was adopted. If the reaction were activation controlled, this should mean that $\alpha=0$, corresponding to the location of the height of the activation barrier at the solution edge of the double layer.

Additional evidence for our choice of B was obtained in the following way. Differentiation of

Eq. (15) leads to the following equation:

$$\frac{d \log I_{Cd}}{d\Delta E} = 33.81\left[1 - R\frac{dI}{d\Delta E}\right]. \qquad (21)$$

Then, if it can be assumed that $R(dI/d\Delta E)$ is negligibly small compared with unity when $\Delta E = 0$, we have

$$\left[\frac{d \log I_{Cd}}{d\Delta E}\right]_{\Delta E=0} = 33.81. \qquad (22)$$

In Table II we give the values of $\Delta \log I_{Cd}/\Delta(\Delta E) = \log (I_{Cd}^2/I_{Cd}^1)/(\Delta E_2 - \Delta E_1)$ at intervals of 0.01 v as obtained experimentally. It is seen that the average value when $\Delta E_2 = 0.01$ and $\Delta E_1 = 0$ is almost exactly equal to the required theoretical value. In Fig. 6 are plotted the average values of $\Delta \log I_{Cd}/\Delta(\Delta E)$ against ΔE. The dotted horizontal line represents the theoretical value. The portion of the curve beyond $\Delta E = 0.04$ v is based on the assumption of equality between cadmium and observed currents. In this region,

TABLE III. *Comparison of* I_{Cd} *(ma) at different stirring rates.*

ΔE	200 r.p.m.	600 r.p.m.	I_{600}/I_{200}
0.00	1.99 1.93	3.68 4.24	2.02
0.01	4.67 4.24	8.41 8.95	1.95
0.02	9.32 8.39	16.7 17.2	1.92
0.03	15.2 13.1	25.5 27.6	1.89
0.04	22.4 18.9	38.0 40.1	1.88

TABLE IV. *Values of* $\Delta \log I_{Cd}/\Delta(\Delta E)$ *1N* H_2SO_4*; 200 r.p.m.*

$\Delta E_2 - \Delta E_1$	0.01 −0.00	0.02 −0.01	0.03 −0.02	0.04 −0.03
	31.2	35.6	23.0	17.6
	26.7	27.0	18.5	11.7
	21.2	31.2	24.8	18.2
	38.4	30.5	22.3	16.7
	35.4		21.0	
Average	30.6	31.1	21.9	16.1
a.d.	±2.4	±1.2	±0.8	±1.1

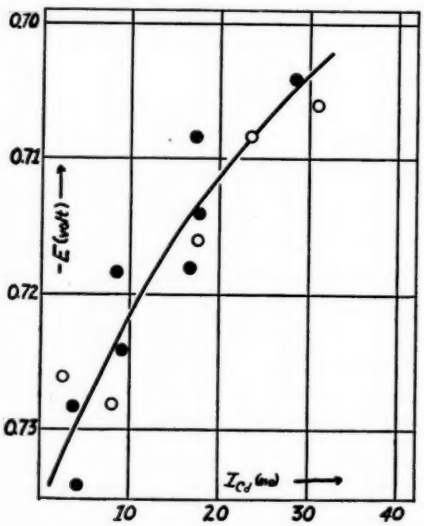

FIG. 7. The effect of concentration of acid on solution rate. Open circles, 0.4*N* H_2SO_4. Black circles, 1*N* H_2SO_4.

then, differentiation of Eq. (15) requires that

$$\frac{d \log I}{d\Delta E} = \frac{33.81}{1 + 33.81RI}. \qquad (23)$$

In view of the linearity between current and potential at higher values of the current as given by (20), it is predicted that in this region a plot of $d \log I/d\Delta E$ *versus* ΔE should give a hyperbola. This was found to be true in examination.

Thus far no distinction can be made between the diffusion controlled and activation controlled mechanisms. Theory[2] predicts, however, that in the former case the value of I_0^q should vary with the stirring rate, whereas I_0^p does not. An examination of the influence of stirring rate was undertaken by ascertaining the values of I_{Cd} when the speed of rotation was reduced from 600 r.p.m. to 200 r.p.m. A comparison of the data collected on a single surface is shown in

TABLE V. *Values of* $\Delta \log I_{Cd}/\Delta(\Delta E)$ *0.4N* H_2SO_4*; 600 r.p.m.*

$\Delta E_2 - \Delta E_1$	0.01 −0.00	0.02 −0.01	0.03 −0.02	0.04 −0.03
	31.6	36.2	19.0	17.9
	36.6	36.6	24.3	12.1
	37.7	32.2	15.5	
	32.8	31.8	25.8	
	35.8			
Average	34.9	34.2	21.2	15.0
a.d.	±1.0	±1.1	±2.0	±2.9

Table III. It is seen that the predictions of diffusion control are fulfilled. It is found that I_{600}/I_{200} is independent of potential. Thus it can definitely be stated that the solution of cadmium in sulfuric acid is diffusion controlled.

In Table IV values of $\Delta \log I_{Cd}/\Delta(\Delta E)$ for various potentials at the low stirring rate are listed. Comparison with Table II of values at the same potential indicate no significant differences that can be attributed to change in stirring rate.

Equation (4) was derived on the assumption that the metallic ion diffuses independently of the other ions. To check this experimentally, the concentration of acid was changed from $1N$ to $0.4N$. Comparison of the rate constants should be made at the same potential. In Fig. 7 we give a plot of I_{Cd} against the values of E as measured by the calomel electrode. The open circles indicate values obtained with weak acid, the black circles values obtained on the same surface with stronger acid. The differences are seen to be erratic, and are due to changes in the cadmium surface. The change due to the change in acid concentration is less than the experimental error. Further, in Table V we give values of $\Delta \log I_{Cd}/\Delta(\Delta E)$, and comparison of these with corresponding values in Tables II and IV exhibit no significant differences.

OCTOBER, 1940 JOURNAL OF CHEMICAL PHYSICS VOLUME 8

Solvent Action on Optical Rotatory Power*

III. The Influence of Liquid Structure on the Interaction of Dipoles

CHARLES O. BECKMANN AND HENRY C. MARKS
Department of Chemistry, Columbia University, New York, New York

(Received July 20, 1940)

By taking into account the London "dispersion" forces and the structural characteristics of a liquid system, an equation for the change of rotivity per mole of dipole solvent in unit volume for liquid solutions is obtained which has the same form as the equation obtained by Beckmann and Cohen for a mixture of gases that are perfect except for dipole interaction, namely,

$$S=G(\alpha, \beta, \gamma)+K_\gamma P_\gamma.$$

This is due to the fact that the polarization term arises from the integration over the angles of orientation alone. The constants, $G(\alpha, \beta, \gamma)$ and K_γ have, of course, a new significance in the present work.

INTRODUCTION

THE change in optical rotatory power with solvent can be attributed to a deformation of the active molecule as has been demonstrated theoretically by de Mallemann,[1] by Kuhn,[2] and by Beckmann and Cohen.[3] The correlation of this change and the dielectric constant of the solvent was suggested by P. Walden[4] in 1905 and recently by Rule and McLean,[5] who used dipole moments and molar polarizations instead of dielectric constants.

The fundamental assumption underlying the theory of Beckmann and Cohen is that the rotivity,[6] Ω, is a linear function of the average electrostatic field, $[\mathbf{F}]_{Av}$, acting on the optically active molecule, i.e.,

$$\Omega=\Omega_1+\Omega'[\mathbf{F}]_{Av}, \qquad (1)$$

where Ω_1 is the rotivity in a zero field and Ω' is a deformability constant characteristic of the active molecule. Kauzmann, Walter and Eyring[7] have pointed out in a recent review article that this linear relationship could arise from a number

* Publication assisted by the Ernest Kempton Adams Fund for Physical Research of Columbia University.

[1] R. de Mallemann, Ann. de physique (10) **2**, 170 (1924).

[2] W. Kuhn and K. Freudenberg, *Hand- und Jahrbuch der chemischen Physik* (Akademische Verlagsgesellschaft, Leipzig, 1932), Vol. 8, Part 3.

[3] C. O. Beckmann and K. Cohen, J. Chem. Phys. **4**, 784 (1936); K. Cohen and C. O. Beckmann, J. Chem. Phys. **6**, 163 (1938).

[4] P. Walden, Ber. d. Phys. Ges. **38**, 345 (1905).

[5] H. G. Rule and A. McLean, J. Chem. Soc. 1400 (1932).

[6] Rotivity $=\Omega=[\alpha]/(n^2+2)$, see references 3 and 7.

[7] W. J. Kauzmann, J. E. Walter and H. Eyring, Chem. Rev. **26**, 339 (1940).

of different mechanisms: (1) the electrostatic field could produce a molecular distortion as originally assumed by Beckmann and Cohen;[3] (2) for molecules that possess a group which is predominantly found in either of two positions with respect to rotation about a bond, the field could change the distribution between these two positions; and (3) the field could have a direct vicinal action on a chromophoric group of the active molecule. Of these mechanisms, the last is probably most important.

The final equation derived by Beckmann and Cohen from Eq. (1) and a calculation of $[\mathbf{F}]_{Av}$ expresses the change of rotatory power as a function of the molar polarization of the solvent. The experimental success of this equation for a class of solvents that show "van Arkel association,"[8] warrants a more detailed analysis, for it was originally derived for mixed gases. Although it was expected to hold for dilute solutions, its validity actually extends over almost a complete concentration range from zero to 100 percent dipolar solvent.

The foremost problem is the calculation of $[\mathbf{F}]_{Av}$. As in the previous papers,[3] the optically active molecule will be designated the α-molecule, the nonpolar solvent molecule, the β-molecule, and the polar solvent molecule, the γ-molecule. The Cartesian system of coordinates in the chosen α-molecule will be indicated by the axes δ, ($\delta=1,2,3$) and the direction of the dipole in this molecule by $\delta=3$. The total average field of the three varieties of molecules along the axis δ is given by

$$[\mathbf{F}_\delta]_{Av}=[\mathbf{F}_{(\alpha)\delta}]_{Av}+[\mathbf{F}_{(\beta)\delta}]_{Av}+[\mathbf{F}_{(\gamma)\delta}]_{Av}. \quad (2)$$

Since all terms will have the same form, only $[\mathbf{F}_{(\gamma)\delta}]_{Av}$ will be considered in detail.

The Case of a Liquid Solution

It was shown that[3]

$$[\mathbf{F}_{(\gamma)\delta}]_{Av}=\frac{n_\gamma}{8\pi^2}\int\theta^{E_{\alpha\gamma}}\mathbf{F}_{(\gamma)\delta}d\omega_\gamma, \quad (3)$$

where n_γ is the number of γ-molecules per cc, $\theta=\exp(1/kT)$, $E_{\alpha\gamma}$, the interaction energy of one α-molecule and one γ-molecule and $d\omega_\gamma$ is the differential element of the 6-space of relative coordinates of the two molecules. Since the interaction of the two molecules does not depend on the dipoles alone (as previously assumed), an additional term for the London[9] "dispersion" forces, $Q_{\alpha\gamma}/r^6$ is added, so that,

$$E_{\alpha\gamma}=\frac{\boldsymbol{\mu}_\alpha\cdot\boldsymbol{\mu}_\gamma}{r^3}-\frac{3(\boldsymbol{\mu}_\alpha\cdot\mathbf{r})(\boldsymbol{\mu}_\gamma\cdot\mathbf{r})}{r^5}-\frac{Q_{\alpha\gamma}}{r^6}, \quad (4)$$

where $\boldsymbol{\mu}_\alpha$ and $\boldsymbol{\mu}_\gamma$ are the dipoles located at the center of the α- and γ-molecules, respectively, these being assumed spherical for this discussion, $\mathbf{r}$ is the distance between the centers of the two molecules and $Q_{\alpha\gamma}$ is a constant characteristic of the "dispersion" interaction of the molecules. The Debye induction effect can be neglected without introducing an error of more than two percent. The electrostatic field of the γ-molecule at the α-molecule is given by the expression

$$\mathbf{F}_{(\gamma)}=-\frac{\boldsymbol{\mu}_\gamma}{r^3}+\frac{3\mathbf{r}(\mathbf{r}\cdot\boldsymbol{\mu}_\gamma)}{r^5}+\frac{C\boldsymbol{\mu}_\alpha}{r^6}+\frac{3C\mathbf{r}(\mathbf{r}\cdot\boldsymbol{\mu}_\alpha)}{r^8}, \quad (5)$$

where C is the polarizability of the γ-molecule.

In order to apply this method to liquid solutions, one must take into account at least two other factors, namely, the effect of repulsive forces and the structure of the liquid. The effect of the repulsive forces is approximated, as is usual in problems of this type, by assigning an effective distance of closest approach of the two molecules, which then sets the lower limit of r. The structural characteristics of the liquid will to a large extent determine the distribution of the γ-molecules in the space about the α-molecule. Even elementary geometrical restrictions will modify molecular arrangements in condensed systems, as was shown by Prins[10] and others. Since a detailed calculation of these factors is not possible at present, we can only indicate their presence by the introduction as a modifying factor,[11] w', characteristic of the liquid structure, in the distribution function which then takes the form,

$$w'\theta^{E_{\alpha\gamma}},$$

where $E_{\alpha\gamma}$ is given by (4).

[8] See H. Müller, Physik. Zeits. **38**, 498 (1937).

[9] F. London, Zeits. f. physik. Chemie **B11**, 222 (1930).

[10] J. A. Prins, Zeits. f. Physik **56**, 617 (1929).

[11] J. H. Hildebrand, *Solubility*, Am. Chem. Soc. Monograph Series (Reinhold Publishing Corp., New York, 1936); J. Chem. Phys. **7**, 1 (1939).

If w' represents an average which does not affect the average orientation of the molecules and $Q_{\alpha\gamma}$ is independent of orientation, we may separate the radial and angular variables and perform that part of the integration which gives rise to the molar polarization term. The result of this integration is

$$[\mathbf{F}_{(\gamma)1}]_{Av}=[\mathbf{F}_{(\gamma)2}]_{Av}=0,$$

$$[\mathbf{F}_{(\gamma)3}]_{Av}=6\mathfrak{y}_{\alpha}\frac{n_{\gamma}}{N}{}_{0}P_{\gamma}\int\frac{w'\theta^{-Q_{\alpha\gamma}/r6}}{r^{4}}dr, \quad (6)$$

$$=6\mathfrak{y}_{\alpha}\frac{n_{\gamma}}{N}{}_{0}P_{\gamma}\int W(r)dr, \quad (7)$$

$${}_{0}P_{\gamma}=\frac{4\pi}{3}N\left(C+\frac{\mu_{\gamma}^{2}}{3kT}\right),$$

where $W(r)$ is now some function which expresses the radial distribution pattern of the γ-molecules around the given α-molecule, ${}_{0}P_{\gamma}$ is the molar polarization of the γ-molecules at infinite dilution[12] and N is Avogadro's number. The expression

$$6\mathfrak{y}_{\alpha}\frac{n_{\gamma}}{N}{}_{0}P_{\gamma}W(r)dr$$

gives the average field at the given α-molecule of all the γ-molecules lying in the spherical shell of thickness, dr, and radius, r. The nature of $W_{\gamma}(r)$ is determined by all the forces of molecular interaction and by the geometrical restrictions imposed on a condensed system.

Because the interaction of the γ-molecules with one another has been neglected, Eq. (7) is applicable only to infinitely dilute solutions. The difference between ${}_{0}P_{\gamma}$ and P_{γ} for a finite concentration is usually attributed to the hindrance of rotation of the dipole molecules.[13] If it can be assumed that this factor will affect the $[\mathbf{F}_{(\gamma)}]_{Av}$ in the same way that it will affect the polarization of the medium, I,[12] then the molar polarization at infinite dilution, ${}_{0}P_{\gamma}$, can be replaced by P_{γ} for a particular concentration of γ-molecules. This assumption is not unreasonable, for an interaction which results in a hindrance of the orientation of a dipole molecule in an external field should also be operative in hindering the orientation in the field of another molecule. Furthermore, the relations obtained on this basis have been shown by Beckmann and Cohen[3] and by Marks and Beckmann[14] to be in excellent agreement with experiment. Thus, we may write

$$[\mathbf{F}_{(\gamma)3}]_{Av}=6\mathfrak{y}_{\alpha}\frac{n_{\gamma}}{N}P_{\gamma}J_{\gamma}, \quad (8)$$

where

$$J_{\gamma}=\int W_{\gamma}(r)dr.$$

In order to apply this result to the general case of a mixture containing an optically active substance, it is necessary to take into account the effect of other kinds of molecules that may be present. We consider a three-component system of optically active molecules (α), nonpolar solvent molecules (β), and dipole solvent molecules (γ). The total field acting on an α-molecule will be the sum of the average fields of the three species of molecules and we may write Eq. (1) as

$$\Omega=\Omega_{1}+\Omega'[\mathbf{F}_{(\alpha)3}]_{Av}+\Omega'[\mathbf{F}_{(\beta)3}]_{Av}+\Omega'[\mathbf{F}_{(\gamma)3}]_{Av}. \quad (9)$$

$[\mathbf{F}_{(\alpha)3}]_{Av}$ and $[\mathbf{F}_{(\beta)3}]_{Av}$ will be given by expressions analogous to (8) for $[\mathbf{F}_{(\gamma)3}]_{Av}$. Limiting the discussion to mixtures in which the volume concentration of the optically active molecules (α) is constant, we substitute the appropriate expressions for $[\mathbf{F}_{(\alpha)3}]_{Av}$, $[\mathbf{F}_{(\beta)3}]_{Av}$ and $[\mathbf{F}_{(\gamma)3}]_{Av}$ in Eq. (9) and find for the change in rotivity produced by the substitution of N_{γ} γ-molecules for $(N_{\beta}{}^{0}-N_{\beta})$ β-molecules,

$$S\equiv(\Omega-\Omega_{0})\frac{VM_{\gamma}}{w_{\gamma}}$$
$$=6\Omega'\mu_{\alpha}w_{\alpha}\frac{M_{\gamma}}{M_{\alpha}}\left(\frac{P_{\alpha}J_{\alpha}-P_{\alpha}{}^{0}J_{\alpha}{}^{0}}{w_{\gamma}}\right)$$
$$+6\Omega'\mu_{\alpha}\frac{M_{\gamma}}{M_{\beta}}\left(\frac{w_{\beta}P_{\beta}J_{\beta}-w_{\beta}{}^{0}P_{\beta}{}^{0}J_{\beta}{}^{0}}{w_{\gamma}}\right)$$
$$+6\Omega'\mu_{\alpha}P_{\gamma}J_{\gamma}, \quad (10)$$

where Ω_{0} is the rotivity when $n_{\gamma}=0$; M_{α}, M_{β}, and M_{γ} are the molecular weights of α, β, and γ,

[12] P. Debye, *Polar Molecules* (Chemical Catalog Company, New York, 1929).
[13] P. Debye, Physik. Zeits. **36**, 100 (1935).
[14] H. C. Marks and C. O. Beckmann, J. Chem. Phys., following paper.

respectively; w_α, w_β, and w_γ are the weights contained in the volume V; and the superscript ^{0} refers to the value of the quantity when $w_\gamma=0$. $n_\alpha V/N$, $n_\beta V/N$, and $n_\gamma V/N$ have been replaced by w_α/M_α, w_β/M_β, and w_γ/M_γ, respectively.

P_α and P_β may be assumed constant. This is reasonable for the latter but not necessarily for the former. However, the variations that occur in P_α due to change in concentration of γ-molecules may be counted in as variations in P_γ and the effect determined from the law of mixtures. Since the factors, J, represent distribution patterns rather than actual concentrations, it is reasonable to suppose that they are constant over a range of concentrations of γ-molecules. Even in regions where this constancy would not be expected, if the variation with n_γ is smooth, factors of the form $(wJ-w^0J^0)/w_\gamma$, would be constant with respect to variations in P_γ. Thus, Eq. (10) reduces to the linear form,

$$S=G(\alpha,\beta,\gamma)+K_\gamma P_\gamma, \tag{11}$$

provided also that the term $(w_\beta-w_\beta{}^0)/w_\gamma$ is a constant as in ideal solutions or is linear in P_γ as was actually found by experiment.[14]

The Case of a Real Gas

The significance of the general form of Eq. (11) is made more obvious by reducing it to a simpler form which will describe the behavior of a mixture of real gases. If the pressure is sufficiently low, one may neglect (1) the structural term w' and (2) the hindrance of rotation due to dipole interaction. Thus by setting $w'=1$, and integrating Eq. (6), we obtain for the average electrostatic field at an α-molecule due to a γ-molecule

$$[\mathbf{F}_{(\gamma)3}]_{Av}=\frac{2\mathfrak{y}_\alpha}{d_{\alpha\gamma}{}^3}\frac{n_\gamma}{N}{}_0P_\gamma\sum_{\nu=0}^{\infty}\frac{Q_{\alpha\gamma}{}^\nu(1/d_{\alpha\gamma}{}^3)^{2\nu}}{\nu!(2\nu+1)(kT)^\nu}, \tag{12}$$

$$Q_{\alpha\gamma}{}^0=0!=1,$$

where $d_{\alpha\gamma}$ is the distance of closest approach of an α- and γ-molecule. This equation reduces to the one obtained by Beckmann and Cohen,[3] which took into account dipole interaction alone as the source of imperfection in the gas, when one takes only the first term, i.e., $\nu=0$,

$$[\mathbf{F}_{(\gamma)3}]_{Av}=\frac{2\mathfrak{y}_\alpha}{d_{\alpha\gamma}{}^3}\frac{n_\gamma}{N}{}_0P_\gamma. \tag{13}$$

By carrying out the same procedure as in the previous section starting with Eq. (9), one obtains for the change in rotivity due to added dipole molecules,

$$S\equiv(\Omega-\Omega_0)\frac{VM_\gamma}{w_\gamma}$$

$$=\frac{2\mu_\alpha}{d_{\alpha\beta}{}^3}\Omega'\frac{M_\gamma}{M_\beta}\cdot\frac{w_\beta-w_\beta{}^0}{w_\gamma}P_\beta D_\beta+\frac{2\mu_\alpha}{d_{\alpha\gamma}{}^3}\Omega'P_\gamma D_\gamma,$$

where

$$D_\beta=\sum_{\nu=0}^{\infty}\frac{Q_{\alpha\beta}{}^\nu(1/d_{\alpha\beta}{}^3)^{2\nu}}{\nu!(2\nu+1)(kT)^\nu}$$

and

$$D_\gamma=\sum_{\nu=0}^{\infty}\frac{Q_{\alpha\gamma}{}^\nu(1/d_{\alpha\gamma}{}^3)^{2\nu}}{\nu!(2\nu+1)(kT)^\nu}.$$

The fact that D_β and D_γ cannot be evaluated for molecules of the complexity required in experiments to confirm this theory and the fact that the necessary optical and electrical data are not available for the case of the imperfect gas, do not completely destroy the usefulness of the equation. Since D_γ (as well as D_β) is always larger than 1, this consideration of the "dispersion" forces has introduced a multiplicative factor which always enhances the effect of the dipole field on the rotatory power. In view of the magnitude of these forces as calculated by London[9] for simple molecules, an equation of this form will explain changes in rotatory power too large to be accounted for by the earlier form based on dipole interaction alone.

Solvent Action on Optical Rotatory Power*

IV. The Rotivity of Dipropionyl-Diethyl-*d*-Tartrate and *l*-Menthyl Acetate in Aromatic and Aliphatic Solvents

HENRY C. MARKS AND CHARLES O. BECKMANN
Department of Chemistry, Columbia University, New York, New York

(Received July 20, 1940)

Experimental data are presented to demonstrate the validity of the equations of Beckmann and Cohen and Beckmann and Marks for the change of rotivity with solvent. Mixtures of polar and nonpolar solvents of both aromatic and aliphatic types were used with dipropionyl-diethyl-*d*-tartrate and *l*-menthyl acetate as optically active substances. The data are discussed in terms of the theory and essential agreement is found in all cases over a wide range of concentrations.

THE theory of Beckmann and Cohen,[1] which treats the solvent effect on optical rotatory power as a deformation of the active molecule by the electrostatic field of the solvent molecules, has been extended by Beckmann and Marks[2] to take into account the London[3] "dispersion" forces and the effects of liquid structural characteristics as well as dipole forces. This calculation led to the following expression for the change in optical rotatory power produced by the progressive replacement of nonpolar solvent by polar solvent,

$$S\equiv(\Omega-\Omega_0)\frac{VM_\gamma}{w_\gamma}=6\Omega'\mu_\alpha w_\alpha\frac{M_\gamma}{M_\alpha}\left(\frac{P_\alpha J_\alpha-P_\alpha{}^0J_\alpha{}^0}{w_\gamma}\right)$$
$$+6\Omega'\mu_\alpha\frac{M_\gamma}{M_\beta}\left(\frac{w_\beta P_\beta J_\beta-w_\beta{}^0P_\beta{}^0J_\beta{}^0}{w_\gamma}\right)+6\Omega'\mu_\alpha P_\gamma J_\gamma=G(\alpha,\beta,\gamma)+K_{\alpha\gamma}P_\gamma,$$

where Ω is the rotivity[4] of the solution, V, the volume of the system, M, a molecular weight, w, a weight of substance, Ω', the deformability constant of the optically active substance, μ_α, the dipole moment of the optically active substance, P, a molar polarization and J, an integral describing the radial distribution of molecules. The subscripts α, β, and γ, refer to the optically active substance, the nonpolar solvent and the polar solvent, respectively, and the subscript or superscript 0, refers to the value of the quantity when $w_\gamma=0$.

That S varies linearly with $P\gamma$ for a number of such mixtures of aromatic solvents has been demonstrated experimentally by Beckmann and Cohen.[1] Since the aromatic nucleus has a special type of field,[5] it was desirable to extend the data to nonaromatic mixtures and to combinations of the two types of substances in order to test some of the more general results of the theory. Accordingly, the rotivities of two compounds of widely differing structures, dipropionyl-diethyl-*d*-tartrate and *l*-menthyl acetate, were studied in various mixtures of polar and nonpolar solvents. The nitro- and cyano-derivatives of benzene and of cyclohexane[6] as polar components and benzene and cyclohexane as nonpolar components were chosen for reasons of desirable physical properties, chemical inertness, relative geometrical simplicity and the magnitude of the effect on optical rotatory power. Hydroaromatic rather than straight chain aliphatic derivatives were chosen in order to avoid unnecessary geometrical complications.

* Publication assisted by the Ernest Kempton Adams Fund for Physical Research of Columbia University.

[1] C. O. Beckmann and K. Cohen, J. Chem. Phys. **4**, 784 (1936).

[2] C. O. Beckmann and H. C. Marks, J. Chem. Phys. preceding paper.

[3] F. London, Zeits. f. physik. Chemie **B11**, 222 (1930).

[4] Rotivity $=\Omega=[\alpha]/(n^2+2)$.

[5] G. Briegleb, Zeits. f. physik. Chemie **B31**, 58 (1935).

[6] Because of the difficulty of nitrating cyclohexane, 1-nitro-1-methyl cyclohexane was used instead of nitrocyclohexane.

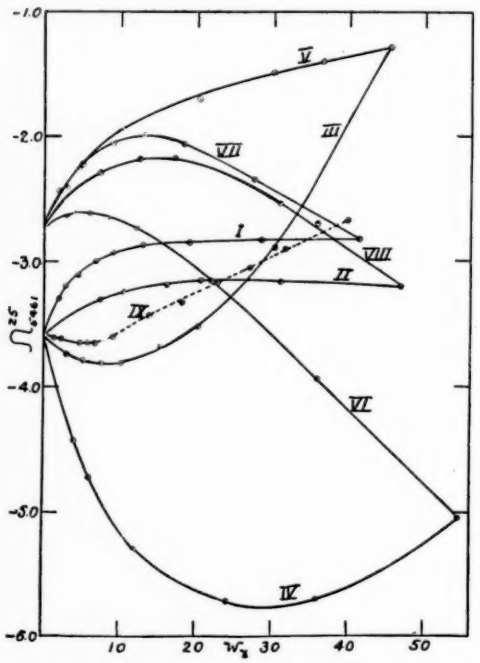

FIG. 1. Dipropionyl diethyl *d*-tartrate in the following solvent mixtures: I. cyclohexane-cyclohexylcyanide, II. cyclohexane-1-nitro-1-methyl cyclohexane, III. cyclohexane-benzonitrile, IV. cyclohexane-nitrobenzene, V. benzene-benzonitrile, VI. benzene-nitrobenzene, VII. benzene-cyclohexylcyanide, VIII. benzene-1-nitro-1-methyl cyclohexane, IX. cyclohexane-benzene.

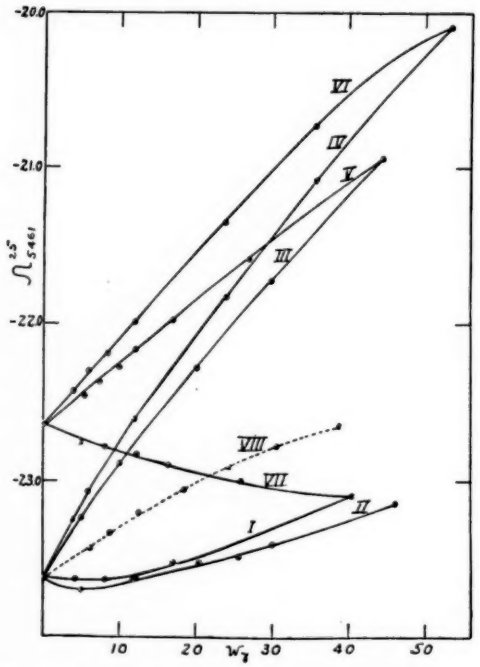

FIG. 2. *l*-Menthyl acetate in the following solvent mixtures: I. cyclohexane-cyclohexylcyanide, II. cyclohexane-1-nitro-1-methyl cyclohexane, III. cyclohexane-benzonitrile, IV. cyclohexane-nitrobenzene, V. benzene-benzonitrile, VI. benzene-nitrobenzene, VII. benzene-cyclohexylcyanide, VIII. cyclohexane-benzene.

The experimental procedure and methods of calculation were those described by Beckmann and Cohen,[1] except that measurements of rotatory power and refractive index were made with both the sodium *D* line and the mercury 5461 line. Since the following discussion applies equally well to either set of data, only the latter set has been completely illustrated in the accompanying tables and figures.

ROTIVITY AS A FUNCTION OF CONCENTRATION

When $\Omega - \Omega_0$ is plotted against w_γ, as shown in Figs. 1 and 2, one is impressed by the great variety of detail exhibited by curves which are more or less of the same general type. For example, the large curvature shown by dipropionyl-diethyl-tartrate in every solvent mixture is in striking contrast to the nearly linear variation shown by *l*-menthyl acetate. Beckmann and Cohen[1] have shown that curves such as these can be resolved into two components, one of which can be attributed solely to changes in the field of the dipoles as measured by changes in P_γ, while the other is due simply to the change in the total field of the nonpolar molecules as their concentration changes. The first component will have a curvature comparable to that ordinarily found when molar polarization is plotted against concentration; the second component will be linear in w_γ. On this basis, it would appear that for *l*-menthyl acetate the change in rotivity is predominately a "concentration effect," while in the case of dipropionyl-diethyl-tartrate the two contributions are nearly the same. This relationship is further evidenced by the fact that the rotivity of menthyl acetate is influenced to a much greater extent by a change from aromatic to hydroaromatic solvent than by a change from nonpolar to polar. Thus, the addition of dipoles without other change consistently makes the rotivity more positive, while replacing aromatic by hydroaromatic solvent (benzene by cyclohexane) makes it more negative. Yet, it is the latter effect which predominates when an aromatic nonpolar solvent is

replaced by a hydroaromatic polar solvent. On the other hand, the equality of the two contributions to the changes in the rotivity of dipropionyl-diethyl tartrate leads to the result that the change from hydroaromatic to aromatic substance is manifested chiefly in the sign of the curvature: The positive curvature of the cyclohexane-benzene series is impressed on all hydroaromatic-aromatic mixtures. This latter circumstance has a further interesting consequence; the change in sign of $\Omega-\Omega_0$, predicted by Beckmann and Cohen,[1] becomes a comparatively frequent occurrence. This difference in the behavior of the two substances will be considered in more detail in one of the following sections.

The Linearity of S with P_γ

As investigation into mixtures of greater complexity discloses a larger and larger variety of rotivity curves, increasing significance must be attached to the essential linearity that is always observed when S is plotted against P_γ, as shown in Figs. 3 and 4. The fact that deviations from linearity do appear in some of the more concentrated solutions (with respect to dipoles) is in no way surprising. Rather, it would be expected that as the concentration of dipoles is increased, a region would sooner or later be reached in which the type of liquid structure would undergo a profound change. In terms of the ideas discussed in the previous publication[2] this would mean that the functions $K_{\alpha\gamma}$ would have to be considered as changing with concentration to an extent no longer negligible. Further, this linear relation in P_γ, because it effectively (though perhaps artificially) separates the two factors contributing to the change in rotivity, provides a more satisfactory basis for analysis than do the rotivity-concentration curves. This is most evident for an optically active compound of the type of dipropionyl-diethyl tartrate where neither factor predominates. Here, rotivity curves which appear to be very different (for example the systems benzene-benzonitrile and

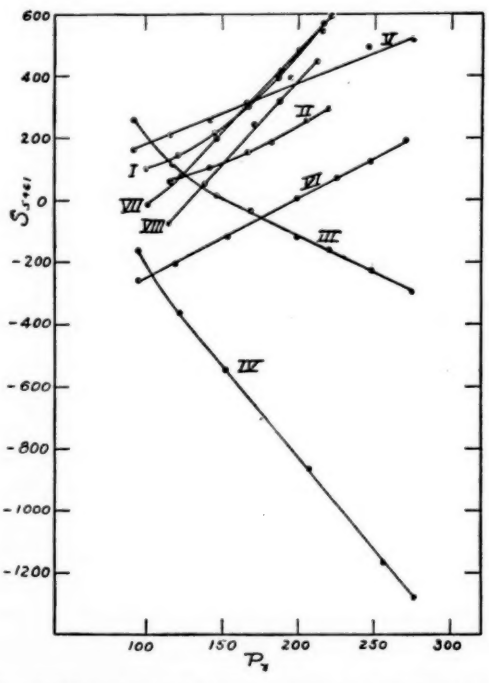

FIG. 3. Dipropionyl diethyl *d*-tartrate in the following solvent mixtures: I. cyclohexane-cyclohexylcyanide, II. cyclohexane-1-nitro-1-methyl cyclohexane, III. cyclohexane-benzonitrile, IV. cyclohexane-nitrobenzene, V. benzene-benzonitrile, VI. benzene-nitrobenzene, VII. benzene-cyclohexylcyanide, VIII. benzene-1-nitro-1-methyl cyclohexane.

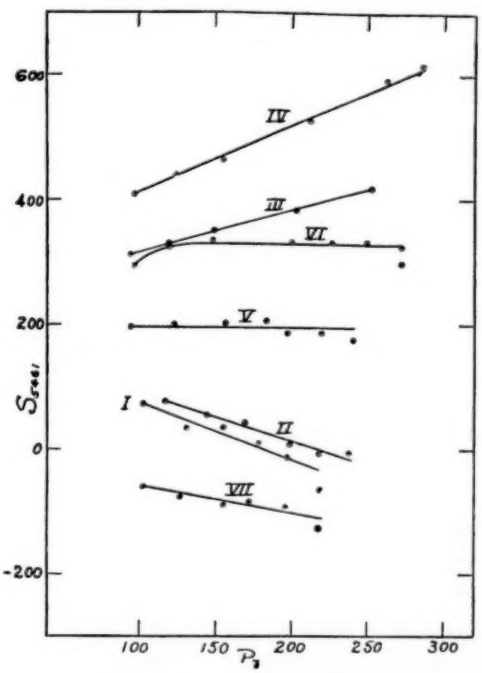

FIG. 4. *l*-Menthyl acetate in the following solvent mixtures: I. cyclohexane-cyclohexylcyanide, II. cyclohexane-1-nitro-1-methyl cyclohexane, III. cyclohexane-benzonitrile, IV. cyclohexane-nitrobenzene, V. benzene-benzonitrile, VI. benzene-nitrobenzene, VII. benzene-cyclohexylcyanide.

benzene-nitrobenzene) are shown to be quite similar with respect to the parts due to changes in the dipole field.

Discussion of $K_{\alpha\gamma}$

A consideration of the structural properties of liquids has indicated that the coefficient of P_γ will contain a factor which is just as much a property of the nonpolar as it is of the polar component. On this basis we still expect to find similar slopes when the effect of similarly constituted dipole molecules on the same optically active substance is measured in the same nonpolar solvent. It will be seen that for every combination this expectation is fulfilled quite satisfactorily, just as Beckmann and Cohen found in comparing the effects of nitrobenzene and of benzonitrile on diacetyl-diethyl tartrate in benzene. In the same way it is clear why they found reasonable agreement in the values of $d_{\alpha\gamma}$ calculated for these two substances. However, it is now also evident that any significant change in the nonpolar constituent, such as the change from benzene to cyclohexane, may very well bring about a radically different manner of variation with P_γ. It is by no means inconceivable that different structural limitations imposed by solvent molecules characterized by very different electron configurations could cause the changes in the dipole field, as measured by the changes in P_γ, to affect the optically active molecule in dissimilar or even opposite ways. Thus in the systems: *l*-menthyl acetate-benzene-nitrobenzene and *l*-menthyl acetate-benzene-benzonitrile, we find two instances where the effect of changes in P_γ is completely vitiated; S remains practically constant while P_γ varies rapidly. Although a theoretical demonstration of these phenomena is not possible at present, a study of the experimental relationships shown in Figs. 3 and 4 and in Table II indicates that such considerations have a real significance. In general, the slopes of the lines fall into a definite order which depends in a regular manner on what we may call the aromatic-hydroaromatic relationship between the two components of the solvent mixture. Thus, going from one extreme to the other in order as shown in Table I we have the following combinations: hydroaromatic nonpolar-aromatic polar; aromatic nonpolar-aromatic polar; aromatic nonpolar-hydroaromatic polar; and hydroaromatic nonpolar-hydroaromatic polar.

Table I. *Experimental values of* $K_{\alpha\gamma}$.

Solvent Mixture	$K_{\alpha\gamma}$ Dipropionyl diethyl *d*-tartrate	$K_{\alpha\gamma}$ *l*-Menthyl Acetate
Cyclohexane-cyclohexylcyanide	5.9	−0.90
Cyclohexane-1-nitro-1-methyl cyclohexane	(2.5)	−0.77
Benzene-1-nitro-1-methyl cyclohexane	5.4	—
Benzene-cyclohexylcyanide	5.4	−0.47
Benzene-nitrobenzene	2.6	0.0
Benzene-benzonitrile	2.3	0.0
Cyclohexane-benzonitrile	−2.4	0.66
Cyclohexane-nitrobenzene	−5.9	1.1

Further, this order is identical for the two optically active compounds (the fact that the signs of the slopes are reversed merely indicates that the signs of the deformability coefficients, are opposite). This is particularly significant in view of the fact that the rotivities of these two substances show such different types of variation with changes of solvent and considering that they present basic structural differences. Wherefore, the conclusion is almost inescapable that this observed regularity is a manifestation of fundamental structural characteristics of these particular solvent mixtures.

There are a number of factors which were necessarily neglected in making an approximate calculation, but one of the most obvious has to do with the effect of the field of the added dipoles on the nonpolar solvent molecules. Weigle[7] has shown that this is by no means negligible, particularly for molecules that do not possess spherical symmetry. Consideration of this interaction would lead to the conclusion that $G(\alpha, \beta, \gamma)$ is not constant to a good approximation; that is, the field of the nonpolar molecules is not linear in their concentration. But if this is true, we must suppose that this effect of the dipole field is measured by P_γ in much the same way as its effect on the optically active molecule. For the experimental fact remains that S is linear in P_γ and therefore any appreciable

[7] J. Weigle, Helv. Phys. Acta **6**, 68 (1933).

TABLE II.*

w_α	w_β	w_γ	$-[\alpha]^{25}_{5461}$	$-[\alpha]_D^{25}$	n^{25}_{5461}	n_D^{25}	$-[\Omega]^{25}_{5461}$	S^{25}_{5461}	ϵ	P_γ
(a) Dipropionyl diethyl d-tartrate-cyclohexane-cyclohexylcyanide.										
5.003	35.059	0.000	14.491	11.243	1.42408	1.42226	3.598		2.277	
5.004	35.063	0.000	14.388	11.191	1.42433	1.42256	3.571		2.278	
4.996	33.403	1.979	13.311	10.308	1.42562	1.42381	3.301	783	2.793	238.1
4.997	32.660	2.844	12.909	10.007	1.42597	1.42416	3.201	737	3.022	229.7
5.010	31.249	4.487	12.576	9.632	1.42697	1.42516	3.116	570	3.468	215.8
5.007	31.094	4.675	12.583	9.587	1.42712	1.42526	3.117	546	3.523	214.7
4.990	29.341	6.761	12.075	9.219	1.42861	1.42681	2.988	482	4.100	199.5
4.996	27.356	9.095	11.859	9.107	1.43016	1.42842	2.932	392	4.784	185.7
5.011	24.084	12.941	11.624	8.980	1.43271	1.43088	2.868	302	5.966	167.1
5.005	18.988	18.970	11.539	8.792	1.43651	1.43465	2.840	214	7.949	145.2
5.002	10.971	28.388	11.545	8.846	1.44267	1.44083	2.829	145	11.147	121.2
5.000	00.000	41.328	11.601	8.901	1.45079	1.44886	2.826	100	15.637	100.4

* In this and the following tables, the subscripts α, β, and γ refer to the substances in the order in which they appear in the title. In all cases w_α, etc. refers to the weight of the substance in a volume of 50 cc at 25°C. ϵ is the dielectric constant at 25°C.

(b) Dipropionyl diethyl d-tartrate-cyclohexane-1-nitro-1-methyl cyclohexane.										
5.003	35.069	0.000	14.491	11.243	1.42428	1.42246	3.597		2.278	
5.001	35.075	0.000	14.549	11.249	1.42438	1.42256	3.611		2.278	
4.995	29.640	7.256	13.364	10.311	1.42891	1.42702	3.306	294	3.832	219.5
5.002	27.330	10.312	13.095	10.096	1.43080	1.42892	3.236	255	4.564	204.6
5.001	23.112	15.960	12.947	9.998	1.43420	1.43229	3.191	185	6.021	181.8
5.001	19.696	20.506	12.847	9.898	1.43732	1.43535	3.160	155	7.228	166.4
5.005	11.987	30.840	12.936	9.989	1.44403	1.44210	3.167	101	10.154	140.5
4.998	00.000	46.885	13.204	10.153	1.45444	1.45227	3.208	60.4	14.788	114.8
(c) Dipropionyl diethyl d-tartrate-cyclohexane-benzonitrile.										
5.014	35.079	0.000	14.361	11.170	1.42403	1.42226	3.565		2.281	
5.004	35.068	0.000	14.389	11.191	1.42428	1.42251	3.572		2.278	
4.996	34.299	1.008	14.661	11.409	1.42622	1.42441	3.634	−332	2.654	315.1
5.009	32.797	2.936	15.122	11.728	1.43061	1.42867	3.737	−295	3.366	275.1
5.003	31.143	5.069	15.390	12.043	1.43486	1.43284	3.792	−227	4.207	247.5
5.012	29.184	7.599	15.511	11.970	1.44047	1.43822	3.806	−161	5.230	220.1
5.007	27.260	10.105	15.578	12.083	1.44629	1.44390	3.807	−121	6.305	199.4
4.995	23.309	15.218	15.115	11.712	1.45733	1.45462	3.665	−32.5	8.613	167.8
5.015	19.551	20.114	14.607	11.217	1.46812	1.46513	3.515	13.8	10.937	146.2
4.995	11.815	30.195	12.161	9.158	1.49058	1.48700	2.881	117	15.804	116.9
5.009	00.000	45.530	5.540	3.593	1.52247	1.51806	1.283	259	22.964	92.18
(d) Dipropionyl diethyl d-tartrate-cyclohexane-nitrobenzene.										
5.005	35.067	0.000	14.484	11.238	1.42423	1.42241	3.595		2.284	
4.996	32.478	4.033	17.963	13.960	1.43281	1.43073	4.432	−1277	3.597	276.9
5.004	31.194	5.960	19.185	14.888	1.43697	1.43480	4.720	−1161	4.286	256.6
5.001	27.283	12.048	21.696	16.947	1.45035	1.44776	5.287	−864	6.699	207.7
5.006	19.467	24.114	23.922	18.628	1.47728	1.47381	5.720	−542	12.446	151.9
5.003	11.937	35.878	24.335	18.689	1.50459	1.50036	5.707	−362	19.009	121.7
5.001	00.000	54.515	22.144	16.645	1.54501	1.53938	5.048	−164	30.544	94.67
(e) Dipropionyl diethyl d-tartrate-benzene-benzonitrile.										
5.013	39.728	0.000	11.320	8.527	1.49513	1.49136	2.673		2.519	
4.990	39.773	0.000	11.573	8.617	1.49528	1.49146	2.732		2.519	
5.014	39.737	0.000	11.517	8.675	1.49499	1.49122	2.719		2.535	
5.002	37.982	2.041	10.296	7.547	1.49646	1.49260	2.429	704	3.357	290.9
5.001	37.139	3.013	10.197	7.548	1.49689	1.49307	2.405	518	3.764	274.5
5.008	35.374	5.019	9.434	6.839	1.49737	1.49345	2.224	497	4.610	245.5
5.006	30.972	10.099	8.240	5.993	1.50120	1.49734	1.937	393	6.806	195.1
4.996	22.101	20.262	7.256	5.054	1.50747	1.50316	1.698	257	11.327	142.1
5.010	13.618	29.983	6.387	4.241	1.51325	1.50908	1.489	210	15.692	115.5
5.009	00.000	45.530	5.540	3.593	1.52247	1.51806	1.283	161	22.964	92.18
(f) Dipropionyl diethyl d-tartrate-benzene-nitrobenzene.										
4.997	39.780	0.000	11.606	8.655	1.49509	1.49126	2.740		2.524	
5.006	37.504	3.092	11.237	8.291	1.49808	1.49421	2.648	183	3.590	282.3
5.000	36.820	4.043	11.101	8.151	1.49884	1.49488	2.614	192	3.932	270.3
5.009	35.395	5.994	11.129	8.085	1.50054	1.49654	2.618	125	4.638	247.4
5.000	33.616	8.474	11.250	8.250	1.50300	1.49895	2.641	71.9	5.577	224.5
4.996	31.030	12.021	11.660	8.457	1.50627	1.50204	2.731	4.61	6.964	198.7
4.991	23.894	21.846	13.575	9.918	1.51526	1.51064	3.160	−118	11.140	153.1
4.999	13.714	35.762	17.053	12.602	1.52786	1.52284	3.934	−205	18.276	119.3
5.000	00.000	54.524	22.049	16.499	1.54485	1.53918	5.026	−258	30.512	95.09

TABLE II.—*Continued.*

w_α	w_β	w_γ	$-[\alpha]^{25}_{5461}$	$-[\alpha]_D^{25}$	n^{25}_{5461}	nD^{25}	$-[\Omega]^{25}_{5461}$	S^{25}_{5461}	ϵ	P_γ
				(*g*) *Dipropionyl diethyl d-tartrate-benzene-cyclohexylcyanide.*						
4.996	39.751	0.000	11.610		1.49523		2.741		2.519	
4.996	39.767	0.000	11.559	8.556	1.49523	1.49141	2.729		2.526	
5.000	35.425	4.532	9.451	6.950	1.49025	1.48661	2.239	597	3.894	221.4
4.998	31.080	9.054	8.604	6.253	1.48504	1.48164	2.046	415	5.291	187.5
5.006	27.212	13.079	8.340	5.993	1.48051	1.47734	1.990	311	6.568	166.4
5.006	22.227	18.231	8.639	6.242	1.47482	1.47185	2.069	199	8.207	146.4
5.007	13.496	27.299	9.736	7.190	1.46489	1.46225	2.348	77.3	11.164	122.9
5.000	00.000	41.328	11.601	8.901	1.45079	1.44886	2.826	−12.0	15.637	101.0
				(*h*) *Dipropionyl diethyl d-tartrate-benzene-1-nitro-1-methyl cyclohexane.*						
5.002	39.724	0.000	11.495	8.596	1.49494	1.49112	2.714		2.516	
5.001	39.738	0.000	11.599	8.649	1.49485	1.49107	2.739		2.518	
4.996	33.578	7.303	9.608	7.006	1.48804	1.48444	2.280	438	4.126	212.2
5.002	29.220	12.445	9.146	6.597	1.48265	1.47929	2.179	315	5.339	188.2
5.000	25.262	17.128	9.000	6.550	1.47865	1.47558	2.150	241	6.496	171.3
4.998	13.728	30.753	10.503	7.802	1.46728	1.46454	2.529	46.1	10.055	138.0
5.005	00.000	46.971	13.187	10.140	1.45384	1.45177	3.206	−73.0	14.816	115.4
				(*i*) *l-menthyl acetate-cyclohexane-cyclohexylcyanide.*						
5.005	34.423	0.000	95.412	80.676	1.42657	1.42476	23.646		2.226	
5.001	34.400	0.000	95.373	80.777	1.42632	1.42451	23.640		2.228	
4.999	34.391	0.000	95.321	80.718	1.42652	1.42476	23.624		2.227	
5.001	30.031	5.142	95.838	81.090	1.42976	1.42792	23.698	−64.7	3.637	218.7
4.995	27.594	8.012	95.792	81.078	1.43170	1.42992	23.654	−11.6	4.450	196.9
5.006	24.422	11.779	95.785	81.053	1.43385	1.43204	23.616	9.73	5.678	177.9
5.004	19.976	16.977	95.629	80.990	1.43727	1.43545	23.521	37.3	7.325	155.0
4.995	12.821	25.485	95.803	81.038	1.44252	1.44063	23.476	34.5	10.469	130.6
5.004	00.000	40.472	94.884	80.294	1.45209	1.45017	23.094	73.2	15.658	103.1
				(*j*) *l-menthyl acetate-cyclohexane-1-nitro-1-methyl cyclohexane.*						
4.996	34.413	0.000	95.324	80.713	1.42687	1.42506	23.619		2.226	
5.005	34.419	0.000	95.347	80.713	1.42677	1.42496	23.626		2.225	
5.002	31.244	4.221	95.519	80.824	1.42926	1.42747	23.627	−6.78	3.082	238.0
4.995	28.361	8.071	95.701	80.936	1.43165	1.42982	23.632	−7.98	3.954	218.0
4.999	25.337	12.095	95.775	81.021	1.43405	1.43219	23.610	7.69	4.939	199.4
5.000	19.257	20.271	95.708	80.956	1.43912	1.43716	23.509	40.2	7.098	169.3
5.004	12.020	29.980	95.672	80.934	1.44543	1.44345	23.396	54.2	9.882	144.2
5.003	00.000	46.734	95.291	80.650	1.45554	1.45347	23.137	75.4	14.653	117.1
				(*k*) *l-menthyl acetate-cyclohexane-benzonitrile.*						
5.005	34.423	0.000	95.412	80.676	1.42657	1.42476	23.646		2.226	
5.001	34.400	0.000	95.373	80.777	1.42632	1.42451	23.640		2.228	
4.999	34.391	0.000	95.321	80.718	1.42652	1.42476	23.624		2.227	
4.998	30.523	4.957	94.440	79.984	1.43692	1.43490	23.234	419	4.097	252.6
5.008	26.621	9.993	93.800	79.423	1.44824	1.44586	22.893	384	6.195	203.4
4.997	18.927	19.970	92.665	78.555	1.46966	1.46667	22.276	351	10.779	148.7
4.995	11.297	29.922	91.795	77.781	1.49126	1.48777	21.732	328	15.599	118.9
5.004	00.000	44.640	90.381	76.542	1.52220	1.51783	20.936	312	22.514	93.75
				(*l*) *l-menthyl acetate-cyclohexane-nitrobenzene.*						
5.005	34.423	0.000	95.412	80.676	1.42657	1.42476	23.646		2.226	
5.001	34.400	0.000	95.373	80.777	1.42632	1.42451	23.640		2.228	
4.999	34.391	0.000	95.321	80.718	1.42652	1.42476	23.624		2.227	
5.005	31.851	3.902	94.354	79.869	1.43491	1.43284	23.246	617	3.504	285.9
5.000	30.551	5.926	93.894	79.495	1.43907	1.43680	23.065	594	4.231	263.2
5.002	26.631	11.983	92.913	78.719	1.45239	1.44982	22.610	527	6.646	212.3
5.004	18.893	23.959	91.377	77.488	1.47874	1.47523	21.826	465	12.378	154.7
4.995	11.301	35.780	89.936	76.423	1.50557	1.50124	21.078	440	19.004	123.5
4.997	00.000	53.423	88.103	74.795	1.54456	1.53893	20.089	409	30.110	96.89

TABLE II.—*Concluded.*

w_α	w_β	w_γ	$-[\alpha]^{25}_{5461}$	$-[\alpha]_D^{25}$	n^{25}_{5461}	n_D^{25}	$-[\Omega]^{25}_{5461}$	S^{25}_{5461}	ϵ	P_γ
				(*m*) *l-menthyl acetate-benzene-benzonitrile.*						
5.007	38.795	0.000	95.858	81.130	1.49394	1.49012	22.652		2.486	
5.002	38.796	0.000	95.816	81.171	1.49361	1.48983	22.647		2.486	
4.995	38.816	0.000	95.740	81.076	1.49375	1.48998	22.627		2.485	
5.002	34.056	5.494	95.266	80.671	1.49751	1.49369	22.455	175	4.739	240.2
5.000	32.376	7.440	95.006	80.455	1.49874	1.49483	22.374	186	5.566	219.1
4.994	30.154	10.029	94.716	80.198	1.50044	1.49654	22.279	187	6.684	196.6
5.003	28.444	11.996	94.301	79.858	1.50181	1.49781	22.160	207	7.541	182.7
4.996	24.115	16.960	93.732	79.420	1.50492	1.50092	21.978	202	9.725	156.0
4.998	15.362	26.995	92.481	78.327	1.51103	1.50695	21.592	200	14.246	123.1
5.004	00.000	44.640	90.381	76.542	1.52220	1.51783	20.936	197	22.514	93.73
				(*n*) *l-menthyl acetate-benzene-nitrobenzene.*						
5.007	38.795	0.000	95.858	81.130	1.49394	1.49012	22.652		2.486	
5.002	38.796	0.000	95.816	81.171	1.49361	1.48983	22.647		2.486	
4.995	38.816	0.000	95.740	81.076	1.49375	1.48998	22.627		2.485	
5.005	35.998	3.914	95.259	80.673	1.49751	1.49360	22.453	297	3.824	271.7
5.000	35.969	3.952	95.192	80.544	1.49779	1.49388	22.433	325	3.844	272.3
5.004	34.529	5.947	94.828	80.289	1.49960	1.49559	22.319	334	4.552	248.5
5.009	34.524	5.956	94.731	80.257	1.49950	1.49550	22.298	355	4.571	249.5
5.002	32.724	8.429	94.422	80.076	1.50196	1.49796	22.186	333	5.485	226.0
5.004	30.189	11.956	93.817	79.480	1.50520	1.50101	21.994	333	6.852	200.1
5.003	21.670	23.700	91.797	77.855	1.51653	1.51196	21.349	336	11.988	148.4
4.997	12.835	35.820	89.859	76.350	1.52781	1.52279	20.733	328	18.405	120.2
4.997	00.000	53.423	88.103	74.795	1.54456	1.53893	20.089	294	30.110	96.87
				(*o*) *l-menthyl acetate-benzene-cyclohexylcyanide.*						
5.007	38.795	0.000	95.858	81.130	1.49394	1.49012	22.652		2.486	
5.002	38.796	0.000	95.816	81.171	1.49361	1.48983	22.647		2.486	
4.995	38.816	0.000	95.740	81.076	1.49375	1.48998	22.627		2.485	
4.998	33.939	5.110	95.933	81.228	1.48837	1.48483	22.759	−125	4.036	219.0
5.005	31.098	8.053	95.814	81.227	1.48528	1.48183	22.780	−93	4.931	195.6
4.998	27.172	12.169	95.733	80.978	1.48095	1.47778	22.830	−84	6.238	172.3
4.996	23.273	16.280	95.730	81.018	1.47635	1.47332	22.904	−88	7.626	155.3
5.004	14.084	25.915	95.474	80.835	1.46644	1.46374	23.003	−76	10.807	127.1
5.004	00.000	40.472	94.884	80.294	1.45209	1.45017	23.094	−61	15.658	103.1
				(*p*) *dipropionyl diethyl d-tartrate-cyclohexane-benzene.*						
5.005	35.098	0.000	14.335	11.290	1.42453	1.42271	3.558		2.279	
4.997	35.080	0.000	14.108	11.056	1.42428	1.42251	3.502		2.276	
5.014	35.079	0.000	14.361	11.170	1.42403	1.42226	3.565		2.281	
5.029	34.565	0.558	14.515	11.234	1.42492	1.42311	3.601	−45.5	2.280	23.5
5.011	33.822	1.374	14.569	11.226	1.42632	1.42446	3.611	−21.3	2.284	25.8
4.990	32.985	2.336	14.628	11.372	1.42791	1.42596	3.622	−14.4	2.290	26.4
5.014	30.853	4.708	14.810	11.420	1.43135	1.42942	3.658	−10.1	2.302	26.1
4.995	29.893	5.760	14.765	11.512	1.43296	1.43093	3.643	−7.25	2.308	26.4
5.018	29.065	6.687	14.847	11.359	1.43470	1.43259	3.658	−7.12	2.314	26.3
5.003	26.875	9.140	14.590	11.345	1.43857	1.43635	3.585	−2.09	2.326	26.3
5.008	22.756	13.739	14.030	10.835	1.44734	1.44385	3.426	3.12	2.352	26.3
4.999	19.033	17.978	13.705	10.450	1.45374	1.45112	3.332	4.43	2.377	26.3
4.996	14.995	22.584	13.110	9.960	1.46197	1.45916	3.169	6.34	2.407	26.3
4.990	11.165	26.944	12.725	9.570	1.47000	1.46682	3.058	6.92	2.433	26.3
5.023	7.164	31.529	12.145	9.060	1.47855	1.47523	2.901	7.86	2.466	26.3
4.996	3.395	35.887	11.310	8.555	1.48707	1.48353	2.686	9.24	2.496	26.3
5.013	0.000	39.728	11.320	8.527	1.49513	1.49136	2.673	8.48	2.519	26.2
4.990	0.000	39.773	11.573	8.617	1.49528	1.49146	2.732	7.89	2.519	26.2
				(*q*) *l-menthyl acetate-cyclohexane-benzene.*						
5.001	34.400	0.000	95.373	80.777	1.42632	1.42451	23.640		2.228	
4.999	28.830	6.143	95.177	80.523	1.43586	1.43375	23.433	130	2.263	27.0
5.006	26.511	8.733	95.028	80.397	1.43987	1.43766	23.330	137	2.281	27.1
5.002	23.203	12.450	94.918	80.323	1.44619	1.44375	23.199	137	2.302	26.9
5.008	17.851	18.457	95.004	80.426	1.45639	1.45362	23.053	124	2.342	26.8
5.009	12.638	24.359	95.083	80.558	1.46669	1.46369	22.905	117	2.383	26.8
5.002	7.194	30.570	95.354	80.711	1.47822	1.47484	22.784	109	2.441	27.1
5.002	0.000	38.796	95.816	81.171	1.49361	1.48983	22.647	100	2.486	26.7

variation in $G(\alpha, \beta, \gamma)$ must also be linear in P_γ.[8] It is apparent, however, that a change of this type in $G(\alpha, \beta, \gamma)$ would not be separable from the other term in P_γ, so that the observed slope would be the sum of the two terms and would still be expected to show the regularities described above.

Discussion of $G(\alpha, \beta, \gamma)$

On the basis of our previous definition we might expect to find some regularities in the various values of $G(\alpha, \beta, \gamma)$, if only for the reason that they occur in the coefficient of P_γ. That such is not the case can easily be verified by extrapolation of the lines in Figs. 3 and 4 to $P_\gamma=0$. The values so obtained for the various mixtures are distributed in a random manner.[9] But it should be remembered that the change in rotivity with solvent is probably the resultant of a number of causes. The change in the dipole field is one of these and the complete understanding of it will constitute a step in the solution of the whole problem. Therefore, for the present, we recognize that the quantity $G(\alpha, \beta, \gamma)$ contains other factors which have not been specified.

[8] In this connection, there exists a relation that is very suggestive, although its precise connection is not clear. The expression for $G(\alpha, \beta, \gamma)$ obtained for the case of an imperfect gas contains the factor $(w_\beta - w_\beta^0)/w_\gamma$. Since the solutions studied are not ideal, this quantity would be expected to vary with the concentration of the polar constituent and consequently, with P_γ. Actually, in those cases where good data are available, $(w_\beta - w_\beta^0)/w_\gamma$ is found to be practically linear in P_γ. The magnitude of this variation is of lower order than that of the change in S. Nevertheless, here is an example of the linear dependence on P_γ of a quantity that is related to the molecular interaction between the two components of the solvent mixture.

[9] In the menthyl acetate experiments there occurs an apparent regularity in the following derived relationship. Using the expression for $G(\alpha, \beta, \gamma)$ derived for the imperfect gas case, one obtains the equation

$$\Delta\Omega_{\beta_1\beta_2} + \Delta\Omega_{\beta_2\gamma} = \Delta\Omega_{\beta_1\gamma},$$

where $\Delta\Omega_{\beta_1\beta_2}$ is the change in rotivity on replacing the necessary amount of nonpolar substance β_1, with a given number of moles of nonpolar substance β_2; $\Delta\Omega_{\beta_2\gamma}$, the change on replacing nonpolar substance β_2 by the same number of moles of polar substance γ; etc., the volume remaining constant in the usual way. For menthyl acetate cyclohexane-benzene and the various polar substances used, the agreement between calculated and observed values is fairly good. However, this is probably due to the almost linear character of the rotivity curves for this compound. The constant part of $G(\alpha, \beta, \gamma)$ is the predominating factor in $\Delta\Omega$, which might permit the observed agreement regardless of the actual significance of the expression for $G(\alpha, \beta, \gamma)$ that was used.

The Aromatic Nucleus

It is apparent that the field of the aromatic nucleus originating in an aromatic dipole molecule, such as a substituted benzene, will be very different from that originating in a benzene molecule. For example, Kortüm[10] has demonstrated by measurements of absorption spectra that nitrobenzene has characteristics other than those obtainable by superposition of a nitro group and a benzene ring. Therefore, it is most advantageous to study the variations in rotivity as cyclohexane is gradually replaced by benzene. Throughout the experiment the molar polarization of the benzene should remain practically constant. That it apparently does so can be seen from Table II, (p) and (q). Accordingly, the theory predicts that S should remain constant, or that the change in rotivity should be linear in the concentration of benzene. For dipropionyl-diethyl-*d*-tartrate, the data shown in Table II(p) and Fig. 1 (dotted line) are seen to fulfill this condition over the greater part of the concentration range, with a small but significant deviation in the region of small benzene concentrations. While the agreement in the case of menthyl acetate is also fairly satisfactory (see Table II(q) and Fig. 2), its significance is lost because all rotivity curves for it are nearly linear even in those cases where P_γ varies widely, a fact which is discussed more fully in the following section. It is recognized that the benzene molecule has a field which may affect rotivity and which cannot be specified by calculations based on a dipole distribution.

The Optically Active Substance

The two optically active substances used are seen to exhibit striking differences in behavior in accordance with their very different structures. Dipropionyl-diethyl-*d*-tartrate contains two assymetric carbon atoms which are identical and, therefore, can be characterized by the same deformability coefficient. In contrast to this, *l*-menthyl acetate contains three different assymetric carbon atoms and at least three different deformability coefficients will be required to describe a change in its optical rotatory power. Not only may these coefficients differ

[10] G. Kortüm, Zeits. f. physik. Chemie **B42**, 39 (1939).

greatly in magnitude and in sign, but in addition the acting dipole field will not be the same at that region in the molecule where each is effective. Consequently, it can be readily understood how internal cancellations might cause the reaction to a dipole field to take on a character very different from that of a molecule of simpler structure.

Preparation of Materials

Dipropionyl diethyl-*d*-tartrate

Diethyl *d*-tartrate was prepared according to the method of Lowry and Cutter[11] and purified by distillation at 2 mm $\alpha^{20}{}_{5461}$(obs.)=18.95° (2 dm.). This was refluxed with propionic anhydride according to the method of McCrae and Patterson[12] for diacetyl diethyl tartrate. After distilling off the excess anhydride under reduced pressure, the product was quickly washed several times with cold sodium bicarbonate solution, then with water, and dried. It was purified by repeated distillation[13] at 2 mm, each time retaining only the middle fraction.

$$\alpha_{5461}{}^{25}(\text{obs.}) = -2.26° \text{ (2 dm.)},$$

$$\alpha_D{}^{25}(\text{obs.}) = 0.14° \text{ (2 dm.)}.$$

Analysis: Calculated, $C=52.80$ percent, $H=6.93$ percent; found, $C=52.65$ percent, $H=6.96$ percent.

l-Menthyl acetate

Prepared from *l*-menthol and acetic anhydride by the method of Tchugaeff[14]

$$\alpha_D{}^{25}(\text{obs.}) = -146.03° \text{ (2 dm.)}.$$

Cyclohexyl cyanide

Cyclohexyl bromide was prepared from cyclohexanol and dry hydrogen bromide.[15] This was converted to the cyanide by the action of dry cyanogen (in ether solution) on the Grignard reagent.[16] It was finally purified by fractionation at 18 mm pressure, b. p. 78–80°C $n_D{}^{25}=1.4511$.

1-nitro-1 methyl cyclohexane

A mixture of 400 g of methyl cyclohexane, 284 cc of 69 percent nitric acid, 900 cc of acetic acid, and 600 cc of acetic anhydride was refluxed for 12 hours.[17] After cooling, a large volume of water was added, the oily layer separated, washed with dilute sodium hydroxide and then with water until neutral. After drying, the unchanged hydrocarbon was distilled off under slightly reduced pressure and the mixed nitro derivatives distilled from the tar at 35 mm. The unwanted isomers were then removed by treatment with hot concentrated potassium hydroxide according to Nametkin.[18] The product was finally purified by two fractionations. The yield was poor and the unreacted hydrocarbon was continually reworked. b.p. (35 mm) 105.5–107.5°C $n_D{}^{20}=1.4568$.

Benzonitrile

Eastman Kodak benzonitrile was dried with anhydrous calcium sulfate for two days and fractionated, b.p. (14 mm) 75–76°C $n_D{}^{25}=1.5265$.

Cyclohexane, benzene, and nitrobenzene were purified as described by Beckmann and Cohen,[1] the physical constants agreeing within experimental error.

When the differences in boiling points permitted, cyclohexane, cyclohexyl cyanide, 1-nitro-1-methyl cyclohexane, benzonitrile, and dipropionyl diethyl tartrate were recovered from mixtures by fractionation. If, after purification, the constants were the same as the original, the substances were re-used.

Apparatus and Precision

These having been previously[1] described, it is only necessary to add that the source of the sodium *D* line was a small Osram sodium lamp.

[11] J. M. Lowry and J. O. Cutter, J. Chem. Soc. **121**, 532 (1922).
[12] J. McCrae and I. S. Patterson, J. Chem. Soc. **77**, 1098 (1900).
[13] P. Freundler, Ann. Chim. Phys. (7) **3**, 457 (1894).
[14] L. Tchugaeff, Ber. d. D. chem. Ges. **31**, 363 (1898).
[15] *Organic Synthesis* (John Wiley & Sons, New York 1935), Vol. XV, p. 24.
[16] V. Grignard, E. Bellet and Ch. Courtot, Ann. Chim. (9) **12**, 368 (1919).
[17] J. Houben, *Die Methoden der Organischen Chemie* (Georg Thieme, Leipzig, 1934), Vol. 4, p. 146.
[18] S. Nametkin, J. Russ. Phys. Chem. Soc. **42**, 692 (1910).

Lattice Vibrations of Crystals and the Corresponding Vibrations of Their Solutions. II

SIMON FREED AND S. I. WEISSMAN
G. H. Jones Laboratory, University of Chicago, Chicago, Illinois

(Received June 24, 1940)

Because vibrations have been found in liquids which closely resemble what have been regarded as lattice vibrations in crystals, we examine whether the vibrations in crystals are to be ascribed to local complexes rather than to an extended lattice. Our experiments confirm the appropriateness of the term "lattice vibrations" and analogous vibrations must, it seems, be accepted as taking place in solutions. Alcohol with a more regular arrangement within the liquid than water gives rise to greater sharpness in the quasi-lattice vibrations of the solution. Correspondingly, a mixed solvent gives a greater spread and diffuseness to the vibrations even though the electric fields immediately surrounding the positive ions in such a solution are as sharp in their effect on the electronic levels as in the pure solvents separately. With absolute alcohol, europium chloride and europium nitrate form solutions which show different quasi-lattice vibrations in their spectra; but when these salts are dissolved in water, the vibrations of the solutions appear about the same. The hydrated crystals of europium chloride exhibit lattice vibrations which are different from those of the hydrated mixed magnesium europium nitrate. In the ionic crystals of anhydrous europium fluoride, a lattice frequency appears; this is considerably greater than any yet measured. A discussion concerning the nature of the systems partaking in the quasi-lattice vibrations is included.

IN a recent communication[1] we called attention to the fact that certain intervals in the spectra of crystals which have been ascribed to lattice oscillations are roughly reproduced in the spectra of their solutions. The correspondence in the intervals is unmistakable experimentally. Not only are they of the same order of magnitude but they accompany the same electronic transitions. These in turn are easily identified since they appear as widely separated groups of lines of considerable intensity. We have observed that corresponding intervals are present in the fluorescence spectra as well as in the absorption spectra. The discovery of lattice oscillations in the visible spectra of crystals resulted from the observation[2] that faint repetitions of the electronic patterns appeared at intervals which in many instances conformed to well-known vibrational frequencies. In the spectra of hydrated neodymium nitrate, for example, some of the intervals were in excellent agreement with the well-known vibrational frequencies of H_2O and of NO_3^-. In addition, rather faint repetitions occurred at smaller intervals. These diminished in magnitude as the lattice was made more massive by replacing H_2O by D_2O, or when in the mixed crystal $3Mg(NO_3)_2 \cdot 2Nd(NO_3)_3 \cdot 24H_2O$ the magnesium was replaced by zinc. The latter intervals were then identified with lattice oscillations. Hellwege[3] confirmed the existence of these frequencies by direct measurement with reststrahlen.

In view of the effect on these frequencies by zinc ion Zn^{++} which is remote from Nd^{+++} in the lattice the term "lattice vibration" does not seem inappropriate. However, no x-ray analysis of the mixed nitrate has as yet been made. Because the vibrations take place in solutions also, it is natural to assume that they originate in local "independent" complexes and to ascribe the oscillations to the motion of molecules, such as water in the first coordination sphere. We therefore examined the spectra of anhydrous europium fluoride (EuF_3) where such a model does not apply. The crystal structure of anhydrous rare earth fluorides is well known, being ionic in character with no molecular clusters in the lattice. Because of the long range ionic forces any disturbance such as an electronic excitation would be expected to set the entire lattice into oscillation.

The symmetry of the lattice has been determined[4] as D^3_{6h} and the point group about the

[1] S. I. Weissman and S. Freed, J. Chem. Phys. **8**, 227 (1940).
[2] H. Ewald, Ann. d. Physik (5) **34**, 209 (1939).
[3] K. H. Hellwege, Zeits. f. Physik **113**, 192 (1939).
[4] I. Oftedal, Zeits. f. physik. Chemie **B5**, 272 (1929); **13**, 190 (1930).

rare earth ions is C_{2v}. The fluorides LaF_3, CeF_3, PrF_3, NdF_3, and SmF_3 were all found to have the same symmetry and there are many reasons for expecting that the fluoride of europium, the element after samarium (Sm) in the periodic table, also has the same structure. The absorption spectra of crystals EuF_3 are in excellent agreement with the supposition that the point group about Eu^{+++} is also C_{2v}. The degeneracy of the energy levels of Eu^{+++} would be completely lifted by an electric field having this symmetry and indeed we found the maximum number of component lines in each group. An electronic transition which had been accepted on the basis of much data as originating in $J=0$ and ending in $J=3$ contained a group of seven lines; another transition from $J=0$ to $J=2$ consisted of a group of five lines. It has in fact been found that as in other salts of europium an interval at 4650A occurs, in this instance of about 340 cm^{-1}. Here the group induced by the electric fields spread over 63 cm^{-1}. The relative intensities of the lines within the modulated group were not the same as within the main group. The intervals, however, between corresponding lines were accurately the same. The vibrational interval 340 cm^{-1} is from two to three times what has appeared in various hydrated crystals. In the hydrated chloride the smallest frequency which coupled with the electronic frequency at 4650A was about 115 cm^{-1} whereas in the mixed magnesium nitrate it was about 175 cm^{-1}. The latter value was equal to the most intense lattice vibration observed by Ewald[2] in the homologous neodymium salt. The magnitude of the lattice oscillations which will couple with a particular electronic frequency may be expected to depend on the lattice symmetry also but one may infer that the higher frequency in the fluoride is a reflection of the greater tightness of binding in the lattice as compared with the hydrated crystals. It should be recorded that the intensity of the lattice vibration, that is the intensity of the repetition of the pure electronic transition is not as great as in hydrated crystals.

The effect of the regularity in the packing of the solvent molecules on the quasi-lattice-vibration-in-the-liquid which hereafter will be called the L-vibration is evident in alcoholic solutions. X-ray diffraction data reveal a higher measure of regularity in alcohol than in water and in fact the L-vibrations in alcoholic solutions are much more definitely outlined than in aqueous solutions. When anhydrous europium nitrate is dissolved in absolute alcohol the L-vibrations are 210 cm^{-1}, 90 cm^{-1} and with anhydrous chloride the principal one is 165 cm^{-1}. In water both the nitrate and chloride have about the same frequency 125 cm^{-1}.[5]

It has been shown[5] that when a little water is added to an anhydrous alcoholic solution of europium chloride, for example, the spectrum of the pure aqueous solution appears superimposed upon the original alcoholic spectrum. It required but relatively little water to suppress the spectrum of "alcoholate" altogether. However, on examining the spectrum from such a solution (i.e. one with the electronic pattern the same as that from an aqueous solution but from a solvent preponderant in alcohol), the L-vibrations were found to be diffuse and spread over the combined ranges which prevail in pure alcohol and in pure water as solvents. In other words, even though the symmetry and strength of the local electric fields about Eu^{+++} were the same as when the ion was in pure water, both alcohol and water took part in the oscillations.

Evidence consistent with the idea that L-vibrations in solutions are not principally due to the first coordination sphere about the positive ion comes from a study of the europium acetyl acetonates dissolved in the nonpolar solvents carbon tetrachloride and benzene. Crystals of various acetylacetonate have been analyzed by Astbury[6] and he concluded that six oxygen atoms at the corners of an octahedron occupy the region of first coordination. As in the case of scandium, for example, which is often classed with the rare earths, one may schematize the structure as in Fig. 1. The solution of such a structure in benzene or carbon tetrachloride might be expected to be a good example of local and independent vibrating systems to which we have previously referred. However, we were unable to observe the coupling of these vibrations with the electronic frequency in the region of

[5] S. Freed, S. I. Weissman, F. E. Fortess and H. F. Jacobson, J. Chem. Phys. **7**, 824 (1939).
[6] W. T. Astbury, Proc. Roy. Soc. **112**, 448 (1926).

the spectrum where the lattice oscillations had always been found. The pure electronic frequency was exceptionally intense in our spectra and in no other instance which we have examined had the lattice interval failed to appear when such intense electronic transitions were present. It should be stated, however, that the amount of europium in the light path was not as great as in some of our other solutions. An attempt to concentrate the solution led to a dimerization of the acetylacetonate and another spectrum* appeared. The dimer may be represented as in Fig. 2. When the amount of europium in the light path was the same as with the monomer, a faint sign of a L-vibration was observed, considerably fainter than when the solvent consisted of dipoles such as water or alcohol.

For the present, it appears to us that the quasi-lattice vibrations of the solutions may be represented in the following way. The modes of

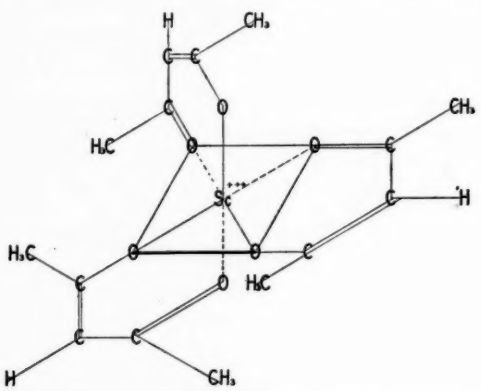

FIG. 1. A structure for scandium acetylacetonate.

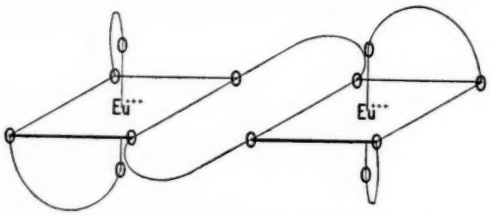

FIG. 2. A structure for the dimer of europium acetylacetonate.

vibration of the solution insofar as they couple with the electronic motions of the positive ions may be approximated by the vibrations of a region extending over several coordination layers from the ions. The main body of the vibrating system is the solvent modified by the presence of the dissolved ions. The roles these play resemble that of a substance which dissolves in a crystal and embeds itself in the lattice. The ions endow the neighboring solvent with crystalline-like properties which diminish in their regularity with distance from the ions. Finally, the outer fringe of the effective vibrating system takes on a character more nearly that of the pure solvent with whatever order is present there,—especially in dilute solutions. How many coordination layers should be assumed to take part actively in the oscillations would depend on the range of the forces of interaction. Even if the structure of a region of such dimensions were idealized into a perfectly regular micro-lattice, its vibrational spectrum would, of course, be rather diffuse.

This investigation has received support from the Penrose Fund of the American Philosophical Society.

* It is intended to publish a description of these spectra soon in the *Journal of the American Chemical Society.*

A Confirmation of the Theory of Thermal Diffusion

T. I. TAYLOR AND GEORGE GLOCKLER
School of Chemistry, University of Minnesota, Minneapolis, Minnesota
(Received July 8, 1940)

THE experiments reported by Nier[1] and Bardeen[2] demonstrated that the theory of the thermal diffusion column[3] as given by Furry, Jones and Onsager[4] describes reasonably well the separation of the carbon isotopes using methane. Since the construction of a 40-foot column by the authors,[5] further experimental verification of this theory has been obtained.

As described previously, the column was constructed from a 2-inch pipe concentric with a 1-inch standard galvanized pipe from which the galvanizing was removed. (More favorable sizes can be obtained in steel tubes.) The difficulties originally experienced with the heating element were overcome by using four parallel loops of No. 16 Nichrome wire running to the bottom and back through 8-hole porcelain insulators. A one-quarter-inch rod running through a hole in the center of the insulators served as a method of holding them in place and facilitated removing the whole heating element when necessary. The following figures give a description of the column: width of annular space = 0.95 cm; mean circumference of annular space = 13.68 cm; area of annular space = 13.0 sq. cm; volume of annular space 14.2 liters; volume of bulb on the bottom = 1.2 liters; volume of reservoir on top = 24.6 liters; height of heating surface 10.9 meters.

In order to study the performance of the column, methane kindly supplied to us by the Southern California Gas Company, Los Angeles, was admitted at different pressures. Small samples were drawn from the top and bottom of the column periodically and the ratio of the isotopes determined by analysis on a mass spectrometer. The temperature of the hot surface was maintained at an average value of 316°C, while the cold surface was that of the cold water supply, about 6°C. The average temperature difference was, therefore, 310°C. A current of 27 amperes passing through the heating element at 195 volts gave an average power consumption of about 5.25 kilowatts.

The results of several experiments at 74 cm, 50 cm, 28 cm and 19 cm of mercury are plotted in Fig. 1. The maximum concentration for a given pressure is reached after 125 to 150 hours. A pressure of 28 cm gave larger concentration than either lower or higher pressures. This is to be compared with Nier's[1] results using a column with a spacing of 0.712 cm. The optimum pressure for that spacing was about 45 cm. A further comparison shows that the smaller spacing gives a larger separation for the same length of column. It, therefore, appears that an annular spacing of about 0.5 cm to 0.7 cm is preferable for the type of column described.

Analyses were also made on samples from the top of the column but owing to the difficulty of correcting the mass-spectrographic analyses for the presence of $O^{16}H^+$ (mass $17 = C^{13}H_4^+$) they were not considered as reliable as the analyses for samples at the bottom of the column. Correc-

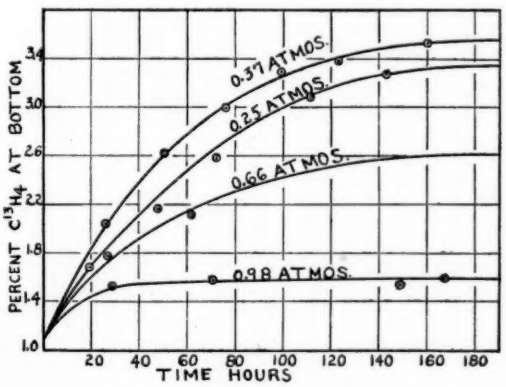

FIG. 1. Variation in the concentration of $C^{13}H_4$ at the bottom of the column with pressure.

[1] Nier, Phys. Rev. **57**, 30 (1940).
[2] Bardeen, Phys. Rev. **57**, 35 (1940).
[3] Clusius and Dickel, Naturwiss. **26**, 546 (1938); **27**, 148 (1939); Brewer and Bramley, Phys. Rev. **55**, 590A (1939); Brewer and Bramley, J. Chem. Phys. **7**, 553 (1939); Groth, Naturwiss. **27**, 260 (1939); H. S. Taylor, Nature **144**, 8 (1939); T. I. Taylor and Glockler, J. Chem. Phys. **7**, 851 (1939); Watson, Phys. Rev. **56**, 703 (1939); Gillespie, J. Chem. Phys. **7**, 530 (1939); Waldmann, Naturwiss. **27**, 230 (1939); Nier, Phys. Rev. **56**, 1009 (1939); Onsager and Watson, Phys. Rev. **56**, 474 (1939); Debye, Ann. d. Physik. **56**, 284 (1939); Waldmann, Zeits. f. Physik. **114**, 53 (1939).
[4] Furry, Jones and Onsager, Phys. Rev. **55**, 1083 (1939).
[5] Taylor and Glockler, J. Chem. Phys. **7**, 851 (1939).

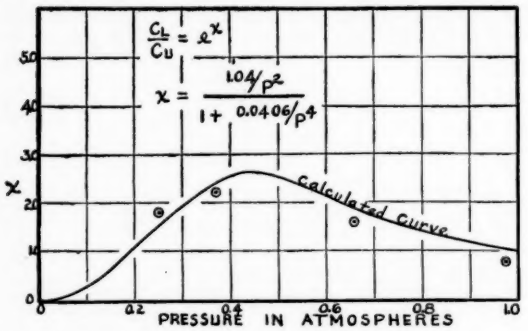

FIG. 2. Variation in the separation factor with pressure.

tions are made empirically by determining the relative heights of the peaks corresponding to masses 16, 17 and 18. The height of the $O^{16}H^+$ peak for water vapor varied from 25 percent to 30 percent of the height of the H_2O^{16+}. Subtraction of the calculated height of the $O^{16}H^+$ peak from the total height at mass 17 for the sample gave the height of $C^{13}H_4^+$ peak. Careful regulation of the energy of the ionizing electron beam in Nier's previous analyses[1] eliminated much of this difficulty. However, weighted mean of the values after equilibrium had been reached gave the following values for the percent of $C^{13}H_4^+$ at the top of the column: 74 cm = 0.70 percent, 50 cm = 0.53 percent, 28 cm = 0.40 percent, 19 cm = 0.60 percent. The corresponding ratios for the maximum concentration of $C^{13}H_4$ at the bottom divided by the concentrate at the top gives, respectively, 2.13, 4.9, 9.0, and 6.2. There was a very large separation of the impurities. The ratio of the concentration of carbon dioxide at the bottom to that at the top was often more than 1000 to 1.

The variation in the ratio of the concentration of $C^{13}H_4$ at the bottom to that at the top, C_L/C_U, can be calculated from the theoretical equations of Furry, Jones and Onsager.[4] For any given column, the dependence upon pressure can be reduced to a simplified equation of the form

$$\frac{C_L}{C_U} = e^{(a/p^2)/(1+b/p^4)} = e^x,$$

where a and b are constants and p is the pressure in atmospheres. Using the dimensions for our column and calculating the constants a and b from the theoretical equations in a manner described by Nier[1] and using his value for the coefficient of thermal diffusion, the value of x is given by

$$x = \frac{1.04/p^2}{1+0.0406/p^4}.$$

Figure 2 shows a comparison of the theoretical curve with experimental points. The results show reasonable agreement. The theory predicts the observed pressure for maximum separation and the manner in which the separation decreases with increasing pressure. If the observed deviations are real, they seem to indicate that the separation is less at higher pressures than would be predicted by the theory. This may easily result from mass movement of the gas or mixing due to assymmetry and irregularities in the column. This effect may also be more likely in a column with a large spacing (0.95 cm) compared to one with smaller spacing. From a study of the theoretical curves for columns of different annular space separations and from consideration of the transport of heavy carbon, it appears that the spacing in thermal diffusion columns of this type should preferably be between 0.5 cm and 0.7 cm.

We wish to thank Mr. B. M. Laulhere, Technical Supervisor of the Southern California Gas Company, Los Angeles, for the supply of methane gas, and we are indebted to Dr. A. O. Nier for carrying out the mass-spectrographic analyses.

On the Theory of Fusion

JOHN G. KIRKWOOD AND ELIZABETH MONROE
Cornell University, Ithaca, New York
(Received September 5, 1940)

IT is the purpose of the present note to present a brief outline of a theory of fusion based upon the concept of an order-disorder transformation. The theory is similar in principle to that of Lennard-Jones and Devonshire,[1] but goes beyond it by allowing to the molecules of the liquid phase a continuum of sites, rather than restricting them to a lattice with merely a somewhat greater multiplicity of sites than are accessible in the solid.

For a system of N molecules confined in a volume v, we define a function $g(\mathbf{r})$, specifying the local molecular density $Ng(\mathbf{r})/v$ at the point $\mathbf{r}$ in the region v. The Helmholtz free energy A, with the suppression of constant terms appropriate to the free molecule, may be exactly expressed in the form

$$\frac{A}{RT}=\frac{1}{v}\int^{v} g\log(g/v)dv+\frac{N}{2v^2}kT\int^{v}\int^{v} W(\mathbf{r}',\mathbf{r},[g])g(\mathbf{r}')g(\mathbf{r})dvdv',$$

$$W(\mathbf{r}',\mathbf{r},[g])=\int_0^1 V(|\mathbf{r}'-\mathbf{r}|)e^{-w(\mathbf{r}',\mathbf{r},\sigma)/kT}, \tag{1}$$

where V is the mutual potential energy of a pair of molecules situated at the points $\mathbf{r}$ and $\mathbf{r}'$, respectively, and $w(\mathbf{r}',\mathbf{r},\sigma)$ is the local free energy of this configuration, when intermolecular forces in the system are reduced to a fraction σ of their full value. Here $W(\mathbf{r}',\mathbf{r},[g])$ is a functional of g in the sense of Volterra.[2] When g is unity, we have the liquid state and $W(\mathbf{r}',\mathbf{r},[g])$ is equal to $W(|\mathbf{r}'-\mathbf{r}|)$, which, in turn, is related to the free volume v_f and the mean potential energy $\bar{V}$ of a pair of molecules in the fluid, in the following manner,

$$\frac{1}{kT}\int^{v} W(r)dv=\log\frac{v}{v_f}+\bar{V}/2kT \tag{2}$$

if the free volume is defined by the relation

$$A/RT=-\log v_f+\bar{V}/2kT+\log\left[\left(\frac{2\pi mkT}{h^2}\right)^{\frac{3}{2}}e\right]. \tag{3}$$

For the present, we approximate $W(\mathbf{r}',\mathbf{r},[g])$ by its liquid value $W(|\mathbf{r}'-\mathbf{r}|)$ and minimize the free energy A with respect to the function g, by means of the calculus of variations.[3] In this manner, we obtain the following integral equation for the equilibrium form of the function g

$$\log\lambda g(\mathbf{r})=-\frac{N}{vkT}\int^{v} W(|\mathbf{r}'-\mathbf{r}|)g(\mathbf{r}')dv', \quad \frac{1}{v}\int^{v} gdv=1. \tag{4}$$

In order to investigate the possibility of a crystalline phase we seek solutions of Eq. (4), which are periodic in the unit cell Δ of a specified lattice. Let $\mathbf{a}_1$, $\mathbf{a}_2$, $\mathbf{a}_3$ be the vectors defining the unit cell, and $\mathbf{b}_1$, $\mathbf{b}_2$, $\mathbf{b}_3$ the corresponding reciprocal vectors. If x, y, z are the contravariant components of $\mathbf{r}$, that is $\mathbf{r}\cdot\mathbf{b}_1$, $\mathbf{r}\cdot\mathbf{b}_2$, $\mathbf{r}\cdot\mathbf{b}_3$, the periodic function $g(r)$ may be expanded in the Fourier series

$$g(\mathbf{r})=\sum_{l_1l_2l_3=-\infty}^{+\infty} s_{l_1l_2l_3}e^{2\pi i[l_1x+l_2y+l_3z]}. \tag{5}$$

[1] Lennard-Jones and Devonshire, Proc. Roy. Soc. **A170**, 464 (1939).
[2] Volterra, *Theory of Functionals and of Integral and Integro-Differential Equations* (Blackie and Son, Ltd., 1930).
[3] Kirkwood, J. Chem. Phys. **8**, 205 (1940).

Substitution in (4) yields

$$\log \lambda g = \sum_{l_1 l_2 l_3 = -\infty}^{+\infty} \alpha(\mathbf{p}) s_{l_1 l_2 l_3} e^{2\pi i [l_1 x + l_2 y + l_3 z]},$$

$$\alpha(\mathbf{p}) = -\frac{N}{vkT} \int^v W(r) e^{i\mathbf{p}\mathbf{r}} dv, \tag{6}$$

$$\mathbf{p} = 2\pi [l_1 \mathbf{b}_1 + l_2 \mathbf{b}_2 + l_3 \mathbf{b}_3].$$

From the normalization condition, $(1/v)\int^v g dv$, it follows that s_{000} must be unity. Equations (5) and (6) yield a system of transcendental equations for the remaining Fourier coefficients $s_{l_1 l_2 l_3}$. We shall here consider the face-centered cubic lattice, supposing for purposes of approximation that the Fourier transform $\alpha(\mathbf{p})$ can be treated as negligibly small for $|l_1|, |l_2|, |l_3| > 1$. We choose a cubic cell containing four molecules with $\mathbf{a}_1 = \mathbf{i}a$; $\mathbf{a}_2 = \mathbf{j}a$; $\mathbf{a}_3 = \mathbf{k}a$ where i, j, k are a set of mutually orthogonal unit vectors, and a is equal to $(4v/N)^{\frac{1}{3}}$. By symmetry, Eqs. (5) and (6) yield

$$g(\mathbf{r}) = \frac{1}{\lambda_0} e^{\alpha_1 s_1 \cos(2\pi x) \cos(2\pi y) \cos(2\pi z)},$$

$$\lambda_0 = \int_0^1 \int_0^1 \int_0^1 e^{\alpha_1 s_1 \cos(2\pi x) \cos(2\pi y) \cos(2\pi z)} dx dy dz, \tag{7}$$

where

$$s_1 = G(\alpha_1 s_1) = \frac{\partial \log \lambda_0}{\partial(\alpha_1 s_1)},$$

$$\alpha_1 = -\frac{8}{\sqrt{3}\Delta^{\frac{3}{2}} kT} \int_0^\infty r W(r) \sin\left(2\pi\sqrt{3}\frac{r}{a}\right) dr, \tag{8}$$

$$\alpha_0 = \frac{-16\pi}{\Delta kT} \int_0^\infty r^2 W(r) dr,$$

and s_1 is the common value of $s_{\pm 1, \pm 1, \pm 1}$.

It is found that the transcendental equation (8) has zero as its unique real solution when α_1 is less than unity and g is constrained to the uniform value unity throughout the volume v. In the range $0.979 \leqslant \alpha_1 \leqslant 1$, the solution s_1 equal to zero remains that of minimum free energy. When $\alpha_1 = 0.979$, phases with $s_1 = 0$ and $s_1 = 0.452$ are in equilibrium, and when $\alpha_1 > 0.979$ ($s_1 > 0.452$), the disordered phase s_1 becomes unstable. When s_1 is nonvanishing, we have a periodic density distribution corresponding to a face-centered cubic lattice, which concentrates more sharply around the lattice points as α_1 increases. The theory predicts a first-order transition from a completely disordered density distribution to one of crystalline order at constant volume. This eliminates the possibility of a critical temperature for fusion and provides a basis for the calculation of melting parameters at constant pressure. The Lennard-Jones Devonshire theory, on the other hand, leads to a second-order transition at constant volume and consequently to a critical point.

In a later article, the proposed theory will be developed in greater detail and applied to the liquid-solid transition in argon.

LETTERS TO THE EDITOR

This section will accept reports of new work, provided these are terse and contain few figures, and especially few halftone cuts. The Editorial Board will not hold itself responsible for opinions expressed by the correspondents. Contributions to this section should not exceed 600 words in length and must reach the office of the Managing Editor not later than the 15th of the month preceding that of the issue in which the letter is to appear. No proof will be sent to the authors. The usual publication charge ($3.00 per page) will not be made and no reprints will be furnished free.

On the Elasticity of Crystals

Interest in the variation with temperature of the elastic moduli of metal crystals, especially in the neighborhood of the melting point, has been stimulated by a suggestion by Brillouin[1] and a paper by Born[2] in which the melting temperature is assumed to be that at which the rigidity of a solid vanishes.

In a recent letter Birch and Bancroft[3] report measurements of the rigidity modulus of polycrystalline Al up to 650°C, 13° below the melting point. It is of interest to compare these results with other existing data on other substances, and with some unpublished data in the variation of Young's modulus of a single crystal of Pb up to 325°C, 2° below the melting point. Single crystals were prepared in vacuum by the Bridgman method, and the elastic measurements carried out from 80°K to 598°K, by the composite piezoelectric oscillator method.[4]

In Fig. 1 we plot as abscissae the reduced temperature θ, equal to the absolute temperature divided by the melting temperature, T/T_m. Ordinates are the ratio of the value of the elastic modulus at T°K to its value at $\theta=0.5$. The points for Al are taken from Birch and Bancroft's table, for Na from the data of Quimby and Siegel,[5] for NaCl from the data of Rose[6] and Durand.[7] The dotted curve is obtained from that of Sutherland,[8] quoted by Brillouin.

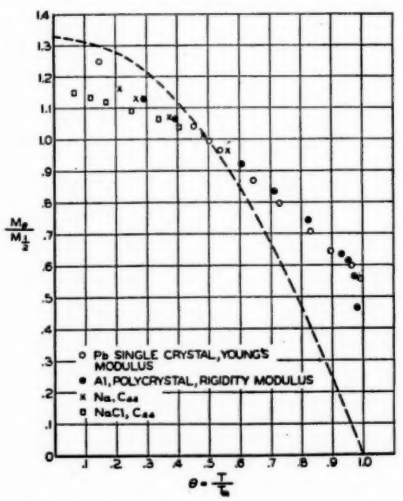

FIG. 1. The variation with temperature of the elastic moduli of several solids.

It appears that the more modern data do not agree well with Sutherland's curve, probably because at high temperatures the static methods used in the earlier work were invalidated by the plastic flow produced by the relatively large stresses needed. It is important to note that the data for the three metals here plotted fall together on one curve, but do not appear to approach zero rigidity at the melting point. The data for NaCl, an ionic salt, do not fall on the same curve as those for the metals. It is perhaps appropriate to mention here that Dr. Joseph Slepian, of these laboratories, has pointed out to us in this connection that the ice cubes in a highball are at the melting point of the solid, but still possess finite rigidity.

SIDNEY SIEGEL
Westinghouse Research Laboratories,
East Pittsburgh, Pennsylvania,

ROBERT CUMMEROW
Physics Department,
University of Pittsburgh,
Pittsburgh, Pennsylvania,
August 25, 1940.

[1] L. Brillouin, Phys. Rev. **54**, 916 (1938).
[2] M. Born, J. Chem. Phys. **7**, 591 (1939).
[3] F. Birch and D. Bancroft, J. Chem. Phys. **8**, 642 (1940).
[4] L. Balamuth, Phys. Rev. **45**, 715 (1934); S. Siegel, Phys. Rev. **57**, 537 (1940).
[5] S. L. Quimby and S. Siegel, Phys. Rev. **54**, 293 (1938).
[6] F. C. Rose, Phys. Rev. **49**, 50 (1936).
[7] M. Durand, Phys. Rev. **50**, 449 (1936).
[8] Sutherland, Phil. Mag. **32**, 42 (1891).

On the Presence of HNC in Hydrogen Cyanide

About ten years ago Dadieu[1] obtained what he considered proof that ordinary hydrogen cyanide consists of a mixture of the two tautomeric forms HCN (99.5 percent) and HNC (0.5 percent). Since there is also some chemical evidence for the existence of these two tautomers (see texts of organic chemistry) it is perhaps in order to point out that the Raman spectrum does *not* support this assumption.

Dadieu's conclusion was based on the observation of a weak Raman line at 2062 cm^{-1} which accompanies the strong CN frequency 2094 in the Raman spectrum of hydrogen cyanide. Since the CN frequency of the nitriles was found to be always higher than that of the corresponding *iso*-nitriles he concluded that the presence of the two lines in prussic acid indicates the presence of both the nitrile and *iso*-nitrile forms (HCN and HNC). However, the weak Raman line 2062 can be quantitatively explained as due to the isotopic molecule $HC^{13}N$. Using the potential constants of Bartunek and Barker,[2] which represent the

vibration frequencies of both HCN and DCN within less than 1 cm^{-1}, one obtains for the $C^{12}-C^{13}$ isotopic shift of the CN vibration 32.9 cm^{-1} in close agreement with the frequency difference of Dadieu's two lines which is 32 cm^{-1}. The $HC^{13}N$ line should have about 1/100 of the intensity of the $HC^{12}N$ line which agrees well with Dadieu's estimate of ½ percent as the "order of magnitude" of the concentration of HNC.

Since the $HC^{13}N$ line must necessarily be there and since the calculated position and intensity agrees with the observed, it follows that *if any* HNC *is present in prussic acid its concentration must be considerably smaller than that of* $HC^{13}N$ *in* HCN.

Somewhat more recently Gordy and Williams[3] have observed a weak band at 4.95μ in addition to the strong C−N band at 4.75μ in a saturated aqueous solution of HCN vapor. They interpret it as due to HNC whose concentration they estimate as between 2 and 4 percent. The band at 4.95μ cannot be interpreted as an isotopic band, the displacement from the main band being about 80 cm^{-1}. However, the fact that no band with a similar displacement occurs in the Raman spectrum of liquid HCN even though the weaker $HC^{13}N$ line does appear, tends to show that the weak band of Gordy and Williams is due to something else (for example, association of HCN to the H_2O molecules in the solution) unless one wants to conclude that the concentration of HNC is appreciably higher in dissolved HCN than in liquid HCN where it definitely is smaller than 1 percent, if it exists at all.

G. HERZBERG

Department of Physics,
University of Saskatchewan,
Saskatoon, Saskatchewan, Canada,
August 27, 1940.

[1] A. Dadieu, Naturwiss. **18**, 895 (1930); Monats. f. Chem. **57**, 437 (1931).
[2] P. F. Bartunek and E. F. Barker, Phys. Rev. **48**, 516 (1935).
[3] W. Gordy and D. Williams, J. Chem. Phys. **4**, 85 (1936).